

**Constraining air-sea equilibrium and biological
end-members for marine gross productivity
estimates using oxygen triple isotopes**

by
Anne van der Meer

Thesis submitted in fulfillment of the requirements
for the degree of

MSc by Research

University of East Anglia
School of Environmental Sciences

August, 2015

© This copy of the thesis has been supplied on condition that anyone who consults it is understood to recognise that its copyright rests with the author and that use of any information derived there from must be in accordance with current UK Copyright Law. In addition, any quotation or extract must include full attribution.

Acknowledgements

My warmest thanks go out to my supervisors, Jan Kaiser and Alina Marca, whom I cannot thank enough, as they have taught me so much, not only about performing research, but also about myself. Thank you so much for your incredible support and commitment during the whole process of research and writing. I could not have wished for, or imagine, more involved, encouraging and dedicated supervisors. In addition, I wish to thank Erik Buitenhuis, Rob Utting, Beate Stawiarsky and Moritz Heinle for introducing me to phytoplankton culturing and kindly allowing me to use their cultures, all the people of the INTRAMIF network, with a special thanks to Amaëlle Landais, for the wonderful experiences during my year as a Marie Curie fellow, and Martin and Pablo for helping me with the formatting and layout of the thesis. Finally, thanks to Paul Dennis and Jack Middelburg for attending my viva and providing me with useful comments on my thesis, my friends and family for their support from a distance, and, very importantly, to Lisanne for cheering me up, sometimes pulling me out of the lab and taking daily walks with me around the lake. This work was supported by a EU FP7 Marie Curie International Training Network grant (agreement no. 237890).

Abstract

The measurement of biological production rates is essential for our understanding how marine ecosystems are sustained and how much CO₂ is taken up through aquatic photosynthesis. Traditional techniques to measure marine production are laborious and subject to systematic errors. A new biogeochemical approach based on triple oxygen isotope measurements in dissolved oxygen (O₂) has been developed over the last few years, which allows the derivation of gross productivity integrated over the depth of the mixed layer and the time-scale of O₂ gas exchange (Luz & Barkan 2000). This approach exploits the relative ¹⁷O/¹⁶O and ¹⁸O/¹⁶O isotope ratio differences of dissolved O₂ compared to atmospheric O₂ to work out the rate of biological production. Two parameters are key for this calculation: the isotopic composition of dissolved O₂ in equilibrium with air and the isotopic composition of photosynthetic oxygen. Recently, a controversy has emerged in the literature over these parameters (Kaiser, 2011) and the main goal of this research was to provide additional data to help resolve this controversy. In order to obtain more information on the isotopic composition of marine biological oxygen, gas from the headspace of airtight bottles with *Picochlorum* sp. and *Emiliana huxleyi* cultures was sampled every 48 hours during eight days, after which the triple oxygen isotopic composition was determined. Results indicate the ¹⁷O excess obtained for both species is in the range of estimations by Kaiser and Abe (2012) based on different triple oxygen isotope measurements of VSMOW vs. air and the species-specific photosynthetic fractionation reported by Eisenstadt et al. (2010). The obtained ¹⁷O excess for *E. huxleyi* was higher (249±11 ppm) than for *Picochlorum* (180±13 ppm), which seems consistent with results of Eisenstadt et al. (2010). In addition, the triple isotopic composition of dissolved oxygen at air saturation was determined for different temperature (0, 22 and 39 °C) and salinity conditions. While 22 °C tests yielded a Δ¹⁷O of ~15-20 ppm, ~10 ppm lower values were obtained for tests at either zero or 39 °C.

List of figures and tables

Figures

Chapter 1

Figure 1: Triple oxygen isotopes in surface ocean and triple isotope plot.	14
---	----

Chapter 2

Figure 2: Schematic drawing of the small extraction line	25
Figure 3: Schematic drawing of the separation line.....	32
Figure 4: $\delta^{18}\text{O}$ results of imbalance tests April 2013	40
Figure 5: Relationship $\Delta^{17}\text{O}$ and imbalance in results of imbalance tests	41
Figure 6: Relationship between $\delta^{18}\text{O}$ and imbalance from zero enrichment data.....	41
Figure 7: Relationship between $\Delta^{17}\text{O}$ and imbalance from zero enrichment data	42
Figure 8: Relationship between imbalance and $\Delta^{17}\text{O}$ before filament change.....	43
Figure 9: $\delta^{17}\text{O}$ results of N_2 dilution series.....	45
Figure 10: $\Delta^{17}\text{O}$ results of N_2 dilution series	45
Figure 11: Effect of variations in $\delta(\text{Ar}/\text{O}_2)$ on the $\Delta^{17}\text{O}$	47
Figure 12: Effect of variations in the $\delta(\text{Ar}/\text{O}_2)$ on $\Delta^{17}\text{O}$	47
Figure 13: Effect of changes in $\delta(\text{Ar}/\text{O}_2)$ on the $\delta^{17}\text{O}$ and $\delta^{18}\text{O}$	48
Figure 14: Effect of changes in $\delta(\text{Ar}/\text{O}_2)$ on the $\delta^{17}\text{O}$ and $\delta^{18}\text{O}$	48

Chapter 3

Figure 15: Schematic drawing of the small extraction line	62
Figure 16: $\delta^{17}\text{O}$ results of different transfer scenarios	65
Figure 17: $\delta^{18}\text{O}$ results of transfer tests.....	66
Figure 18: $\Delta^{17}\text{O}$ results of transfer tests	67
Figure 19: $\delta(\text{O}_2/\text{Ar})$ results of transfer tests	68

Chapter 4

Figure 20: $\delta^{17}\text{O}$ and $\delta^{18}\text{O}$ (vs. air) results of the air-equilibrated water tests.....	84
Figure 21: Average $\Delta^{17}\text{O}$ (0.5179, vs. air) results of the air-equilibrated water tests.....	85
Figure 22: Individual $\Delta^{17}\text{O}$ (vs. air) results of the air-equilibrated water tests	86
Figure 23: $\delta(\text{O}_2/\text{Ar})$ (vs. air) results of the air-equilibrated water tests	91

Chapter 5

Figure 24: Culture bottles in growth chamber	104
Figure 25: Schematic of the extraction line	105
Figure 26: Needle connected to the extraction line.....	108
Figure 27: Picture of the extraction line, just prior to sampling	109

Figure 28: $\Delta^{17}\text{O}$, $\delta(\text{O}_2/\text{Ar})$, $\delta^{17}\text{O}$ and $\delta^{18}\text{O}$ results for <i>E. huxleyi</i>	116
Figure 29: Average $\Delta^{17}\text{O}$ <i>Picochlorum</i> first sampling.....	119
Figure 30: <i>E. huxleyi</i> , $\Delta^{17}\text{O}$ results of different sample patterns.....	122
Figure 31: <i>E. huxleyi</i> , $\Delta^{17}\text{O}$ results of different sample patterns.....	123
Figure 32: $\delta^{18}\text{O}$ results of <i>E. huxleyi</i> different sample patterns	125
Figure 33: $\delta^{18}\text{O}$ results of <i>E. huxleyi</i> different sample patterns	126
Figure 34: $\delta(\text{O}_2/\text{Ar})$ results vs. air for all <i>E. huxleyi</i> series.....	127
Figure 35: Nitrogen content of <i>E.huxleyi</i> samples.....	128
Figure 36: Fluorescence results of trials in March.....	130
Figure 37: Fluorescence and Coulter Counter results of <i>E. huxleyi</i> June experiments..	130
Figure 38: Fluorescence results for <i>Picochlorum</i> (June-July)	131

Appendix

Figure 39: Effect of used definitions on $\Delta^{17}\text{O}$ <i>E. huxleyi</i>	158
Figure 40: Effect of used definitions on $\Delta^{17}\text{O}$ <i>Picochlorum</i>	158
Figure 41: Expected variations $\Delta^{17}\text{O}$ with f for <i>E. huxleyi</i>	159
Figure 42: Expected variations $\Delta^{17}\text{O}$ with f for <i>Nannochloropsis</i>	160
Figure 43: Expected variations $\Delta^{17}\text{O}$ with f for <i>E. huxleyi</i> with $^{18}\epsilon_{\text{R}} = -10$ and -30	160
Figure 44: Expected variations $\Delta^{17}\text{O}$ with f for <i>E. huxleyi</i> with $\gamma_{\text{R}} = 0.52$ and 0.5225 ...	160

Tables

Table 1: Results of performance tests of the separation line and mass spectrometer.....	52
Table 2: Overview of MSZ transfer test results and characteristics	70
Table 3: Results of injection experiments.....	71
Table 4: Overview of published air-equilibrated water experiment results.....	79
Table 5: Results of air-equilibrated water tests conducted at different temperatures and salinities	83
Table 6: Results of Eisenstadt et al. 2010, table adapted from Kaiser & Abe (2012)	98
Table 7: Adaptation of section of Table 3 from Kaiser and Abe (2012).	99
Table 8: Measurements of the triple oxygen isotope composition of VSMOW vs. air...	99
Table 9: Table 3 from Kaiser and Abe 2012.....	164
Table 10: Overview of all transfer test results and characteristics of the molecular sieve transfer tests (Chapter 3).....	164

Table of Contents

Acknowledgements.....	1
Abstract.....	3
List of figures and tables.....	4
Figures.....	4
Tables.....	5
Table of Contents.....	6
Chapter 1: Introduction.....	10
1.1 Aims of research and structure of the thesis.....	10
1.2 Motivation.....	10
1.3 Deriving gross oxygen production with the triple oxygen isotope method.....	11
1.3.1 Definition of ^{17}O excess ($\Delta^{17}\text{O}$).....	14
1.3.2 Calculation of GOP in the surface ocean.....	18
1.4 Advantages and problems of the triple isotope method.....	19
1.4.1 Advantages.....	19
1.4.2 Current uncertainties and debates in the literature.....	19
1.4.3 The triple isotopic composition of photosynthetic oxygen.....	20
1.4.4 The triple isotopic composition of dissolved oxygen at air saturation.....	21
Chapter 2: Methods.....	23
Abstract.....	23
2.1. Introduction.....	23
2.2. Extraction and preparation of gas samples.....	24
2.2.1. Extraction line.....	24
2.2.2. Separation line.....	30
2.2.3. Encountered problems.....	33
2.3. Isotope Ratio Mass Spectrometry.....	34

2.3.1 Description of instrument and IRMS measurements	34
2.3.2 Nitrogen, Argon and imbalance corrections	39
2.3.3 Standardisation with respect to atmospheric air.....	50
2.3.4 Calculation of ^{17}O excess	51
2.4. Reproducibility and performance tests of MS and separation line.....	51
 Chapter 3 – Method development and improvement: molecular sieve transfer tests	55
Abstract.....	55
3.1 Introduction.....	56
3.2 Methods	58
3.2.1 Description of transfer tests.....	58
3.2.2 Description of materials and extraction line	61
3.2.3 Description of procedure.....	62
3.3 Results.....	64
3.3.1 $\delta^{17}\text{O}$ and $\delta^{18}\text{O}$ results	64
3.3.2 $\Delta^{17}\text{O}$	68
3.3.3 $\delta(\text{O}_2/\text{Ar})$	69
3.3.4 Freezing times and additional data.....	70
3.4.1 Summary of results.....	72
3.4 Discussion and conclusions	73
3.4.1 Discussion	73
3.4.2 Conclusions	77
 Chapter 4: The triple isotopic composition of dissolved oxygen at air saturation.....	78
Abstract.....	78
4.1 Introduction.....	78
4.2 Methods	80

4.2.1 Preparation of air-equilibrated water.....	80
4.2.2 Gas extraction and preparation.....	81
4.2.3 IRMS measurements	82
4.3 Results.....	83
4.4 Discussion.....	85
4.4.1 $\Delta^{17}\text{O}$ results compared to previous results.....	85
4.4.2 $\delta^{18}\text{O}$ results compared to previous results	87
4.4.3 $\delta(\text{O}_2/\text{Ar})$ results compared to previous results	89
4.5 Conclusions.....	91
Chapter 5: The isotopic signature of photosynthetic oxygen.....	93
Abstract.....	93
5.1 Introduction.....	94
5.2 Methods	100
5.2.1 Goals and summary methods	100
5.2.2 Phytoplankton culturing	101
5.2.3 Sampling procedure.....	104
5.2.4 Gas preparation and IRMS measurements	110
5.2.5 Initial trials and sampling strategy	114
5.3 Results.....	116
5.3.1 First time sampling (new bottles).....	116
5.3.2 <i>E. huxleyi</i> different sample series.....	122
5.3.3 Additional results ($\delta(\text{O}_2/\text{Ar})$, $d(\text{N}_2/\text{O}_2)$)	127
5.3.4 Fluorescence and Coulter Counter results.....	130
5.3.5 Variability in results	132
5.4 Discussion.....	133

5.4.1 Introduction: overview results.....	133
5.4.2 Steady state.....	134
5.4.3 Comparison results to values from literature (Luz and Barkan 2000, Kaiser and Abe 2012).....	138
5.4.4 Additional considerations.....	142
5.5 Conclusions.....	146
Bibliography.....	147
Appendix.....	158

Chapter 1: Introduction

1.1 Aims of research and structure of the thesis

In this chapter, first, an introduction will be given to the triple oxygen isotope method for estimating gross oxygen production and its advantages over other methods. Secondly, uncertainties of the method will be discussed, including wind speed-based parameterisations of gas exchange coefficients, respiration triple isotope coefficients and the triple oxygen isotopic composition of biological and air-saturated dissolved O₂ end-members.

Chapter 2 focuses on the methodology of extraction and preparation of gas samples for triple oxygen isotope analysis, and the subsequent analysis of these gas samples using isotope ratio mass spectrometry.

Chapter 3 is dedicated to method development of transfer of gas samples using molecular sieves, to improve the efficiency of the current sample processing method in the U.E.A. Stable Isotope Lab.

Chapter 4 concerns air-equilibrated water experiments at different temperatures and salinities, conducted in order to obtain more information on the triple isotopic signature of dissolved oxygen at air saturation, one of the two end-members in the derivation of gross oxygen productivity using triple oxygen isotopes (isotopic signature of dissolved oxygen at air saturation).

In Chapter 5, results are described from laboratory batch culture experiments conducted to determine the triple isotope composition of oxygen produced by two different phytoplankton species, *Emiliana huxleyi* and *Picochlorum* (isotopic signature of biological oxygen).

1.2 Motivation

Despite its relatively small biomass, marine phytoplankton is responsible for nearly half of global primary production and carbon fixation (Field 1998). This makes the oceans an important sink of anthropogenic, mostly fossil fuel-derived CO₂, but the exact amount of carbon fixed by marine organisms and the metabolic balance of large areas of the oceans are still debated (Ducklow & Doney 2013, Duarte et al. 2013, Williams et al. 2013). Most current methods to estimate gross primary production and net carbon fixation (including satellite remote sensing and global carbon budgets) are calibrated using data from ¹⁴C, H₂¹⁸O or light-dark O₂ bottle incubations, which have been reported to

sometimes underestimate, sometimes overestimate, primary production, and which are subject to containment effects.

Incubation-independent in situ methods to derive oceanic productivity, including fast repetition rate fluorometry (FRRF) and the use of triple O₂ isotopes (Juranek and Quay 2013), can help trace potential biases in incubation results and evaluate satellite-based estimates, and – due to the ease of sample collection – provide information over larger spatial and temporal scales and give more insight into marine biological carbon fixation and cycling.

1.3 Deriving gross oxygen production with the triple oxygen isotope method

Luz and Barkan (2000) developed a method to estimate oceanic productivity using the triple-oxygen isotope composition (¹⁸O/¹⁶O and ¹⁷O/¹⁶O) of oxygen dissolved in seawater. This method is based on the knowledge that atmospheric O₂ has a different triple oxygen isotopic composition from biologically produced and respired O₂. The reason for this difference is that terrestrial processes generally fractionate oxygen in a mass-dependent way: for a given enrichment in ¹⁸O over ¹⁶O, ¹⁷O is enriched approximately 0.52 times as much, relative to ¹⁶O. As a result, $\delta^{17}\text{O}$ and $\delta^{18}\text{O}$ (where $\delta^x\text{O} = \frac{R_{\text{sample}}}{R_{\text{reference}}} - 1$; R is the ^xO/¹⁶O abundance ratio and $x = 17, 18$) of mass-dependently fractionated oxygen can be plotted along a line with a slope of about 0.52 ($\delta^{17}\text{O} \approx 0.52 \delta^{18}\text{O}$) (Matsuhisa et al. 1978, Young et al. 2002, Kaiser et al. 2004).

Due to non-mass-dependent photochemical isotope exchange reactions in the stratosphere involving O₂, O₃ and CO₂, which remove more ¹⁷O from O₂ relative to ¹⁸O than would be expected for mass-dependent fractionation (relationship 1 to 1.7 instead of 0.52) (Thiemens et al. 1995, Yung et al. 1997, Lämmerzahl et al. 2002), atmospheric O₂ is depleted in ¹⁷O/¹⁶O relative to ¹⁸O/¹⁶O compared to O₂ that is produced mass-dependently/biologically (Bender et al. 1994, Luz et al. 1999).

In order to describe the relationship between $\delta^{17}\text{O}$ and $\delta^{18}\text{O}$ and express the deviation from mass-dependent fractionation, the ¹⁷O 'anomaly' or 'excess' can be defined as $\Delta^{17}\text{O} = \delta^{17}\text{O} - \lambda \delta^{18}\text{O}$, where $\lambda \approx 0.52$. Other values of λ between 0.5 and 0.53 may also be adopted, depending on the mass-dependent process under consideration (Matsuhisa et al. 1978, Young et al. 2002, Angert et al. 2003, Kaiser et al. 2004, Helman et al. 2005, Luz and Barkan 2005). This definition is based on a linear approximation of the non-linear mass-dependent fractionation law $^{17}\alpha = ^{18}\alpha^\lambda$, with fractionation factor $^x\alpha = \frac{R_a}{R_b}$ where R is the ^xO/¹⁶O abundance ratio, 'a' and 'b' are two compounds at equilibrium or a product and substrate affected by the same mass-dependent fractionation process

(Young et al. 2002, Miller 2002, Kaiser et al. 2004, Blunier et al. 2002). Instead of this linear approximation, Miller (2002) suggested a logarithmic definition based on the more accurate power-relationship between $\delta^{17}\text{O}$ and $\delta^{18}\text{O}$ ($\Delta^{17}\text{O} \approx \ln(\delta^{17}\text{O} + 1) - \lambda \ln(\delta^{18}\text{O} + 1)$) (Miller 2002, Kaiser et al. 2004, **Section 1.3.1**).

Different definitions of $\Delta^{17}\text{O}$ and corresponding λ values have been used over the past years (Kaiser 2011, Section 1.3.1). Here the kinetic fractionation slope (γ_{R}) of respiration (0.5179) is used, as respiration is the most widespread O_2 consuming process and setting $\lambda = \gamma_{\text{R}}$ makes the resulting $\Delta^{17}\text{O}$ insensitive to the effect of respiration. In 2005, Luz and Barkan found an average γ_{R} of 0.5179 ± 0.0006 for respiration for a wide range of organisms and experimental conditions (Barkan and Luz 2005), this value has since then been adopted for λ in most studies involving dissolved oxygen (Kaiser 2011). $\Delta^{17}\text{O}$ is generally small ($< 1 \text{ ‰}$), and therefore reported in parts per million (ppm). In the triple isotope study of molecular oxygen, air O_2 is generally taken as the reference (Luz & Barkan 2005).

Oxygen in the surface ocean mixed layer has two main sources, introduction from the atmosphere through air-sea gas exchange, and biological O_2 production (photosynthesis, O_2 production through water splitting). Due to the relative $^{17}\text{O}/^{16}\text{O}$ depletion in the atmosphere, oxygen from these two sources has a distinctly different triple isotopic composition. Depending on the relative contribution from each source, the triple isotopic composition of oxygen dissolved in the surface mixed layer will vary between the compositions of these two 'end members' (**Figure 1**).

When the triple isotopic composition of both atmospherically introduced oxygen and biologically produced oxygen is known, and the rate of O_2 exchange with the atmosphere is known, the rate of biological gross O_2 production (GOP), integrated over the depth of the mixed layer and the residence time of O_2 in the mixed layer, can be derived from the triple isotope composition of dissolved oxygen, using a simple mass balance, neglecting vertical mixing with deeper waters and fractionation during gas exchange, and assuming oxygen concentrations and the ^{17}O excess of dissolved O_2 , $\Delta^{17}\text{O}_{\text{dis}}$, to be at steady state (Luz & Barkan 2000):

$$GOP \approx k[\text{O}_2]_{\text{sat}} \frac{\Delta^{17}\text{O}_{\text{dis}} - \Delta^{17}\text{O}_{\text{sat}}}{\Delta^{17}\text{O}_{\text{bio}} - \Delta^{17}\text{O}_{\text{dis}}}$$

where $[\text{O}_2]_{\text{sat}}$ is the dissolved O_2 concentration at air saturation, k is the gas-exchange coefficient (based on wind-speed parameterisations (Wanninkhof 1992, Ho et al. 2006, Juranek & Quay 2010)), $\Delta^{17}\text{O}_{\text{sat}}$ is the ^{17}O excess of dissolved oxygen at air saturation and $\Delta^{17}\text{O}_{\text{bio}}$ is the ^{17}O excess of biological oxygen.

Experiments performed by Barkan and Luz in 2000, yielded a $\Delta^{17}\text{O}$ (calculated using $\delta^{17}\text{O} - 0.521 \delta^{18}\text{O}$) of (16 ± 2) ppm for oxygen at air saturation and (249 ± 15) ppm for biological oxygen (obtained from steady-state experiments with cultures of *Acropora* and *Nannochloropsis*). These values have since then been used for $\Delta^{17}\text{O}_{\text{sat}}$ and $\Delta^{17}\text{O}_{\text{bio}}$ in most studies.

The dissolved O_2 concentration, $[\text{O}_2]$, is affected by biological as well as physical processes (temperature changes, atmospheric pressure changes, bubble injection). Because argon has a similar solubility to O_2 and is affected by physical processes in a similar way, but does not have biological sources or sinks, the O_2/Ar ratio can be used to express the 'biological oxygen saturation', which can be used to estimate mixed-layer net community oxygen production (*NOP*) (assuming steady-state and no vertical/horizontal mixing) (Craig & Hayward 1987, Quay et al. 1993, Barkan & Luz 2002, Hendricks et al 2004, Kaiser et al 2005, Barkan & Luz 2009):

$$\left(\frac{[\text{O}_2]}{[\text{O}_2]_{\text{sat}}}\right)_{\text{bio}} = \frac{([\text{O}_2]/[\text{Ar}])}{([\text{O}_2]_{\text{sat}}/[\text{Ar}]_{\text{sat}})} = \frac{\delta(\text{O}_2/\text{Ar}) + 1}{\delta(\text{O}_2/\text{Ar})_{\text{sat}} + 1}$$

$$NOP = k[\text{O}_2]_{\text{sat}} \left(\left(\frac{[\text{O}_2]}{[\text{O}_2]_{\text{sat}}} \right)_{\text{bio}} - 1 \right)$$

NOP is the rate of net (community) oxygen production and $\left(\left(\frac{[\text{O}_2]}{[\text{O}_2]_{\text{sat}}} \right)_{\text{bio}} - 1 \right)$ is the 'biological oxygen supersaturation', the oxygen supersaturation in excess of argon supersaturation.

$$\delta(\text{O}_2/\text{Ar}) = \frac{(\text{O}_2/\text{Ar})_{\text{sam}}}{(\text{O}_2/\text{Ar})_{\text{ref}}} - 1$$

Gas exchange coefficient k is based on wind-speed parameterisations (Wanninkhof 1992, Ho et al. 2006) and relatively uncertain. However when $f = NOP/GOP$ (the ratio of net over gross O_2 production) is calculated, k cancels from the calculation, providing an estimate of the metabolic state of the marine biological ecosystem:

$$f = NOP/GOP = \left(\left(\frac{[\text{O}_2]}{[\text{O}_2]_{\text{sat}}} \right)_{\text{bio}} - 1 \right) \frac{\Delta^{17}\text{O}_{\text{bio}} - \Delta^{17}\text{O}_{\text{dis}}}{\Delta^{17}\text{O}_{\text{dis}} - \Delta^{17}\text{O}_{\text{sat}}}$$

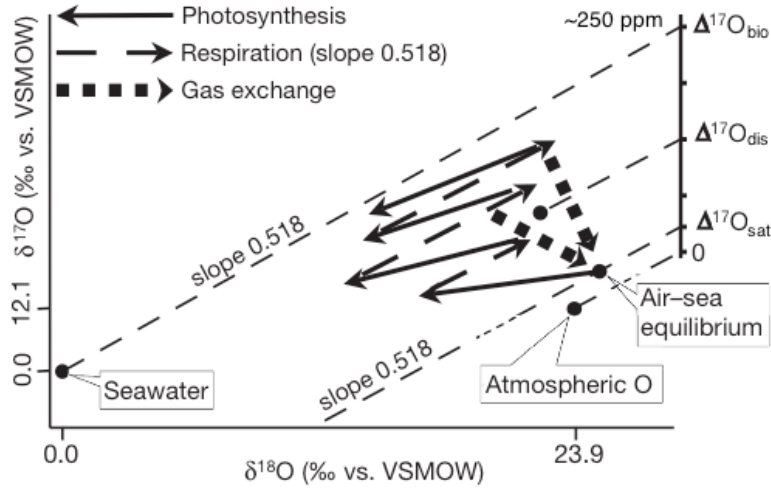


Figure 1: Triple isotope plot (not to scale and simplified), illustrating the idea behind the use of triple oxygen isotopes to derive marine productivity. Biological oxygen is produced with a composition close to that of the substrate water (which has a positive $\Delta^{17}\text{O}$ and negative $\delta^{17}\text{O}$ and $\delta^{18}\text{O}$ values with respect to atmospheric oxygen $\Delta^{17}\text{O} = \sim 250$ ppm, $\delta^{18}\text{O} = \sim 23\text{‰}$). Respiration discriminates against ^{17}O and ^{18}O and increases the $\delta^{17}\text{O}$ and $\delta^{18}\text{O}$ values (along a slope of ~ 0.518), but does not significantly change the $\Delta^{17}\text{O}$, because this effect is accounted for in the calculation of $\Delta^{17}\text{O}$ (with λ set equal to ~ 0.518). Air-sea gas exchange introduces oxygen with a $\Delta^{17}\text{O}$ of ~ 0 (in reality, the $\Delta^{17}\text{O}$ of dissolved O_2 at air saturation in the absence of biological productivity is slightly higher (8-17 ppm) due to fractionation during invasion and evasion). Depending on the relative rates of air-sea gas exchange and biological O_2 production, the $\Delta^{17}\text{O}$ of dissolved oxygen in the mixed layer is thus expected to vary between ~ 0 and ~ 250 ppm. Figure adapted from Luz and Barkan (2009).

1.3.1 Definition of ^{17}O excess ($\Delta^{17}\text{O}$)

For both kinetic and equilibrium mass-dependent fractionation, the following relationship (fractionation law) applies between fractionation factors or isotope ratios

$$\frac{{}^{17}R_a}{{}^{17}R_b} = (1 + K) \left(\frac{{}^{18}R_a}{{}^{18}R_b} \right)^\lambda$$

where xR is the ratio of the abundance of ${}^x\text{O}$ ($x = 17$ or 18) over ${}^{16}\text{O}$, 'a' and 'b' are two compounds affected by the same fractionation process and K is a measure of the offset between 'a' and the mass-dependent fractionation (MDF) curve on which 'b' lies (Young et al. 2002, Blunier et al. 2002). When 'a' and 'b' plot on the same MDF line on a three-isotope plot, the offset K is 0. λ is close to 0.52 but its actual value depends on the fractionation process under consideration (Kaiser et al. 2004; Young et al. 2002; Matsuhisa et al. 1978).

For equilibrium isotope exchange, $\lambda = \frac{\frac{1}{m_1} - \frac{1}{m_2}}{\frac{1}{m_1} - \frac{1}{m_3}}$, where $m_{1,3}$ are atomic masses and $m_1 < m_2$

$< m_3$ (Young et al. 2002, Blunier et al. 2002). For kinetic isotope fractionation,

$$\lambda = \frac{\ln\left(\frac{m_2}{m_1}\right)}{\ln\left(\frac{m_3}{m_1}\right)}$$

Using the definition of the fractionation factor

$${}^x\alpha = \frac{{}^xR_a}{{}^xR_b}$$

where x is 17 or 18, the above equation can also be written as

$${}^{17}\alpha = (1 + K)({}^{18}\alpha)^\lambda$$

The fractionation factor is generally close to 1. Therefore, a related quantity defined as

$${}^x\varepsilon = {}^x\alpha - 1$$

is often used. It is called 'fractionation constant', 'discrimination', 'fractionation' or 'isotope effect'. It gives an indication of the resulting change or difference in $\delta^x\text{O}$ between 'a' and 'b', due to a certain fractionation process.

When 'a' and 'b' plot on the same MDF line on a three-isotope plot, the offset K is 0 and the fractionation law becomes

$$\frac{{}^{17}R_a}{{}^{17}R_b} = \left(\frac{{}^{18}R_a}{{}^{18}R_b}\right)^\lambda$$

In δ -notation this gives

$$(\delta^{17}\text{O} + 1) = (\delta^{18}\text{O} + 1)^\lambda,$$

so, the fractionation curve in a plot of $\delta^{17}\text{O}$ against $\delta^{18}\text{O}$ is given by

$$\delta^{17}\text{O} = (\delta^{18}\text{O} + 1)^\lambda - 1$$

As can be observed, this curve is not linear.

However, when taking the natural logarithm and using δ -notation, the above-described fractionation law (with '1 + K ' term) becomes

$$\ln(\delta^{17}\text{O} + 1) = \ln(1 + K) + \lambda \ln(\delta^{18}\text{O} + 1)$$

So, λ is the slope of the line on a $\ln(\delta^{17}\text{O} + 1)$ vs. $\ln(\delta^{18}\text{O} + 1)$ plot and $\ln(1 + K)$ is the intercept with the y-axis. A deviation from mass-dependent fractionation can thus be observed as a deviation from a line with slope 0.52, resulting in $\ln(1 + K) \neq 0$.

Miller (2002) proposed to define the deviation from MDF (^{17}O anomaly or excess) as

$$\ln(1 + \Delta^{17}\text{O}) = \ln(1 + K) = \ln(\delta^{17}\text{O} + 1) - \lambda \ln(\delta^{18}\text{O} + 1)$$

where, for $K \ll 1$,

$$\Delta^{17}\text{O} = K \approx \ln(1 + K) = \ln(\delta^{17}\text{O} + 1) - \lambda \ln(\delta^{18}\text{O} + 1)$$

Through Taylor expansion the following approximation can be obtained

$$\Delta^{17}\text{O} = \delta^{17}\text{O} - \lambda' \delta^{18}\text{O}$$

However, in contrast to λ , λ' (the local slope in a $\delta^{17}\text{O}$ vs. $\delta^{18}\text{O}$ plot) is not constant but a function of $\delta^{18}\text{O}$, and thus dependent on the underlying isotopic composition and the reference used. When a constant value is inserted for λ' , this can yield non-zero $\Delta^{17}\text{O}$ values for MDF processes with $\lambda = 0.52$, since λ' is actually more closely estimated by

$$\lambda \left(1 - \frac{(1 - \lambda) \delta^{18}\text{O}}{2} \right)$$

which includes the second-order term in the Taylor series (Kaiser et al. 2004).

If the linearised approximation, $\Delta^{17}\text{O} = \delta^{17}\text{O} - \lambda \delta^{18}\text{O}$, is adopted as $\Delta^{17}\text{O}$ definition, this gives approximately the same result as the logarithmic definition for $\delta^{18}\text{O}$ values close to zero. However, already when $\delta^{18}\text{O} = -20\text{‰}$, the resulting difference in $\Delta^{17}\text{O}$ is 50 ppm (Clayton & Mayeda 1996, Miller 2002, Kaiser et al. 2004).

$\Delta^{17}\text{O}$ has been defined in various ways by different authors, using different slopes for the reference mass-dependent fractionation line (λ). The most commonly used definition of $\Delta^{17}\text{O}$ is now the logarithmic formula ($\Delta^{17}\text{O} = \ln(\delta^{17}\text{O} + 1) - \lambda \ln(\delta^{18}\text{O} + 1)$) with a reference slope of $\lambda = 0.5179$ (which corresponds to the ratio between fractionation of ^{17}O and ^{18}O in the most common respiration processes in a wide range of marine organisms) (Miller 2002, Angert et al. 2003, Luz and Barkan 2005, Kaiser 2011). However, which λ is most suited to eliminate effects of respiration from $\Delta^{17}\text{O}$ in a certain situation, depends on the process of fractionation under consideration.

As shown by Angert et al. (2003), for equilibrium fractionation processes $\ln(\delta^{17}\text{O} + 1)$ and $\ln(\delta^{18}\text{O} + 1)$ evolve along a slope of

$$\lambda = \theta = \frac{\ln(^{17}\alpha)}{\ln(^{18}\alpha)}$$

For systems at biological steady-state specifically, $\lambda = \theta_{\text{R}} = \ln(^{17}\alpha_{\text{R}})/\ln(^{18}\alpha_{\text{R}})$, where 'R' stands for respiration. If this λ value is used in the calculation of $\Delta^{17}\text{O}$ using the 'ln' definition, respiration does not change $\Delta^{17}\text{O}$. Partly for this reason, Angert et al. (2003) and Luz & Barkan (2011) recommend using the 'ln' definition. However, because of the non-linearity of this definition, it is less suitable for use in the approximated calculation of *GOP* and leads to larger errors when used in this calculation (Kaiser & Abe 2012 and Prokopenko et al. 2011).

In systems with uptake only, $\ln(\delta^{17}\text{O} + 1)$ and $\ln(\delta^{18}\text{O} + 1)$ evolve along a different slope (Angert et al. 2003, Luz & Barkan 2005, Kaiser 2011).

For one-way, Rayleigh fractionation the following relationship applies:

$$\frac{{}^xR}{{}^xR_0} = \left(\frac{c}{c_0}\right)^{x\varepsilon}$$

where x can be 17 or 18, xR_0 is the initial ratio of either ^{17}O or ^{18}O over ^{16}O , and c/c_0 is the remaining O_2 fraction. Taking the natural logarithm and using delta-notation gives

$$\ln(\delta^x\text{O} + 1) = x\varepsilon \ln\left(\frac{c}{c_0}\right)$$

So, for kinetic fractionation, the local slope in a $\ln(\delta^{17}\text{O} + 1)$ vs. $\ln(\delta^{18}\text{O} + 1)$ plot is given by

$$\lambda = \gamma = \ln(\delta^{17}\text{O} + 1) / \ln(\delta^{18}\text{O} + 1) = {}^{17}\varepsilon / {}^{18}\varepsilon$$

λ In case of Rayleigh fractionation is therefore equal to $\gamma = {}^{17}\varepsilon / {}^{18}\varepsilon$. For a biological system with uptake only, $\lambda = \gamma_R = {}^{17}\varepsilon_R / {}^{18}\varepsilon_R$, where ‘R’ stands for respiration (Angert et al. 2003).

Even though a definition of $\Delta^{17}\text{O}$ with $\lambda = 0.5179$ is often chosen so that $\Delta^{17}\text{O}$ is not changed by respiration, the triple isotopic composition of photosynthetic oxygen, in the absence of any respiration, is generally not equal to that of biological oxygen in a system with both production and respiration. The $\delta^x\text{O}$ of photosynthetic O_2 with respect to air- O_2 ($\delta^x\text{O}_p$) can be calculated as follows:

$$\delta^x\text{O}_p = (1 + \delta^x\text{O}_w)(1 + {}^x\varepsilon_p) - 1$$

where $\delta^x\text{O}_w$ is the $\delta^x\text{O}$ of the source water relative to air- O_2 , ${}^x\varepsilon_p$ is the photosynthetic isotope fractionation and x refers to 17 or 18 (Kaiser and Abe 2012). $\delta^x\text{O}$ of oxygen (at isotopic steady state) under conditions of both photosynthesis and respiration can be calculated as

$$\delta^x\text{O} = \frac{\delta^x\text{O}_p - (1 - f)^x\varepsilon_R}{1 + (1 - f)^x\varepsilon_R}$$

where ${}^x\varepsilon_R$ is the respiratory isotope effect, x is 17 or 18 and f is the ratio of net to gross production. It can be observed the $\delta^x\text{O}$ is dependent on f , ${}^{18}\varepsilon_R$ and γ_R ($\gamma_R = {}^{17}\varepsilon_R / {}^{18}\varepsilon_R$, where ‘R’ stands for respiration). At biological or concentration steady state (S0), the net to gross production ratio f is zero, so

$$\delta\text{O}_{S0} = \frac{\delta^x\text{O}_p - {}^x\varepsilon_R}{1 + {}^x\varepsilon_R}$$

As a result, the $\Delta^{17}\text{O}$ of oxygen at steady state between respiration and photosynthesis is generally not equal to the $\Delta^{17}\text{O}$ of photosynthetic oxygen.

As shown by various authors (Angert et al. 2003, Kaiser 2011, Nicholson 2011, Kaiser & Abe 2012),

$$\Delta^{17}\text{O}_{\text{s0}(\ln)} = \Delta^{17}\text{O}_{\text{P}(\ln)} - \ln(1 + {}^{17}\varepsilon_{\text{R}}) + \lambda \ln(1 + {}^{18}\varepsilon_{\text{R}})$$

So, $\Delta^{17}\text{O}_{\text{S0}}$ is only equal to $\Delta^{17}\text{O}_{\text{P}}$ if the ‘ln’ definition is used with λ equal to

$$\theta_{\text{R}} = \frac{\ln({}^{17}\alpha_{\text{R}})}{\ln({}^{18}\alpha_{\text{R}})} = \frac{\ln(1 + {}^{17}\varepsilon_{\text{R}})}{\ln(1 + {}^{18}\varepsilon_{\text{R}})} = \frac{\ln(1 + \gamma_{\text{R}} {}^{18}\varepsilon_{\text{R}})}{\ln(1 + {}^{18}\varepsilon_{\text{R}})}$$

Barkan and Luz (2005, 2011) and Nicholson (2011) therefore propose using a λ of 0.5154 for systems at biological steady-state, which is equal to θ calculated using a γ_{R} of 0.5179 and ${}^{18}\varepsilon_{\text{R}}$ of -20‰ (values associated with average dark respiration). However, this only works when the exact ${}^{18}\varepsilon_{\text{R}}$ and γ_{R} of the involved processes are known, and ${}^{18}\varepsilon_{\text{R}}$ varies between processes and organisms and is generally not as well constrained as γ_{R} . In addition, in nature f is seldom equal to zero.

Barkan and Luz (2005) state that the kinetic respiratory slope $\gamma_{\text{R}} = {}^{17}\varepsilon_{\text{R}}/{}^{18}\varepsilon_{\text{R}} = 0.5179$ should be used not only for respiration only systems, but also for dissolved O_2 (because it produces better results when $f \neq 0$, i.e. under variable light/quasi-steady state conditions, while the steady-state respiratory slope θ (0.5154 for average dark respiration) should be used for steady-state systems, including atmospheric oxygen (both: with a logarithmic $\Delta^{17}\text{O}$ definition).

1.3.2 Calculation of *GOP* in the surface ocean

Use of different definitions of $\Delta^{17}\text{O}$ in combination with different λ values in the past makes it difficult to compare and correctly interpret resulting *GOP* values. Therefore it has been recently suggested to calculate *GOP* directly from the measured $\delta^{17}\text{O}$ and $\delta^{18}\text{O}$ instead of the approximated $\Delta^{17}\text{O}$ (Kaiser 2011; Prokopenko et al. 2011). Because this method does not involve approximations it gives more accurate results and has now been widely accepted as the preferred method to calculate *GOP*.

$$g = \frac{GOP}{k[\text{O}_2]_{\text{sat}}} = \frac{(1 + {}^{17}\varepsilon_{\text{E}}) \frac{{}^{17}\delta - {}^{17}\delta_{\text{sat}}}{1 + {}^{17}\delta} - \gamma_{\text{R}}(1 + {}^{18}\varepsilon_{\text{E}}) \frac{{}^{18}\delta - {}^{18}\delta_{\text{sat}}}{1 + {}^{18}\delta} + s({}^{17}\varepsilon_{\text{E}} - \gamma_{\text{R}} {}^{18}\varepsilon_{\text{E}})}{\frac{{}^{17}\delta_{\text{P}} - {}^{17}\delta}{1 + {}^{17}\delta} - \gamma_{\text{R}} \frac{{}^{18}\delta_{\text{P}} - {}^{18}\delta}{1 + {}^{18}\delta}}$$

Where g is the ratio of gross production to gross air invasion, *GOP* is the gross oxygen production, ${}^{17}\delta$ and ${}^{18}\delta$ are $\delta^{17}\text{O}$ and $\delta^{18}\text{O}$ of dissolved O_2 with respect to air- O_2 , ${}^{17}\delta_{\text{sat}}$ and ${}^{18}\delta_{\text{sat}}$ are the $\delta^{17}\text{O}$ and $\delta^{18}\text{O}$ of dissolved O_2 at air saturation, ${}^{17}\delta_{\text{P}}$ and ${}^{18}\delta_{\text{P}}$ are the $\delta^{17}\text{O}$ and $\delta^{18}\text{O}$ of photosynthetic oxygen, ε_{E} is the kinetic fractionation during evasion from sea to air, s is the relative supersaturation of dissolved O_2 ($s = c/c_{\text{sat}} - 1$, where $c = [\text{O}_2]$,

the dissolved O₂ concentration), and k and $[\text{O}_2]_{\text{sat}}$ are the gas exchange coefficient and dissolved oxygen concentration at air-saturation (Kaiser 2011).

When you do not take into account isotopic fractionation during invasion and evasion, the equation becomes identical to the one suggested by Prokopenko et al. (2011):

$$g = \frac{\frac{^{17}\delta - ^{17}\delta_{\text{sat}}}{1 + ^{17}\delta} - \gamma_{\text{R}} \frac{^{18}\delta - ^{18}\delta_{\text{sat}}}{1 + ^{18}\delta}}{\frac{^{17}\delta_{\text{p}} - ^{17}\delta}{1 + ^{17}\delta} - \gamma_{\text{R}} \frac{^{18}\delta_{\text{p}} - ^{18}\delta}{1 + ^{18}\delta}}$$

1.4 Advantages and problems of the triple isotope method

1.4.1 Advantages

This method has since 2000 been applied in the determination of *GOP* for several oceans (Barkan & Luz 2000, 2011; Hendricks et al. 2004, 2005, Sarma et al. 2005, 2006, Juranek & Quay et al. 2005, 2010, 2012, 2013, Reuer et al. 2007). Compared to traditional methods, it has the important advantage that it eliminates containment artifacts associated with bottle incubations, and that it provides the *GOP* integrated over a timescale of weeks (the residence time of O₂ in the mixed layer), as a result of which the temporal heterogeneity in algal productivity (episodic pulses of productivity, blooms) is better captured than through traditional, nearly-instantaneous methods. In addition, surface seawater samples required for triple oxygen isotope analysis can be very easily collected on many different ships, including commercial cargo ships of opportunity, which makes it possible to collect samples over much larger areas, including parts of the ocean that are difficult to access and for which data on biological production are sparse, and at higher spatial and temporal resolution. Finally, it provides an independent measure of *GOP*, which can be used to evaluate data derived from bottle incubations and satellite productivity algorithms (Juranek & Quay 2013).

1.4.2 Current uncertainties and debates in the literature

Uncertainty exists around the gas exchange coefficient k (which is estimated based on wind-speed parameterisations and introduces a relatively large error to the calculation of *GOP*, but can be eliminated from the results by calculating f (Wanninkhof 1992, Ho et al. 2006, Juranek & Quay 2010, Section 1.3)), and neglecting the effects of entrainment, upwelling, horizontal/vertical transport/mixing/advection (Hendricks et al. 2005, Juranek & Quay 2010, Castro-Morales et al. 2013; Nicholson et al. 2014). Furthermore, the method does not measure production below the mixed layer and assumes steady state

if applied in its simplest form. In $GOP(^{17}\text{O})$ studies over the past years, several alterations and additions have therefore been made to the method described in Section 1.3, for instance in order to include the effects of upwelling, vertical mixing or time rate of change (Hendricks et al. 2005, Juranek & Quay 2010, Castro-Morales et al. 2013; Nicholson et al. 2014).

Finally, as explained above, two parameters are crucial for the derivation of GOP :

- The isotopic signature of dissolved O_2 at saturation ($\Delta^{17}\text{O}_{\text{sat}}, \delta^{17}\text{O}_{\text{sat}}, \delta^{18}\text{O}_{\text{sat}}$)
- The isotopic signature of biological oxygen ($\Delta^{17}\text{O}_{\text{bio}}, \delta^{17}\text{O}_{\text{bio}}, \delta^{18}\text{O}_{\text{bio}}$)

The $\Delta^{17}\text{O}$ of dissolved oxygen in the surface mixed layer fluctuates between these two extremes, depending on the relative rate of air-sea gas exchange and biological oxygen production. Therefore, for the correct assessment of gross oxygen production using triple O_2 isotopes, next to accurate determination of the rate of air-sea gas exchange, accurate knowledge of the triple O_2 composition of biological O_2 and dissolved O_2 at air saturation, is crucial. However, there is still a lot of uncertainty concerning the exact value of both of these end-members.

Different laboratories are not in agreement on the value of $\Delta^{17}\text{O}_{\text{sat}}$ and reported values range between 8 and 18 ppm (Kaiser 2011). One study indicated temperature dependence, but other data of $\Delta^{17}\text{O}_{\text{sat}}$ at temperatures other than room temperature are sparse and should be independently re-measured (Barkan & Luz 2009, Stanley et al. 2010, Kaiser 2011) (**Section 1.4.4**). In the case of $\Delta^{17}\text{O}_{\text{bio}}$, most studies use 249 ppm, obtained from one study with two biological species (Barkan & Luz 2000) of which $\delta^{17}\text{O}$ and $\delta^{18}\text{O}$ values were not preserved. While it was previously assumed the $\Delta^{17}\text{O}$ of photosynthetic oxygen was approximately equal to the $\Delta^{17}\text{O}$ of water used in its production, a recent study indicated photosynthetic fractionation and a species-specific $\Delta^{17}\text{O}_{\text{bio}}$ (Eisenstadt et al. 2010). $\Delta^{17}\text{O}_{\text{bio}}$ estimates based on the isotopic composition of ocean water and the photosynthetic isotopic fractionation reported by Eisenstadt et al. (2010) may not agree with the value derived by Barkan & Luz (2000), depending on the correct triple oxygen isotope composition of VSMOW (Vienna Standard Mean Ocean Water) versus air- O_2 , which is currently being debated (Kaiser & Abe 2012) (**Section 1.4.3**). In both cases, more experiments are needed.

1.4.3 The triple isotopic composition of photosynthetic oxygen

For the triple O_2 isotopic composition of biological O_2 ($\Delta^{17}\text{O}_{\text{bio}}$), there are only limited experimental data available, originating from two sets of experiments by one research group (Luz and Barkan 2000, Eisenstadt et al. 2010). While it was previously assumed

that photosynthetic O₂ would be approximately equal in composition to the source water (Guy et al. 1993, Helman et al. 2005, Tcherkez & Farquhar 2007), recently conducted experiments indicated isotopic fractionation between H₂O and O₂ during photosynthesis, possibly related to O₂ consumption close to the site of water splitting, with the degree of fractionation differing between species (Eisenstadt et al. 2010). This would make the resulting $\Delta^{17}\text{O}_{\text{bio}}$ a combination of the triple-isotope composition of the source water and a species-specific addition due to photosynthetic fractionation. Unfortunately, information regarding this potential fractionation is only available from one set of experiments with a limited number of species (Eisenstadt et al. 2010). The other original sources of information on $\Delta^{17}\text{O}_{\text{bio}}$ are steady-state culture experiments conducted by Luz & Barkan in 2000 (Luz et al. 1999, Luz and Barkan 2000), in which plants, corals and algae were allowed to produce and consume O₂ in airtight flasks and the triple isotope composition of the resulting O₂ was determined. These experiments yielded the currently widely used value for marine $\Delta^{17}\text{O}_{\text{bio}}$ of 249 ppm, but were only conducted with ‘two’ species (coral *Acropora* with symbiotic algae, and alga *Nannochloropsis*) and results have since then not been reproduced.

In order to obtain more information on the $\Delta^{17}\text{O}_{\text{bio}}$ at steady state for different species, experiments were conducted with two marine phytoplankton species, coccolithophore *E. huxleyi* and green alga *Picochlorum* sp., growing cultures in airtight flasks and sampling the headspace gas for triple O₂ isotope analysis, after allowing accumulation and recycling of oxygen for several days (**Chapter 5**).

1.4.4 The triple isotopic composition of dissolved oxygen at air saturation

As explained in **Section 1.3**, the triple isotopic composition of dissolved oxygen in equilibrium with air (at air saturation) in the absence of any biological activity is not zero (when the composition of air-O₂ is taken as reference) due to fractionation during invasion and evasion. Initially, a $\Delta^{17}\text{O}_{\text{sat}}$ value of 16 ppm was reported, based on air-equilibrated water experiments (Luz & Barkan 2000). A value of 16-18 ppm was confirmed by several subsequent studies conducted in different laboratories (Kaiser et al. 2011). However, two laboratories reported a value of 8 ppm instead (Reuer et al. 2007, Stanley et al. 2010). Comparison of results is complicated by the fact that different water types and experimental methods were used in different laboratories, and often few experimental details (such as experimental conditions or $\delta^{17}\text{O}$, $\delta^{18}\text{O}$ and $\delta(\text{O}_2/\text{Ar})$ values) were reported. Barkan and Luz (2009) reported $\Delta^{17}\text{O}_{\text{sat}}$ might be temperature-dependent, based on experiments conducted at three temperatures from 3.5 to 25 °C. However, so far no other publication has confirmed such a dependence, and apart from Reuer et al. (2007), no other research group has reported $\Delta^{17}\text{O}_{\text{sat}}$ for temperatures below room

temperature (~20-25 °C). Finally, no research group has reported $\Delta^{17}\text{O}_{\text{sat}}$ for temperatures above room temperature. Since $\Delta^{17}\text{O}_{\text{dis}}$ is often close to $\Delta^{17}\text{O}_{\text{sat}}$, errors in $\Delta^{17}\text{O}_{\text{sat}}$ of only a few parts per million could easily lead to significant errors in the calculation of *GOP*.

In order to obtain more information on the triple isotopic composition of dissolved oxygen at air saturation and its possible relationship with temperature, air-equilibrated water experiments were conducted over a wide temperature range (at 0 °C, 22 °C and 39 °C) with both saline (35 g l⁻¹ NaCl) and fresh (distilled) water. Details are provided in **Chapter 4**.

Chapter 2: Methods

Abstract

This chapter focuses on the extraction and preparation of gas samples for triple oxygen isotope analysis, and the subsequent analysis of these gas samples using Isotope Ratio Mass Spectrometry. Details on the biological experiments are given in **Chapter 5**, details on the preparation of air-equilibrated water and sampling of dissolved air are given in **Chapter 4**. Gas purification took place using a home-built automated separation line, built after the example of Barkan and Luz (2003) by former U.E.A. PhD students J. Gloël and A. González-Posada. Triple oxygen isotope and O₂/Ar ratio measurements were performed on a Dual-Inlet *Finnigan MAT 252* Isotope Ratio Mass Spectrometer.

Unless otherwise stated, all experiments were conducted at the University of East Anglia in Norwich. Air-equilibrated water tests (**Chapter 4**), gas transfer tests (**Chapter 3**), gas extraction and purification and triple oxygen isotope measurements were performed at the Stable Isotope Lab, under supervision of A. Marca and J. Kaiser. Phytoplankton cultures for the study of biological oxygen (**Chapter 5**) were grown in the marine trace gas laboratory under supervision of R. Utting. Phytoplankton cultures were supplied by M. Heinle and B. Stawiarski.

2.1. Introduction

This study focuses on the triple oxygen isotope composition of dissolved oxygen at air saturation and oxygen produced by marine phytoplankton. In order to be able to measure the oxygen isotopic composition of air samples in the mass spectrometer, gas samples first have to be collected and purified, because next to oxygen and argon, the two gases relevant for this study, samples usually also contain substantial amounts of CO₂, H₂O and N₂. If not removed, these gases will interfere with the triple oxygen mass spectrometric measurements. Evidently, during the collection and preparation of gas samples for O₂-Ar analysis, contamination with outside air, or isotopic or elemental fractionation of the sampled gas has to be prevented or kept to a minimum.

At the Stable Isotope Lab at U.E.A., all gas species are first extracted from sample bottles on a small, high-vacuum, extraction line, and cryogenically collected on molecular sieve pellets in sealable glass tubes. At this stage most CO₂ and H₂O are removed from the gas sample by cryogenic trapping. From these tubes, samples are

transferred to an automated purification line, built after the example of Barkan and Luz (2003), where N_2 and any remaining CO_2 and H_2O are removed, through gas chromatography and cryogenic trapping respectively. This results in O_2 -Ar samples with negligible N_2 content, which can subsequently be analysed for their triple oxygen isotope composition and O_2/Ar ratio on a Dual-Inlet Isotope Ratio Mass Spectrometer (IRMS, *Thermo Finnigan MAT 252*).

The processing of samples using the above-described set up has been repeatedly tested by J. Gloël (2012), A. González-Posada (2012) and A. Marca (pers. com. 2012), as well as during this study, and it was found it did not lead to significant contamination or fractionation of the sampled gas (Gloël 2012, González-Posada 2012, **Paragraph 2.4 (Chapter 3 and 4)**).

In this chapter, the general procedure of gas extraction, preparation and analysis for the study of triple oxygen isotopes, as applied during this research, will be described.

First, in **Section 2.1**, a description is given of the method of gas sample extraction and collection on molecular sieves ('the extraction line'). In **Section 2.2**, a description of the gas separation line and purification process is given ('the separation line'). **Section 2.3** concerns the mass-spectrometric measurements and processing of output data. **Section 2.4** presents the outcomes of performance and reproducibility tests of the applied method.

2.2. Extraction and preparation of gas samples

2.2.1. Extraction line

Currently, at U.E.A., gas samples for triple oxygen isotope analysis are first collected on molecular sieves in glass tubes using an extraction line (from now on referred to as 'the extraction line'), before being introduced to the gas purification line (described in **Section 2.2**). There are two reasons for this approach. Firstly, it was found that freezing a sample directly from a seawater sample bottle (~350 ml) into the gas purification line required a collection time of 30-45 minutes per sample (time required to freeze > 99.7% of the sample in the first trap), due to the line dimensions, while the collection of a similar sample on the extraction line could be achieved within ~15 minutes (the exact time depending on the quantity of molecular sieves used) (González-Posada 2012). Secondly, use of this separate line allows the direct transfer of dissolved gases from seawater sample bottles to sealed glass tubes for more leak-proof and efficient storage (Gloël 2012).

Description of the line and materials

For the extraction of sample gases and their transfer to molecular sieve pellets in storage tubes, a small high-vacuum extraction line was used. The line generally consisted of 0.6-1.2 cm outer diameter stainless steel and glass tubing, an optional ~180 ml glass trap, a pressure gauge (*Pfeiffer Vacuum*, Activeline capacitance gauge), three manual high-vacuum valves (*Louwers Hapert*) and two connection ports, connected via a manual (*Swagelok*, bellows-sealed) valve to a turbomolecular drag pump (*Pfeiffer Vacuum*, TMU071P). A schematic of the line is displayed in **Figure 2**. The total volume of the line, including trap, was approximately 200 ml, and generally a vacuum of $1.6-1.9 \times 10^{-7}$ mbar could be obtained all around. A pressure gauge ($> 5 \times 10^{-4}$ mbar) was used to check the line for leaks and monitor the pressure drop during freezing. The collection tube containing molecular sieves, a glass vial of constant dimensions (2.5 ml, ~50 mm length, ~8 mm internal diameter) with a high-vacuum o-ring valve (*GE (Glass Expansion)*, Melbourne), was attached to the line at the connection point closest to the pump (**B**), using a *Swagelok* Ultra-Torr fitting. At point **A**, a sample bottle (350 ml glass bottle with *GE* valve) or reference flask (1 L, 2 ml neck with two *GE* valves) could be connected.

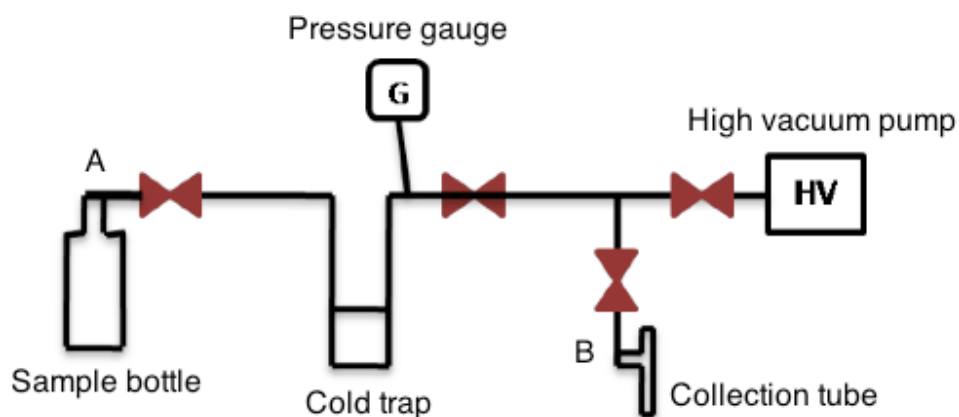


Figure 2: Schematic drawing of the small extraction line, Figure adapted from Gloël (2012). The cold trap was generally kept at liquid nitrogen temperature (-196°C). During the processing of air-equilibrated water or environmental samples, the sample bottle was kept at -78°C in ethanol and dry ice.

Introduction of samples

A sample bottle or reference flask, for introduction of the gas, was connected at point **A** using a *Swagelok* Ultra-Torr connector. Samples were generally introduced after the whole line, including the collection tube, had been evacuated down to 1.9×10^{-7} mbar

(and molecular sieves had been degassed, see below). The pressure in the line before and after introduction of each sample was written down.

Collection of samples

Samples were collected in glass tubes with molecular sieve pellets, connected at point **B**. The glass tubes were either 2.5 ml vials with a *Glass Expansion* high-vacuum, compression o-ring valve, or 20x0.6 (od) cm glass tubes that could be sealed with a flame torch (gas burner).

Molecular sieves

Each tube contained 5-10 new pellets (1.6 x 6 mm) of *Sigma-Aldrich* zeolite 5Å molecular sieve. Molecular sieves are crystalline structures with a specific pore diameter that can be used to trap specific gases based on their molecular diameter and chemical characteristics. Details on the use of molecular sieves are given in **Chapter 3**. These molecular sieves are able to trap O₂, N₂, and Ar at liquid nitrogen temperature (-196 °C). Gases can subsequently be released again from the sieves by increasing the temperature (to room temperature or slightly above room temperature (higher temperatures improve desorption, but too high temperatures (> 200 °C) for extended periods might lead to exchange of oxygen between the sieve lattice and the sample and/or damage to the sieve structure (Karlsson 2004))).

Because it has been reported that the use of zeolite molecular sieves can cause elemental and isotopic fractionation due to incomplete adsorption or desorption, the amount of fractionation increasing with the quantity of molecular sieve used (Barkan and Luz 2003, Abe 2008), transfer of gas species from sampling bottle to Pyrex tube was done until at least 99.8%, (preferably 99.9%), (determined manometrically) of the sample was adsorbed (in which case fractionation due to incomplete adsorption is expected to be negligible (Abe 2008)). In addition, the smallest possible amount of sieves was used, and tubes with molecular sieves were heated prior to release of the sample (~10-20 minutes at ~60 °C (in hot water)) in order to minimize fractionation due to incomplete desorption (following Abe, 2008). Initially, 5 pellets of the above-mentioned type of molecular sieve were used, as it was found this was the minimum number required to cryogenically adsorb gas samples. When this amount was used, in combination with heating before desorption, no significant fractionation of the sample gas was observed (Gloël 2012, González-Posada 2012). Because freezing on to 5 molecular sieve pellets still required a relatively long transfer time per sample (up to 40 minutes), tests were performed with increased numbers of molecular sieve pellets on the extraction line (see **Chapter 3**). It was found that increasing the number of pellets on the extraction line

from 5 to 10 did not lead to significantly increase fractionation (provided transfer to the MS took place using 5 pellets, see **Chapter 3**), but did decrease the transfer time to ~5 minutes per sample. Samples for the equilibrated water tests and biological experiments were therefore collected using 10 pellets of molecular sieve. New pellets of ~6 mm length were used in all cases, which were degassed under vacuum prior to use (in order to remove pre-adsorbed gases that could interfere with the sample and decrease adsorption capacity), by heating them twice with an ethanol burner (~200 °C) (following Abe 2008) for up to ~40 s each time. Each period of heating was carried on until the pressure in the line stopped increasing, and sieves were allowed to cool down before the second period of heating. It had been found in this way sufficient gases could be removed from the sieves, without damaging the sieve structure (A. Marca, pers. com. 2012).

Cryogenic trapping of CO₂ and H₂O

During the transfer of most samples a glass trap, 180 ml in volume, was present on the line, that could be cooled down to -78 °C (using ethanol and dry ice) or -196 °C (using liquid nitrogen), for removal of CO₂ and H₂O from the samples. Initially, the trap was cooled down to -78 °C (Gloël 2012, González-Posada 2012), following recommendations of Barkan and Luz (2003), who reported that oxygen and argon can freeze on ice at -196 °C (which could lead to fractionation) and the use of a liquid nitrogen temperature trap during extraction should thus be avoided (Barkan and Luz 2003). It was however found, during the processing of seawater samples, that due to the high H₂O content of gas samples and proximity of collection tube to the trap, a -78 °C trap did not freeze sufficient H₂O, which complicated the collection of samples. A -196 °C trap was therefore used from 2012 onwards (A. Marca, pers.com. 2012).

Potential fractionation due to liquid nitrogen trap

During the molecular sieve transfer tests, described in **Chapter 3**, O₂-Ar samples were transferred both with and without liquid nitrogen cold trap on the extraction line, and results were compared. It was found that all samples transferred with a -196 °C cold trap on the line, displayed some negative fractionation (negative $\delta^{17}\text{O}$ and $\delta^{18}\text{O}$ values, in the range -0.03 and -0.06‰ for $\delta^{17}\text{O}$ and $\delta^{18}\text{O}$ respectively (see **Chapter 3**)). In all cases, the observed fractionation was however mass dependent, no effect on the $\Delta^{17}\text{O}$ was observed. In addition, tests were performed both at high and low pressure (by introducing the same amount of gas from a large volume sample bottle). It was found that comparable negative fractionation resulted when the line pressure was lowered, the fractionation being worst when both a cold trap and large volume bottle were involved.

In this case, the pressure in the line was also lowest, since the cold trap adds a relatively large volume to the line. It can therefore not be excluded that the negative fractionation was related to the volume rather than the temperature of the trap. (Comparable tests should therefore ideally be performed with the glass trap at room temperature and -78 °C). If the liquid N₂ trap led to fractionation due to freezing of Ar and O₂ on ice, fractionation could potentially be worse during the processing of air-equilibrated water or biological oxygen samples, since these samples would be expected to contain more H₂O. Tests were however performed with the method of sampling used in the culture experiments, and sample bottles containing water bubbled with O₂-Ar reference gas (and a 3 ml O₂-Ar headspace). Results showed a fractionation nearly identical (-0.03 and -0.06% for $\delta^{17}\text{O}$ and $\delta^{18}\text{O}$ respectively) to that observed during the transfer tests with cold trap, for a comparable line volume (**Chapter 3**). Finally, results of air-equilibrated water tests give a good indication of fractionation during the whole process of sampling, extraction and preparation (since atmospheric oxygen is expected to have approximately the same composition at different locations, and resulting $\delta^{18}\text{O}$ values can be compared to equilibrium values from literature). For artificial seawater (35 g l⁻¹ NaCl), $\delta^{18}\text{O}$ values were obtained that were very close (< 0.02‰) to equilibrium values reported in literature (see **Chapter 4**). In addition, in most cases $\delta(\text{O}_2/\text{Ar})$ results were very close to reported equilibrium values (< 1‰), both indicating the presence of a liquid nitrogen trap probably did not significantly affect the results.

Alterations or additions for specific studies

For the equilibrated water tests (**Chapter 4**), samples were introduced from 350 ml sample bottles, which were held in a Dewar with ethanol and dry ice (-78 °C) before and during admission of the sample, in order to freeze most of the H₂O still present in the bottles. This is the general approach for dissolved air samples (González-Posada 2012, Gloël 2012).

For the experiments with phytoplankton cultures, a needle was connected to the line at point **A** (see **Chapter 5**) and introduction of headspace gas took place by piercing the stopper of the sample bottle, after evacuating the line while the needle was halfway down the stopper.

General procedure

The sample bottle, or flask containing the gas to be transferred, was connected to the line at point **A**, and a collection tube containing 10 new molecular sieve pellets was connected at point **B**. The line was then evacuated down to, preferably, 1.6-1.9 x 10⁻⁷ mbar (a pressure of up to 3 x 10⁻⁷ mbar was occasionally accepted). The cold trap was

cooled down to $-196\text{ }^{\circ}\text{C}$ prior to transfer of the samples, by immersing it halfway in liquid nitrogen, after it had been evacuated (during the transfer of samples, the trap stayed in the Dewar with liquid nitrogen, which was regularly topped up). Valves were present between the liquid nitrogen trap and the connection ports, so that sample bottles and tubes could be replaced without significant introduction of air into the trap while it was in liquid nitrogen. Before transfer of a sample, molecular sieves were degassed, by stepwise heating (with an ethanol burner, $\sim 200\text{ }^{\circ}\text{C}$, for two periods of $\sim 40\text{ s}$) while they were being evacuated (see above: 'molecular sieves'). After the whole line and collection tube had been evacuated down to $\sim 1.9 \times 10^{-7}\text{ mbar}$, the valve to the pump was closed and the pressure in the line was written down. The sample was then released into the line, generally up to the valve of the sample tube. The pressure was written down, and the sample was allowed to stay in the main part of the line for ~ 2 minutes. After this time, the valve of the collection tube was opened, and the pressure was written down again. The sample tube was then immersed in liquid nitrogen, and the sample was allowed to freeze on the molecular sieves until at least 99.9% of the sample was adsorbed, which was determined by monitoring the pressure drop (note: for air-equilibrated water and biological samples (**Chapter 4 and 5**) only a recovery of $> 99.9\%$ was accepted. During the transfer tests (**Chapter 3**), occasionally a recovery of 99.8% was accepted). This generally took ~ 5 minutes. After at least 99.9% of the sample had been collected, the collection tube was closed, depending on the tube either with a GE compression o-ring valve, or by flame sealing. After the tube had been closed, the liquid nitrogen could be removed from the tube, and the tube could be removed. The line could then be evacuated and prepared for the next sample.

Note: samples for air-equilibrated water tests and molecular sieve transfer tests (**Chapter 3 and 4**) were collected in valved tubes, while for the biological experiments samples from May were collected in valved tubes, while samples from June-July were collected in flame-seal tubes. Results between May and June-July were comparable, thus not indicating a substantial influence of the collection tube (it could however be expected to make a difference when samples are stored for longer periods of time, as flame-seal tubes are more leak-proof).

Samples collected on molecular sieves in glass tubes were transferred to an automated gas purification line, for removal of N_2 and remaining CO_2 and H_2O , in order to obtain an O_2 -Ar mixture suitable for triple oxygen isotope analysis.

2.2.2. Separation (gas purification) line

After extraction and collection in glass tubes, samples were transferred to an automated gas purification line for the removal of nitrogen and remaining CO₂ and H₂O. This line was built by UEA PhD students J. Gloël and A. González-Posada after the example of Barkan and Luz (2003), with a few modifications. Most importantly, a 10-port two-position valve was used instead of four three-way valves, a 2.74 m GC column was used (*Supelco, 13074-U*, 2.74 m, 2.1 mm diameter, 45/60 molecular sieve) at a temperature of ~0-1 °C, with a helium flow of 8-10 ml/min, instead of the 0.2 m GC column at -80 °C with a 25 ml/min He flow used by Barkan and Luz (2003). Finally, resulting O₂-Ar mixtures were collected under liquid nitrogen, in stainless-steel fingers pre-filled with molecular sieves at the end of the process, instead of using liquid helium, as recommended by Barkan and Luz (2003) (Gloël 2012, González-Posada, 2012).

Liquid helium vs. molecular sieves and liquid nitrogen for final trapping

Barkan and Luz (2003) recommended the use of liquid helium (instead of molecular sieves under liquid nitrogen) for sample collection from the purification line, because they observed elemental and isotopic fractionation due to incomplete desorption from zeolite molecular sieves upon introduction of samples to a dual-inlet mass-spectrometer; the amount of fractionation increasing with the sieve quantity used. This was confirmed by Abe (2008). Abe however reported that fractionation could be negligible as long as a small amount of zeolite 5Å molecular sieves was used, and tubes containing the sieves were heated in hot water prior to desorption of the samples (10 minutes at 60°C) (Abe, 2008). Gloël and González-Posada found that when O₂-Ar gas was transferred to the MS using 5 *Sigma-Aldrich* zeolite 5Å pellets of 1.6x5 mm (corresponding to ~0.2g), in combination with heating prior to transfer to the MS, fractionation was negligible (Gloël 2012, González-Posada, 2012). This was confirmed by transfer tests conducted during this study (**Chapter 3 and Section 2.4**). Since final transfer using molecular sieves and liquid nitrogen was found not to lead to significant fractionation under these conditions, the use of molecular sieves was preferred above the use of liquid helium for safety and economic reasons.

The operation, materials and testing of the gas purification line have been described in detail in the theses of Gloël (2012) and González-Posada (2012).

During this study, the line was used under the same protocol, as described by Gloël (2012) and González-Posada (2012). No important alterations to the line took place, with the exception of using an increased number of molecular sieve pellets in the first collection trap (T3, see **Figure 3**), and the removal of the inline particle filters above this

trap. Initially, 20 pellets of 5Å zeolite sieve were present, but in order to find out whether the freezing speed of samples from 350 ml bottles could be increased, the trap was filled with 2.4 g of sieves. Because the increased number of molecular sieves (which should not affect elemental or isotopic composition, as gas was trapped during desorption (Barkan and Luz 2003, **Chapter 3**)) did not significantly increase the transfer speed into T3, it was considered that the particle inline filters above the trap slowed down the process. These filters had been put in position to prevent solid (glass wool, molecular sieve dust) fragments from entering the line and damaging the valves. Glass wool was used in the traps during the building and testing stage of the line, because molecular sieve powder got sucked into the line and damaged the valves. Now, instead of the filters and glass wool, pieces of cut metal wire were placed on top of the pellets. Unfortunately, this modification did not decrease transfer time directly from glass bottles to < 30 minutes. It was therefore decided to keep using the small extraction line as an intermediate step in the transfer of the dissolved gases from the large volume sample bottles to the purification line (see **Section 2.2.1**).

As mentioned above, the gas purification line has been described in detail in the theses of Gloël (2012) and González-Posada (2012). A short description of the line and purification process will be given below.

Description of the line and purification protocol

The line consisted of a 10-port 2-position valve (*Valco*, A4L10UWM), that could be used i.e. to change the direction of helium flow and open or close off parts of the system, a helium carrier gas (flow rate 8-10 ml/min), which was purified using a trap with 13X sieves at -196 °C, two (1/4 inch stainless steel) traps containing zeolite 5Å molecular sieve pellets for collection of samples (T3 for trapping before GC separation, T4 for trapping O₂ and Ar after GC separation), which could be automatically cooled down to -196 °C (using a pneumatic dewar with liquid nitrogen) for collection of samples, and heated to the required temperature using a heating rope (*Omegalux*, FGR series, 240V), a glass spiral trap at -196 °C for removal of remaining CO₂ and H₂O from the samples, a gas chromatographic column (*Supelco*, 13074-U, 2.74 m, 2.1 mm diameter, 45/60 molecular sieve) for separation of N₂ from O₂ and Ar, and an exit manifold consisting of 7 stainless-steel fingers with molecular sieve pellets. Individual tubes could be opened and closed using pneumatically actuated springless diaphragm valves. Valves and controls were connected to a computer interface via *National Instruments* modules.

Two Pirani gauges ($>5 \times 10^{-4}$ mbar) monitored the pressure in the line, one near the inlet and one near the exit manifold, and a compact cold cathode gauge ($>2 \times 10^{-9}$ mbar) was present near the high-vacuum pump (*Pfeiffer Vacuum*, turbomolecular drag pump).

During the time of processing of the samples for this study, a vacuum of 2.7×10^{-7} mbar was generally achieved in the line. A schematic of the line is given in **Figure 3**.

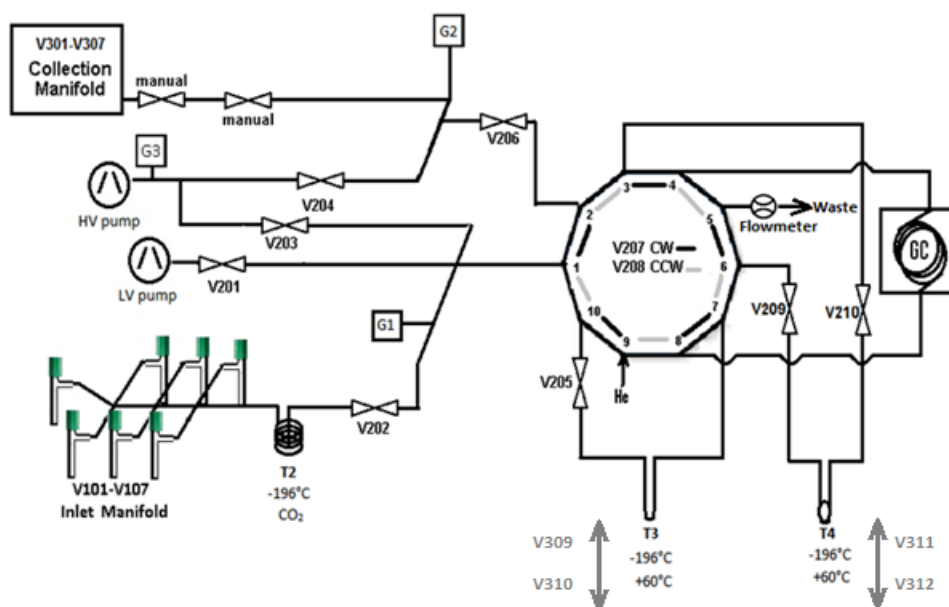


Figure 3: Schematic drawing of the separation line, by González-Posada (2012). Valves are indicated by V, traps by T, pressure gauges by G. HV = high-vacuum pump, while LV = (optional) low vacuum pump, GC = gas chromatographic column. The 10-port valve has two positions, in the first position, the grey connections are open and the black connections are closed (as a result, He gas flows directly through the GC to waste), in the second position, grey connections are closed and black connections are opened (He gas flows through trap 3, GC and trap 4 before going to waste).

Preparation procedure

Samples were connected to the inlet the evening before processing (so that the inlet could be evacuated overnight), and heated for 10-20 minutes at ~ 60 °C prior to release. Before the start of each sample run, the manual valve of the sample tube was opened or the tube was cracked (flame-seal tubes), and the program was started.

Before starting the automated preparation sequence, the 10-port 2-way valve was positioned so that helium flow was directed straight through the GC and then to waste (**Figure 3**).

After obtaining the right vacuum in the first part of the inlet ($< 2.9 \times 10^{-7}$ mbar), the valve to the sample was opened and the sample was released into the first part of the line (up to valve 202), where a glass spiral trap at -196 °C was present to remove any

remaining CO₂ and H₂O. The first collection trap (T3, containing zeolite 5 Å molecular sieve) was then immersed in liquid nitrogen and the sample was frozen into the trap (for ~15 minutes). After collection of ~99.5% of the sample, the trap was removed from the liquid nitrogen and heated to 60 °C and the He flow (8-10 ml/min) was directed over the trap (by switching the 10-port valve), so that the helium carrier gas could guide the sample from the T3 through the GC column, where O₂ and Ar were separated from nitrogen. O₂ and Ar eluted first, and were collected in the second trap (T4, also containing zeolite 5 Å molecular sieve) which was held at -196 °C. After O₂ and Ar had been collected, but before elution of N₂, which was retained in the GC longer, the 10-port valve was switched again, so that the He flow was redirected, back to its initial position, to go straight into the GC and then to waste. In this way N₂ eluting from the GC was carried to waste instead of ending up in the sample. Finally, the second collection trap was also heated to 60 °C, and the sample (now a purified O₂-Ar mixture, suitable for MS analysis) was collected into a stainless-steel holding tube of the exit manifold, which was held in liquid nitrogen and contained five pellets of zeolite 5 Å molecular sieve per tube. As mentioned above, it had been found no fractionation of the sample gas took place as long as this type and amount of sieves were used, and sample tubes were heated prior to release of the sample (Gloël 2012, González-Posada, 2012, **Chapter 3**). The purification process took ~75 minutes per sample. The line was automatically evacuated at the end of each sample run, while trap T3 and T4 were degassed by heating to 180 °C.

Together with each set of up to six samples, one aliquot of dry air (DA) was processed, so that the functioning of the line could be monitored and sample results could later be referenced against air (see **Section 2.3.3**). After collection of all samples and one DA aliquot, the exit manifold was disconnected from the purification line and connected to the Isotope Ratio Mass Spectrometer (*Thermo Finnigan* MAT 252, dual-inlet), for determination of the triple oxygen isotope composition and O₂/Ar ratio of the resulting O₂-Ar mixtures.

2.2.3. Encountered problems

During the processing of biological oxygen samples, in the summer of 2013, several samples suddenly contained very high amounts of nitrogen when they were measured on the MS (> 10 V instead of ~0.5 V). Such high amounts of nitrogen severely influence the measurement, and cannot be corrected for, so the samples were lost. After examining several options, it was found that the helium flow sensor (*Honeywell*) no longer displayed the correct helium flow rate on screen. The flow rate on screen was 8-10

ml/min, while the actual flow rate (measured using a calibrated manual flow meter) was 14-15 ml/min. As a result of this high flow rate, nitrogen eluted from the GC earlier, sometimes before the moment of switchover of the 10-port valve, so that part of the nitrogen was collected with the sample instead of being carried to waste. As a result, some of the biological samples were lost. For subsequent samples, a calibrated manual flow meter was used, and the helium flow rate was closely monitored. Because the first batch of samples had been processed at a relatively high flow rate (~14 ml/min), later samples were processed at a flow rate (manual meter) of ~11-12 ml/min (it was ensured there was still sufficient time between the 10-port valve switch-over and elution of nitrogen at this rate), in order to keep conditions as similar as possible between different samples of the same study.

In addition, some of the valves on the entry manifold had to be replaced, because they were suddenly leaking, probably due to the presence of small glass fragments introduced through the breaking of Pyrex tubes. Since this was immediately noticed, no samples were lost or affected.

2.3. Isotope Ratio Mass Spectrometry

2.3.1 Description of instrument and IRMS measurements

After collection of a set of maximally 6 samples and minimally one DA aliquot, the exit manifold was disconnected from the purification line and connected to the dual-inlet isotope ratio mass spectrometer (*Thermo Finnigan MAT 252*), for determination of the triple oxygen isotope composition and O₂/Ar ratio of the resulting O₂-Ar mixtures (with respect to a O₂-Ar reference mixture (4.7% Ar in O₂, *BOC Ltd.*)). Because molecular sieves were used for sample collection from the separation line, the tubes containing the samples were heated for ~20 minutes at ~50-80 °C (hot water, cooling down) prior to release of the samples into the MS (following Abe 2008), in order to minimise the risk of incomplete desorption.

Initially, sample tubes were heated in hot tap water, with a temperature of approximately ~60 °C, which was allowed to cool down over the period of heating. Later, tests were performed heating aliquots of O₂-Ar reference gas to either 60 or ~80-90 °C (still cooling down during the period of heating) prior to release into the mass spectrometer. No significant difference was observed in the $\Delta^{17}\text{O}$, but resulting $\delta^{17}\text{O}$ and $\delta^{18}\text{O}$ values were closer to zero (indicating less fractionation) when the start temperature was ~80-90 °C. Because results were slightly better when a higher temperature was applied (too high

temperatures should be avoided in order to prevent exchange of molecules between the sieves and the sample (Karlsson 2004, Abe 2008) samples were from thereon heated with a start temperature of ~80 °C.

Analysis of samples took place on a *Thermo Finnigan* MAT 252 Dual-Inlet Isotope Ratio Mass Spectrometer. Aliquots of sample and standard gas (in this case an O₂-Ar mixture (4.7% Ar in O₂, *BOC Ltd.*)) are simultaneously introduced into the sample and standard-bellows of the MS-inlet respectively. Bellows are receptacles with adjustable volume, in which gas is kept for analysis in the MS. Sample and standard bellows are connected to the ionization chamber through independent capillaries, and flow on the capillaries, and the resulting signal intensity, is determined by the pressure in the bellows, which can be adjusted by adjusting the bellow opening. At the beginning of each measurement cycle, the bellows are adjusted automatically in order to achieve an *m/z* 32 signal intensity of 2.5 V. The $\delta^{17}\text{O}$ and $\delta^{18}\text{O}$ of the sample relative to the reference are then determined by alternately analysing the reference and sample gas (determining the ion beam intensities/relative amounts of *m/z* 32, 33 and 34).

Oxygen isotopologues ¹⁶O¹⁶O (*m/z* 32), ¹⁷O¹⁶O (*m/z* 33) and ¹⁸O¹⁶O (*m/z* 34) were collected (and their signal was analysed) simultaneously in cup three (3 x 10⁻⁸ Ohm resistor), five (3 x 10⁻¹¹ Ohm resistor) and six (1 x 10⁻¹¹ Ohm resistor) respectively.

During each measurement cycle, the reference gas is first introduced into the mass spectrometer and analysed during a set amount of time (integration time), after which valves are switched and the remaining gas is pumped away during a set amount of time (idle time), after which the sample gas is introduced and analysed in the same way. This cycle was repeated 30 times within one block of measurements.

Procedure of introduction of samples

Before the measurement of each set of sample gases from the separation line, a 'zero enrichment' was performed, in order to test the functioning of the instrument and to condition the source to almost pure oxygen gas. For this measurement the same O₂-Ar reference gas was introduced to both sides on the inlet and measured against each other. (Results of zero enrichments conducted during the period of this study are displayed in **Section 2.4, Table 1**). Approximately 30 minutes before the end of the zero enrichment measurement, the manifold containing the samples was attached to the sample side of the inlet, while a flask with a reference O₂-Ar mixture (4.7% Ar in O₂, *BOC Ltd.*) was attached to the standard side.

After the whole inlet system, including the bellows, had been properly evacuated, and an aliquot of reference gas had been expanded in the expansion volume in the neck of the

flask, valves to the pump were closed and the sample and standard gas were introduced into the sample and standard bellow respectively. Gas was allowed to equilibrate for one minute before valves were closed.

Because it had been found that differences in amount of gas between the sample and standard side of the inlet could influence the results (different depletion rates) (Stanley 2010), the variable volume bellows were manually adjusted upon introduction of sample and reference in order to expand equal amounts of gas on both sides (approximately the same pressure for the same bellow volume).

At the beginning of each measurement cycle, the bellows were adjusted automatically in order to achieve an m/z 32 signal intensity of 2.5 V. The $\delta^{17}\text{O}$ and $\delta^{18}\text{O}$ were then determined 90 times (in 3 blocks of 30 cycles of sample-reference measurement), and an average $\delta^{17}\text{O}$ and $\delta^{18}\text{O}$ were calculated for each run.

As explained in **Chapter 1**, the isotope-ratio difference of a sample relative to a reference is in standard delta-notation:

$$\delta \left(\frac{\text{sample}}{\text{reference}} \right) = \frac{R_{\text{sam}}}{R_{\text{ref}}} - 1$$

$$R \left(\frac{^*\text{O}}{^{16}\text{O}} \right) = \frac{n(^*\text{O})}{n(^{16}\text{O})} \approx \frac{n(^*\text{O}^{16}\text{O})}{n(^{16}\text{O}^{16}\text{O})}$$

where R is the isotope ratio, the ratio of the abundance (n) of the minor isotope over the major isotope (in this case, the ratio of the amount of either, ^{17}O or ^{18}O over ^{16}O), and $^*\text{O}$ is either ^{17}O or ^{18}O .

$\delta^{17}\text{O}$ and $\delta^{18}\text{O}$ were calculated from the measured ion beam intensities of m/z 34 and 33 relative to 32 in the sample and reference according to:

$$\delta^{17}\text{O}/\text{‰} = \left[\frac{\left(\frac{n(^{17}\text{O})}{n(^{16}\text{O})} \right)_{\text{sam}}}{\left(\frac{n(^{17}\text{O})}{n(^{16}\text{O})} \right)_{\text{ref}}} - 1 \right] \cdot 1000 \approx \left[\frac{\left(\frac{n(^{17}\text{O}^{16}\text{O})}{n(^{16}\text{O}^{16}\text{O})} \right)_{\text{sam}}}{\left(\frac{n(^{17}\text{O}^{16}\text{O})}{n(^{16}\text{O}^{16}\text{O})} \right)_{\text{ref}}} - 1 \right] \cdot 1000$$

$$\approx \left[\frac{\left(\frac{U_{33}}{U_{32}} \right)_{\text{sam}}}{\left(\frac{U_{33}}{U_{32}} \right)_{\text{ref}}} - 1 \right] \cdot 1000$$

$$\delta^{18}\text{O}/\text{‰} \approx \left[\frac{\left(\frac{U_{34}}{U_{32}} \right)_{\text{sam}}}{\left(\frac{U_{34}}{U_{32}} \right)_{\text{ref}}} - 1 \right] \cdot 1000$$

Where ' U_{33} ', ' U_{34} ' and ' U_{32} ' are the ion beam intensities (V) of m/z 33, 34 and 32 respectively, representing the amounts of $^{17}\text{O}^{16}\text{O}$, $^{18}\text{O}^{16}\text{O}$ and $^{16}\text{O}^{16}\text{O}$.

At the time of measurement of samples for this study, the average standard deviations between 30 measurements of one run (internal precision of the MS) were 0.047 and 0.020‰ for $\delta^{17}\text{O}$ and $\delta^{18}\text{O}$ respectively. The corresponding standard errors were 0.009 and 0.004‰.

Tests had been performed by Gloël (2012) and González-Posada (2012) in order to find the measurement settings that produced maximal measurement precision (smallest standard deviation and error) while minimising measurement time. It was found best results were obtained when the idle time was 5 seconds, the integration time was 16 seconds and samples were measured against the reference 90 times, in three runs of 30 measurement cycles. The chosen signal height for m/z 32 was 2.5 V (3×10^{-8} Ohm resistor) during the time of the measurements for this study.

At the end of each 3 measurement blocks, an ‘interfering masses’ measurement was performed, during which the ion beam intensities (ion current \cdot resistance, in V) of m/z 32 ($^{16}\text{O}_2$), 40 (Ar) and 28 ($^{14}\text{N}_2$) were determined. The signal intensities of m/z 32 and 40 were measured in cup 3 (peak jumping), after which m/z 28 was measured in cup 5.

From the results of these measurements, the $\delta(\text{O}_2/\text{Ar})$ and $d(\text{N}_2/\text{O}_2)$ could be calculated according to the following formulas:

$$\delta(\text{O}_2/\text{Ar})/\text{‰} = \left[\left(\frac{\left(\frac{U_{32}}{U_{40}} \right)_{\text{sam}}}{\left(\frac{U_{32}}{U_{40}} \right)_{\text{ref}}} \right) - 1 \right] \cdot 1000$$

$d(\text{N}_2/\text{O}_2)$ was calculated according to:

$$d(\text{N}_2/\text{O}_2)/\text{‰} = \left[\left(\frac{U_{28}}{U_{32}} \right)_{\text{sam}} - \left(\frac{U_{28}}{U_{32}} \right)_{\text{ref}} \right] \cdot 1000$$

Where ‘ U_{28} ’, ‘ U_{32} ’ and ‘ U_{40} ’ are the measured ion beam intensities (V) for m/z 28 (N_2), 32 ($^{16}\text{O}_2$) and 40 (Ar) respectively.

As measure for N_2 content and for use in N_2 corrections (**Section 2.3.2**), the above-defined $d(\text{N}_2/\text{O}_2)$ was used instead of the standard delta-value ($\delta(\text{N}_2/\text{O}_2)$) because it was less affected by changes in the background N_2 concentration in the MS (Gloël 2012). As a result, a stronger, more consistent, relationship was observed between $d(\text{N}_2/\text{O}_2)$ and the isotopic results than between $\delta(\text{N}_2/\text{O}_2)$ and isotopic results, which made $d(\text{N}_2/\text{O}_2)$ more suitable for use in the nitrogen interference corrections (**Section 2.3.2**).

In total, a full measurement on the MS consisting of 3 blocks of 30 determinations of $\delta^{17}\text{O}$ and $\delta^{18}\text{O}$ and one interfering masses measurement took 1 hour and 25 minutes.

As mentioned above, zero enrichment tests were performed regularly, and always before introduction of samples, in order to test the performance of the mass-spectrometer. Results for the zero enrichment measurements are displayed in **Table 1**. As can be observed, the deviations from zero in $\Delta^{17}\text{O}$, $\delta^{17}\text{O}$, $\delta^{18}\text{O}$ (-3 ppm, -0.010 and -0.012‰ resp.) are small (considering the standard deviation, see below), and results are comparable to those obtained in 2011 and 2012 by Gloël (2012) and González-Posada (2012). Standard deviations obtained for $\Delta^{17}\text{O}$, $\delta^{17}\text{O}$ and $\delta^{18}\text{O}$ were 10 ppm, 0.010 and 0.012‰ respectively, while the associated standard errors, based on 54 runs, were 3 ppm, 0.003 and 0.003‰ (calculated using the 95% CI function in MS Excel).

For each sample, three $\delta^{17}\text{O}$ and $\delta^{18}\text{O}$ values and one $\delta(\text{O}_2/\text{Ar})$ value were obtained. These could later be used for the calculation of $\Delta^{17}\text{O}$, and be averaged per sample, but first corrections had to be applied to the individual $\delta^{17}\text{O}$ and $\delta^{18}\text{O}$ results to account for imbalance and N_2 and Ar interference (**Section 2.3.2**), after which the corrected values (in case of biological and air-equilibrated water samples) had to be standardised with respect to air (**Section 2.3.3**).

2.3.2 Nitrogen, Argon and imbalance corrections

Any differences in (m/z 32) signal (depletion rate) between the standard and sample gas (imbalance) during the mass spectrometric measurement, as well as the presence of interfering gases N_2 and Ar, are known to influence the isotopic measurements and affect resulting $\delta^{17}O$ and $\delta^{18}O$ values; the magnitude of the corrections depending i.e. on the used instrument, settings and conditions within the MS (Bender et al. 1994, Emerson et al. 1999, Abe and Yoshida 2003, Barkan and Luz 2003, Sarma et al. 2003). Therefore, corrections had to be applied.

The exact effects of imbalance, N_2 and Ar content on the results are variable, they depend, next to on the specific instrument used, on many factors, including filament, ion source settings and conditions within the MS. Correction factors therefore have to be determined regularly, and always after filament change or source cleaning (Barkan & Luz 2003).

2.3.2.1 Imbalance correction

As described above, the MS automatically balances the pressure in the sample and reference bellows before each measurement run, so that comparable signal intensities for m/z 32 (of ~ 2.5 V) are obtained for the sample and the standard gases. However, small differences in the signal intensity between the sample and standard can strongly affect the resulting $\delta^{17}O$, $\delta^{18}O$ and $\Delta^{17}O$ values.

The effect of imbalance on the resulting $\delta^{17}O$ and $\delta^{18}O$ values was assessed using two different approaches. Firstly, imbalance tests were performed. For these tests, the same O_2 -Ar reference gas was admitted to both the sample and reference side of the inlet, the automatic signal intensity adjustment by the IRMS was turned off and the intensities of m/z 32 on the sample and reference side were instead manually adjusted before each measurement block, so that the m/z 32 signal intensity on the reference side was kept constant at 2.5 V, while the signal intensity on the sample side was varied from 2.3 to 2.7 V in steps of approximately 0.1 V. For each combination of signal intensities, three measurement blocks were performed. During each block the gases were measured for 30 minutes, consisting of 30 sample-reference pair measurements, and $\delta^{17}O$, $\delta^{18}O$ and $\Delta^{17}O$ were calculated. Results are displayed in **Figure 4 and 5**. Secondly, the resulting $\delta^{17}O$, $\delta^{18}O$ and $\Delta^{17}O$ values (of individual runs) of all zero enrichments performed over the months relevant for these studies (summer 2013), were plotted against the difference in signal intensity of m/z 32 ($U_{32, \text{sample}} - U_{32, \text{reference}}$, where U is the ion beam intensity in V) measured at the beginning of each measurement run (**Figure 6 and 7**).

In both cases, a strong linear relationship was found between the difference in voltage for m/z 32 on sample and reference side and the resulting $\delta^{18}\text{O}$ (linear regression line slope 1.72, $R^2 > 0.99$ for imbalance test results and 1.86, $R^2 = 0.92$ for zero enrichment results) and $\Delta^{17}\text{O}$ (-1534.2, $R^2 > 0.99$ and -1416.6, $R^2 = 0.91$ for imbalance tests and zero enrichments respectively (see **Figure 4-8**). A strong relationship between imbalance and $\delta^{17}\text{O}$ was also found in the imbalance test results (linear regression line slope -0.64, $R^2 = 0.97$), but in the zero enrichment results this relationship was less pronounced (slope -0.45, $R^2 = 0.51$). The correction factors were obtained through linear regression.

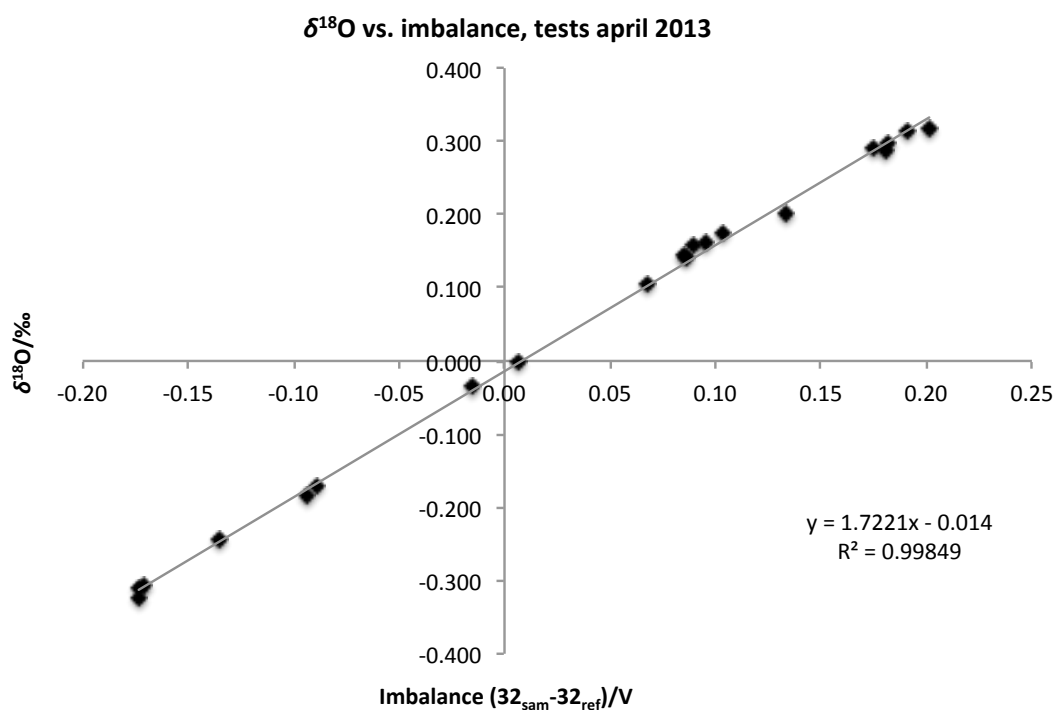


Figure 4: $\delta^{18}\text{O}$ results of imbalance tests April 2013 (after filament change and ion source tuning): reference side 2.5 V for all tests, sample side varied from 2.3 to 2.7 V, 3 samples/tests per voltage difference. ‘32’ indicates the ion beam intensity of m/z 32 in volts, recorded at the beginning of the measurement.

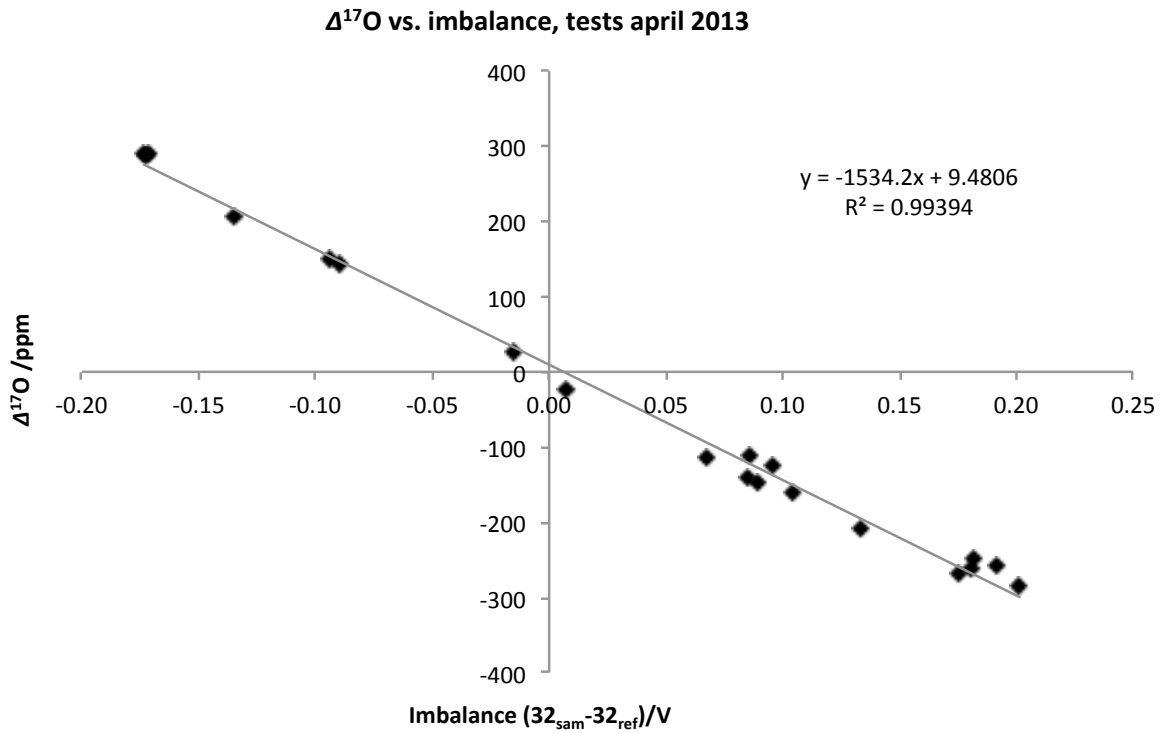


Figure 5: Relationship $\Delta^{17}\text{O}$ and imbalance in results of imbalance tests April 2013 (after filament change and ion source tuning): reference side 2.5 V for all tests, sample side varied from 2.3-2.7 V, 3 tests per voltage difference.

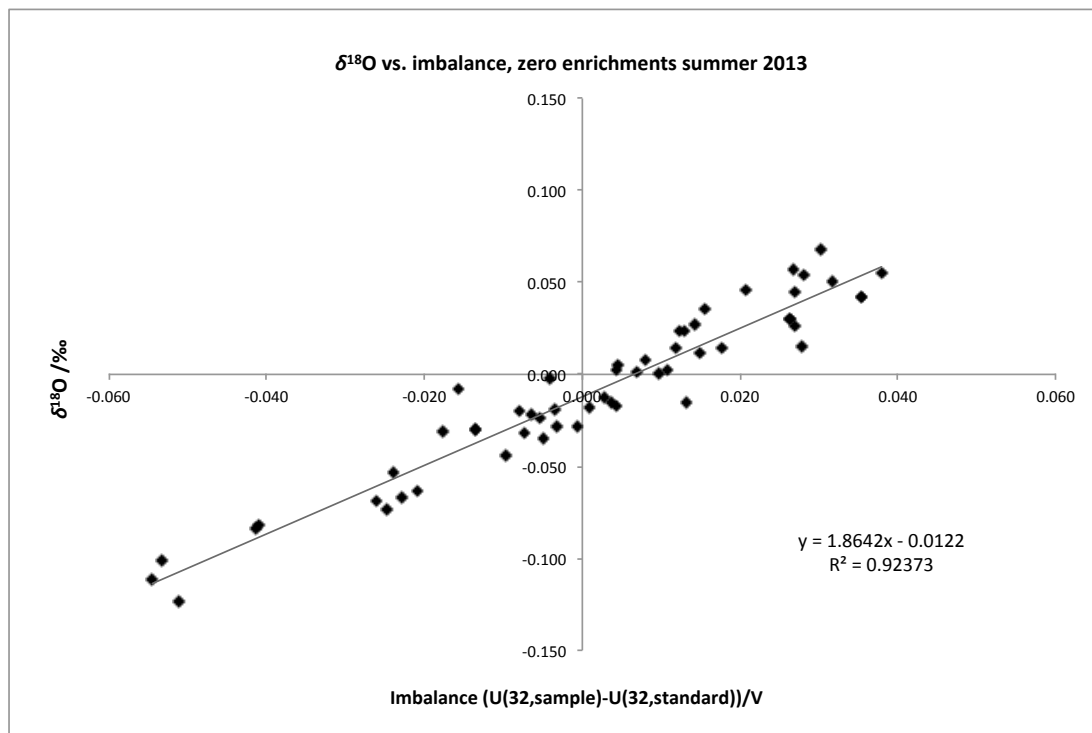


Figure 6: The relationship between $\delta^{18}\text{O}$ and imbalance (difference in m/z 32 signal on sample and standard side) from zero enrichment data (from 06-09/2013) (the time of measurement of

biological and air-equilibrated water samples). U is the ion beam intensity in volts, 32 refers to m/z 32.

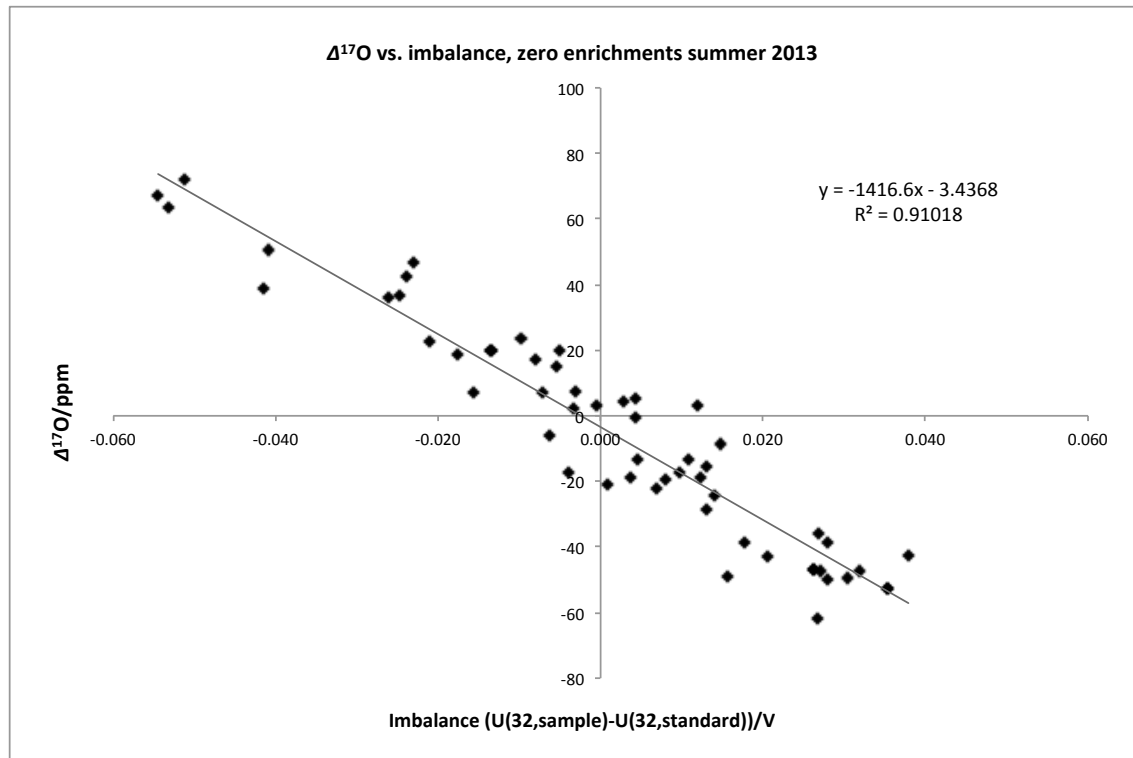


Figure 7: The relationship between $\Delta^{17}\text{O}$ and imbalance (difference in m/z 32 signal intensity on sample and standard side) from zero enrichment data (from 06-09/2013). U is the ion beam intensity in V, '32' refers to m/z 32.

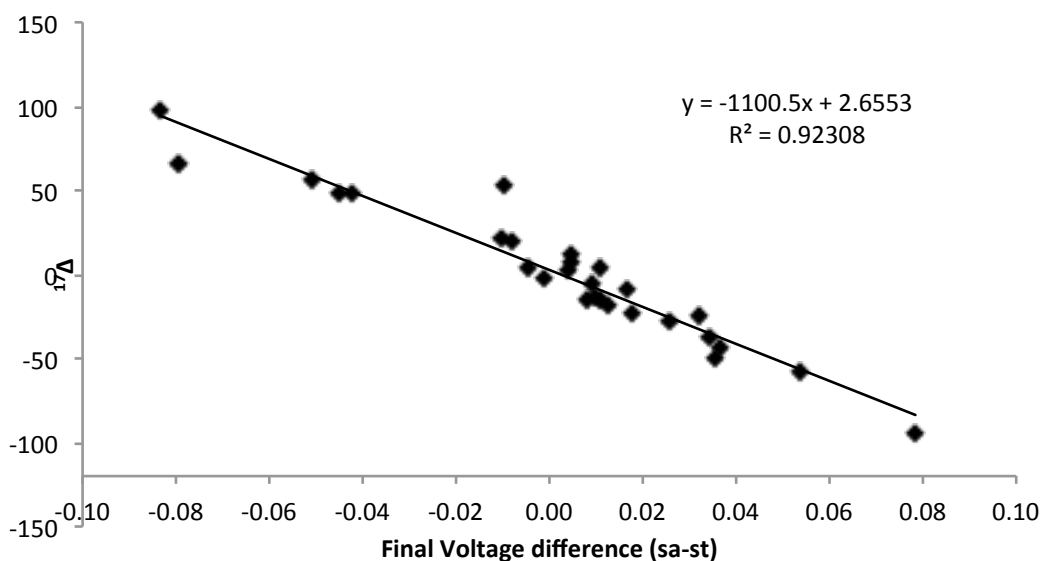


Figure 8: Relationship between imbalance (difference in m/z 32 signal intensity (V) between sample and standard) and resulting $\Delta^{17}\text{O}$ before filament change and tuning in April 2013. Data from measurements conducted in summer 2012 by González-Posada (2012).

Since imbalance tests gave results close to the results based on the zero enrichments, the slopes of the relationships based on zero enrichments were used for the imbalance correction because these relationships were based on more data points. Also, zero enrichment data were obtained in the months the samples for biological O_2 and air-equilibrated water tests were measured, while imbalance tests were conducted a few months earlier, and zero enrichments were obtained over several months, while the imbalance tests were conducted on one day, as a result of which the zero enrichments are more likely to capture daily fluctuations in the MS conditions. Finally, the zero enrichment tests cover the range of imbalance likely to be experienced in actual measurements.

Results of biological experiments and air-equilibrated water tests (and other tests performed in summer 2013) were therefore corrected using a correction factor of 1.86 for $\delta^{18}\text{O}$ and -0.45 for $\delta^{17}\text{O}$. Correction was performed as follows:

$$\delta^{18}\text{O}_{\text{corr}} = \delta^{18}\text{O}_{\text{meas}} - 1.86 \cdot (U_{32,\text{sam}} - U_{32,\text{ref}})$$

$$\delta^{17}\text{O}_{\text{corr}} = \delta^{17}\text{O}_{\text{meas}} - (-0.45) \cdot (U_{32,\text{sam}} - U_{32,\text{ref}})$$

Where $U_{32,\text{sam}}$ and $U_{32,\text{ref}}$ are the ion beam intensities (V) of m/z 32 measured at the beginning of the measurement run, for the sample and standard side, respectively. The result of each individual run was corrected separately. It was found the use of these correction factors led to good, consistent results for data from summer 2013.

In April 2013, the filament was changed, emission was decreased from 1200 to 1000 μA and the ion source was tuned for maximum sensitivity. This resulted in a change in the imbalance effect and the required correction factors. Zero enrichments from late 2012 and early 2013 plotted against imbalance indicated a relationship with imbalance of ~ 1100 for $\Delta^{17}\text{O}$ and ~ 1.1 for $\delta^{18}\text{O}$, while imbalance tests and zero enrichments performed after the filament change indicated a relationship with imbalance of ~ 1400 - 1500 for $\Delta^{17}\text{O}$, ~ 1.8 for $\delta^{18}\text{O}$ (as mentioned above).

Molecular sieve transfer test samples (**Chapter 3**) were measured in 2012, before the filament change. For imbalance correction of these samples, the results of zero enrichments performed by A. González-Posada from summer 2012 were used (**Figure 8**). The relationship with imbalance found in these results was comparable to the relationship found in zero enrichments performed in late 2012 (start of this study) and early 2013 (which all indicated a relationship with $\Delta^{17}\text{O}$ close to 1100 and with $\delta^{18}\text{O}$ close to 1), but summer 2012 results were used because the number of data points was higher.

Molecular sieve transfer test results dating from autumn 2012 were therefore corrected using a correction factor of -0.52 ($R^2 = 0.84$) and 1.12 ($R^2 = 0.86$) for $\delta^{17}\text{O}$ and $\delta^{18}\text{O}$ respectively, corresponding to a relationship between imbalance and $\Delta^{17}\text{O}$ of 1100.5 ($R^2 = 0.92$) (**Figure 8**).

2.3.2.2 Nitrogen correction

Because nitrogen will interfere with triple oxygen isotope measurements if left in the sample, it is removed from samples beforehand through gas chromatography (on the separation line, see **Section 2.2.2**). Small amounts of nitrogen will however always be present, and these can still influence the results. In order to assess the effect of nitrogen on the $\delta^{17}\text{O}$ and $\delta^{18}\text{O}$ results, aliquots of O_2 -Ar reference gas were mixed with different amounts of pure nitrogen gas, and the resulting mixtures were frozen onto molecular sieves in glass tubes at liquid nitrogen temperature and measured on the MS against the same O_2 -Ar reference gas without added nitrogen. The $\delta^{17}\text{O}$, $\delta^{18}\text{O}$ and $\Delta^{17}\text{O}$ results were then plotted against the nitrogen content (quantified as the difference in the 28/32 between the sample and reference gas, $d(\text{N}_2/\text{O}_2)$) and the correction factors were determined through linear regression. Results of different dilution series are displayed in **Figure 9 and 10**.

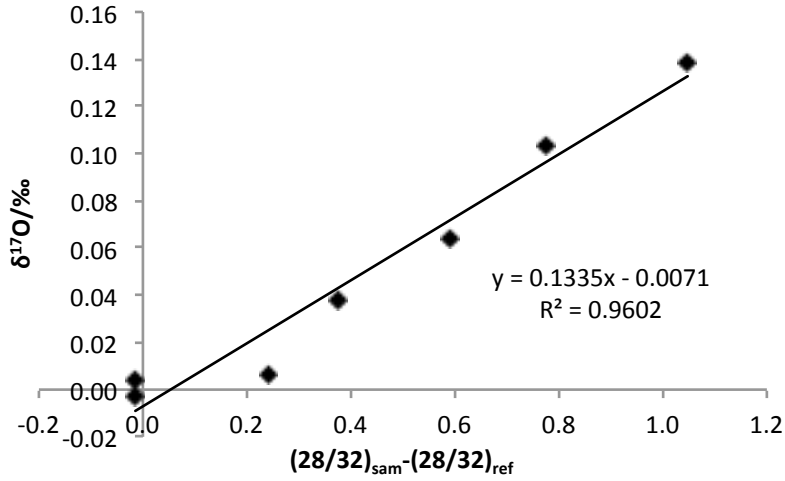


Figure 9: $\delta^{17}\text{O}$ results of N_2 dilution series

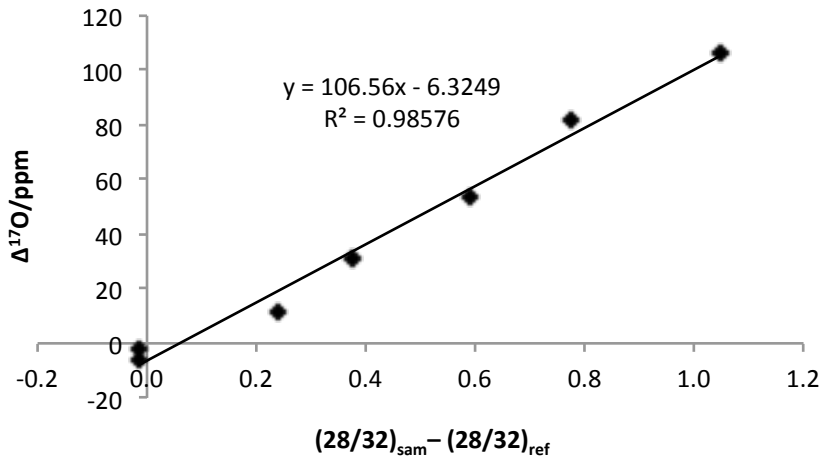


Figure 10: $\Delta^{17}\text{O}$ results of N_2 dilution series

A strong linear relationship was observed between $\delta^{17}\text{O}$ ($R^2 = \sim 0.96$) and $\Delta^{17}\text{O}$ ($R^2 = \sim 0.99$) and $d(\text{N}_2/\text{O}_2)$ (absolute value).

Based on dilution series, results of this study were corrected using a correction factor of 0.052 ($R^2 = 0.75$) for $\delta^{18}\text{O}$ and 0.1335 ($R^2 = 0.96$) for $\delta^{17}\text{O}$.

$\delta^{17}\text{O}$ and $\delta^{18}\text{O}$ were corrected as follows:

$$\delta^{18}\text{O}_{\text{corr}} = \delta^{18}\text{O}_{\text{meas}} - 0.052 \cdot d(\text{N}_2/\text{O}_2)$$

$$\delta^{17}\text{O}_{\text{corr}} = \delta^{17}\text{O}_{\text{meas}} - 0.1335 \cdot d(\text{N}_2/\text{O}_2)$$

Where

$$d(\text{N}_2/\text{O}_2) = (U_{28}/U_{32})_{\text{sam}} - (U_{28}/U_{32})_{\text{ref}}$$

Note: $d(\text{N}_2/\text{O}_2)$ here refers to the absolute value, not the per mill value.

2.3.2.3 Argon correction

Next to nitrogen, argon has also been reported to interfere with triple oxygen isotope measurements (Barkan and Luz 2003, Abe and Yoshida 2003, Sarma et al. 2003). Abe and Yoshida (2003) found a strong effect of increased Ar contents on the $\delta^{17}\text{O}$ and $\delta^{18}\text{O}$. However, they performed tests with Ar/O₂ ratios of 0.4-9, while Ar/O₂ ratios in nature are generally much lower (0.04-0.2) (Barkan and Luz 2003). In dissolved air samples from seawater, the fluctuations in Ar are expected to be so small ($\delta(\text{Ar}/\text{O}_2)$ close to 10-20‰) that the effect on $\delta^{17}\text{O}$ and $\delta^{18}\text{O}$ will be negligible (Barkan and Luz 2003, J. Kaiser pers. com. 2013). However, in samples from the experiments with marine phytoplankton (**Chapter 5**), due to the production of biological oxygen, the $\delta(\text{O}_2/\text{Ar})$ was in all cases much higher, and $\delta(\text{Ar}/\text{O}_2)$ thus lower, than in the reference gas ($\delta(\text{O}_2/\text{Ar}) \sim 1000\text{-}10,000\text{‰}$ vs. the reference gas (see **Section 5.3**), corresponding $\delta(\text{Ar}/\text{O}_2)$ down to $\sim -900\text{‰}$). In addition, Barkan and Luz (2003) reported that the measurement of a gas mixture against a pure gas would lead to less accurate results. Therefore, it had to be tested whether a difference in the Ar/O₂ ratio between sample and reference of this magnitude would influence the resulting $\delta^{17}\text{O}$ and $\delta^{18}\text{O}$.

For this, different amounts of pure argon were added to pure oxygen, creating mixtures of $\sim 0\text{-}5\%$ Ar in oxygen (in steps of 1%), and measuring the resulting mixtures (collected using molecular sieves) against both the pure oxygen (0% Ar) used for the mixtures, and against the O₂-Ar reference mixture (4.7% Ar in O₂) on the MAT 252. (In addition, the pure oxygen was measured as sample against the different O₂-Ar mixtures.)

The O₂-Ar reference gas had a different isotopic composition from the pure O₂ reference gas (offset ~ -3.45 , ~ -6.76 ‰ and ~ 50 ppm for $\delta^{17}\text{O}$ and $\delta^{18}\text{O}$ and $\Delta^{17}\text{O}$ respectively). Results are displayed in **Figure 11-14**.

In all cases, results indicated differences in the Ar content between the sample and the reference (variations in $\delta(\text{Ar}/\text{O}_2)$) in this range (0-5% Ar in O₂, $\delta(\text{Ar}/\text{O}_2)$ down to -1000‰ relative to the 4.7% Ar in O₂ reference), did not significantly affect the $\Delta^{17}\text{O}$ (**Figure 11 and 12**). A linear relationship was found between $\delta(\text{Ar}/\text{O}_2)$ and $\delta^{17}\text{O}$ and $\delta^{18}\text{O}$, with $\delta^{17}\text{O}$ and $\delta^{18}\text{O}$ increasing with increasing $\delta(\text{Ar}/\text{O}_2)$ (as reported by Barkan and Luz and Abe and Yoshida (2003)).

However, within this $\delta(\text{Ar}/\text{O}_2)$ range, the effect and thus corresponding correction of the $\delta^{17}\text{O}$ and $\delta^{18}\text{O}$ results was very small (for biological samples, the effect of the applied correction was up to $\sim +0.003\text{‰}$ for $\delta^{17}\text{O}$ and $\sim +0.005\text{‰}$ for $\delta^{18}\text{O}$, while the corresponding effect on $\Delta^{17}\text{O}$ was 0-1 ppm, see next page).

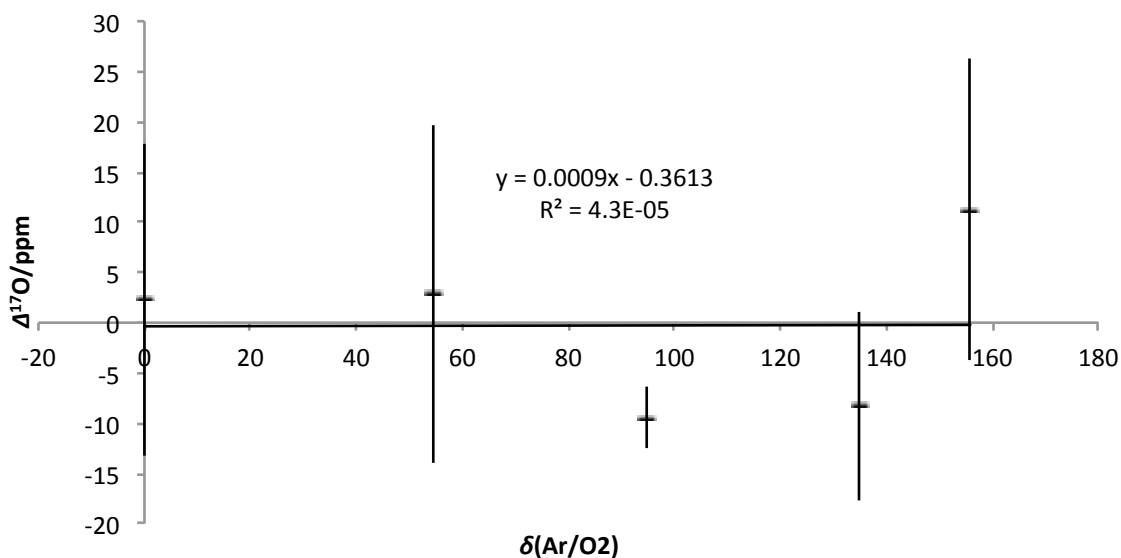


Figure 11: Effect of variations in $\delta(\text{Ar}/\text{O}_2)$ (relative Ar content) on the $\Delta^{17}\text{O}$ (ppm). Pure O_2 mixed with 1-5% Ar, collected on molecular sieves and measured on the MAT 252 against the pure O_2 gas (0% Ar). $\delta(\text{Ar}/\text{O}_2)$ is displayed as absolute value. All measurements were performed in triplicate and error bars show ± 1 SD.

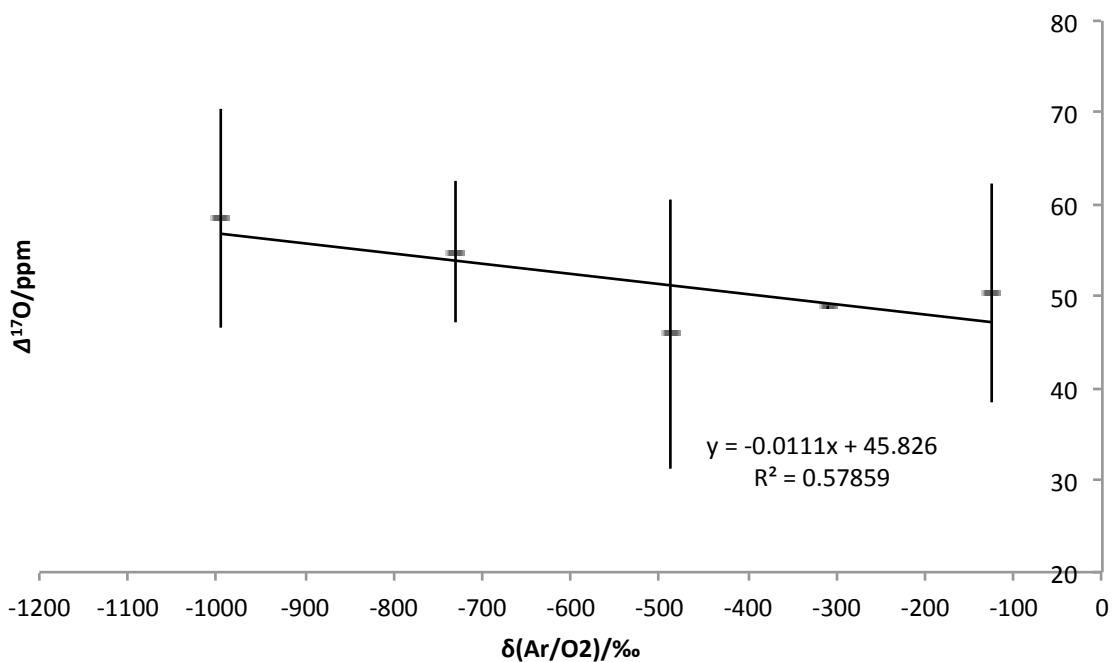


Figure 12: Effect of variations in the $\delta(\text{Ar}/\text{O}_2)$ (relative Ar content) on the $\Delta^{17}\text{O}$. Mixtures of pure O_2 with 0-5% added Ar, collected on molecular sieves and measured on the MAT 252 against an O_2 -Ar reference gas (4.7% Ar in O_2). Direct comparison of the isotopic composition of both reference gases indicated the pure O_2 gas has a $\delta^{17}\text{O}$, $\delta^{18}\text{O}$ and $\Delta^{17}\text{O}$ of ~ -3.45 , ~ -6.76 ‰ and ~ 50 ppm relative to the O_2 -Ar reference gas. All measurements were performed in triplicate and error bars show ± 1 SD. (Note: the $\Delta^{17}\text{O}$ at $\delta(\text{Ar}/\text{O}_2) = \sim -1000$ ‰ is relatively high, but in this case the

sample contained ~0% while the reference contained 4.7% Ar, which might have led to less precise results (Barkan and Luz 2003)).

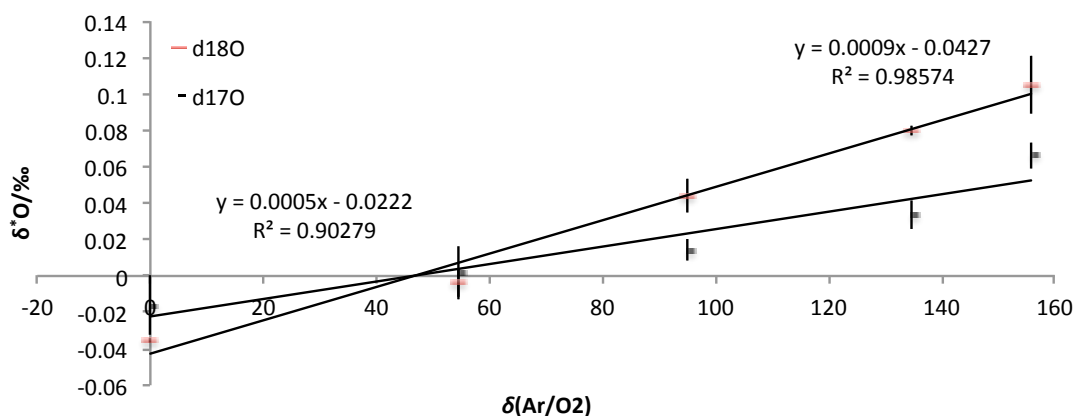


Figure 13: Effect of changes in $\delta(\text{Ar}/\text{O}_2)$ on the $\delta^{17}\text{O}$ and $\delta^{18}\text{O}$. Pure O_2 mixed with 0-5% Ar, collected on molecular sieves and measured on the MAT 252 against the pure O_2 gas. Note: $\delta(\text{Ar}/\text{O}_2)$ is displayed as absolute (not %) value. All measurements were performed in triplicate and error bars show ± 1 SD.

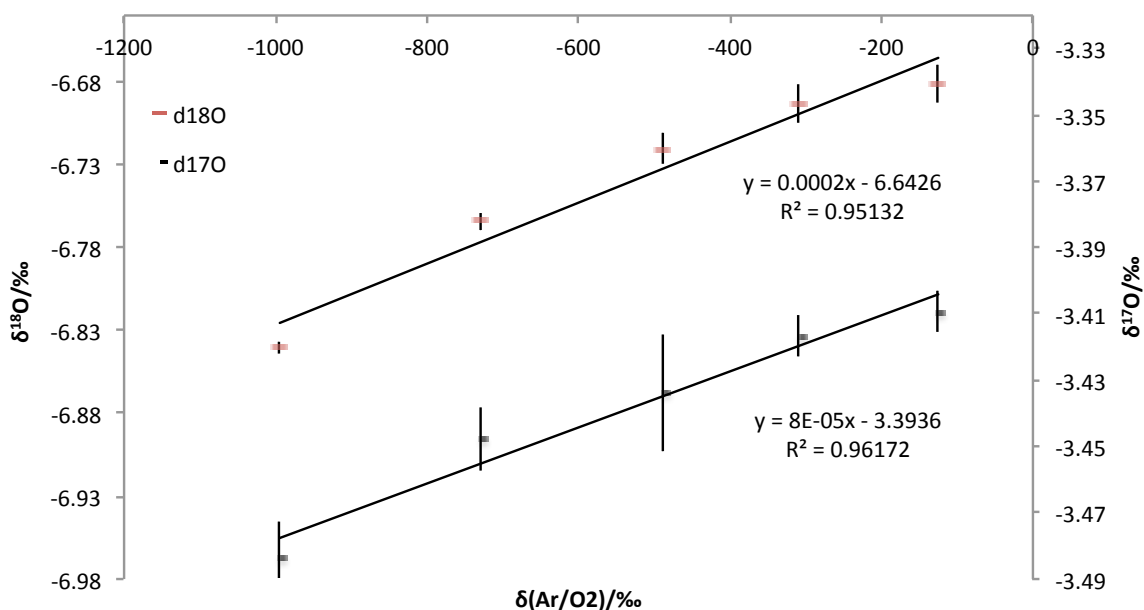


Figure 14: Effect of variations in the $\delta(\text{Ar}/\text{O}_2)$ on the $\delta^{17}\text{O}$ and $\delta^{18}\text{O}$, mixtures of pure O_2 with 0-5% added Ar, collected on molecular sieves and measured on the MAT 252 against a an O_2 -Ar reference gas (4.7% Ar in O_2). Direct comparison of the isotopic composition of both reference gases indicated the pure O_2 gas has a $\delta^{17}\text{O}$, $\delta^{18}\text{O}$ and $\Delta^{17}\text{O}$ of ~ -3.45 , ~ -6.76 ‰ and ~ 50 ppm relative to the O_2 -Ar reference gas. All measurements were performed in triplicate and error bars show ± 1 SD.

For the biological O₂ samples, the correction based on measurements against pure O₂ does not change $\delta^{17}\text{O}$ and $\delta^{18}\text{O}$ values more than $\sim 0.005\%$, and $\Delta^{17}\text{O}$ more than 1 ppm. The correction based on measurements of the mixtures against a different O₂-Ar mixture (4.7% Ar in O₂, *BOC Ltd.*, Australia ($\Delta^{17}\text{O}$ offset ~ 50 ppm, $\delta^{17}\text{O}$ and $\delta^{18}\text{O}$ ~ -3.45 and ~ -6.76 resp.)), would increase $\delta^{17}\text{O}$ values with ~ 0.050 - 0.070% and $\delta^{18}\text{O}$ values with ~ 0.130 - 0.160% . The corresponding change in $\Delta^{17}\text{O}$ is a decrease of 7 ppm for all days of *Picochlorum* and the first days of *E. huxleyi*, and a (maximal) decrease of 9 ppm, for the final days of *E. huxleyi* (10 ppm for the final day of the 5-day repetition, 9 ppm for the final day samples of other series). This would decrease the resulting $\Delta^{17}\text{O}_{\text{S0}}$ values to ~ 173 and ~ 240 ppm, respectively. This difference is within the error of the results, and would not substantially change the conclusions. Because this correction would introduce an extra error, while it would not significantly change the results, and the measurements against pure O₂ indicated no effect on the $\Delta^{17}\text{O}$, while for the measurements against O₂-Ar only a weak relationship ($R^2 = 0.58$) was found between $\delta(\text{Ar}/\text{O}_2)$ and $\Delta^{17}\text{O}$, it was chosen to apply the weak correction, based on measurements against pure O₂, to the results (corresponding to $+0.0003 \cdot \delta(\text{O}_2/\text{Ar})$ and $+0.0007 \cdot \delta(\text{O}_2/\text{Ar})$ for $\delta^{17}\text{O}$ and $\delta^{18}\text{O}$ resp., where $\delta(\text{O}_2/\text{Ar})$ is the absolute value).

2.3.2.4 Solubility correction

Correction for solubility/distribution between headspace and water phase

For air-equilibrated water tests, $\delta^{17}\text{O}$, $\delta^{18}\text{O}$ and $\delta(\text{O}_2/\text{Ar})$ values had to be corrected for the distribution of gases between headspace and water phase in sample bottles.

$\delta(\text{O}_2/\text{Ar})$ was corrected (following Luz et al. 2002) according to:

$$\delta(\text{O}_2/\text{Ar})_{\text{corr}}/\text{‰} = [Q \cdot (\delta(\text{O}_2/\text{Ar})_{\text{meas}} + 1) - 1] \cdot 1000$$

(note: $\delta(\text{O}_2/\text{Ar})_{\text{meas}}$ here refers to the absolute value),

where

$$Q = \frac{1 + L(\text{O}_2) \cdot f_V}{1 + L(\text{Ar}) \cdot f_V}$$

L is the Ostwald solubility coefficient in $\text{ml L}^{-1} \text{atm}^{-1}$ for the temperature in the laboratory, and f_V is the ratio of water over headspace volume ($V_{\text{aq}}/V_{\text{gas}}$).

$$f_V = V_{\text{aq}}/V_{\text{gas}}$$

$\delta^*\text{O}$ values (* refers to either ¹⁷ or ¹⁸) were corrected according to:

$$\delta^*\text{O}_{\text{corr}} = Q \cdot \delta^*\text{O}_{\text{meas}}$$

Where

$$Q = \frac{1 + L(^*\text{O}^{16}\text{O}) \cdot f_V}{1 + L(^{16}\text{O}_2) \cdot f_V}$$

and

$$L(*O^{16}O) = L(^{16}O_2) \cdot (1 + \delta^*O_{\text{sat}})$$

In the air-equilibrated water tests (**Chapter 4**), f_V was close to 1. For $\delta(O_2/Ar)$, Q was ~ 0.997 and the resulting correction was -2 to -3% . For $\delta^{18}O$, Q was ~ 1.02 and the correction was $+0.01$ to $+0.02\%$. For $\delta^{17}O$, no definite $\delta^{17}O_{\text{sat}}$ value is available from literature, but the effect is expected to be mass dependent, and not to significantly affect the $\Delta^{17}O$ (J. Kaiser, pers. com. 2013).

2.3.3 Standardisation with respect to atmospheric air

All values were initially calculated relative to the O_2 -Ar working reference, and, for biological and equilibrated water samples, had to be standardised against atmospheric air. For this, results were recalculated using the composition of dry air aliquots prepared together with the samples and measured against the same reference.

Atmospheric O_2 is the preferred isotopic reference for natural molecular oxygen because it is closest in composition to the samples (Barkan and Luz 2003, 2005). Also atmospheric air is assumed to have a (globally) constant composition, which facilitates comparison of results. Therefore all results were standardized against atmospheric air.

This was done by processing aliquots of cryogenically dried atmospheric air (dry air, or DA) on the separation line in an identical way to the samples and subsequently measuring their composition against the same O_2 -Ar reference gas (and applying the same corrections). The average composition of DA (with respect to the O_2 -Ar reference gas) over the time frame of sample processing could then be used to standardize the (N_2 and imbalance corrected) $\delta^{17}O$, $\delta^{18}O$ and $\delta(O_2/Ar)$ results of the samples vs. atmospheric air according to:

$$\delta^*_{\text{sa/air}}/\text{‰} \approx \delta^*_{\text{sa/DA}}/\text{‰} = \left[\frac{\delta^*_{\text{sa/ref}} - \delta^*_{\text{DA/ref}}}{\delta^*_{\text{DA/ref}} + 1} \right] \cdot 1000$$

Where ‘*’ can be ^{17}O , ^{18}O or O_2/Ar , ‘sa’ stands for sample, ‘DA’ stands for dry air and ‘ref’ stands for the working reference O_2 -Ar mixture. Note: δ -values in this equation are absolute (not ‰) values.

Used $\delta^{17}O$, $\delta^{18}O$ and $\delta(O_2/Ar)$ values for dry air in the above formula were $-0.477 \cdot 10^{-3}$, $-0.879 \cdot 10^{-3}$ and $136.1 \cdot 10^{-3}$ respectively, based on the average of (corrected) dry air results obtained in the period 06-09/2013 (see **Table 1**).

Because the DA standard went through the same purification process as the samples, any fractionation during the purification process would be expected to affect the sample and standard in the same way, and would thus be cancelled out in the final results.

2.3.4 Calculation of ^{17}O excess

From the resulting $\delta^{17}\text{O}$ and $\delta^{18}\text{O}$ values, the $\Delta^{17}\text{O}$ (^{17}O excess) could be calculated. Different definitions for ^{17}O excess have been used and recommended in the past (Barkan and Luz 2000, Miller et al. 2002, Angert et al. 2003, Barkan and Luz 2005, Kaiser 2011a, Nicholson 2011, Kaiser and Abe 2012), each with their own merits and/or disadvantages. As explained by Kaiser (2011) it does not really matter which definition is used, as long as it is used consistently, it is clearly stated which definition was used and underlying $\delta^{17}\text{O}$ and $\delta^{18}\text{O}$ results are reported with any calculated $\Delta^{17}\text{O}$ values (Kaiser 2011). In this study, the linear definition is used, following Kaiser 2011 and Kaiser and Abe 2012, because of its mathematical simplicity. For the lambda coefficient the value of 0.5179 was adopted, which corresponds to the weighted average ratio between discrimination against $^{17}\text{O}^{16}\text{O}$ and $^{18}\text{O}^{16}\text{O}$ during respiration for a wide range of organisms and experimental conditions (Barkan and Luz, 2005):

$$\Delta^{17}\text{O}/\text{ppm} = [\delta^{17}\text{O} - 0.5179 \cdot \delta^{18}\text{O}] \cdot 1000$$

where $\delta^{17}\text{O}$ and $\delta^{18}\text{O}$ are the values in ‰.

2.4. Reproducibility and performance tests of MS and separation line

In order to test the performance of the purification line, aliquots of O_2 -Ar reference gas and dry air were regularly processed on the line in the same way as samples and measured on the MS against the same O_2 -Ar reference gas. Results are displayed in **Table 1**. In addition, as mentioned in **Section 2.3.1**, zero enrichments were performed on the MAT 252 on each measurement day, during which the O_2 -Ar reference gas was measured against itself, in order to test the functioning of the mass spectrometer. Results of zero enrichments are displayed in **Table 1**. All results were corrected for imbalance and nitrogen interference using the corrections described in **Section 2.3.2**, and $\Delta^{17}\text{O}$, $\delta(\text{O}_2/\text{Ar})$ and $d(\text{N}_2/\text{O}_2)$ were calculated using above-mentioned equations. Values are averages of all conducted MS runs, and the error is based on the number of individual runs. All results are reported with respect to the O_2 -Ar reference gas. For comparison purposes, results of similar tests conducted by Gloël (2012) and González-Posada (2012) during 2011 and 2012 are included in **Table 1**.

Table 1: Results of performance tests of the separation line, mass spectrometer and transfer to the MS using 5 zeolite molecular sieve pellets. Results of this study are displayed in bold. For comparison purposes, results of similar tests conducted in 2011 and 2012 by J. Gloël (2012) (G) and A. González-Posada (2012) (GP) are included in the same table.

Procedure	Time frame	$\delta^{17}\text{O}/\text{‰}$	SD	95% CI	$\delta^{18}\text{O}/\text{‰}$	SD	95% CI	$\Delta^{17}\text{O}/\text{ppm}$	SD	95% CI	$\delta(\text{O}_2/\text{Ar})/\text{‰}$	SD	95% CI	n
Zero enrichment	06-09/2013	-0.010	0.010	0.003	-0.012	0.012	0.003	-3	10	3	0.1	0.1	0.0	54
	06-08/2012 (GP)	-0.006	0.011	0.003	-0.004	0.015	0.003	-4	14	3	0.1	0.1	0.0	98
	03-05/2011 (G, GP)	-0.006	0.018	0.003	-0.023	0.020	0.003	6	20	3	0.1	1.2	0.2	140
O ₂ -Ar through line	06-09/2013	0.010	0.031	0.011	0.026	0.053	0.019	-4	13	5	0.3	0.9	0.3	30
	03/2011 (G, GP)	0.008	0.025	0.007	0.017	0.046	0.013	0	13	4	-2.2	3.1	0.9	45
Dry air through line	06-09/2013	-0.477	0.026	0.006	-0.879	0.049	0.012	-21	11	5	136.1	0.8	0.2	80
	05/2011 (G, GP)	-0.471	0.022	0.007	-0.864	0.043	0.013	-23	15	5	133.1	1.3	0.4	42
O ₂ -Ar 5 mol. sieve to MS	06-09/2013	-0.008	0.011	0.012	-0.021	0.013	0.015	3	6	7	-9.8	0.7	0.8	3
	04/2011 (G, GP)	-0.004	0.010	0.005	-0.013	0.021	0.010	2	9	4	-3.0	1.6	0.8	17
Internal precision MS '13		$\delta^{17}\text{O}/\text{‰}$			$\delta^{18}\text{O}/\text{‰}$									
Avg std. dev.		0.047			0.020									
Avg std. error		0.009			0.004									

As can be observed, results obtained during 2013 are comparable to those obtained by Gloël (2012) and González-Posada (2012) in 2011 and 2012. Differences in $\Delta^{17}\text{O}$ and $\delta^{17}\text{O}$, $\delta^{18}\text{O}$ values (for either zero enrichments, dry air or processed O₂-Ar aliquots) are not significant, considering the standard deviations. While the standard deviation in zero enrichment results is slightly smaller than during similar tests in 2011 and 2012, the standard deviation in the results of dry air and O₂-Ar reference aliquots processed through the separation line is slightly larger than during similar tests conducted by Gloël (2012) and González-Posada (2012) (0.026-0.031 and 0.049-0.053‰ vs. 0.022-0.025 and 0.043-0.046‰ for $\delta^{17}\text{O}$ and $\delta^{18}\text{O}$ results from 2013 and 2011, respectively). However, differences are small.

The standard deviation of $\delta(\text{O}_2/\text{Ar})$ results has however considerably decreased since 2011 (0.1‰ (2013) vs. 1.2‰ (2011) for zero enrichments and 0.9‰ (2013) vs. 3.1‰ (2011) for O₂-Ar through the line). Since this difference can also be observed in the zero enrichments results, the improvement is probably largely related to changes in the mass spectrometer.

In addition, for O₂-Ar aliquots processed though the line in 2011 a slightly negative $\delta(\text{O}_2/\text{Ar})$ was obtained (-2.2‰ for aliquots processed through the separation line vs. 0.1‰ for zero enrichments), possibly indicating some loss of oxygen. This could however be (partly) related to the uncertainty in the MS results, since the SD was 3.1‰. In this study, no significant elemental fractionation due to the purification process was observed, the resulting $\delta(\text{O}_2/\text{Ar})$ for O₂-Ar aliquots processed through the line being (0.3±0.9)‰ (±SD) vs. (0.1±0.0)‰ for zero enrichments.

The slightly more negative $\delta(\text{O}_2/\text{Ar})$ obtained for line-processed O₂-Ar in 2011 compared to 2013 is accompanied by a slightly more negative $\delta(\text{O}_2/\text{Ar})$ for dry air for

2011 compared to 2013 ((133.1±1.3)‰ vs. (136.1±0.8)‰ for 2013). It should however be realised the results for dry air relative to the reference gas depend on the specific composition of both standards, and it is not likely exactly the same reference gas flasks were used in 2011 and 2013 (since reference gas flasks are refilled regularly). However, results for dry air are still comparable between tests from 2011 and 2013.

Results of O₂-Ar aliquots processed through the line indicate a small increase in $\delta^{17}\text{O}$ and $\delta^{18}\text{O}$, and thus enrichment in heavy isotopes, due to the purification process (values of 0.010 and 0.026‰ were obtained for O₂-Ar aliquots processed through the line, while $\delta^{17}\text{O}$ and $\delta^{18}\text{O}$ average values obtained during zero enrichments are -0.010 and -0.012‰ respectively). The same was observed in 2011 (values of 0.008 and 0.017‰ for processed O₂-Ar vs. -0.006 and -0.023‰ for directly introduced O₂-Ar). However, differences are small, and because the DA standard went through the same purification process as the samples, any fractionation during the purification process would be expected to affect the sample and standard in the same way, and thus to be cancelled out in the final results. No significant effect of the purification process on the $\Delta^{17}\text{O}$ was observed, which for this study was (-3±10) ppm (±1 SD) for zero enrichments and (-4±13) ppm for O₂-Ar processed on the separation line.

In order to test the effect of using molecular sieve pellets in the final transfer of samples to the MS, Gloël and González-Posada also conducted tests freezing aliquots of O₂-Ar reference gas into stainless steel fingers with 5 molecular sieve pellets at -196 °C and then transferring the samples to the MS. Comparable tests were conducted for this study during the molecular sieve transfer tests (**Chapter 3, Section 3.2**). Just as for the tests of Gloël and González-Posada, slightly negative $\delta^{17}\text{O}$ and $\delta^{18}\text{O}$ values were obtained ((-0.008±0.012) and (-0.021±0.015)‰ (±95% confidence interval) for $\delta^{17}\text{O}$ and $\delta^{18}\text{O}$ resp.), but results were not significantly different from those obtained during zero enrichments (average results of zero enrichments also being slightly negative, see **Table 1**). The $\Delta^{17}\text{O}$ was also within the standard deviation of zero enrichments ((3±6) ppm). It should be noted that these tests were performed in triplicate, so the error is relatively large compared to the error for results displayed in this table. Finally, the effect of this transfer step is of course included in the results of the DA and processed O₂-Ar aliquots.

Air-equilibrated water tests

Finally, to test the combined effect of the whole procedure (water sampling, extraction of dissolved air, and the processing of air samples on the extraction and separation line and MS) air-equilibrated water tests were performed. Because air is assumed to have an approximately globally constant O₂ isotopic composition and O₂/Ar ratio, and the

expected equilibrium values of $\delta^{18}\text{O}$ and $\delta(\text{O}_2/\text{Ar})$ of dissolved air are known, results can be directly compared to equilibrium values from literature and results from other labs, and in this way the performance and accuracy of the whole method can be tested.

Air-equilibrated water tests were performed with different water types and temperatures. Tests and results are described in detail in **Chapter 4**. Tests with distilled water with 35 g l^{-1} NaCl produced $\delta^{18}\text{O}$ values very close (within $\sim 0.02\text{‰}$) to equilibrium values reported by Benson and Krause (1984) ($(0.695 \pm 0.06)\text{‰}$ (± 1 SD) vs. 0.717‰ ($22 \text{ }^\circ\text{C}$) and $(0.619 \pm 0.02)\text{‰}$ vs 0.638‰ ($39 \text{ }^\circ\text{C}$) respectively). Both for tests with distilled and saline water, obtained $\delta(\text{O}_2/\text{Ar})$ values were very close (within $\sim 1\text{‰}$) to equilibrium values reported in literature (Hamme and Emerson 2004) and observed in similar studies (for room temperature tests ($22 \text{ }^\circ\text{C}$) average $\delta(\text{O}_2/\text{Ar})$ results were $(-88.5 \pm 0.9)\text{‰}$ for distilled and $(-89.2 \pm 0.9)\text{‰}$ for 35 g l^{-1} NaCl water, close to results of Barkan and Luz 2003 ($(-88.8 \pm 0.4)\text{‰}$), Sarma et al. 2006b ($(-87.4 \pm 1)\text{‰}$) and Castro-Morales 2010 ($(-88.4 \pm 1)\text{‰}$) for comparable tests). Finally, over all tests conducted at room temperature ($22 \text{ }^\circ\text{C}$), an average $\Delta^{17}\text{O}$ of (17 ± 9) ppm (± 1 SD) was obtained, which is in the range of $\Delta^{17}\text{O}$ values found by other laboratories for comparable tests (Kaiser 2011).

These results indicate elemental and isotopic fractionation over the whole sample preparation process is probably small, and there is no indication that the extraction procedure involving molecular sieves and a liquid nitrogen cold trap severely influences the results.

Chapter 3 – Method development and improvement: molecular sieve transfer tests

Abstract

In the stable isotope lab at UEA, zeolite 5Å molecular sieves and liquid nitrogen are currently used to trap and transfer samples for triple O₂ isotope analysis at different stages of the preparation process (from the extraction line to the separation line, in between traps on the separation line and from the separation line to the IRMS). Because it has been reported that elemental and isotopic fractionation can take place due to incomplete desorption of samples from molecular sieve zeolite (MSZ), the amount of fractionation increasing with the quantity of MSZ used (Barkan & Luz 2003, Abe 2008), the used amount of molecular sieve is kept to a minimum (5 pellets, 1.6 x 6 mm). However, with the currently used amount of MSZ, collection of samples under low pressure can take up to 30-40 minutes per sample. Increasing the number of molecular sieve pellets used during extraction would decrease freezing time, but could potentially lead to increased fractionation of the sample gas. In order to assess the effect of increasing the molecular sieve amount used during transfer of O₂-Ar samples for triple oxygen isotope analysis, tests were performed transferring O₂-Ar reference gas using different quantities of zeolite 5Å molecular sieves and liquid nitrogen, and measuring the isotopic and elemental composition of the transferred gas on a MAT 252 IRMS against the directly-introduced reference gas. Tests were performed with different line volumes and both with and without a cold trap on line, in order to simulate conditions generally encountered during sample processing. Results indicate that increasing the number of pellets used during extraction from 5 or 6 to 10 will lead to a decrease in transfer time of 20-30 minutes per sample, and can take place without significant increase in fractionation, as long as the gas is desorbed from these pellets under cryotrapping and final transfer to the MS takes place using 5 pellets. Increasing the number of pellets used during transfer to the MS from 5 to 10 would lead to a strong increase in (mass-dependent) fractionation and should therefore be discouraged. In all cases, small but significant negative fractionation (loss of heavy isotopes) was observed when a liquid nitrogen trap was present on the line and when the pressure in the line was lowered by expansion into a sample bottle. All observed fractionation was however mass-dependent, no effect was observed on the $\Delta^{17}\text{O}$ for any of the tested scenarios.

3.1 Introduction

Molecular sieves are microporous crystalline solids with a specific pore diameter that allows them to cryogenically trap, transfer and separate certain gases based on their specific diameter, polarity and boiling point. Different types of molecular sieves exist, with different chemical compositions and pore diameters, each suited to trap molecules within a specific size range. In stable isotope studies, synthetic zeolite molecular sieves are often used, which have an aluminosilicate structure that can include different cations, the cation included determining the pore size of the sieve. In triple oxygen isotope studies, zeolite 5Å (the Ca-type of zeolite, which can trap molecules with a diameter < 5 Å; 1 Å = 0.1 nm) molecular sieves are often used for the cryogenic trapping and transfer of oxygen-argon samples within vacuum systems and separation of oxygen and argon from nitrogen (Karlsson 2004).

It has however been reported (Barkan & Luz 2003, Abe 2008) that the use of molecular sieves can lead to fractionation of the transferred gas. Reported reasons for this fractionation include chemisorption, exchange of oxygen between host lattice and guest molecules, exchange of oxygen with other guest molecules and fractionation due to different diffusion rates of the isotopologues into and out of the molecular sieve structure (Karlsson 2004). Different diffusion rates in and out of the molecular sieves will only lead to fractionation when recovery of the gas during adsorption or desorption is not complete. This is, however, the case when molecular sieves are used to introduce gas into a dual-inlet mass spectrometer. In this case, the gas is expanded based on a pressure difference, and an equilibrium fraction of gas will always stay adsorbed on the sieves, the exact amount depending on the pressure, temperature and void volume of the molecular sieves (Barkan & Luz, 2003, Abe 2008).

Recently, fractionation of oxygen during transfer to the mass spectrometer, due to incomplete desorption from zeolite molecular sieves (type 13X and 5Å) was reported by Barkan and Luz (2003) and Abe (2008). In both studies fractionation against the heavy isotopes was observed ($\delta^{17}\text{O}$ and $\delta^{18}\text{O}$: -0.05 to -0.3‰) when sample gas was expanded from 5Å molecular sieves into the inlet system of a dual-inlet (IR) mass-spectrometer, the fractionation increasing with the quantity of molecular sieve material used. Barkan and Luz therefore suggest the use of liquid Helium for transfer of samples to the MS, while Abe suggests using a minimum amount of MSZ and heating the molecular sieves before admission to the MS (10 minutes at 60 °C) in order to maximise desorption (Barkan & Luz 2003, Abe 2008).

According to Barkan and Luz (2003), fractionation during desorption from molecular sieves is not an issue when desorption is complete due to simultaneous trapping of the desorbed gas. According to Abe (2008), incomplete recovery during adsorption on molecular sieves can also lead to (mass-dependent) fractionation against the heavy isotopes, but this effect is smaller and can be minimised by assuring sufficient (close to 100%) adsorption of the sample.

Currently, in the stable isotope lab at UEA, molecular sieves of type zeolite 5Å and liquid nitrogen are used for the transfer of samples for triple oxygen isotope analysis from the sample extraction line to the separation line, between parts of the separation line and from the separation line to the IRMS (see **Chapter 2**). In order to minimise the risk of fractionation due to incomplete desorption, 5 pellets (*Sigma-Aldrich*, 1.6 x 6 mm, comparable in volume to 1-2 pellets in the study of Abe, 2008) are used for transfer to the MS, while 5 or 6 pellets are used during extraction, and pellets are heated to 60 °C for 10-20 minutes prior to release of the sample gas (Gloël 2012, González-Posada 2012, A. Marca, personal communication, 2013). It had been found that when these sieve amounts were used, in combination with heating prior to sample release, the amount of fractionation of the transferred gas was negligible (Gloël 2012, González-Posada 2012). This approach was chosen over the use of liquid Helium, as recommended by Barkan and Luz (2003), for safety and economic reasons.

However, when using 5 or 6 pellets, collection of samples from large volume (350 ml) sample bottles can take up to 40 minutes per sample on the currently-used extraction and separation line (taking a minimum recovery of 99.8%). Increasing the number of pellets used during extraction would decrease freezing time (by increasing the total adsorption capacity of the sieves), but could potentially lead to increased fractionation of the sample gas.

In order to assess whether increasing the amount of molecular sieves used during extraction would be possible without significantly increasing fractionation, tests were performed, transferring O₂-Ar reference gas with different quantities of zeolite 5Å molecular sieve, under different line conditions, and measuring the isotopic and elemental composition of the transferred gas on a MAT 252 isotope ratio mass spectrometer against the directly-introduced reference gas. In order to simulate conditions generally encountered during sample processing, tests were performed with

either one or two transfer steps, different line volumes and both with and without a -196 °C trap on line.

This chapter is dedicated to tests to optimise the amount of molecular sieve pellets used that leads to minimum transfer time without sample fractionation. In addition, the effect of different transfer conditions (cold trap, line pressure, heating) on the isotopic and elemental composition of transferred gas is assessed.

3.2 Methods

In order to assess whether increasing the molecular sieve amount used during extraction would be possible without fractionating the sample gas, transfer tests were conducted with different numbers of molecular sieve pellets under different conditions. An aliquot of O₂-Ar reference gas was collected on 5, 6 or 10 pellets (Sigma-Aldrich zeolite 5Å, 1.6 by 6 mm), and either released straight from these pellets into the MS, or first transferred to 5 pellets and then released into the MS (comparable to the current approach at the end of sample preparation).

In the next three paragraphs, a description of the performed tests, the extraction line and the experimental procedure will be given.

3.2.1 Description of transfer tests

Tests were performed by freezing an aliquot of a working reference O₂-Ar mixture on to different numbers of molecular sieve pellets at liquid-N₂ temperature under different (pressure and cold trap) conditions, and subsequently measuring the transferred gas on the IRMS against the same reference gas, introduced directly (differences in isotopic composition between the directly admitted reference gas and the reference gas transferred using molecular sieves being an indication of fractionation during the transfer process).

In addition to ‘single transfer’ tests, in which gas was frozen on 5, 6 or 10 pellets of MSZ and subsequently released into the DI-IRMS (in order to test the effect of MSZ quantity during final transfer), tests were performed in which gas was frozen on 6 or 10 pellets and subsequently on 5 pellets before being released into the MS (‘double transfer’ tests). The use of 5 pellets for transfer to the MS has been tested thoroughly and is currently the general approach in the UEA stable isotope lab. In this way, the effect of increasing the quantity of MSZ during extraction or intermediate transfer could

be assessed. Double transfer tests were performed both with and without heating (20 minutes at ~ 60 °C) of the molecular sieves with sample before the second transfer to 5 pellets. In all cases, tubes containing molecular sieves with samples were heated (as described above) prior to release of the samples in the MS, as advocated by Abe (2008).

In order to simulate the extraction of gas from a 350 ml sample bottle, which generally takes place at relatively low pressure and thus requires a relatively long freezing time, one aliquot of reference gas was first expanded into a 350 ml sample bottle and then transferred from this bottle on to the molecular sieves. Due to the large volume of the sample bottles, their presence resulted in a relatively low pressure in the line (~ 2 -4 vs. ~ 50 -60 mbar for transfers straight from the reference flask). In this way the freezing of samples at both high and low pressure could be tested. Sample bottles were evacuated down to $\sim 1.9 \times 10^{-7}$ mbar and gas was left to mix for 10 minutes after expansion.

In addition, the effect of the presence of a liquid nitrogen (-196 °C) trap on the extraction line was assessed. During the processing of gas samples from seawater for triple oxygen isotope analysis, a cold trap is always present on the extraction line for the removal of H_2O and CO_2 . According to Barkan and Luz (2003), oxygen and argon can freeze on water ice at liquid nitrogen temperature, which could lead to isotopic and elemental fractionation. They therefore suggest the trapping of water vapour at dry ice temperature (-78 °C) before introduction of the sample to a liquid nitrogen trap (-196 °C). For this reason, Gonzalez-Posada (2012) and Gloël (2012) only used -78 °C traps on the extraction line, while currently a -78 °C and -196 °C trap are used. The effect of admitting the sample straight to a -196 °C trap, without prior removal of water vapour, was tested by performing transfer tests with and without liquid nitrogen cold trap on the line. The cold trap used in these tests had a volume of ~ 180 ml. As a result its presence strongly increased the line volume, and decreased the pressure after loading of a sample from ~ 50 to ~ 5 mbar. Tests conducted with liquid nitrogen trap on line are indicated by 'cold trap'.

The following transfer tests were performed:

- 5 pellets, high pressure (*HP*);
- 5 pellets, cold trap;
- 5 pellets, low pressure (*LP*), cold trap;
- 6 pellets, *HP*;
- 6 pellets, *LP*, cold trap;
- 10 pellets, *HP*;
- 10 pellets, *LP*, cold trap;
- 6>5 pellets, *HP*;
- 6>5 pellets, *HP*, not heated;
- 10>5 pellets, *HP*;
- 10>5 pellets, *LP*;
- 10>5 pellets, *LP*, not heated;
- 10>5 pellets, *LP*, cold trap.

Numbers refer to the number of molecular sieve pellets the O₂-Ar reference gas was frozen on. '6>5' indicates gas was first frozen on to 6 pellets and then transferred from these 6 pellets to 5 pellets, prior introduction to the IRMS. 'Not heated' indicates samples were not heated before the second transfer to 5 pellets. 'High pressure' or '*HP*' indicates the gas was transferred directly from the reference flask, which resulted in an initial line pressure of ~50-60 mbar, while 'low pressure' ('*LP*') indicates gas was first expanded into a 350 ml sample bottle, which resulted in a low pressure in the line (~2-5 mbar) at the start of transfer. 'Cold trap' indicates the presence of a liquid nitrogen trap on the line (-196°C), which increased the line volume from ~20 to ~200 ml. In the second test, '5 pellets, cold trap', the O₂-Ar reference gas was transferred straight from the flask, but at a relatively low pressure due to the presence of the cold trap.

In each case, an aliquot of a working reference O₂-Ar mixture was frozen on to a specific number of zeolite 5Å molecular sieve pellets at liquid nitrogen temperature. After transfer, tubes containing the molecular sieves were heated for 20 minutes at ~60 °C (in hot water) after which samples were released into the Dual-Inlet IRMS where their oxygen triple isotopic composition was measured relative to that of an aliquot of the same O₂-Ar mixture introduced directly.

A more detailed description of the materials and procedure will be given in the next sections.

3.2.2 Description of materials and extraction line

The used molecular sieves were pellets of synthetic zeolite 5Å from *Sigma-Aldrich* with a 1.6 mm diameter. Only pellets of ~5-7 mm length were selected. Pellets were kept in 2.5 ml glass collection tubes, with high-vacuum compression o-ring valves (*Glass Expansion*, Melbourne), which were immersed in liquid nitrogen during sample collection and in heated water before sample release. The transferred gas was a working reference mixture of 4.7% Ar in O₂, (*BOC Ltd., Australia*). Transfer tests were performed on the extraction line described in **Section 2.1**, and samples were analysed on a MAT 252 DI-IRMS. A brief description of the line and transfer procedure for these specific tests will be given below.

As described in **Chapter 2 Section 2.2.1**, for the extraction of sample gases and their transfer to molecular sieve pellets in storage tubes, a small high-vacuum extraction line was used. The line consisted of (6-12 mm o.d.) stainless steel and glass tubing, an optional ~180 ml glass trap, a pressure gauge (*Pfeiffer Vacuum, Activeline* capacitance gauge), three manual high-vacuum valves (*Louwers Hapert*) and two connection ports, connected via a manual valve to a turbomolecular drag pump (*Pfeiffer Vacuum, TMU071P*). The total volume of the line was approximately 200 ml, and generally a vacuum of $1.6-1.9 \times 10^{-7}$ mbar could be obtained all around. For these tests a maximum pressure of 3×10^{-7} mbar was accepted. A pressure gauge ($> 5 \times 10^{-4}$ mbar) was used to check the line for leaks and monitor the pressure drop during freezing. The collection tube containing the molecular sieves, a glass sample tube of constant dimensions (2.5 ml, ~50 mm length, ~8 mm internal diameter) with a compression o-ring high-vacuum valve (*Glass Expansion (GE)*), was attached to the line at the connection point closest to the pump, using a *Swagelok Ultra-Torr* fitting. At the location furthest from the pump, the sample bottle (350 ml glass bottle with *GE* valve) or reference flask (1L, ~2 ml neck with two *GE* valves) was connected. A schematic drawing of the line is given in **Figure 15**.

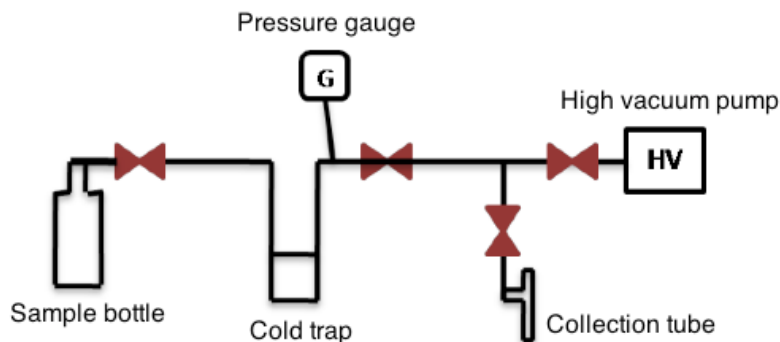


Figure 15: Schematic drawing of the small extraction line, figure adapted from Gloël (2012).

3.2.3 Description of procedure

Before transfer of a sample, the line was evacuated down to a vacuum of preferably $1.6\text{--}1.9 \times 10^{-7}$ and maximally 3×10^{-7} mbar. A sample tube with new molecular sieve pellets was attached, and the molecular sieve pellets were degassed step-wise, in order to remove adsorbed gases (H_2O , CO_2) that could interfere with the sample and decrease the sorption capacity (Karlsson 2004). Pellets were degassed, by heating the sample tube twice with an ethanol burner ($> \sim 200$ °C) for up to 40-60 s, while it was under vacuum. Heating was stopped at the moment the pressure in the line stopped increasing, after which the tube was allowed to cool down until a pressure of $\sim 1 \times 10^{-6}$ mbar was reached. At this point the second period of heating was started, which, again, lasted until the pressure stopped increasing. This resulted in two periods of heating of up to approximately 40 seconds. According to the molecular sieves manufacturer's manual and literature, temperatures for regeneration generally should not exceed 300-500 °C (Sigma-Aldrich, Karlsson 2004). In this case, relatively high temperatures were applied, but only for brief amounts of time, in order to prevent damage of the molecular sieve structure.

After degassing of the molecular sieves, a vacuum of 1.9×10^{-7} mbar was generally achieved in the line. After obtaining the required vacuum, the valve to the pump was closed and the sample was released. The pressure before and after introduction of the sample was recorded. The sample tube was then immersed in liquid nitrogen (-196 °C) and the sample gas was frozen on to the molecular sieves, until at least 99.9% of the sample was adsorbed (ascertained manometrically). In case the pressure in the line was relatively low and the freezing time exceeded 10 minutes, a minimum recovery of 99.8% was accepted. After collection, the final pressure and freezing time were written down and the collection tube was closed and disconnected. The line could then be evacuated and prepared for the next sample.

For some of the tests, a 180 ml glass trap was connected to the line, which could be cooled down to liquid nitrogen temperature (-196 °C). The presence of this trap strongly increased the total line volume (from ~20 to ~200 ml) and thus had an important influence on the starting pressure in the line after loading the sample.

After transfer, all samples were heated for 20 minutes at ~60 °C in hot tap water, which was left to cool down during this period, after which their triple oxygen isotopic composition was determined by measurement against the reference O₂-Ar mixture on the IRMS (*Thermo Finnigan MAT 252*, Dual-Inlet mode). Each sample was measured during one run of 30 cycles of sample-reference analysis. The bellows were adjusted manually upon introduction of the sample, in order to achieve a minimum difference in sample size between the reference and sample side. The used idle and integration times were 5 and 16 s respectively, the signal height of *m/z* 32 was 2.5 V. Internal standard errors over one acquisition of 30 measurements were generally 0.009 and 0.004‰ for δ¹⁷O and δ¹⁸O respectively. Resulting δ¹⁷O and δ¹⁸O values were corrected for the effects of nitrogen interference and imbalance (difference in output voltage of *m/z* 32 signal between standard and sample), according to the linear relationships derived in **Chapter 2**. The Δ¹⁷O was calculated, for each sample, according to

$$\Delta^{17}\text{O}/\text{ppm} = (\delta^{17}\text{O} - 0.5179 \delta^{18}\text{O}) \cdot 1000.$$

At the end of each block of 30 measurements, an interfering-masses measurement was performed, during which the ion currents of *m/z* 28 (N₂), 40 (Ar) and 32 (¹⁶O₂) were measured for both sample and reference. *d*(N₂/O₂) and δ(O₂/Ar) were then calculated according to

$$d(\text{N}_2/\text{O}_2)/\text{‰} = ((U_{28}/U_{32})_{\text{sa}} - (U_{28}/U_{32})_{\text{ref}}) \cdot 1000,$$

$$\delta(\text{O}_2/\text{Ar})/\text{‰} = \left(\frac{(U_{32}/U_{40})_{\text{sa}}}{(U_{32}/U_{40})_{\text{ref}}} - 1 \right) \cdot 1000,$$

where *U*₂₈, *U*₃₂ and *U*₄₀ are the voltages of the ion beam intensities of *m/z* 28 (N₂), 32 (¹⁶O₂) and 40 (Ar) respectively, ‘sa’ stands for sample and ‘ref’ for working reference. The resulting δ¹⁷O, δ¹⁸O, Δ¹⁷O and δ(O₂/Ar) are displayed in **Figure 16-19**. *d*(N₂/O₂) and transfer characteristics are given in **Table 2**.

3.3 Results

In order to improve the efficiency of the extraction and separation line, transfer tests were performed with different numbers of molecular sieve pellets under different conditions. In each case, a working reference O₂-Ar-mixture was frozen on to zeolite 5Å molecular sieve pellets and then introduced to a dual-inlet isotope ratio mass spectrometer (IRMS), where its O₂ isotopic composition was determined relative to that of the same reference gas introduced directly.

$\delta^{17}\text{O}$ and $\delta^{18}\text{O}$ results of the transfer tests are displayed in **Figure 16 and 17**, while $\Delta^{17}\text{O}$ results are displayed in **Figure 18**. $\delta(\text{O}_2/\text{Ar})$ results of the transfer tests are given in **Figure 19**. A detailed overview of all test results and characteristics (including $d(\text{N}_2/\text{O}_2)$ and transfer conditions) is given in **Table 2**. Results of injection experiments are given in **Table 3**.

3.3.1 $\delta^{17}\text{O}$ and $\delta^{18}\text{O}$ results

The results for $\delta^{17}\text{O}$ and $\delta^{18}\text{O}$ of the transfer tests are displayed in **Figure 16 and 17**.

All tests resulted in slightly negative $\delta^{17}\text{O}$ and $\delta^{18}\text{O}$ values, possibly indicating some fractionation against the heavy isotopes due to transfer using MSZ 5Å. However, for all *HP* tests except for single transfer using 10 pellets, values were close to zero and not significantly different from results of zero enrichments (t-test, α : 0.05). The extent of fractionation strongly depended on the used pellet number and transfer conditions.

For most tests, $\delta^{17}\text{O}$ and $\delta^{18}\text{O}$ are in the range of -0.01 to -0.10‰, a strong exception being the results of the single transfer tests with 10 pellets. Small but insignificant fractionation was observed for *HP* tests with 5, 6, 6>5 or 10>5 pellets (0.01-0.02‰ for $\delta^{17}\text{O}$ (**Figure 16**), 0.02-0.04‰ for $\delta^{18}\text{O}$ (**Figure 17**)). Fractionation was however significantly higher when a liquid nitrogen cold trap or *LP* procedure was included (-0.04 to -0.06‰ for $\delta^{17}\text{O}$, -0.06 to -0.10‰ for $\delta^{18}\text{O}$). Strongest fractionation was observed for tests in which gas was frozen onto 10 pellets and then released into the MS (-0.15 to -0.21‰ for $\delta^{17}\text{O}$, -0.29 to -0.42‰ for $\delta^{18}\text{O}$ (**Figure 16 & 17**)).

Observed $\delta^{17}\text{O}$ values are close to half of the $\delta^{18}\text{O}$ values. The only exception to this general trend appears in the $\delta^{17}\text{O}$ values for the 6>5 tests, which are slightly more negative than expected.

High pressure, single transfer

Best results, in terms of least fractionation in $\delta^{18}\text{O}$ and $\delta^{17}\text{O}$, were obtained for the single transfer tests with 5 pellets under high pressure ((-0.008±0.011)‰ and (-

0.021±0.013)‰, for $\delta^{17}\text{O}$ and $\delta^{18}\text{O}$ respectively (**Figure 16 and 17**). These tests most closely represent the current procedure of transferring samples from the separation line to the mass spectrometer. Resulting values for these tests were slightly negative, but within the range of ‘zero enrichment’ results (**Table 2**).

Increasing the number of molecular sieve pellets during single transfer decreased the $\delta^{17}\text{O}$ and $\delta^{18}\text{O}$, indicating an increased negative fractionation with increased sieve amount. Although fractionation was still reasonably small when 6 pellets were used ((-0.011±0.006) and (-0.034±0.015)‰, for $\delta^{17}\text{O}$ (**Figure 16**) and $\delta^{18}\text{O}$ (**Figure 17**) respectively, which is not significantly different from 5 pellet test and zero enrichment results (**Table 2**)), the amount of observed fractionation became significantly higher when 10 pellets were used for transfer to the mass spectrometer, in which case very negative $\delta^{17}\text{O}$ and $\delta^{18}\text{O}$ values were measured, accompanied by a relatively large standard deviation ((-0.146±0.031) and (-0.292±0.046)‰ for $\delta^{17}\text{O}$ and $\delta^{18}\text{O}$ respectively, see **Figure 16 and 17**).

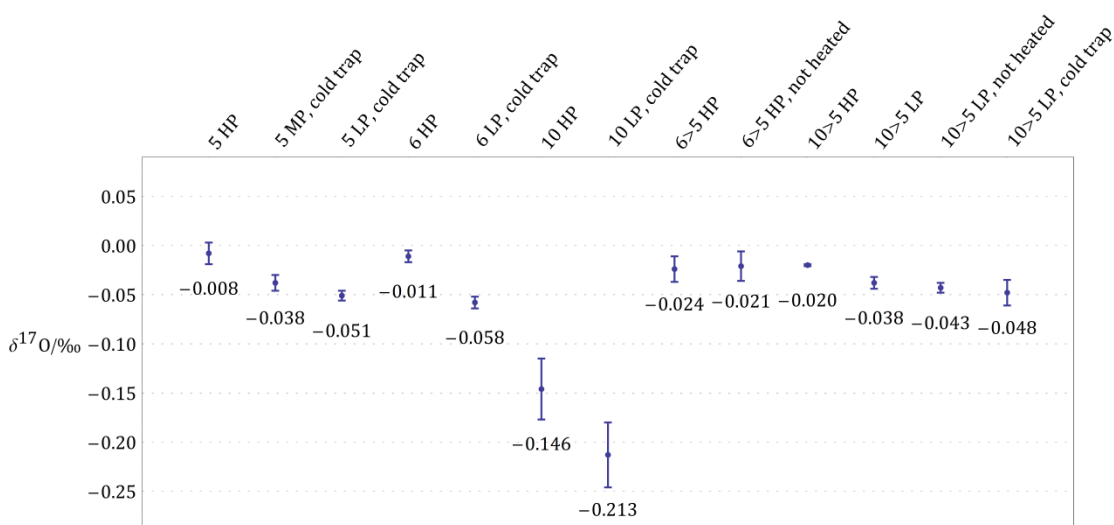


Figure 16: $\delta^{17}\text{O}$ results of different transfer tests. Each test was performed in triplicate and plotted values are averages. All samples were measured during one run of 30 cycles on the IRMS. Error bars show ± 1 standard deviation.

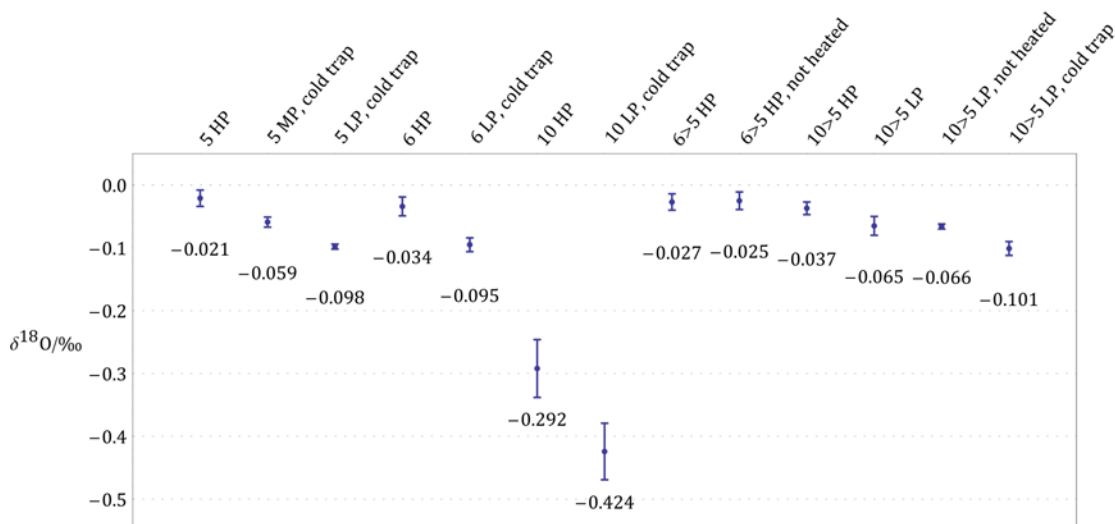


Figure 17: $\delta^{18}\text{O}$ results of different transfer tests. The transfer tests on the x -axis correspond to the different tests listed in the previous section. Each test was performed in triplicate and the plotted values are averages. All samples were measured against the directly introduced O_2 -Ar reference gas in one run of 30 cycles on the IRMS. Error bars show ± 1 standard deviation.

High pressure, double transfer

When gas was transferred from 6 or 10 pellets to 5 before introduction to the MS (6>5, 10>5 tests), the strong fractionation due to the use of 10 pellets was no longer observed. 10>5 test results were not significantly different (t-test, α : 0.05) from 6>5 test results, results of single transfer using 5 or 6 pellets or zero enrichments (**Table 2**).

Comparable results were obtained for the 6>5 and 10>5 *HP* tests (6>5: (-0.024 ± 0.013) and $(-0.027 \pm 0.013)\text{‰}$ and 10>5: (-0.020 ± 0.001) and $(-0.037 \pm 0.010)\text{‰}$ for $\delta^{17}\text{O}$ (**Figure 16**) and $\delta^{18}\text{O}$ (**Figure 17**) respectively), the 10>5 tests yielding a slightly more negative (but not significantly different) $\delta^{18}\text{O}$, the 6>5 test results having a slightly larger variability. Although results of 6>5 and 10>5 tests are slightly more negative than those of single transfers using 5 pellets, this might be due to the addition of an extra transfer step, and multiple transfers cannot be avoided during gas preparation. Tests with 5>5 pellets, or tests with more than two transfer steps were not performed, but would be interesting, to see whether fractionation would increase further. However, in this case fractionation for *HP* 10>5 and 6>5 tests was still negligible (not significant statistically).

The strong fractionation observed for single transfer tests with 10 pellets is not observable for 10>5 tests. The fact that results are comparable between 6>5 and 10>5 tests, could indicate increasing the pellet number from 6 to 10 in the first step would not lead to a significant difference in the results, or addition of fractionation, as long as the gas is released from the 10 pellets during simultaneous cryotrapping and 5 pellets are used in the final step.

Effect of expansion procedure and cold trap

For all tests, including single transfers with 5, 6 or 10 pellets and double transfers, significantly increased fractionation was observed when a liquid nitrogen cold trap or *LP* (low pressure/expansion) procedure was included. As can be observed from results of 5 pellet and 10>5 pellet tests (see **Figure 16** and **17**), fractionation was strongest in the presence of both cold trap and the extra expansion procedure (*LP*) (-0.05 to -0.06‰ for $\delta^{17}\text{O}$ and -0.10‰ for $\delta^{18}\text{O}$) and intermediate in the presence of either cold trap or *LP* procedure (-0.04‰ for $\delta^{17}\text{O}$, -0.06 to -0.07‰ for $\delta^{18}\text{O}$). It should be noted that because the cold trap added a large volume to the line, both the cold trap and *LP* procedure increased the extraction line volume. As a result, sample pressure in the line was lowest when both were involved (2-3 mbar), and intermediate when one of the two was included (4-6 mbar) (50-60 mbar when neither was included) (**Table 2**). The effects of addition of cold trap and/or '*LP*' procedure are comparable between single transfer tests with 5 or 6 pellets and double transfer tests with 10>5 pellets. The combined effect leading to respective $\delta^{17}\text{O}$ and $\delta^{18}\text{O}$ values of -0.051 and -0.098‰ for 5 pellet tests and -0.048 and -0.101‰ for 10>5 pellet tests.

Effect of heating before second transfer

No significant or consistent effect of heating before the second transfer was found in any of the results ($\delta^{17}\text{O}$, $\delta^{18}\text{O}$, $\delta(\text{O}_2/\text{Ar})$, $\Delta^{17}\text{O}$). The resulting $\delta^{18}\text{O}$ values of similar 6>5 and 10>5 tests with and without heating were only different by 0.001‰ and 0.002‰, and $\delta^{17}\text{O}$ values were changed by 0.003‰ and 0.005‰ respectively, well within the error of the measurement.

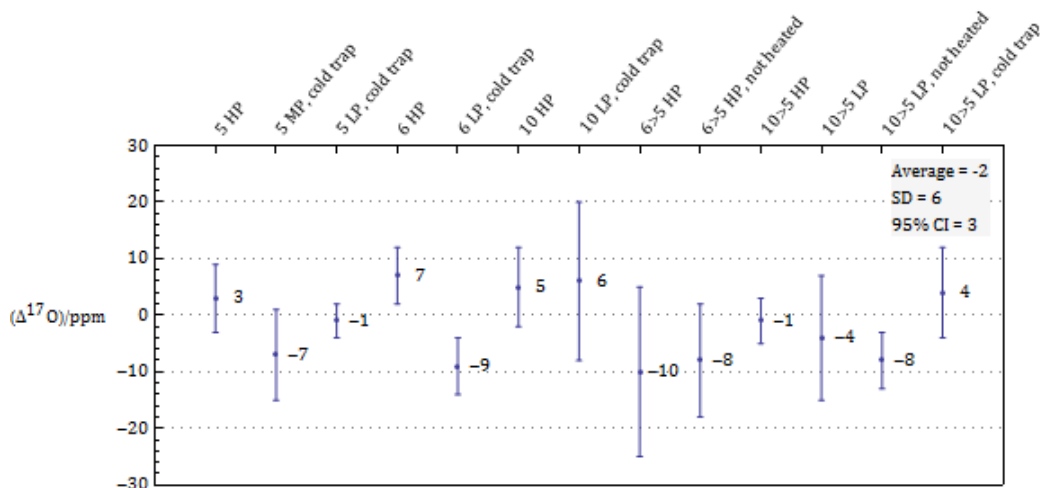


Figure 18: $\Delta^{17}\text{O}$ results of transfer tests. $\Delta^{17}\text{O} = 1000 \times (\delta^{17}\text{O} - 0.5179 \times \delta^{18}\text{O})$. Error bars show ± 1 SD. The average $\Delta^{17}\text{O}$ is -2 ± 6 (SD).

3.3.2 $\Delta^{17}\text{O}$

As can be observed from **Figure 18**, all $\Delta^{17}\text{O}$ results are close to zero and within the range of zero enrichment results (**Table 2**), and no consistent effect of any of the tested parameters on the $\Delta^{17}\text{O}$ could be observed. The average resulting $\Delta^{17}\text{O}$ was (-2 ± 6) ppm, which is very close to results of zero enrichments performed in 2012 and 2013 (see **Table 2**). In all cases, observed $\delta^{17}\text{O}$ values are close to half of the $\delta^{18}\text{O}$ values (see **Figure 16** and **17**), indicating mass-dependent fractionation, and consequently variations in $\Delta^{17}\text{O}$ are small and do not reflect the observed variations in $\delta^{17}\text{O}$ and $\delta^{18}\text{O}$.

No significant difference between the $\Delta^{17}\text{O}$ results of *HP* tests with 5, 6 or 10 pellets is observable, although strong differences were observed in their $\delta^{17}\text{O}$ and $\delta^{18}\text{O}$ results. The 6>5 tests yielded relatively negative and variable $\Delta^{17}\text{O}$ values due to the relatively negative and variable $\delta^{17}\text{O}$ results. The presence of a cold trap and/or *LP* scenario is accompanied by relatively negative $\Delta^{17}\text{O}$ values in most cases, but by a relatively positive value in the 10>5 *LP* cold trap test case. So, based on these data, no consistent relationship can be observed between any of the tested parameters and $\Delta^{17}\text{O}$. Whether there is any relationship between *LP* and/or cold trap or heating before second transfer and the $\Delta^{17}\text{O}$ cannot be concluded based on these data, since all results are very close to zero and within the standard deviation of the zero enrichments, so any effects would be obscured by the measurement error.

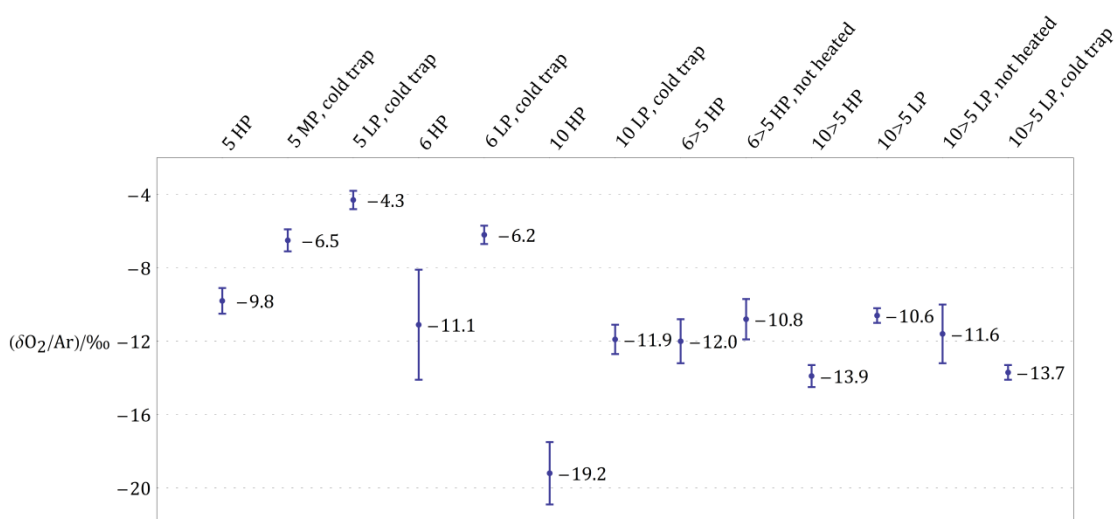


Figure 19: $\delta(\text{O}_2/\text{Ar})$ results of different transfer tests. The transfer tests on the x-axis correspond to the different tests listed in the previous section. Each test was performed three times and the plotted values are averages. All samples were measured against the directly introduced O_2 -Ar reference gas in one run of 30 cycles on the IRMS. Error bars show ± 1 standard deviation.

3.3.3 $\delta(\text{O}_2/\text{Ar})$

$\delta(\text{O}_2/\text{Ar})$ results, which give an indication of elemental fractionation, are displayed in **Figure 19**. As can be observed from **Figure 19**, relatively negative $\delta(\text{O}_2/\text{Ar})$ values, indicating elemental fractionation, were observed for all tests (average $(-11 \pm 1)\%$). The deviation from zero increases with the used molecular sieve quantity during transfer to the MS (single transfer tests with 5, 6 or 10 pellets yielding $\delta(\text{O}_2/\text{Ar})$ values of -9.8, -11.1 and -19.2‰ respectively, see **Figure 19** and **Table 2**). This is in agreement with findings by Barkan and Luz (2003) and Abe (2008). Just as for the $\delta^{17}\text{O}$ and $\delta^{18}\text{O}$ results, the relatively strong fractionation observed for tests with desorption from 10 pellets into the MS (-19.2‰) is no longer observed when gas is transferred from 10 to 5 pellets (10>5 pellet test) (-13.9‰). A slightly stronger fractionation is observed when transfer takes place from 6 or 10 pellets to 5 pellets before introduction to the MS, compared to tests in which this first step is omitted (5 pellet single transfer), as was also observed in $\delta^{17}\text{O}$ and $\delta^{18}\text{O}$ results.

The effect of the ‘LP’ procedure and cold trap is however not the same as for the isotopic composition. As can be observed from **Table 2** and **Figure 19**, elemental fractionation was always smaller (the $\delta(\text{O}_2/\text{Ar})$ more positive), when the pressure in the line was lower (through larger line volume, either by cold trap or ‘LP’ procedure). Results of the 10>5 test indicate the presence of a liquid nitrogen trap slightly increases the fractionation (the $\delta(\text{O}_2/\text{Ar})$ being more negative for the ‘10>5 LP cold trap’ test ($(-13.7 \pm 0.4)\%$) than for the ‘10>5 LP’ tests ((-10.6 ± 0.4) and $(-11.6 \pm 1.6)\%$ for tests with and without heating respectively, see **Figure 19**, **Table 2**). Again, no effect of heating before transfer from 6 or 10 to 5 pellets can be observed.

As mentioned above, negative $\delta(\text{O}_2/\text{Ar})$ values were observed for all tests (average -10.9‰, see **Table 2**). The observed fractionation is strong, compared to expectations based on studies from the same lab (Gloël 2012, Gonzalez-Posada 2012) and literature (Barkan and Luz 2003) (-4 to -10‰ (single transfer using 5 pellets), vs. -3 and -3 to -5‰ for comparable experiments conducted by Gloël and Gonzalez-Posada (2012, 2012) and Barkan and Luz (2003) respectively). It should however be noted exact line conditions (line volume, sample tube volume) during the other experiments are not known, and here-presented results and the study by Abe (2008) indicate these factors might have an important influence on the results. Finally, as can be observed from **Figure 19**, the deviation from zero increases with the used molecular sieve quantity during transfer to the MS, and it cannot be included larger sieve quantities were used in these tests (on

average selected pellets might have been slightly longer in this study than in the studies of Gloël and Gonzalez-Posada (2012, 2012)).

3.3.4 Freezing times and additional data

A detailed overview of test results and characteristics, is given in **Table 2**, including $d(N_2/O_2)$ and transfer conditions. Results of zero enrichments (reference gas vs. reference gas) in the time period surrounding these experiments (2012-2013) are included for comparison purposes. A complete overview, including $\delta^{17}O$ and $\delta^{18}O$ and injection test data is displayed in the Appendix (**Table 10**).

Table 2: Overview of transfer test results and characteristics (including $d(N_2/O_2)$, $\delta(O_2/Ar)$ and transfer conditions). In addition, results of zero enrichments in the period surrounding the tests are included. $t_{freezing}$ indicates the total time required for a sample to freeze on the molecular sieves during transfer, while P_{start} is the pressure in the line after loading the sample. ‘-’ indicates the starting pressure could not be measured because a <10 mbar gauge was present on the line and the pressure was above 10 mbar. Entry ‘10[2]’, in column 5, row 1, indicates the actual freezing time in these experiments was 10 minutes, while the required time to reach 99.9% recovery was 2 minutes. ‘n’ gives the number of samples transferred for each scenario. All tests were performed in triplicate. One sample was lost due to high nitrogen content. $\delta(O_2/Ar)$, freezing time and line pressure of this sample were comparable to the values of the other two samples.

Procedure	$\Delta(^{17}O)/ppm$	SD	$P_{start}/mbar$	$t_{freezing}/min$	$d(N_2/O_2)/\text{‰}$	$\delta(O_2/Ar)/\text{‰}$	SD	n
1a) 5 hp	3	6	64	10 (2)	99	-9.8	0.7	3
1b) 5 mp cold trap	-7	8	6	25	88	-6.5	0.6	3
1c) 5 lp cold trap	-1	3	3	35	563	-4.3	0.5	2
2a) 6 hp	7	5	54	2	43	-11.1	3.0	3
2b) 6 lp cold trap	-9	5	3	39	107	-6.2	0.5	3
3a) 10 hp	5	7	-	2	25	-19.2	1.7	3
3b) 10 lp cold trap	6	14	2	5	228	-11.9	0.8	3
4a) 6>5 hp	-10	15	53	4	93	-12.0	1.2	3
4b) 6>5 hp not heated	-8	10	53	5	69	-10.8	1.1	3
5a) 10>5 hp	-1	4	-	7	41	-13.9	0.6	3
5b) 10>5 lp	-4	11	4	13	265	-10.6	0.4	3
5c) 10>5 lp not heated	-8	5	4	12	152	-11.6	1.6	3
5d) 10>5 lp cold trap	4	8	2	15	224	-13.7	0.4	3
Average	-2	8			154	-10.9	1.0	
SD	6							
95% CI	3							

Zero enrichments				n: 54
Year	$\Delta(^{17}O)/ppm$	$\delta(^{17}O)/\text{‰}$	$\delta(^{18}O)/\text{‰}$	
2013	-3	-0.010	-0.012	
Average	-3	-0.010	-0.012	
SD	10	0.010	0.012	
95% CI	3	0.003	0.003	
2012	-4	-0.006	-0.004	n: 98
Average	-4	-0.006	-0.004	
SD	14	0.011	0.015	
95% CI	3	0.003	0.003	

Freezing time

When starting pressures were high (50-60 mbar), all samples froze relatively fast (within 2-7 minutes total). At low starting pressures, the number of pellets started to make a

substantial difference. As can be observed from **Table 2**, freezing time at high (50-60 mbar) starting pressure was similar for transfer on to 5, 6 or 10 pellets (2-3 minutes) (for ‘6>5’ and ‘10>5’ tests, the total freezing time was longer due to the addition of an extra transfer step). However, at low starting pressures (2-6 mbar), the used number of molecular sieve pellets had a large influence on the freezing time, which varied from 30-40 minutes for 5 or 6 pellet transfer to 5 minutes for 10 pellet transfer under similar conditions. This means that while using 6 pellets instead of 5 during extraction does not make a big difference, using 10 pellets instead of 5 or 6 implies a time gain of approximately 30 minutes per sample.

N₂ content

Samples did not have to be treated for separation of N₂, since the tested gas was a pure O₂-Ar mixture, and the N₂ introduced during the process as a result of leakage was in the range for which corrections could be applied (**Chapter 2**). Since no separation procedure was applied, $d(N_2/O_2)$ results give an indication of the air contamination during transfer. In all cases, relatively high nitrogen contents were observed for results of ‘LP’ tests (average $d(N_2/O_2)$ values between 100 and 563‰), compared to the samples that not undergo expansion into a sample bottle (all below 100‰), which might indicate increased contamination due to the expansion procedure. (Note: the ‘LP’ procedure also led to low line pressures, which led to longer freezing times. However, longer freezing times are not always accompanied by high nitrogen contents, and high $d(N_2/O_2)$ values were also observed for ‘LP’ tests with relatively short freezing times (see **Table 2**)). Most sets of three samples (9 out of 13) had an average $d(N_2/O_2)$ of 25 to 200 ‰ (N₂ voltage of 0.2-0.5 V). In this range corrections for N₂ interference can be applied with good results (**Chapter 2**). The only exception are the ‘5 LP’ samples, which had an average $d(N_2/O_2)$ of 563 ‰. The corrected O₂ isotopic results of these samples are not significantly different from the general trend, but the O₂/Ar ratio ($\delta(O_2/Ar)$) is slightly more positive than for the other samples. An effect of contamination cannot be ruled out.

Table 3: Results of injection experiments (± 1 SD).

Injection tests, 10>5, cold trap			
$\delta^{17}O/‰$	$\Delta^{18}O/‰$	$\Delta^{17}O/ppm$	$\delta(O_2/Ar)/‰$
-0.031±0.012	-0.057±0.019	-1±9	-11.9±1.6
$d(N_2/O_2)/‰$	$P_{start}/mbar$	$t_{freezing}/min$	n
257	9	16	12

Pressure in line

Both the cold trap and ‘LP’ procedure increased the line volume and thus led to a lower starting pressure in the line. As can be observed in **Table 2**, the starting pressure in the line varied from 2 mbar when cold trap and ‘HP’ procedure were involved, to 50-60 mbar when neither was involved (‘HP’ tests). When either cold trap or ‘LP’ procedure was included, the pressure was intermediate (4-6 mbar). Lower starting pressures always resulted in longer freezing times.

Injection tests

For comparison, results of later performed ‘injection’ experiments are displayed in **Table 3** and the bottom row of **Table 10 (Appendix)**. During these experiments, O₂-Ar reference gas from the headspace of airtight 165 ml bottles containing distilled water bubbled with O₂-Ar, was inserted into the same extraction line (through an evacuated needle, see **Chapter 4**) and transferred, with cold trap on line, onto 10 and then 5 molecular sieve pellets, with heating of the pellets before the second transfer. In this case, the line conditions were relatively similar to those of the ‘5 cold trap’ scenario (no expansion procedure, intermediate starting pressure) and ‘10>5 LP’ scenarios, but more water vapour was introduced into the line. The results are very similar to those of the ‘5 cold trap’ and ‘10>5 LP’ tests. This could indicate the presence of more water vapour does not increase the fractionating effect of the cold trap. However, it cannot be excluded that due to the different gas introduction procedure applied here, other fractionation processes were involved, and the relatively similar result is a coincidence.

3.4.1 Summary of results

Results indicate that increasing the number of pellets used during extraction from 5 or 6 to 10 will lead to a decrease in transfer time of 20-30 minutes per sample, and can take place without significant increase in fractionation, as long as the gas is desorbed from these pellets under simultaneous cryotrapping and transfer to the MS takes place using 5 pellets. However, increasing the number of pellets used during transfer to the MS from 5 to 10 would lead to a strong increase in fractionation. The change from 5 to 6 pellets in this step would lead to a small increase in fractionation but no substantial decrease in freezing time. In all cases, increased fractionation was observed when a liquid nitrogen trap was present on the line and when the pressure in the line was lowered by expansion into a sample bottle, which was accompanied by longer freezing times. Fractionation was strongest in the presence of both a cold trap and a ‘LP’ procedure and intermediate when only a cold trap or ‘LP’ procedure was involved. Fractionation was not reflected in the ¹⁷O excess, which was in the range obtained during zero enrichments.

3.4 Discussion and conclusions

3.4.1 Discussion

Use of molecular sieves during transfer to the MS Isotopic fractionation

Results confirm findings by Abe (2008) and Barkan and Luz (2003), who reported isotopic and elemental fractionation (loss of oxygen, ^{17}O and ^{18}O) with transfer of O_2 or O_2 -Ar to the dual-inlet MS using zeolite (5\AA) molecular sieves, the amount of fractionation increasing with the amount of molecular sieve used. It was however found, confirming results of Gloël (2012) and González-Posada (2012), that isotopic fractionation is negligible when 5 pellets of molecular sieve are used (*Sigma-Aldrich*, zeolite 5\AA , 1.6/5 mm in size) for final transfer to the MS (and samples are heated before release into the MS as suggested by Abe (2008)). Results therefore confirm that under these specific conditions, molecular sieves can be used for final transfer instead of liquid helium.

Elemental fractionation

However, in all cases, strong elemental fractionation was observed due to the use of molecular sieve pellets ($\sim 10\text{‰}$), stronger than reported by Barkan and Luz (2003) and Gloël (2012) and González-Posada (2012), the amount of fractionation increasing with the amount of sieves used. For transfer using 5 pellets, a more negative $\delta(\text{O}_2/\text{Ar})$ was observed than in the study of Gloël (2012) and González-Posada (2012) (-9.8 ± 0.7 vs. $-3\pm 1.6\text{‰}$). However, it cannot be excluded that in this study on average slightly larger pellets were selected (~ 6 mm instead of ~ 5 mm (Gloël 2012, González-Posada 2012)), In addition it has been reported differences in gas pressure and the line volume during desorption affect the resulting fractionation (Barkan and Luz 2003, Abe 2008), so the difference might be due to differences in sample size, or line volume during desorption, next to possible differences adsorption recovery, air contamination or transfer conditions (in this study, less fractionation was observed for samples expanded into a sample bottle before transfer. However, Since all (air-equilibrated and biological) samples processed for this research were transferred from the separation line to the MS using the 5 pellets and manifold and line volumes used by Gloël (2012) and González-Posada (2012), such strong fractionation would not be expected to have affected the samples. In addition, the air standard was processed on the separation line together with the samples, so any fractionation due to transfer using molecular sieve pellets would be expected to affect sample and standard in the same way, and would thus be cancelled out in the final results.

Use of molecular sieves during extraction

It was found that adding an extra molecular sieve transfer step, (transferring from 6 or 10 pellets to 5 and then to the MS), as currently happens on the extraction line, slightly increased the observed isotopic and elemental fractionation (decreased resulting values with ~ -0.004 - 0.016‰ for $\delta^{17}\text{O}$ and $\delta^{18}\text{O}$ and -1 - 4‰ for $\delta(\text{O}_2/\text{Ar})$ respectively) with respect to single transfer using 5 pellets. Differences were however small, and for $\delta^{17}\text{O}$ and $\delta^{18}\text{O}$ not significant. No significant increase in fractionation was observed when the number of pellets used during first transfer was increased from 6 to 10 pellets, and although significant isotopic fractionation was observed when samples were released straight from 10 pellets into the MS, no significant fractionation was observed when samples were transferred using 10 pellets and then transferred to the MS using 5 pellets. This indicates, as reported by Barkan and Luz (2003), that fractionation due to incomplete desorption from molecular sieves is not an issue when samples are desorbed during simultaneous trapping (in which case the desorption is expected to be close to complete) and only during release into the MS, which happens based on a pressure difference only. As a result, increasing the molecular sieve amount on the extraction line, or in intermediate traps on the separation line, should not significantly increase fractionation. Therefore, these results indicate increasing the number of molecular sieves on the extraction line from 5 or 6 to 10 should be possible without significantly increasing fractionation, as long as the gas is desorbed from them during simultaneous trapping, and final transfer to the MS takes place using a maximum of 5 pellets. Since these conditions are met when samples are processed on the separation line after extraction, and it was found increasing the number of molecular sieve pellets from 5 or 6 to 10 led to a substantial decrease in transfer time (from 30-40 minutes to 5 minutes), 10 pellets were used during extraction of samples for air-equilibrated water tests and culture experiments described in **Chapter 4 and 5**.

Effect of line pressure/expansion procedure

When the pressure in the line was lowered through expansion of the aliquot of gas into a sample bottle before transfer, in all cases slightly more negative $\delta^{17}\text{O}$ and $\delta^{18}\text{O}$ values were obtained and slightly more positive $\delta(\text{O}_2/\text{Ar})$ values (see **Figure 18, Table 2**). It is difficult to assess what might have caused this increased fractionation.

It could be related to fractionation during the expansion of gas into a sample bottle. The gas was however allowed to equilibrate for several (~ 10) minutes after expansion, so fractionation would be expected to be negligible.

What is however important to note, is that due to this long time of equilibration, the samples from the low pressure experiments might have increased air contamination. In all cases, higher $d(N_2/O_2)$ were observed for low pressure samples (see **Table 2**). Since air has a positive $\delta(O_2/Ar)$ and negative $\delta^{17}O$ and $\delta^{18}O$ values with respect to the reference gas, this might partly explain the results.

Another option would be fractionation during adsorption. Because of the longer freezing time, the recovery was generally slightly lower for low pressure (99.8%) than for high-pressure samples (>99.9%). However, fractionation during adsorption would probably not affect the results to such an extent if the recovery is >99.8% (Abe 2008).

It should be realized, for high and low pressure tests, the sample size should be approximately the same, and thus the pressure should not play an important role during desorption. However, during expansion of an O_2 -Ar aliquot into a sample bottle, not the whole aliquot of O_2 -Ar ends up in the sample bottle, but the gas is distributed over the sample bottle, part of the line and the aliquot volume. Therefore, it is possible the sample size of 'LP' samples would be slightly smaller than for high pressure (straight from flask) samples, which might have resulted in a slightly lower pressure during desorption. Barkan and Luz (2003) reported they observed stronger fractionation effects during molecular sieve transfer for higher gas pressures. However, again this might explain the more positive $\delta(O_2/Ar)$ values, but not the more negative $\delta^{17}O$ and $\delta^{18}O$ values.

In order to assess the effect of the pressure in the line only, without additional effects of an expansion procedure and/or trap temperature effects, it would be interesting to conduct similar tests with the large volume glass trap at room temperature.

Effect of liquid nitrogen trap

O_2 -Ar samples were transferred both with and without liquid nitrogen cold trap on the extraction line, and results were compared. It was found that all samples transferred with a $-196^\circ C$ cold trap on the line, displayed some negative fractionation (negative $\delta^{17}O$ and $\delta^{18}O$ values, in the range ~ -0.03 and -0.06% for $\delta^{17}O$ and $\delta^{18}O$ respectively). In all cases, the observed fractionation was however mass dependent, no effect on the $\Delta^{17}O$ was observed.

In addition, tests were performed both at high and low pressure (by introducing the same amount of gas from a large volume sample bottle). It was found that comparable negative fractionation resulted when the line pressure was lowered through expansion into a sample bottle, the fractionation being worst when both a cold trap and large volume bottle were involved ($\delta^{18}O$: -0.1%). In this case the pressure in the line was also lowest, since the cold trap adds a relatively large volume to the line. It can therefore not

be excluded that the negative fractionation was related to the volume rather than the temperature of the trap. In addition, it cannot be stated a -78°C trap would produce better results. Comparable tests should therefore ideally be performed with the glass trap at room temperature and -78°C .

If the liquid nitrogen trap led to fractionation due to freezing of Ar and O_2 on ice (as reported by Barkan and Luz 2003), fractionation could potentially be worse during the processing of air-equilibrated water or biological oxygen samples, since these samples would be expected to contain more H_2O . Tests were however performed with the method of sampling used in the culture experiments, and sample bottles containing water bubbled with O_2 -Ar reference gas and a 3 ml O_2 -Ar headspace. Results showed a fractionation nearly identical (-0.031 and -0.057% for $\delta^{17}\text{O}$ and $\delta^{18}\text{O}$ respectively) to that observed during the transfer tests with cold trap, for a comparable line volume (**Chapter 5, paragraph 2**). Finally, results of air-equilibrated water tests give a good indication of fractionation during the whole process of sampling, extraction and preparation (since atmospheric oxygen is expected to have approximately the same composition at different locations, and resulting $\delta^{18}\text{O}$ values can be compared to equilibrium values from literature). For artificial seawater (35 g/L NaCl), $\delta^{18}\text{O}$ values were obtained that were very close ($<0.02\%$) to equilibrium values reported in literature (see **Chapter 4**). In addition, in almost all cases $\delta(\text{O}_2/\text{Ar})$ results were very close to reported equilibrium values ($<1\%$), both indicating the presence of a liquid nitrogen trap probably did not significantly affect the results.

Effect of heating before second transfer

No effect of heating before the second transfer was observed on any of the results ($\delta^{17}\text{O}$, $\delta^{18}\text{O}$, $\Delta^{17}\text{O}$ or $\delta(\text{O}_2/\text{Ar})$), values for 6>5 and 10>5 tests with and without this heating procedure being very similar. This could be expected, since gases were desorbed from the first set of sieves under simultaneous trapping, and Barkan and Luz (2003) reported desorption would in this case be close to complete (Barkan and Luz 2003). In this case heating (to improve desorption) would not be expected to have a significant effect.

Effect on $\Delta^{17}\text{O}$

In all cases, observed fractionation due to the presence of a liquid nitrogen trap, pressure lowering or the use of molecular sieves was only observed in the $\delta^{17}\text{O}$ and $\delta^{18}\text{O}$. No significant effect of any of the tested parameters on the $\Delta^{17}\text{O}$ was observed.

3.4.2 Conclusions

No significant difference could be observed between results of transfer tests with 5 or 6 pellets MSZ 5Å in terms of fractionation or time, but, under low-pressure conditions (associated with extraction from sample bottles), the use of 10 pellets instead of 5 considerably speeded up the process. It did however lead to strong mass-dependent negative fractionation, when gas was desorbed directly from these pellets into the inlet of the MAT 252. However, when gas was transferred from these 10 pellets to 5 (as currently happens at the end of sample preparation) and then measured, fractionation was reasonably small, results being comparable to those for single transfer tests with 5 or 6 pellets, and double transfer tests with 6>5 pellets. These results indicate that freezing during extraction can take place on 10 pellets instead of 5 or 6 (as long as the gas is released from these pellets under simultaneous trapping, and final transfer takes place using 5 molecular sieve pellets), which would decrease extraction time from 30-40 to 5-6 minutes per sample. Results indicate the inclusion of a low starting pressure through expansion procedure and/or a liquid nitrogen cold trap led to increased negative mass-dependent fractionation in combination with a lowering of the pressure in the line, strongest fractionation being observed when both were included, in which case the pressure in the line was also lowest. This fractionation is not reflected in the ¹⁷O excess, but would decrease the accuracy of the measurements. Based on these results it is difficult to assess which factors are most important in causing the observed fractionation (whether it were the cold trap or expansion procedure or the low pressure they induced), and further tests should be performed (similar tests could be conducted with a trap at -78°C and room temperature and transfer straight from flask). However, based on these results and recommendations of Barkan and Luz (2003), the choice of a liquid nitrogen trap as first trap during extraction should not be made without careful consideration. Heating before the second transfer did not have an observable effect on the results, and, based on these results, could thus be omitted. This is consistent with the statement by Barkan and Luz (2003) that incomplete desorption from molecular sieves is not an issue when desorption occurs under simultaneous trapping.

Chapter 4: The triple isotopic composition of dissolved oxygen at air saturation

Abstract

The ^{17}O excess of dissolved oxygen at saturation ($\Delta^{17}\text{O}_{\text{sat}}$) and its temperature dependence is still a matter of debate. In the past, $\Delta^{17}\text{O}_{\text{sat}}$ was assumed to be constant at 16 ppm (Luz and Barkan 2000). However, experiments conducted over the past 10 years produced varying results with values clustering around two values at room temperature (8 ppm (Reuer et al. 2007, Stanley et al. 2010) and 16-18 ppm (Barkan and Luz 2000, 2003, 2009, Juranek and Quay 2005, Sarma et al. 2006b), (Stanley et al. 2010, Kaiser 2011). It has also been reported that $\Delta^{17}\text{O}_{\text{sat}}$ might be temperature dependent (Barkan and Luz 2009). To investigate these discrepancies and uncertainties, air-equilibrated water experiments were conducted at different temperatures (0, 22 and 39 °C) for both distilled water and water with 35 g l⁻¹ NaCl. Equilibrated water was prepared by bubbling water containing 0.4 g l⁻¹ HgCl₂ with air in an open 3-L flask, for a minimum of 24 hours. Dissolved gases were extracted by headspace equilibration. After removal of H₂O, CO₂ and N₂ they were analysed for their triple oxygen isotopic composition and O₂/Ar ratio on a dual-inlet IRMS (Finnigan MAT 252). For both distilled and 35 g l⁻¹ NaCl water, $\Delta^{17}\text{O}$ results were in the range of 15-20 ppm for experiments conducted at room temperature, but lower values (2-9 ppm) were obtained for tests conducted at 0 °C and 39 °C. While results for 0 and 22 °C are in agreement with the temperature relationship reported by Barkan and Luz (2009), results for 39 °C are not. However, the spread in the results was relatively large (standard deviation: 5-12 ppm) and sample numbers were small (3 or 4). It would therefore be advisable to repeat the experiments with larger sample numbers and an increased number of temperatures.

4.1 Introduction

As discussed in **Chapter 1**, for the accurate estimation of aquatic gross oxygen production (*GOP*) using triple oxygen isotopes, correct assessment of the triple isotopic composition of dissolved oxygen at air saturation is crucial. The triple oxygen isotopic composition of dissolved oxygen that entered the sea through air-sea gas exchange is not identical to that of atmospheric oxygen, as a result of fractionation processes during dissolution and degassing, but slightly enriched in ^{17}O and ^{18}O (Benson & Krause 1979). The air-seawater equilibrium experiments conducted by Barkan and Luz in 2000

indicated a positive $\Delta^{17}\text{O}_{\text{sat}}$ of (16±2) ppm, equivalent to (18±2) ppm using the $\Delta^{17}\text{O}$ definition applied in this study. This value has since then been adopted in most aquatic productivity studies. Over the past 10 years, tests comparable to those of Barkan and Luz (2000) have been conducted by several research groups (see **Table 4**). Although several experiments confirmed the findings of Barkan and Luz (2000), yielding values in the range of 16-18 ppm (Barkan & Luz 2003, Juranek & Quay 2005, Sarma et al. 2006b, Barkan & Luz 2009), two laboratories reported a significantly lower value of 8 ppm (Reuer et al. 2007, Stanley et al. 2010).

The reason for this discrepancy is not known, but different research groups used different water types and experimental methods and many of the reported results are based on a relatively small number of samples ($n < 10$) or carry a relatively large measurement uncertainty (**Table 4**) (in several cases standard deviations of ~5-11 ppm were reported or are visible from the data (Reuer et al. 2007 (SD:11), Sarma et al. 2006b (SD:7), Castro-Morales (SD:9), Gloel and Gonzalez-Posada (SD:5)).

Table 4: Overview of air-equilibrated water experiments published over the past 15 years. Table adapted from Kaiser (2011). ‘-’ indicates data was not reported. ^a According to Stanley et al. (2010), ^b According to Kaiser (2011), ^c Gloel (2012) and Gonzalez-Posada (2012) reported on the same study but did not report the same temperature. For Reuer et al. (2007) the standard deviation can be determined from reported data as 11 ppm.

Reference	Preparation	Water	$\vartheta/^\circ\text{C}$	$^{17}\Delta/\text{ppm (0.5179)}$	SD/ppm	(SE × t)/ppm	n
Luz and Barkan (2000)	bubbling	seawater	25	18	-	2	5
Luz and Barkan (2003)	bubbling	distilled	25	17	3	3	7
Sarma et al. (2003)	bubbling ^b	distilled	22	13	-	5	10
Juranek and Quay (2005)	stirring ^a	deionised	-	17	-	3	4
Sarma et al. (2006b)	bubbling ^b	distilled	24	18	7	2	10
Reuer et al. (2007)	stirring	35 gl ⁻¹ NaCl	11.2	6	-	2	14
Reuer et al. (2007)	stirring	35 gl ⁻¹ NaCl	24.8	8	-	3	14
Luz and Barkan (2009)	bubbling	seawater	3.5	4	3	3	5
Luz and Barkan (2009)	bubbling	seawater	12.2	9	2	2	5
Luz and Barkan (2009)	bubbling	seawater	25.0	17	4	4	5
Stanley et al. (2010)	stirring	-	-	8	-	3	-
Stanley et al. (2010)	stirring	distilled	-	9	-	2	16
Castro-Morales (2010)	stirring	distilled	21	20	9	5	11
Gloel & Gonzalez-Posada (2012)	bubbling	35 gl ⁻¹ NaCl	15.5-20 ^c	15	5	5	13

In 2009, Barkan and Luz reported that $\Delta^{17}\text{O}_{\text{sat}}$ is temperature dependent. They observed a linear increase in $\Delta^{17}\text{O}_{\text{sat}}$ from 4 to 17 ppm going from 3.5 °C to 25 °C, which they parameterised as $\Delta^{17}\text{O}_{\text{sat}}(0.5179)/\text{ppm} = 0.6 \vartheta/^\circ\text{C} + 1.8$, where ϑ is the Celsius temperature (Barkan & Luz 2009). While such a temperature relationship could explain the low $\Delta^{17}\text{O}_{\text{sat}}$ obtained in the 11 °C experiment of Reuer et al. (2007), it would not explain the low value obtained in the 25 °C experiment. Apart from that of the experiment by Reuer et al. at 11 °C, no results were reported by other research groups for temperatures below 20 °C, or above 25 °C. Although the error in the results of Barkan and Luz (2009) is small, the reported relationship is based on only 3

temperatures and 5 samples per temperature, and has so far not been confirmed by other laboratories.

Because in marine environments $\Delta^{17}\text{O}_{\text{dis}}$ is often very close to $\Delta^{17}\text{O}_{\text{sat}}$, estimates of GOP are very sensitive to the value of $\Delta^{17}\text{O}_{\text{sat}}$ used for their calculation. It is therefore crucial to decrease the uncertainty in this value by obtaining more experimental data on the triple isotopic composition of dissolved oxygen at air saturation at different temperatures.

Thus, for this study, air-equilibrated water experiments were conducted under different temperature (0, 22 and 39 °C) and salinity conditions (0 and 35 g l⁻¹ NaCl).

4.2 Methods

4.2.1 Preparation of air-equilibrated water

Air-equilibrated water was prepared by constantly bubbling ca. 3 l of distilled water (to which 1.2 ml of HgCl₂ saturated solution was added to prevent biological activity) with air, for a minimum of 24 hours, in a flask open to the atmosphere, but covered with aluminium foil to reduce evaporation. For tests conducted at 0 °C or 39 °C, the flask was kept in a water bath at the required temperature during equilibration and sampling. For tests conducted at seawater salinity 35 g l⁻¹ NaCl was added to distilled water prior to the equilibration.

Air-equilibrated water samples were collected and processed in the same way as seawater samples (see **Chapter 2**). After a minimum equilibration period of 24 hours, 175 ml water samples were collected through siphoning into pre-evacuated glass (350 ml) sample bottles with high-vacuum o-ring valves (*Glass Expansion*), ensuring the inlet neck was continuously filled with water without bubbles, while the valve was carefully opened to slowly suck water in, the water seal preventing air from entering. After filling the bottles halfway, they were closed using the vacuum valve and sealed by filling the neck with water and capping the inlet.

During equilibration of the 35 g l⁻¹ NaCl water, O₂ concentration and temperature were continuously monitored using an oxygen optode, and sampling started after values had stabilised (which was after 30 h at room temperature and after 40 h at 39 °C). In addition, times between the stop of bubbling and sampling were recorded for each sample. All bottles were filled within 1 hour after the stop of bubbling. During preparation of the earlier distilled water experiments, O₂ concentration and saturation were not monitored and water was equilibrated for a longer period (up to 7 days). For these samples, exact times between end of bubbling and sampling were not recorded.

4.2.2 Gas extraction and preparation

After filling, bottles were stored on a shaker table in the dark at room temperature for a minimum of 24 hours in order to equilibrate gases between the water phase and headspace of the bottles. After equilibration, water was carefully drawn out of the bottles under vacuum, while the bottles were held upside down, so that the valve was sealed with water during the process. The valve was closed when only 1 cm of water was left above the valve. The headspace gas was subsequently transferred onto pellets of molecular sieve (10 pellets of zeolite 5Å (*Sigma-Aldrich*, 1.6 mm diameter, 6 mm length, degassed before use)), using the small high-vacuum extraction line described in **Section 2.2.1** and **Chapter 3**. Samples were extracted with two cold traps on the line, a -78 °C trap surrounding the sample bottle and a liquid nitrogen trap further down the line. Transfer took place until at least 99.9% of the sample had been adsorbed.

After collection on molecular sieve pellets in valved glass tubes, gas samples were transferred to the automated gas purification line described in **Chapter 2** for removal of CO₂ and N₂ from the sample, which could interfere with the oxygen isotope measurements.

Samples were introduced after heating the tubes for 20 minutes at 60 °C. Briefly, the procedure was as follows. First, remaining CO₂ and H₂O were removed at -196 °C, after which samples were collected at -196 °C on molecular sieve pellets. Subsequently, the pellets were heated to 60 °C and the gas was carried through the GC column using a purified He carrier gas. O₂ and Ar eluted before N₂ and were trapped on a second trap with molecular sieve pellets at -196 °C. After O₂ and Ar had eluted, the flow through the line was redirected so that N₂ was carried to waste. After pumping away excess He, the trap containing the sample was heated to 60 °C and the samples were collected into stainless steel fingers by cryogenic trapping on to 5 molecular sieve pellets at -196 °C. This approach had been tested before (Gloël (2012), Gonzalez-Posada (2012)) and was found not to cause any significant fractionation. Samples on molecular sieves in stainless steel fingers were heated for 20 minutes at ~60 °C prior to introduction to the MS, after which the triple oxygen isotopic and elemental composition (O₂, N₂ and Ar content) of the gas was determined through dual-inlet isotope ratio mass spectrometry in a MAT 252. Samples were directly measured against an O₂-Ar reference gas mixture (4.7% Ar in O₂, *BOC Ltd.*).

4.2.3 IRMS measurements

For each set of samples a sample of dry air was processed as internal laboratory standard in a similar way to the dissolved oxygen samples, and averaged results were used to standardise the triple oxygen isotopic and O₂/Ar results with respect to atmospheric air.

For each sample, three measurement runs were conducted consisting of 30 cycles of alternate sample-reference analyses. Average $\delta^{17}\text{O}$ and $\delta^{18}\text{O}$ were calculated for each run. Interfering masses (N₂ at m/z 28 and Ar at m/z 40) were measured at the end of each run. ^{17}O excess and $\delta\text{O}_2/\text{Ar}$ were calculated using the following formulas:

$$\Delta^{17}\text{O} = \delta^{17}\text{O} - 0.5179 \delta^{18}\text{O}$$

$$\delta(\text{O}_2/\text{Ar}) = \frac{(U_{32}/U_{40})_{\text{sa}}}{(U_{32}/U_{40})_{\text{ref}}} - 1$$

where U_{32} and U_{40} are the voltages of the ion beam intensities at m/z 32 ($^{16}\text{O}_2$) and 40 (^{40}Ar) respectively. ‘sa’ stands for sample and ‘ref’ for working reference.

Results were corrected for N₂ interference and reference-sample voltage imbalance according to the relationships described in **Section 2.3.2**.

In addition, $\delta^{18}\text{O}$ and $\delta(\text{O}_2/\text{Ar})$ results were corrected for the distribution of gases between headspace and water phase in the sample bottles (‘solubility correction’, see **Section 2.3.2.4**) as follows:

$$\delta(\text{O}_2/\text{Ar})_{\text{corr}} = Q [1 + \delta(\text{O}_2/\text{Ar})_{\text{meas}}] - 1$$

where

$$Q = \frac{1 + L(\text{O}_2) \cdot f_V}{1 + L(\text{Ar}) \cdot f_V};$$

$L(\text{O}_2)$ is the Ostwald solubility coefficient of oxygen for the temperature in the laboratory and f_V is the ratio of water over headspace volume ($V_{\text{water}}/V_{\text{gas}}$).

$$\delta^{18}\text{O}_{\text{corr}} = Q (1 + \delta^{18}\text{O}_{\text{meas}}) - 1$$

where

$$Q = \frac{1 + L(^{18}\text{O}^{16}\text{O}) \cdot f_V}{1 + L(^{16}\text{O}_2) \cdot f_V}$$

and

$$L(^{18}\text{O}^{16}\text{O}) = L(^{16}\text{O}_2) \cdot (1 + \delta^{18}\text{O}_{\text{sat}})$$

In these tests, f_V was close to 1. For $\delta(\text{O}_2/\text{Ar})$, Q was 0.997-0.998 and the resulting correction was -2 to -3 ‰. For $\delta^{18}\text{O}$, Q was 1.01-1.02 and the correction was +0.01 to +0.02 ‰. For $\delta^{17}\text{O}$, no definite $\delta^{17}\text{O}_{\text{sat}}$ value is available from literature, but the effect is expected to be mass dependent, and not to significantly affect $\Delta^{17}\text{O}$ (J. Kaiser, personal communication 2013).

4.3 Results

Table 5, and Figure 20 to 23 show the results of the air-equilibrated water tests.

Table 5: $\delta^{17}\text{O}$, $\delta^{18}\text{O}$, $\Delta^{17}\text{O}$ (0.5179) and $\delta(\text{O}_2/\text{Ar})$ of air-equilibrated water vs. air from tests conducted at different temperatures and salinities. Displayed $\delta^{18}\text{O}$ values include a solubility correction (Section 4.2.3), which was not applied to the $\delta^{17}\text{O}$. Results of the non-solubility corrected $\delta^{18}\text{O}$, which was used for the calculation of $\Delta^{17}\text{O}$, are displayed in brackets. Values that are uncertain or different from the general pattern are displayed in italics. Bracketed terms in the third and fourth column are the results without inclusion of these values. Expected equilibrium values based on the temperature dependence reported by Benson and Krause (1984) and Barkan and Luz (2009) are displayed in green.

	Distilled				35g l ⁻¹ NaCl			
	$\delta^{17}\text{O}/\text{‰}$	$\delta^{18}\text{O}_{\text{sc}}/\text{‰}$	$\Delta^{17}\text{O}/\text{ppm}$	$\delta(\text{O}_2/\text{Ar})/\text{‰}$	$\delta^{17}\text{O}/\text{‰}$	$\delta^{18}\text{O}_{\text{sc}}/\text{‰}$	$\Delta^{17}\text{O}/\text{ppm}$	$\delta(\text{O}_2/\text{Ar})/\text{‰}$
0°C								
1	0.458	0.871	16	-85.9				
2	0.490	0.953	6	-89.2				
3	0.474	0.931	4	-88.0				
4	0.552	1.084	3	-89.7				
Average	0.494	0.959(0.939)	7 (4)	-88.2 (-89.0)				
SD (n=4)	0.041	0.090(0.080)	6 (2)	1.7 (0.9)				
		0.833	2					
22°C								
1	0.208	0.369	22	-87.9	0.390	0.767	1	-89.6
2	0.237	0.439	14	-77.0	0.360	0.667	24	-89.0
3	0.258	0.457	25	-89.2	0.347	0.651	17	-88.8
Average	0.234	0.421(0.413)	20	-84.7 (-88.5)	0.366	0.695(0.679)	14	-89.2
SD (n=3)	0.025	0.046(0.048)	6	6.7 (0.9)	0.022	0.063(0.060)	12	0.4
		0.717	15			0.717	15	
39°C								
1	0.189	0.365	4	-87.9	0.327	0.643	1	-90.9
2	0.230	0.440	8	-90.0	0.306	0.605	-3	-91.0
3	0.199	0.373	9	-88.9	0.315	0.610	8	-90.0
4	0.217	0.396	16	-89.9	0.103	0.177	11	-50.0
Average	0.209	0.394(0.385)	9	-89.2	0.316	0.619(0.607)	2	-90.7
SD (n=4)	0.018	0.034(0.032)	5	1.0	0.010	0.021(0.019)	5	0.5
		0.638	25			0.638	25	

Green: expected eq.-values based on T-relationships Benson and Krause (1984) and Barkan and Luz (2009)

One 35 g l⁻¹ NaCl 39 °C sample was contaminated with air during water sampling and is therefore displayed in pale red and not included in the average.

Standard deviations in $\delta^{17}\text{O}$ and $\delta^{18}\text{O}$ are on average 0.02 and 0.05‰, which is comparable to standard deviations obtained for samples of dry air standard and O₂-Ar reference that were processed through the separation line in a similar way to the samples (see Chapter 2). Standard deviations for all individual $\Delta^{17}\text{O}$ results at one temperature are 12-13 ppm, which is also comparable to tests with dry air and O₂-Ar standard processed through the separation line. Variations between 3 samples of one set are 0.010 ‰ for $\delta^{17}\text{O}$ and $\delta^{18}\text{O}$ and 10 ppm for $\Delta^{17}\text{O}$, which is comparable to the standard deviation of zero enrichments (Section 2.4, Table 1).

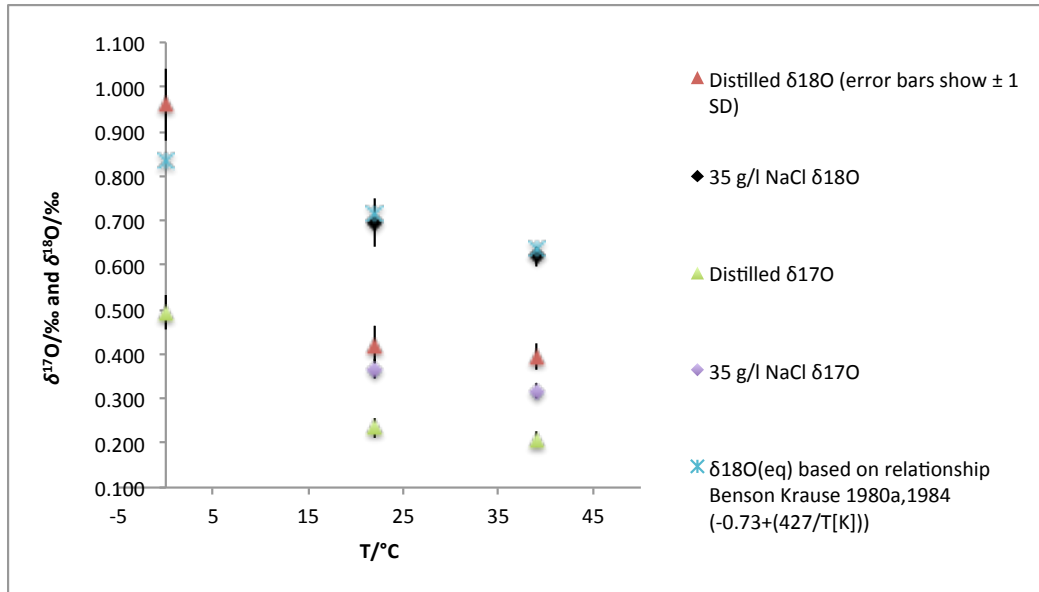


Figure 20: $\delta^{17}\text{O}$ and $\delta^{18}\text{O}$ (vs. air) results of the air-equilibrated water tests. Distilled water results are displayed as triangles (red = $\delta^{18}\text{O}$, green = $\delta^{17}\text{O}$), while diamonds indicate 35 g l⁻¹ NaCl results (black = $\delta^{18}\text{O}$, purple = $\delta^{17}\text{O}$). Error bars are ± 1 SD. Blue symbols show the equilibrium values expected based on the temperature relationship of Benson and Krause (1984).

Average $\Delta^{17}\text{O}$ values are between 2-20 ppm with respect to air, and in the range of $\Delta^{17}\text{O}_{\text{sat}}$ values reported in literature. Values for distilled and salt water at room temperature are (20 \pm 6) ppm and (14 \pm 12) ppm, respectively.

The standard deviation of $\Delta^{17}\text{O}$ for most tests is 5-6 ppm, except for the test with salt water at 22 °C, which gave 12 ppm. These results are comparable to the standard deviations of earlier studies in the same laboratory (Gloël 2012, Gonzalez-Posada 2012), and similar studies conducted by other laboratories (Table 5). Only the lab of Luz and Barkan (2000, 2003, 2009) consistently reports lower uncertainties.

During tests conducted at 39 °C for both distilled and for 35 g l⁻¹ NaCl water $\Delta^{17}\text{O}$ values below the range of 16-18 ppm were obtained (9 \pm 5 for distilled and 2 \pm 5 for 35 g l⁻¹ NaCl). The differences between results of tests at 22 °C and 39 °C in this study are not statistically significant for one water type, due to the large variability in the 22 °C results and small sample numbers. However, they are significant when results of both water types are combined for each temperature, in which case averages of (17 \pm 6) ppm and 6 \pm 6 ppm are obtained for the 22 °C and 39 °C tests, respectively.

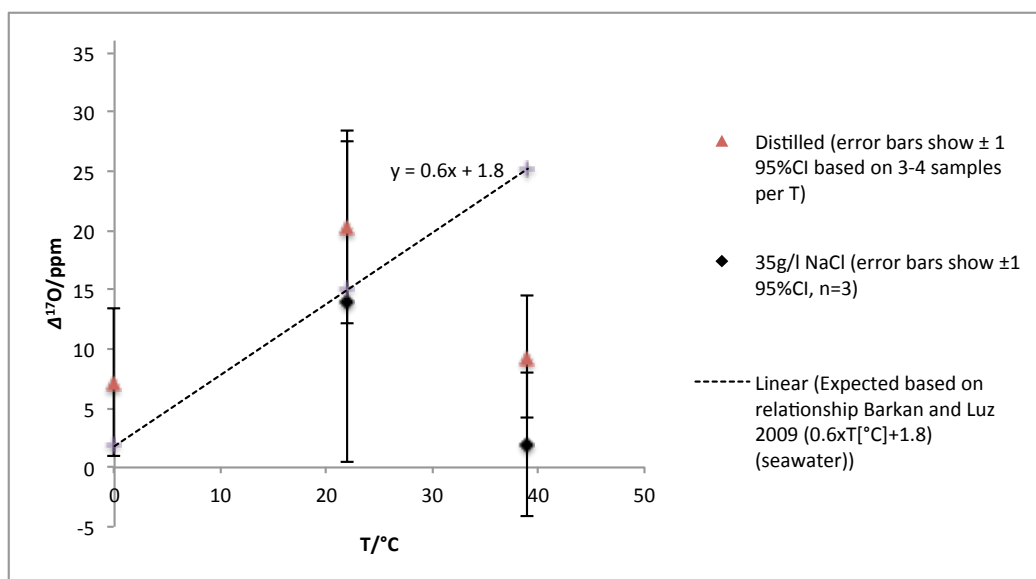


Figure 21: Average $\Delta^{17}\text{O}$ (0.5179, vs. air) results of the air-equilibrated water tests. Red triangles show the averages of 3-4 distilled water samples, while the averages of 3 35 g l⁻¹ NaCl water samples are displayed as black diamonds. Error bars show ± 1 95% CI. Purple symbols show the expected values based on the temperature relationship reported by Barkan and Luz (2009). Note: the value at 39 °C was obtained through extrapolation; Barkan and Luz did not conduct experiments up to this temperature.

4.4 Discussion

4.4.1 $\Delta^{17}\text{O}$ results compared to previous results

As can be observed in **Figure 22**, $\Delta^{17}\text{O}$ values for tests conducted at 22 °C for both distilled and 35 gL⁻¹ NaCl water cluster around 20 ppm, with the exception of one low value of 1 ppm for the 35 g l⁻¹ NaCl scenario. The reason for this relatively low value is not known. It could be due to the uncertainty of the method (however, this value is accompanied by relatively positive $\delta^{17}\text{O}$ and $\delta^{18}\text{O}$ values, see discussion below).

Due to this low value, the resulting average $\Delta^{17}\text{O}$ for water at 35 g l⁻¹ NaCl is slightly lower than for distilled water, i.e. (14 \pm 12) ppm vs. (20 \pm 6) ppm. The difference is however not statistically significant. Both values are relatively close to the values of 16-18 ppm reported in most previous studies at room temperature (**Table 4**) and differ from the value of 8 ppm reported by Reuer et al. (2007) and Stanley et al. (2010).

Expected $\Delta^{17}\text{O}$ values based on the linear relationship between temperature and $\Delta^{17}\text{O}$ reported by Barkan and Luz (2009) (**Section 4.1**) are displayed in **Table 5** and **Figure 21 and 22** (2 ppm at 0 °C, 15 ppm at 22 °C and 25 ppm at 39 °C). Experiments in this study show an average value of 14 ppm for 35 g l⁻¹ NaCl test at 22 °C, which is very

close to the value based on the temperature relationship of Barkan and Luz (2009) (15 ppm for 22 °C).

The results for the 39 °C tests using both distilled and salt water are significantly below the 16-18 ppm values reported in the literature (**Table 4**). They are also in the opposite direction of what would be expected based on the temperature dependence reported by Barkan and Luz (2009) (expected value at 39 °C based on this relationship: 25 ppm). Values reported here are closer to the 8 ppm value reported by Reuer et al. (2007) and Stanley et al. (2010) than the 16-18 ppm reported in studies mentioned above. However, the number of samples in this study (4) is relatively low. It is also important to note that Barkan and Luz did not conduct experiments up to 40 °C, and no other research groups conducted air-equilibrated water tests at temperatures above 25 °C before. Therefore it cannot be excluded that at this high temperature other factors play a role, or the linear temperature-relationship reported by Barkan and Luz (2009) does not apply up to such high temperatures.

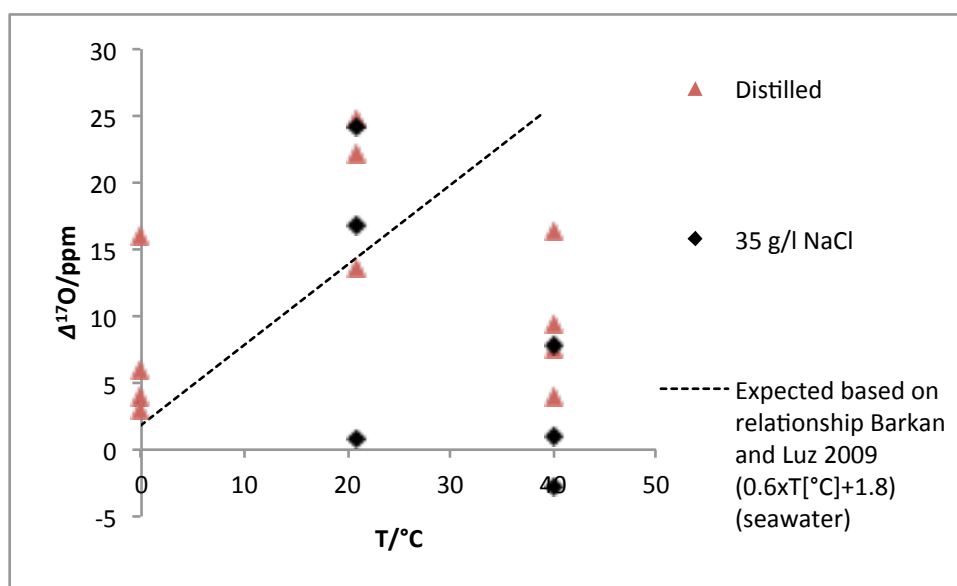


Figure 22: Individual $\Delta^{17}\text{O}$ (vs. air) results of the air-equilibrated water tests. Red triangles indicate distilled water while black diamonds indicate water with 35 g l⁻¹ NaCl. Each symbol shows the result of one sample (average of 3 MS runs of 30 cycles). The dotted line shows the expected values based on the temperature relationship reported by Barkan and Luz (2009) (based on experiments at 3.5-25 °C).

Comparatively low $\Delta^{17}\text{O}$ values of (7±6) ppm (**Table 5**) were also obtained for the test with distilled water at 0 °C. When the first sample is excluded, the average becomes (4±2) ppm. Based on the temperature relationship of Barkan and Luz (2009) a value of 2 ppm would be expected at 0 °C, which is very close to the value obtained here.

The results of experiments conducted at 0 °C and 22 °C are thus close to expectations based on the Barkan and Luz (2009) temperature relationship, while the 39 °C results are not. As mentioned above, this might indicate the proposed linear relationship does not apply up to this temperature. It should however be realised sample numbers were small and the standard deviation was large. The difference of ~10 ppm between results at different temperatures is coincidentally close to the difference between reported $\Delta^{17}\text{O}_{\text{sat}}$ values at room temperature. This is equal to the standard deviation of zero enrichments during this study (**Chapter 2, Table 1**), thus for low sample numbers it cannot be excluded such a difference is related to the intrinsic uncertainty of the method. In this study, unfortunately, no tests were conducted with 35 g l⁻¹ NaCl water at 0 °C.

4.4.2 $\delta^{18}\text{O}$ results compared to previous results

For both distilled water and salt water, lower $\delta^{18}\text{O}$ values were measured for higher temperatures, which is consistent with the findings of Benson and Krause (1979). However, $\delta^{18}\text{O}$ values of distilled water tests are far from expected equilibrium values based on the relationship of Benson and Krause (1984), at 22 °C and 39 °C being 0.2-0.3‰ below expected values and $\delta^{18}\text{O}$ values for distilled water tests at 0 °C being 0.1‰ above expected values. This could be related to handling of the samples, inconsistent bubbling times (up to 7 days, without monitoring O₂ concentration), times between bubbling and sampling, and equilibration times, and relatively long storage times of these samples (2 weeks for 0 °C and 39 °C and 3 months for 22 °C distilled water samples) on molecular sieves in glass tubes with Glass-expansion valve (without water seal) due to problems with the separation line, which might have lead to contamination or alteration of the sample. In addition, for the test at 0 °C, fractionation due to freezing might have played a role (experiments of Benson and Krause were not conducted down to 0 °C).

For all three temperatures the deviation in the $\delta^{18}\text{O}$ values is however very similar between the 3-4 samples, indicating the same process affected all samples in the same way. $\Delta^{17}\text{O}$ and $\delta(\text{O}_2/\text{Ar})$ results do not seem to have been affected by this deviation in the $\delta^{18}\text{O}$, as they are comparable to the results of 35 g l⁻¹ NaCl water tests (see below), and $\delta(\text{O}_2/\text{Ar})$ results are very close to equilibrium values reported in literature.

The 35 g l⁻¹ NaCl tests produced $\delta^{18}\text{O}$ values very close to equilibrium values reported by Benson and Krause (1984) (0.695±0.060 vs. 0.717 ‰ and 0.619±0.020 vs. 0.638 ‰, respectively). For these tests, O₂ concentration and saturation were monitored during the bubbling, bubbling times were 24-48 hours, sampling took place within one hour of bubbling and samples were not stored on molecular sieves for more than one day.

Benson and Krause (1984) stated a difference in salinity from 0 to 40 would not alter $\delta^{18}\text{O}$. Based on this, one would not expect $\delta^{18}\text{O}$ results to differ significantly between distilled water and 35 g l⁻¹ experiments conducted at 22 °C and 40 °C. The fact that they do in this case is probably largely due to errors in the distilled water results due to long storage times or not sampling while at saturation. However, the observed deviation was comparable for distilled water samples prepared at 22 °C and 40 °C, although storage time was 8 times as long for the 22 °C samples. In addition, 0 °C and 40 °C samples were treated in a very comparable way (with similar bubbling and storage times), but in the 40 °C case resulting $\delta^{18}\text{O}$ values were 0.2‰ below the expected value, while in the 0 °C case they are 0.1 ‰ above the expected value. It should however be realised that for the 0° C test, fractionation due to partial freezing of the sample might have played an additional role. Benson and Krause (1979) did not conduct their tests down to 0 °C. It would therefore be interesting to repeat the low temperature experiments at a slightly higher temperature (1-3 °C).

The 35 g l⁻¹ NaCl samples in **Table 5** are numbered according to the order of sampling (note: distilled water samples are not), the first sample having been sampled relatively soon after stopping bubbling (5 (39 °C) to 15 (22 °C) minutes), while the other two samples were collected with a longer delay after stopping bubbling (15-30 minutes for the 39 °C sample 2-3, 30 minutes for 22 °C sample 2 and 1 hour for 22° sample 3.) A decrease can be observed in the individual $\delta^{18}\text{O}$ results with increasing time between bubbling and sampling, samples collected within 15 minutes after bubbling (35 g l⁻¹ NaCl sample 1 of 22 °C and 39°) having a relatively high $\delta^{18}\text{O}$ (higher than the equilibrium value of Benson and Krause (1984)) compared to the samples (2 and 3) that were collected later (**Table 5**). The difference is larger for the room temperature results, which could be explained by a larger time difference between the samples (15 minutes between sample 1 and 2 and 30 minutes between sample 2 and 3 (vs. 10 minutes between 1 and 2 and 5 minutes between 2 and 3 for the 39 °C test). In addition, for the 22 °C test a decrease in the O₂ concentration and saturation was visible over the time of sampling (from 246 µM for sample 1 and 2 to 243 µM for sample 3), while for the 39 °C test the O₂ concentration and saturation were relatively stable (but the time span was shorter). The differences in results between sample 2 and 3 (RT) (in $\delta^{17}\text{O}$, $\delta^{18}\text{O}$, $\Delta^{17}\text{O}$ and $\delta(\text{O}_2/\text{Ar})$) are however smaller than the differences between sample 1 and 2 for both 22 °C and 39 °C tests, which might indicate that values stabilise with increased time between bubbling and sampling.

In addition, the relatively high $\delta^{17}\text{O}$ and $\delta^{18}\text{O}$ values measured for 35 g l⁻¹ NaCl sample 1 at 22 °C are accompanied by a relatively negative $\Delta^{17}\text{O}$ (and $\delta(\text{O}_2/\text{Ar})$) ($\Delta^{17}\text{O} = 1$ ppm versus 24 and 17 ppm for test 2 and 3). While this might be a coincidence, due to the

relatively large variability in $\Delta^{17}\text{O}$ results, it could also be related to the observed (positive) deviation in the small deltas from equilibrium values for this sample. Unfortunately, for the distilled water tests times between bubbling and sampling of individual samples were not recorded (but sampling probably took place relatively fast after bubbling for distilled 0 °C and 39 °C samples).

The decrease in $\delta^{18}\text{O}$ with increasing time between bubbling and sampling, and the relatively positive $\delta^{18}\text{O}$ values (with respect to equilibrium values of Benson and Krause 1984) obtained for samples collected quickly after bubbling, might be related to the fact that a slight supersaturation of oxygen might exist directly after bubbling (which would lead to above equilibrium concentrations and consequently a larger evasion flux and increased fractionation (higher $\delta^{17}\text{O}$ and $\delta^{18}\text{O}$ values) (Kaiser 2011)). In addition, the temperature increased slightly after the stop of bubbling, which would also have led to a decrease in O_2 concentrations with time after bubbling.

This, and the fact that values seem to stabilise with longer time after bubbling, might indicate that adapting a longer time between bubbling and sampling (2 hours, as suggested by Barkan and Luz 2002, 2003 and 2009, based on preliminary experiments) might lead to less variable and more accurate results. However, in all other air-equilibrated water studies using the bubbling approach, the times between bubbling and sampling were not mentioned. If the timing would indeed make a difference for the $\delta^{18}\text{O}$ and possibly $\Delta^{17}\text{O}$ results, the use of different times between bubbling and sampling could potentially have influenced the results. However, here unfortunately times between sampling and bubbling were not recorded for distilled water samples, and based on this limited dataset (3 samples and 2 temperatures) it is impossible to say whether this has truly influenced the results. However, since Barkan and Luz (2009) adopted a period of 2 hours between bubbling and sampling based on preliminary experiments, and values obtained here seem to stabilize with longer time after bubbling, it would be advisable, also for comparison purposes, to conduct any future air-equilibrated water tests with a period of 2 hours between bubbling and sampling.

4.4.3 $\delta(\text{O}_2/\text{Ar})$ results compared to previous results

$\delta(\text{O}_2/\text{Ar})$ results of individual samples are displayed in **Table 5** and **Figure 23**. For most distilled and 35 g l⁻¹ NaCl water samples obtained $\delta(\text{O}_2/\text{Ar})$ values are around -89‰, and very close (within 1‰) to equilibrium values reported in literature (Hamme and Emerson 2004) and observed in similar studies (Barkan and Luz 2003, Sarma 2006b, Castro-Morales 2010). Except for one distilled water sample with a $\delta(\text{O}_2/\text{Ar})$ of -77‰ (22 °C sample 2) and one distilled water sample with a $\delta(\text{O}_2/\text{Ar})$ of -85.9‰ (0 °C sample 1), all $\delta(\text{O}_2/\text{Ar})$ results are in the range of -88 to -91‰, which corresponds to the

equilibrium values reported in literature (Hamme and Emerson 2004). $\delta(\text{O}_2/\text{Ar})$ values are slightly more negative for tests at 39 °C (-90 ‰) and for tests with 35 g l⁻¹ NaCl (compared to tests with distilled water and lower temperatures). This is consistent with expectations based on literature (Hamme and Emerson 2004). The fact that $\delta(\text{O}_2/\text{Ar})$ values of most (all except one) distilled water samples are in close agreement with equilibrium values from literature values is interesting because the $\delta^{17}\text{O}$ and $\delta^{18}\text{O}$ results of the distilled water tests are so far from the equilibrium values. If this was caused by sampling while the water was not in equilibrium with air, or by contamination of the samples with air, one would expect this to be reflected in the $\delta(\text{O}_2/\text{Ar})$ too. However, isotope and elemental ratios would not necessarily be affected to a similar extent.. The relatively positive $\delta(\text{O}_2/\text{Ar})$ that was observed for one 22 °C distilled sample (-77‰, see **Table 5**) is difficult to explain based on these data. Apart from this relatively positive $\delta(\text{O}_2/\text{Ar})$ value, the other results of this sample are not different from those of the other two samples of the same test, $\delta^{17}\text{O}$ and $\delta^{18}\text{O}$ results being in between those of the other two tests, and $\Delta^{17}\text{O}$ results not being significantly different. In the case of sample 1 of the distilled water test at 0 °C, the relatively positive $\delta(\text{O}_2/\text{Ar})$ of -85.9‰ is accompanied by relatively negative $\delta^{17}\text{O}$ and $\delta^{18}\text{O}$ values. Due to a problem during water collection for this particular sample, some outside air might have accidentally entered the bottle. While this could explain the slightly lower $\delta^{17}\text{O}$ and $\delta^{18}\text{O}$ and higher $\delta(\text{O}_2/\text{Ar})$ (both closer to zero = air) for this sample, it would not explain why the $\Delta^{17}\text{O}$ is relatively high for this sample. This could however be a coincidence since the variability between samples is relatively large).

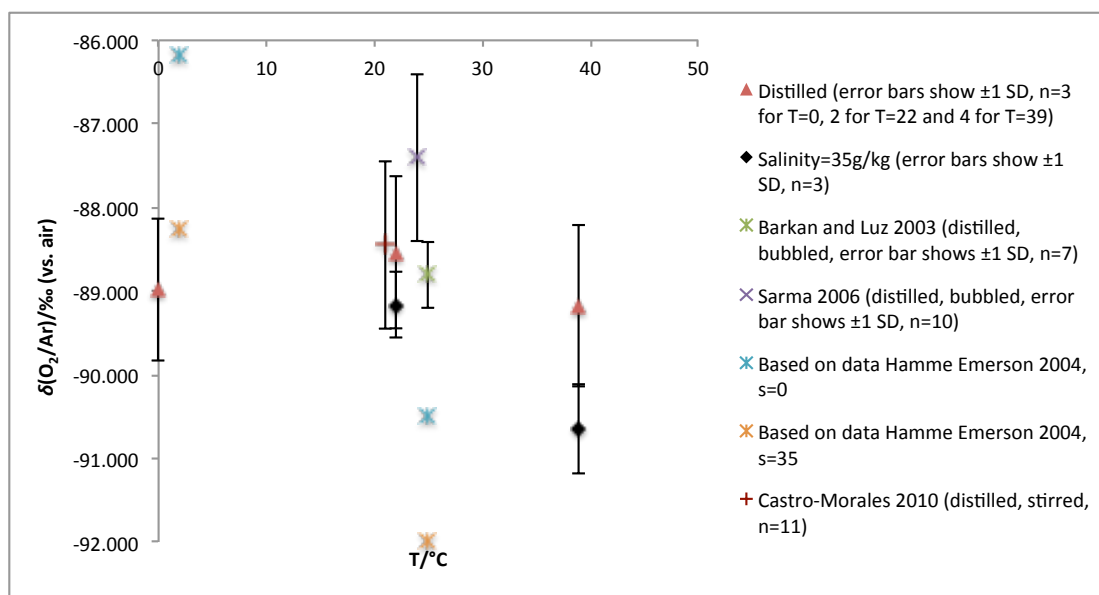


Figure 23: $\delta(\text{O}_2/\text{Ar})$ (vs. air) results of the air-equilibrated water tests. Results of this study are displayed in red triangles (distilled water) and black diamonds ($35 \text{ g l}^{-1} \text{ NaCl}$). Results of comparable studies and expected equilibrium values based on O_2/Ar ratios measured by Hamme and Emerson (2004) are displayed for comparison. Average $\delta(\text{O}_2/\text{Ar})$ values without outliers are displayed (distilled water tests at $0 \text{ }^\circ\text{C}$ and $22 \text{ }^\circ\text{C}$ each yielded one relatively negative $\delta(\text{O}_2/\text{Ar})$ value, which is not included in these averages). Complete $\delta(\text{O}_2/\text{Ar})$ results are given in **Table 5**. As can be observed, for most tests the obtained $\delta(\text{O}_2/\text{Ar})$ values are close (within $\sim 1\text{‰}$) to equilibrium values reported in literature. Room temperature $\delta(\text{O}_2/\text{Ar})$ results ($-88.5 \pm 0.9\text{‰}$ for distilled and $-89.2 \pm 0.9\text{‰}$ for $35 \text{ g l}^{-1} \text{ NaCl}$ water) are very close to the results of Barkan and Luz 2003 ($-88.8 \pm 0.4\text{‰}$), Sarma 2006b ($-87.4 \pm 1\text{‰}$) and Castro-Morales 2010 ($-88.4 \pm 1\text{‰}$) for comparable tests. More negative $\delta(\text{O}_2/\text{Ar})$ values were obtained with increasing temperature and salinity, which is consistent with the data of Hamme and Emerson (2004). For most tests, the SD was in the range $0.5\text{-}1\text{‰}$, which is comparable to the SDs reported in literature.

4.5 Conclusions

Although for both water types at room temperature an average ^{17}O excess in the range of $15\text{-}20 \text{ ppm}$ was obtained, lower values were obtained for both lower ($0 \text{ }^\circ\text{C}$) and higher ($39 \text{ }^\circ\text{C}$) temperature experiments (close to or below 8 ppm). While the low value at $0 \text{ }^\circ\text{C}$ could be in agreement with the temperature-dependence reported by Barkan and Luz (2009), the low ^{17}O excess obtained for both distilled and salt water, at $39 \text{ }^\circ\text{C}$ could not be explained by this relationship. This could indicate the proposed linear relationship does not apply up to this high temperature. However, because the spread in the $22 \text{ }^\circ\text{C}$ data is relatively large (SD: $5\text{-}12 \text{ ppm}$ means, 13 ppm individual measurements), and the sample number per scenario is small ($3\text{-}4$), differences between $22 \text{ }^\circ\text{C}$ and $39 \text{ }^\circ\text{C}$ tests of

the same water type are not statistically significant. Differences between the $\Delta^{17}\text{O}$ at 22 °C and 39 °C are however statistically significant when the water types are combined (combined averages being (17 ± 6) ppm for 22 °C and (6 ± 6) ppm for 39 °C).

Because the observed SD (in $\delta^{17}\text{O}$ and $\delta^{18}\text{O}$ and $\Delta^{17}\text{O}$) was comparable to that obtained when processing dry air or O_2 -Ar samples through the separation line, the large uncertainty is probably mainly due to the uncertainty of the sample processing method and MS measurements. More reliable results can therefore only be obtained by increasing the sample number.

In addition, although obtained $\delta(\text{O}_2/\text{Ar})$ values for both distilled and salt water tests, and $\delta^{18}\text{O}$ values for the salt water tests are very close to equilibrium values reported in literature, $\delta^{18}\text{O}$ values of the distilled water tests were either 0.2-0.3 ‰ lower (22 °C and 40 °C) or 0.1 ‰ higher (0 °C) than expected equilibrium values. The reason for this is not known, but compared to salt water samples, distilled water samples were stored longer on molecular sieves, and bubbled longer, without monitoring of the O_2 concentration (or time between bubbling and sampling). Finally, at 0 °C, fractionation due to freezing could not be excluded.

It would therefore be advisable, based on these results, to repeat the tests with larger sample numbers, preferably at an increased number of temperatures. In addition, in order to obtain data more suitable for comparison, distilled water tests should ideally be repeated with shorter storage and bubble times (24-48 h), monitoring of O_2 concentrations during equilibration and consistent times between stop of bubbling and sampling (preferably 2 hours). Finally, it would be interesting to conduct the low temperature test at a temperature slightly above 0 °C for both water types.

Chapter 5: The isotopic signature of photosynthetic oxygen

Abstract

Recently it was reported that species-specific fractionation takes place during photosynthesis in phytoplankton (Eisenstadt et al. 2010). This would make the $\Delta^{17}\text{O}$ of biological oxygen a combination of the $\Delta^{17}\text{O}$ of the water used in its production and a species-specific change due to fractionation. Kaiser and Abe (2012) estimated $\Delta^{17}\text{O}_{\text{bio}}$ based on different $\Delta^{17}\text{O}$ measurements of Vienna Standard Mean Ocean Water (VSMOW) vs. air and the fractionation per species observed by Eisenstadt et al. (2010) (**Table 7**). In order to obtain more information on the triple isotopic composition of biological oxygen, culture experiments were conducted with two marine phytoplankton species under steady-state conditions. For this, cultures of marine phytoplankton species *Picochlorum* sp. and *Emiliana huxleyi* were grown in airtight 165 ml bottles with a 4 ml N_2 headspace under close-to-natural growth conditions. Oxygen was allowed to accumulate and replace initially present oxygen in the bottles over a period of 5-6 days, after which samples of the headspace gas were collected at different time intervals over a period of 8-15 days, through a needle under vacuum, connected to an extraction line. Samples were analysed for their triple oxygen isotopic composition and O_2/Ar ratio on a *Finnigan MAT 252* dual-inlet isotope ratio mass-spectrometer.

Results indicated biological steady state was reached, and $\Delta^{17}\text{O}$ values stabilised, from the start of sampling for *Picochlorum* and near the end of sampling for *E. huxleyi*. The steady state values were (249 ± 11) ppm (± 1 SD) for *E. huxleyi* and (180 ± 13) ppm for *Picochlorum*. Results were consistent between bottles of the same growth day from different sample series and independent experiments conducted in May and June-July 2013. Results are in the range of $\Delta^{17}\text{O}$ values estimated by Kaiser and Abe (2012) based on different measurements of VSMOW and the photosynthetic fractionation reported by Eisenstadt et al. (2010), and seem to be in agreement with findings of Eisenstadt et al. (2010), who reported species-specific photosynthetic fractionation in *E. huxleyi* and other phytoplankton species.

5.1 Introduction

This chapter focuses on triple isotopic composition of marine biological oxygen. As explained in **Chapter 1**, accurate knowledge of the triple isotopic composition of biological oxygen ($\Delta^{17}\text{O}_{\text{bio}}$) is crucial in the derivation of gross oxygen production using triple oxygen isotopes. However, at the moment there is still a lot of uncertainty regarding the exact value of this parameter. In order to improve our knowledge on $\Delta^{17}\text{O}_{\text{bio}}$, experiments were conducted with different types of marine phytoplankton under biological steady state conditions. In the following section, a brief a description will be given of the current knowledge on $\Delta^{17}\text{O}_{\text{bio}}$ the remaining uncertainties and the reason for this study.

Introduction

For the derivation of oceanic gross oxygen production using oxygen triple isotopes, next to information on air-sea gas exchange and the composition of atmospherically derived oxygen, information is required on the triple isotopic composition of pure biological oxygen*. However, experimental data on the triple isotopic signature of biological oxygen are sparse. Until recently, a universal value of ~ 250 (249 ± 15) ppm was assumed for all marine biological oxygen, based on steady-state culture experiments with two marine species (*Acropora*, a coral with symbiotic algae (252 ± 5 ppm) and planktonic alga *Nannochloropsis*, (244 ± 20 ppm)) by Luz and Barkan (2000). In these experiments, oxygen was allowed to accumulate, and samples were taken after all initially present oxygen had been replaced by biological oxygen, and a steady state between respiration and production was reached. (Note: $\Delta^{17}\text{O}_{\text{bio}}$ values were calculated using the linear definition with slope/ λ 0.521. Unfortunately, they were reported without underlying $\delta^{17}\text{O}$ and $\delta^{18}\text{O}$ values. Fortunately, under steady state conditions, with $\delta^{17}\text{O}$ and $\delta^{18}\text{O}$ values close to zero, the use of different definitions or slopes has a relatively small effect on the resulting $\Delta^{17}\text{O}$ (Barkan and Luz 2011, Kaiser and Abe 2012)).

* Pure biological oxygen can refer to pure photosynthetic oxygen, oxygen at a steady state between photosynthesis and respiration, or oxygen in a system with both photosynthesis and respiration that is not at steady state. A detailed explanation is given on page 97. In this study, because of the focus on application for marine productivity estimates, $\Delta^{17}\text{O}_{\text{bio}}$ refers to marine biological oxygen. For terrestrial biological oxygen, the resulting $\Delta^{17}\text{O}$ is generally (~ 100 ppm) lower due the lower $\Delta^{17}\text{O}$ of fresh water relative to seawater (Luz et al. 1999, Luz and Barkan 2000).

Because several studies indicated the production of oxygen by cleavage of water molecules in photosystem II during photosynthesis would cause negligible isotopic fractionation (Guy et al. 1993, Helman et al. 2005, Tcherkez and Farquhar 2007), it was assumed the isotopic composition of photosynthetic oxygen would be approximately equal to that of the source water used in its production. However, until recently, accurate ($< \pm 80$ ppm) measurements of the triple isotopic composition of seawater (represented by the VSMOW, Vienna Standard Mean Ocean Water, standard) versus air were not available. When results of such measurements were first published in 2005 (Luz and Barkan 2005), they indicated $\Delta^{17}\text{O}$ values for VSMOW versus air in the range of ~ 150 ppm (exact value depending on $\Delta^{17}\text{O}$ definition). This was substantially lower than the (~ 250 ppm) value for biological oxygen reported by Luz and Barkan 2000, and the difference was too large to be easily attributed to the involvement of different oxygen consumption processes or a difference in the used definition or slope for $\Delta^{17}\text{O}$.

However, two recent studies, by the same research group, provided data that could explain this difference.

Firstly, in 2010, Eisenstadt et al. reported photosynthetic fractionation was possibly not negligible, as assumed before, but significant (in the order of 1-7‰ for $\delta^{18}\text{O}$ and 10-70 ppm for $\Delta^{17}\text{O}$), and species-dependent. Results indicated, depending on the species, an increase in $\Delta^{17}\text{O}$ of ~ 10 -70 ppm with respect to the substrate water. Eisenstadt et al. (2010) performed experiments with different fresh water and marine phytoplankton species, both at ~ 0 oxygen levels (assuming no respiration), and with rising oxygen levels. In contrast to what was indicated by earlier studies (Guy et al. 1993, Helman et al. 2005), a significant enrichment in both $^{17}\text{O}/^{16}\text{O}$ and $^{18}\text{O}/^{16}\text{O}$ was observed even at zero oxygen levels, together with an increase in $\Delta^{17}\text{O}$. Since one would expect respiration at these oxygen levels to be negligible, the authors concluded this indicated fractionation took place during photosynthesis (possibly due to cell-internal recycling of oxygen close to the site of production/PTOX or chlororespiration). Results were different from those of comparable studies by Guy et al. 1993 and Helman et al. 2005, in which only a very small, negligible fractionation was observed ($^{18}\epsilon_p < 1\text{‰}$, $\Delta^{17}\text{O} < \sim 10$ ppm) (Guy et al. 1993, Helman et al. 2005). The observed photosynthetic fractionation differed between species, results for all marine species indicating fractionation along a slope (θ_p) of ~ 0.524 , but with different corresponding $^{18}\epsilon_p$ and thus $\Delta^{17}\text{O}$ values. The strongest fractionation (effect on $\delta^{17}\text{O}$ and $\delta^{18}\text{O}$ and $\Delta^{17}\text{O}$ values) was observed for *E. huxleyi* (~ 73 ppm, $^{18}\epsilon_p: 5.814 \pm 0.06\text{‰}$ ($\theta_p: 0.5253$)) and *C. reinhardtii* (~ 49 ppm, $^{18}\epsilon_p: 7.04 \pm 0.1\text{‰}$ (fresh water, $\theta_p: 0.5198$)), while less fractionation was observed for the species *Nannochloropsis* (~ 27 ppm, $^{18}\epsilon_p: 2.850 \pm 0.05\text{‰}$ ($\theta_p: 0.5253$)) and *Synechocystis* (~ 11 ppm, $^{18}\epsilon_p: 0.467 \pm 0.17\text{‰}$ (fresh water, $\theta_p: 0.5354$)) (see **Table 6**). (It should be

noted the result for *Synechocystis* came from an earlier study of Helman et al. (2005). In addition, one of the studied species, *P. tricornutum*, had been studied before by Guy et al. (1993), with different results.) Next to the occurrence of fractionation during photosynthesis, these results thus indicated a difference in photosynthetic fractionation between species.

However, this ~10-70 ppm difference due to photosynthetic fractionation could only partly explain the high value (~250 ppm) for biological oxygen compared to that of VSMOW (~150), not completely. Even if the photosynthetic fractionation is species specific, the same species, *Nannochloropsis*, was studied both in the study of Luz and Barkan (2000) and Eisenstadt et al. (2010). As explained by Kaiser and Abe (2012), the steady-state value of (244±20) ppm obtained in the 2000 Luz and Barkan study cannot easily be explained based on a VSMOW $\Delta^{17}\text{O}$ of 146±4 ppm (lin. def. with $\lambda = 0.5179$) and the photosynthetic fractionation reported by Eisenstadt et al. (2010) (Kaiser and Abe calculated, for different species, the expected $\Delta^{17}\text{O}_{\text{bio}(S_0)}$, see **Table 7**).

However, in 2011, Barkan and Luz published the results of new measurements of VSMOW vs. air, performed in the years 2005-2011, which all indicated a significantly (~50 ppm) higher $\Delta^{17}\text{O}$ of VSMOW vs. air than previous experiments (the new value being 196±4 ppm (calculated with delta-definition, $\lambda = 0.5179$) see **Table 8**). Barkan and Luz (2011) attributed the ~50 ppm difference to improvements in the method. If the value of VSMOW vs. air of ~200 ppm is correct, this would in combination with the photosynthetic fractionation reported by Eisenstadt et al. (2010), perfectly add up to the ~250 ppm value for $\Delta^{17}\text{O}_{\text{bio}}$ reported by Luz and Barkan in 2000. However, in 2012, Kaiser and Abe questioned the reliability of these new measurements, and published values much closer to those originally reported by Luz and Barkan in 2005 (145±6 ppm, delta definition with $\lambda = 0.5179$). The correct value of VSMOW vs. air is therefore still debated, as either ~150 or ~200 ppm.

As mentioned above, even with the photosynthetic fractionation reported by Eisenstadt et al. (2010), the Barkan and Luz (2005) and Kaiser and Abe (2012) VSMOW measurements (~150 ppm) could not explain the ~250 ppm value from the 2000 Luz and Barkan experiments, which is still widely used in the calculation of gross oxygen production.

To summarise, there is still a lot of uncertainty regarding $\Delta^{17}\text{O}_{\text{bio}}$, and the value of ~250 ppm that was assumed to be robust and universal, appears to be less certain than thought before. The only available $\Delta^{17}\text{O}_{S_0}$ (biological steady state $\Delta^{17}\text{O}$ (see side note)), which are widely used in the calculation of gross oxygen production (*GOP*), date from the 2000 experiments and were reported without underlying $\delta^{17}\text{O}$ and $\delta^{18}\text{O}$ values. There is a debate concerning the correct $\delta^{17}\text{O}$ ($\Delta^{17}\text{O}$) value for VSMOW vs. air, and one of the two

proposed values is not compatible with the ~250 ppm value. Finally, recent experiments indicate considerable species-specific photosynthetic fractionation, which would not only imply $\Delta^{17}\text{O}_{\text{bio}}$ is different from $\Delta^{17}\text{O}_{\text{source water}}$ but that $\Delta^{17}\text{O}_{\text{bio}}$ might be species dependent, in contrast to what was initially assumed by Luz and Barkan (2000). This would have important implications for the calculation of gross oxygen production. In order to decrease the uncertainty regarding $\Delta^{17}\text{O}_{\text{bio}}$, experiments were conducted with different species of phytoplankton under steady state conditions, comparable to those conducted by Luz and Barkan in 2000.

Side note: $\Delta^{17}\text{O}_{\text{bio}}$, $\Delta^{17}\text{O}_{\text{S0}}$ and $\Delta^{17}\text{O}_{\text{P}}$

It should be noted that ‘biological’ oxygen can indicate both pure photosynthetic oxygen (P) and oxygen at steady-state between photosynthesis and respiration (concentration or biological steady-state) (S0). Additionally, it can indicate oxygen that is affected by both photosynthesis and respiration, but not at biological steady state (f (ratio of net to gross production) $\neq 0$ or 1).

Eisenstadt et al. (2010) reported $\delta^{17}\text{O}_{\text{P}}$ and $\delta^{18}\text{O}_{\text{P}}$ (pure photosynthetic oxygen in the absence of respiration) values versus the source water, while Luz and Barkan (2000) reported $\Delta^{17}\text{O}_{\text{S0}}$ (concentration or biological steady state) values versus air (atmospheric oxygen).

The relationship between $\delta^{17}\text{O}_{\text{S0}}$ and $\delta^{18}\text{O}_{\text{S0}}$ (values for concentration or biological steady state (ratio net to gross production $f=0$)) can be related to the relationship of $\delta^{17}\text{O}_{\text{P}}$ and $\delta^{18}\text{O}_{\text{P}}$ (values for pure photosynthetic oxygen, in the absence of respiration ($f=1$)), however, this is not straightforward, since it requires knowledge of the exact γ_{R} ($=^{17}\epsilon_{\text{R}}/^{18}\epsilon_{\text{R}}$) and $^{18}\epsilon_{\text{R}}$ (**Chapter 1, 1.3.1**, Kaiser 2011, Kaiser and Abe 2012).

As explained in **Chapter 1 (1.3.1)**,

The δ^* of photosynthetic O_2 with respect to air- O_2 ($^*\delta_{\text{P}}$) can be calculated as follows:

$$^*\delta_{\text{P}} = (1 + ^*\delta_{\text{W}})(1 + ^*\epsilon_{\text{P}}) - 1$$

where $^*\delta_{\text{W}}$ is the δ^* of the source water relative to air- O_2 , $^*\epsilon_{\text{P}}$ is the photosynthetic isotope fractionation and ‘*’ refers to ^{17}O or ^{18}O .

δ^* of oxygen under conditions of both photosynthesis and respiration is calculated (assuming isotopic steady state) as:

$$\delta^* = \frac{\delta^*_{\text{P}} - (1 - f)^*\epsilon_{\text{R}}}{1 + (1 - f)^*\epsilon_{\text{R}}}$$

$^*\epsilon_{\text{R}}$ is the respiratory isotope effect, ‘*’ refers to ^{17}O or ^{18}O and f is the ratio of net to gross production. It can be observed the δ^* is dependent on f , $^{18}\epsilon_{\text{R}}$ and γ_{R} ($\gamma_{\text{R}} = ^{17}\epsilon_{\text{R}}/^{18}\epsilon_{\text{R}}$, where ‘R’ stands for respiration).

At biological or concentration steady state (S0), the net to gross production ratio f is zero, so

$$^*\delta_{\text{S0}} = \frac{^*\delta_{\text{P}} - ^*\epsilon_{\text{R}}}{1 + ^*\epsilon_{\text{R}}}$$

As a result, the $\Delta^{17}\text{O}$ of oxygen at steady state between respiration and photosynthesis is generally not equal to the $\Delta^{17}\text{O}$ of photosynthetic oxygen.

As indicated by Luz and Barkan 2005, Nicholson 2011, Barkan and Luz 2011, and Kaiser 2011, a logarithmic definition with tuned coefficient λ ($\theta = \ln(^{17}\alpha)/\ln(^{18}\alpha) = \ln(\gamma_R^{18}\epsilon_R + 1)/\ln(^{18}\epsilon_R + 1)$) can be used. When this tuned theta is used with the ‘ln’ definition (equation , $\Delta^{17}\text{O}_P$ will be equal to $\Delta^{17}\text{O}_{S_0}$. However, the exact γ_R and $^{18}\epsilon_R$ are generally not known. Although γ_R (kinetic respiratory slope/ratio of $\delta^{17}\text{O}$ and $\delta^{18}\text{O}$ discrimination during respiration) is well known for many different organisms, marine communities, temperatures, light conditions and respiratory pathways (Luz and Barkan 2005, weighted average 0.5179 ± 0.0006), $^{18}\epsilon_R$ is less well constrained, and is in fact known to vary greatly between organisms and involved oxygen consumption reactions, and to be affected by diffusion. Values between -10 and -30‰ have been reported (Kidson et al. 1993, Guy et al. 1989, 1993, Helman et al. 2005, Luz and Barkan 2005), average values for marine (microorganism) communities being $\sim(-20 \pm 3)\%$ (Kidson et al. 1993), but significantly smaller values of $^{18}\epsilon_R$ being associated with larger organisms and the Mehler reaction (-10 and -15.3‰ (Guy et al. 1993, Helman et al. 2005), and larger values with AOX (-24 to -26‰ (vs. -16- to -18‰ for COX), and photorespiration ($\sim-21.5\%$) (Guy et al. 1989, 1993, Angert et al. 2003, Helman et al. 2005, Luz and Barkan 2005). Therefore, depending on the species and exact processes involved, the $^{18}\epsilon_R$ might be different from -20‰. Finally, it should be realised in nature f is often different from zero.

Table 6: Results of Eisenstadt et al. 2010, table adapted from Kaiser and Abe (2012), showing the photosynthetic fractionation reported for different types of phytoplankton by Eisenstadt et al. (2010). $\theta_P = \ln(1+^{17}\epsilon_P)/\ln(1+^{18}\epsilon_P)$, ϵ_P is the photosynthetic isotope effect. Size info from Roscoff/CCAP culture collection.

Reference	Species	Group	Habitat	Cell diam./ μm	θ_P	$^{18}\epsilon_P/\%$
Helman et al. (2005), Eisenstadt et al. (2010)	<i>Synechocystis</i> sp. (PCC 6803)	cyanobacteria	fresh water	~1	0.5354 \pm 0.0020	0.467 \pm 0.17
Eisenstadt et al. (2010)	<i>Nannochloropsis</i> sp. (oculata)	eustigmatophyceae	marine	~1-2	0.5253 \pm 0.0004	2.850 \pm 0.05
Eisenstadt et al. (2010)	<i>P. tricornutum</i> (CCAP 1055/1)	diatoms	marine	~11	0.5234 \pm 0.0004	4.426 \pm 0.01
Eisenstadt et al. (2010)	<i>Emiliania huxleyi</i> (NK8)	coccolithophores	marine	~5	0.5253 \pm 0.0004	5.814 \pm 0.06
Eisenstadt et al. (2010)	<i>Chlamydomonas reinhardtii</i>	green algae	fresh water	~10	0.5198 \pm 0.0001	7.04 \pm 0.10
	mean				0.5203 \pm 0.0027	4.119 \pm 2.6

Table 7: Adaptation of section of Table 3 from Kaiser and Abe (2012), showing calculations of the $\Delta^{17}\text{O}$ of biological oxygen vs. air- O_2 based on two different measurements of VSMOW vs. air (Barkan and Luz 2005 and 2011) and the species-specific photosynthetic fractionation reported by Eisenstadt et al. (2010). ‘P’ indicates photosynthetic oxygen, ‘S0’ indicates oxygen at steady state between photosynthesis and respiration (net to gross production ratio $f = 0$). ‘W’ indicates the triple isotope composition of seawater vs. air (5 ppm below the value for VSMOW (Barkan and Luz 2010)). $\Delta^{17}\text{O}_{\text{S0}}$ was calculated assuming average respiration in marine communities with $^{18}\epsilon_{\text{R}} = (-20 \pm 4)\text{‰}$ and $\gamma_{\text{R}} = ^{17}\epsilon_{\text{R}} / ^{18}\epsilon_{\text{R}} = 0.5179 \pm 0.0006$, using $^*\delta_{\text{S0}} = \frac{^*\delta_{\text{P}} - ^*\epsilon_{\text{R}}}{1 + ^*\epsilon_{\text{R}}}$ and $^*\delta_{\text{P}} = (1 + ^*\delta_{\text{W}})(1 + ^*\epsilon_{\text{P}}) - 1$, where * refers to either ^{17}O or ^{18}O , and ϵ refers to the isotope effect of either respiration (R) or photosynthesis (P). $^*\delta_{\text{W}}$ is the δ^* of the source water relative to air- O_2 . See Kaiser and Abe 2012 for details. Displayed $\Delta^{17}\text{O}$ values were calculated using the linear definition with slope 0.5179.

	$^{18}\delta_{\text{P}}/\text{‰}$	$^{17}\delta_{\text{P}}/\text{‰}$	$\Delta^{17}\text{O}_{\text{P}}/\text{ppm}$	$^{18}\delta_{\text{S0}}/\text{‰}$	$^{17}\delta_{\text{P}}/\text{‰}$	$\Delta^{17}\text{O}_{\text{S0}}/\text{ppm}$
δ_{W} based on Barkan & Luz (2005), $\epsilon_{\text{P}} = 0$	-23.320	-11.936	141 ± 4	-3.388	-1.594	160
ϵ_{P} (<i>Synechocystis</i> sp. PCC 6803)	-22.864	-11.587	152 ± 6	-2.923	-1.345	169
ϵ_{P} (<i>Nannochloropsis</i> sp.)	-20.536	-10.458	178 ± 4	-0.547	-0.101	183
ϵ_{P} (<i>Phaeodactylum tricorutum</i>)	-18.997	-9.649	189 ± 4	1.023	0.716	186
ϵ_{P} (<i>Emiliana huxleyi</i>)	-17.642	-8.922	214 ± 5	2.407	1.451	204
ϵ_{P} (<i>Chlamydomonas reinhardtii</i>)	-16.444	-8.326	190 ± 4	3.628	2.053	174
mean	-19.297	-9.809	185 ± 22	0.718	0.555	183 ± 14
δ_{W} based on Barkan & Luz (2011), $\epsilon_{\text{P}} = 0$	-23.324	-11.888	192 ± 4	-3.392	-1.546	211
ϵ_{P} (<i>Synechocystis</i> sp. PCC 6803)	-22.868	-11.641	202 ± 6	-2.927	-1.297	219
ϵ_{P} (<i>Nannochloropsis</i> sp.)	-20.540	-10.410	228 ± 4	-0.552	-0.052	233
ϵ_{P} (<i>Phaeodactylum tricorutum</i>)	-19.001	-9.601	239 ± 4	1.019	-0.765	237
ϵ_{P} (<i>Emiliana huxleyi</i>)	-17.646	-8.874	264 ± 5	2.402	1.499	255
ϵ_{P} (<i>Chlamydomonas reinhardtii</i>)	-16.448	-8.278	240 ± 4	3.624	2.102	225
mean	-19.301	-9.761	235 ± 22	0.714	0.603	234 ± 14

Table 8: Recent measurements of the triple oxygen isotopic composition of VSMOW (Vienna Standard Mean Ocean Water) vs. air O_2 . Table adapted from Kaiser and Abe (2012). ‘l.d. 0.5179’ refers to the linear definition with slope 0.5179.

	$^{18}\delta_{\text{VSMOW}}/\text{‰}$	$^{17}\delta_{\text{VSMOW}}/\text{‰}$	$^{17}\Delta_{\text{VSMOW}}/\text{ppm}$ (l.d., 0.5179)
Barkan and Luz (2005)	-23.320 ± 0.02	-11.931 ± 0.01	146 ± 4
Barkan and Luz (2011)	-23.324 ± 0.02	-11.883 ± 0.01	196 ± 4
Kaiser and Abe (2012)	-23.647 ± 0.04	-12.102 ± 0.03	145 ± 6

5.2 Methods

5.2.1 Goals and summary methods

In order to obtain more information on the isotopic composition of oxygen produced by different types of phytoplankton, gas from the headspace of airtight bottles containing cultures of *Picochlorum* sp. and *Emiliana huxleyi* was sampled every 48 hours during eight days, after which the triple oxygen isotopic composition was measured.

Summary of methods

The green alga *Picochlorum* sp. and coccolithophore *Emiliana huxleyi* were added to a seawater-based f/2 and K/4 medium respectively (see **Section 5.2.2**), in airtight 165 ml bottles, closed with a thick butyl rubber stopper. A headspace was created, by replacing 4 ml of the medium with pure nitrogen gas. Bottles were stored in a growth chamber under close to natural growth conditions (50 μ E, 17 °C for *E. huxleyi* and 150 μ E, 21 °C for *Picochlorum*, 14:10 h light-dark cycle). Fluorescence and cell number were measured in order to keep track of the phytoplankton growth. Cultures were allowed to grow for 5-6 days before the start of sampling in order to allow sufficient O₂ accumulation and replacement of initial O₂ with biological O₂.

From day 5 (*E. huxleyi*) and 6 (*Picochlorum*) samples of the headspace gas were taken every 48 hours using a needle connected to an extraction line with liquid nitrogen trap, and frozen onto ten molecular sieve pellets at liquid N₂ temperature. Afterwards, 4 ml of nitrogen gas was injected into each bottle. Tests indicated this method of sampling and repressurising did not lead to fractionation or contamination of the sample gas.

Three new bottles were sampled every two days over a period of eight days. Three bottles were resampled every two days from sample day one, and three bottles were resampled every three days from sample day two.

For *E. huxleyi*, a comparable set of experiments was conducted one month earlier, in which three bottles were resampled every five days over a period of 20 days.

Sampled gas, trapped on molecular sieves, was transferred to a line for separation of O₂ and Ar from CO₂, H₂O and N₂, after which oxygen isotope and O₂/Ar ratios were measured on a Dual-Inlet IRMS (*MAT 252*).

Results are presented in **Section 5.3**. Results of first time and repeated sampling of *Emiliana huxleyi* are displayed in **Figure 28** and **30 to 35**.

For *Picochlorum*, oxygen contents were lower and unfortunately, resampling did not yield sufficient oxygen for MS measurements. Results of newly sampled bottles are displayed in **Figure 29**.

5.2.2 Phytoplankton culturing

Inoculation

The green alga *Picochlorum* sp. (RCC 289, strain OLI 26 SA, size 2 µm, origin equatorial Pacific, 15 m depth, 100 µE, 20 °C, <http://roscoff-culture-collection.org/rcc-strain-details/289>) and coccolithophore *Emiliania huxleyi* (RCC1229, strain AC457, size 5 µm, origin North Sea, 28 m depth, 17 °C) were added to respectively a seawater-based modified f/2 (Guillard and Ryther 1962, Guillard, 1975) and K/4 medium (Keller et al. 1987, as modified by Ian Probert, see below), in airtight 165 ml bottles, closed with a 20 mm butyl rubber stopper. Culture media ingredients, bottles and stoppers were sterilised by autoclaving (*ProClave ES:2300*, *Priorclave Tactrol 2*, 121°C, 20 min, 2 h cycle) prior to inoculation and inoculation took place in a Class 2 Microbiological Safety Cabinet (*Walker Safety Cabinets Ltd.*).

Both species were grown in a medium based on seawater, collected near the coast of East Anglia (stored in the dark at low temperature), filtered with a 0.2 µm filter, which was supplemented with either f/2 or K/4 nutrients and vitamins. Seawater and ingredients were separately sterilized before addition of the culture. For the preparation of f/2 (Guillard and Ryther 1962, Guillard 1975), 975 ml of seawater was filtered and topped up to 1 L with distilled water and two drops of HCl. Filtered seawater, and required f/2 ingredients (nutrients N/2 (nitrate), P/2 (phosphate), T/2 (trace metals) and V/2 (vitamins)), were subsequently separately sterilised by autoclaving and afterwards combined (1 ml of each nutrient and 0.5 ml of vitamins per liter of water) in a microbiological safety cabinet. *E. huxleyi* was grown in a seawater-based K/4 medium (Keller et al. 1987, as modified by Ian Probert (<http://roscoff-culture-collection.org/sites/default/files/MediaRecipesPDF-/K2-Ian.pdf>)). For 1 liter of medium, 0.25 ml of NaNO₃, NH₄Cl, KH₂PO₄, H₂SeO₃, FeEDTA and trace-metal solution and 0.5 ml of f/2 vitamin solution were added. Again, seawater and ingredients were separately sterilised by autoclaving and combined in a safety cabinet.

During inoculation, 140 ml of freshly prepared, sterile medium (either f/2 or K/4) was pipetted into sterilised 165 ml glass bottles in the microbiological safety cabinet (*Walker Safety Cabinets Ltd.*). A few ml of culture in logarithmic growth phase was subsequently pipetted into the bottle (8 ml per 160 ml of culture for *E. huxleyi*, 2 ml per 160 ml of culture for *Picochlorum*), after which the bottle was topped up with growth medium to the rim. The bottle was then sealed with a sterile 20 mm thick butyl rubber stopper (*Chemglass*), which was inserted into the bottle with a sterile needle (*BD Microlance*, 23G) inside, so that excess water could flow out. Closed culture bottles (completely

filled with medium, with negligible headspace (max. few mm bubble)) were moved to the Stable Isotope Lab for headspace creation.

Headspace creation

A headspace was created by replacing 4 ml of the medium with nitrogen gas. Nitrogen gas was chosen because an inert gas was required. Helium was considered, but did not freeze on the molecular sieves, which complicated sampling. The headspace was created using a 5 ml gas tight borosilicate glass syringe (*SGE*, SG008770) with removeable luer-lock valve. 25G x 1" (0.5 x 25 mm) sterile hypodermic needles were used (*BD Microlance*, 300400). Nitrogen was injected from a crimp sealed 165 ml bottle, continuously flushed with pure nitrogen gas (flow rate ~125 ml/min for a minimum of 15 minutes prior to extraction) from a cylinder with pressurised nitrogen gas (*BOC Ltd.*, UN1066, oxygen-free), nitrogen flowing in from a long (*BD Yale*, 20G, 4") needle connected to the cylinder via tubing, and flowing out directly via a second needle (*BD Microlance*, 23G, 11/4"). The nitrogen flow rate was continuously monitored. During the pulling of nitrogen into the syringe, the exit needle of the flushed bottle was briefly removed (while N₂ was still flowing in) in order to prevent sucking in of outside air. After pulling the plunger, the exit needle was reinserted, and the increased flow rate was allowed to return to normal, after which the syringe was closed and removed. Culture bottles were held upside down and nitrogen was injected slowly while excess water was allowed to drip out through a second needle (*BD Microlance*, 23G, 11/4"). Bottles were held upside down or sideways during nitrogen injection, so that the stopper and needle tip were continuously sealed with water, in order to prevent contamination with air. Tests with O₂-Ar gas indicated no significant air contamination took place due to this approach.

Growth conditions

Bottles were stored in a growth chamber (*Sanyo (Panasonic, UK)*, ML-350, Versatile Environmental Test Chamber), fluorescent lighting (FL40SS-W/37 lamps) under close to natural growth conditions (14:10 h light-dark cycle, ~50 μE ($\mu\text{mol photons m}^{-2} \text{ s}^{-1}$), 17 °C for *E. huxleyi* and ~150 μE ($\mu\text{mol photons m}^{-2} \text{ s}^{-1}$), 21 °C for *Picochlorum*. These were the conditions stock cultures were kept under, which are comparable to those at site of culture collection. Cultures were kept on the mid shelf of the growth chambers and light intensity was monitored using a Scalar PAR Irradiance Sensor (QSL 2101, *Biospherical Instruments Inc.*). Expected growth rates under these conditions were near 0.5-1 per day for *Picochlorum* (B. Steawarski, pers.com. 2013) and 1-1.5 per day for *E. huxleyi* (Buitenhuis et al., 2008). Although both cultures have their optimum growth at a

light intensity of around 300 μE (B. Steawarski, M. Henle, pers. com. 2013), close to natural growth conditions were preferred for these experiments.

Culture bottles were stored on the mid shelf of the growth chamber, in such a way that all bottles were at approximately the same distance from the lamps. Bottles were stored sideways and transported upside down, so that the stopper was always sealed with water, in order to prevent contamination. Bottles were not moved or shaken, except during transport to the stable isotope lab for sampling.

Cultures were allowed to grow, produce O_2 and recycle initially present, dissolved atmospheric, oxygen for 5-7 days (period decided based on preliminary experiments), after which samples of the headspace gas were taken every 48 hours over a period of two weeks.

Fluorescence and Coulter measurements

Fluorescence and cell number were measured, from separate bottles, in order to keep track of the phytoplankton growth. For both species, In Vivo Fluorescence (which gives an indication of chlorophyll a and cell concentration (Heinle 2013)) was measured in a *Turner 10-AU Field Fluorometer*. ~3 ml culture samples were taken at the same time every day. For *E. huxleyi*, next to fluorescence, cell concentration was measured at the same time every day, using a *Coulter Multisizer 3* (*Beckman Coulter Ltd.*, High Wycombe, UK). Three samples were measured each time, for which 0.5 ml of culture was diluted with 9.5 ml of 0.2 μm filtered seawater. For each sample, triplicate measurements were performed. *Picochlorum* cells were too small ($< 2 \mu\text{m}$) for *Multisizer* measurements. Samples for fluorescence and Coulter counting were extracted using a syringe (SGE gas tight syringe with luer-lock and 23G BD Microlance needle), from a bottle grown together with and further treated similar to the other culture bottles.

Materials

Bottles and stoppers

165 ml glass bottles were used, which were closed off from the atmosphere with thick butyl rubber stoppers (*Chemglass CLS-4209-14*, blue rubber butyl stopper, 20 mm size). Tests had been performed with 165 ml bottles and different types of stoppers, needles and airtight syringes, both with O_2 -Ar reference gas, and distilled water bubbled with O_2 -Ar reference gas. It was found the stoppers sufficiently sealed off the bottles. Thick stoppers were preferred as they allowed sealing the needle halfway before and after sampling (see **Section 5.2.3**). Because the stoppers were nearly too wide for the bottle necks, they sealed the bottles without requirement of crimp caps. As extra precaution,

bottles were always stored and collected sideways or upside down, so that the neck remained sealed in water.

Syringes and needles

Syringes used in these experiments were Gas Tight borosilicate 5 ml Syringes with removable Gas Tight valve and Luer-Lock connection (*SGE Analytical Science*). *BD Microlance* sterile hypodermic needles were used in all cases. For sampling, headspace creation and repressurising, 25G needles were used of 1-inch length (0.5 x 25 mm), while for stopper insertion, fluorescence and Coulter measurements 23G, 1 1/4-inch needles were used.



Figure 24: Culture bottles in growth chamber.

5.2.3 Sampling procedure

Sampling

Headspace gas was extracted by expansion into an evacuated extraction line through a needle connected to the line, which could be evacuated prior to sampling, and subsequent transfer of the extracted gas onto molecular sieves in sealable glass tubes. A detailed description of the line and procedure is given in **Chapter 2, Section 2.1** and below.

Sampling took place using the extraction line described in **Section 2.1**. The line was as described in **Section 2.1.2**, with liquid nitrogen trap, only a needle (*BD Microlance, 25G x 25 mm, 300400*) was connected to it using a Luer-Lock connection (see **Figure 25 and 26**). Prior to sampling, the needle tip was sealed, by pushing the needle halfway down the stopper of the sample bottle, and the line was evacuated up to the needle tip.

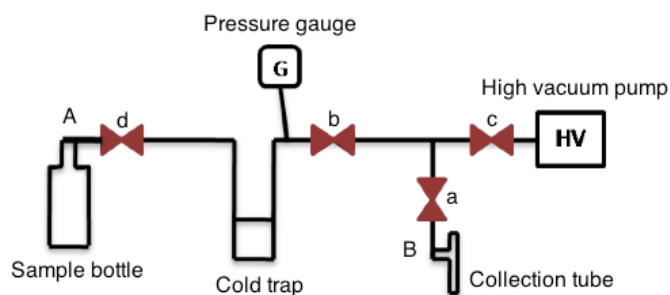


Figure 25: Schematic of the small extraction line, figure adapted from Gloël (2012).

Although the Luer-Lock connection was not high vacuum, a pressure of down to $\sim 1.2 \times 10^{-7}$ mbar could be achieved in the line when the needle tip was sealed.

Occasionally, the pressure in the line was higher than 3×10^{-7} mbar. This was mainly the case when several samples had been processed and the water content in the line was high, or when the needle connection was poor. Often, replacing the needle solved the problem. However, after the processing of many samples, occasionally a vacuum of up to 1×10^{-6} mbar had to be accepted. In order to prevent contamination with outside air, the valve to the needle was closed quickly after sampling (after stabilisation of the pressure in the line, which generally took ~ 10 -30 seconds).

Tests of this sampling method (using sealed 165 ml bottles with O_2 -Ar or water bubbled with O_2 -Ar and a 3 ml headspace, extracting the gas, freezing it onto molecular sieves and analysing it on the MAT 252) indicated contamination with outside air in this case was negligible. In addition, no significant fractionation due to the sample procedure was observed (see **Chapter 3, Section 3.3**).

Extraction line – transfer of gas samples to molecular sieves

For the extraction of sample gases and their transfer to molecular sieve pellets in storage tubes, a small high-vacuum extraction line was used. The line consisted of 0.5-1 cm inner diameter stainless steel and glass tubing, a ~ 180 ml glass trap, which was kept in liquid nitrogen (-196 °C) during sample processing, a pressure gauge (*Pfeiffer Vacuum, capacitance gauge*) to check the line for leaks and monitor the pressure drop during

freezing, three manual high-vacuum valves (*Louwers Hapert*) and two connection ports, connected via a manual valve to a turbomolecular drag pump (*Pfeiffer Vacuum*, TMU071P). A schematic drawing of the line is displayed in **Figure 25**.

The total volume of the line, including trap, was approximately 200 ml, and generally a vacuum of 1.6×10^{-7} mbar could be obtained all around. For these particular tests, occasionally a pressure of up to 1×10^{-6} mbar was accepted.

The collection tube containing molecular sieves, either a 2.5 ml glass vial (~50 mm length, ~8 mm internal diameter) with compression o-ring high-vacuum valve (*Glass expansion*), or a 200 mm length, 5 mm inner diameter Pyrex flame-seal tube, was attached to the line at the connection point closest to the pump (**B**), using a *Swagelok Ultra-Torr* fitting. At point **A**, the sample needle was connected.

Sampling procedure

A sample needle (*BD Microlance*, 25G x 25 mm, 300400) was attached to the line with a Luer-Lock connection, and the needle was inserted exactly halfway down the stopper of the sample bottle, so that the tip was sealed but did not pierce the stopper (See **Figure 27**). The line, including a liquid N₂ trap, was then evacuated up to the needle. In the mean time, the trap on the line was cooled with liquid nitrogen, and a sample tube (either a 2.5 ml tube with *GE* valve or a 20 cm flame-seal tube) containing 10 new molecular sieve pellets (*Sigma-Aldrich Zeolite 5 Å*, 1.6 to ~6 mm) was connected (in a part of the line closed off to the pump, valve **a** (**Figure 25**) closed).

After the whole line had been evacuated (preferably down to $1.6\text{-}1.9 \times 10^{-7}$ mbar), including the collection tube and sample needle, the valve to the pump was closed (either **c** and **b** or **b** only), after which the pressure in the line was recorded, and the sample was released. This was done by pushing the needle through the stopper, allowing it to reach the headspace but not the water. As a result, the sample was expanded up to valve **b** (~200 ml volume). After ~10-30 seconds of sampling (upon stabilisation of the pressure), the valve to the needle (**d**) was closed, the needle was moved upwards in the stopper to seal, and the pressure was written down. The sample then stayed in the part of the line between valve **b** and **d** for 2 minutes, while H₂O was frozen on the liquid nitrogen trap. After two minutes, valve **b** was opened and the sample gas was expanded up to the collection tube. At this point, the pressure was written down again and the collection tube (a 2.5 glass vial with *GE* valve or 20-0.6 cm od flame-seal tube, containing 10 pellets of zeolite 5A molecular sieve) was immersed in liquid nitrogen so that the sample could freeze on the molecular sieves. After at least 99.9% of sample had been collected on the sieves (ascertained manometrically), the tube with sieves was

sealed, either by closing the valve or flame-sealing with a gas burner. After this, the sample tube could be removed and the line could be prepared for the next sample.

Sampling – additional remarks

During sampling of biological oxygen, sometimes, higher pressures were unavoidable, due to the increased amount of water vapour in the line and the luer-lock connection of the needle to the line. The vacuum that could be reached in the line with the needle attached varied between 1.2×10^{-7} and 1×10^{-6} mbar, and depended on the specific needle and the amount of H₂O the line had been exposed to. Because the connection of the needle to the line was not high-vacuum and thus not completely leak-proof the valve next to the sample needle (**D**) was closed relatively quickly after sampling (within seconds, after stabilisation of the pressure, before the needle was removed from the stopper), and the sample was taken immediately after the line was closed off from the pump. Several tests with O₂-Ar ref gas were performed in order to ascertain no significant fractionation or contamination of the sample gas took place during extraction and/or transfer of the samples.

Needle replacement

A new needle was used at least every three bottles and between the sampling of different species. The needle was briefly sterilised with a flame between bottles of the same species. For each moment of sampling, three bottles were sampled.

Collection tubes

All samples from May were collected in valved tubes, while samples from June-July were collected in flame-seal tubes from sample day 3 (*Picochlorum*) and 2 (*E. huxleyi*).

Sampling tests and trials

Tests had been performed using this sampling method, with bottles with O₂-Ar reference gas and distilled water bubbled with O₂-Ar reference gas, with a 3 ml headspace, sampling and transferring the gas on to 10 and subsequently five pellets (as normally happens to samples at the end of the separation line, see **Chapter 2, Section 2.1.2 and Chapter 3, 3.3**) before measurement on the IRMS. A liquid nitrogen cold trap was present on the line during the tests. It was found the sampling method did not lead to significant fractionation or contamination of the gas (see **Section 3.3**). Results were similar to those obtained for extraction tests in which O₂-Ar reference gas was introduced straight from the flask under comparable conditions (liquid nitrogen trap, 10>5 molecular sieve pellets, relatively low pressure, see **Chapter 3**).



Figure 26: Needle connected to the extraction line via glass tube with Luer-Lock connection



Figure 27: Picture of the extraction line, just prior to sampling. The needle tip is sealed in the stopper of the sample bottle.

Repressurising

After the headspace gas had been collected, the pressure in the headspace of the bottles would be lower than atmospheric. In order to minimise contamination risks, and prevent any effects of underpressure on phytoplankton growth, the headspace of the bottles was repressurised with pure nitrogen gas after the collection of samples. This was done using a 165 ml bottle attached to a pure N₂ gas cylinder (*BOC Ltd*, UN1066, oxygen-free, pressurized N₂), which was continuously flushed with nitrogen gas at a rate of ~125 ml/min for a minimum of 10-15 minutes. After this period, N₂ gas was extracted from the bottle using a valved gas tight syringe (*SGE*, 008770) with luer-lock fitted needle (*BD Microlance*, 25G x 25 mm), and injected into the sample bottle, while this was held upside down or sideways so that stopper and needle tip were continuously sealed with water. This was approximately the same method as used for headspace creation. The exit needle of the flushed bottle was briefly removed during extraction of the gas, in order to minimise the possibility of atmospheric air introduction, and reinserted after the plunger had been pulled. Tests (with O₂-Ar gas) had been performed using this method of

repressurising, which indicated it led to negligible introduction of atmospheric air in the bottles. Repressurised bottles were moved back to the growth chamber.

5.2.4 Gas preparation and IRMS measurements

Gas preparation

Samples collected on molecular sieves in valved or flame-sealed glass tubes could be transported to the separation line (built after the example of Barkan and Luz (2003) with minor alterations, see **Section 2.1.2**) for cryogenic removal of remaining CO₂ and H₂O, and gas-chromatographic separation of N₂. Prior to release of the samples into the separation line, sample tubes were heated for 10-20 minutes at 50-70 °C (hot water, cooling down) in order to maximise desorption from the sieves (Abe 2008).

The separation procedure is described in detail in **Section 2.1.2**. The procedure was semi-automated, took approximately 45 minutes per sample, and resulted in O₂-Ar mixtures with negligible N₂ content.

At the end of the separation procedure, purified gas samples were cryogenically collected on zeolite 5Å molecular sieves (5 pellets, 1.6 by ~5 mm, see **Section 2.1.2**) in stainless steel tubes. After collection of a processed set of samples and one dry air aliquot, the exit manifold was removed from the separation line and attached to the mass spectrometer (*Thermo Finnigan MAT 252*), where the elemental and isotopic composition of the gas samples could be determined.

Mass-spectrometric measurements

Removal of CO₂, H₂O and N₂ resulted in purified O₂-Ar mixtures with negligible nitrogen content, which could be introduced to the Isotope Ratio Mass Spectrometer (*Thermo Finnigan MAT 252*, Dual-Inlet Mode) for determination of their triple oxygen isotopic composition and O₂/Ar ratio. Samples were analysed on a *Thermo Finnigan MAT 252* Isotope Ratio Mass Spectrometer, in Dual-Inlet Mode, against a simultaneously introduced O₂-Ar working reference gas (BOC Australia, 4.7% Ar in O₂).

Before introduction to the mass spectrometer, tubes with purified samples on molecular sieves were heated for ~20 minutes at ~50-80 °C (hot water, cooling down), after which their contents were released, and the triple oxygen isotopic composition was determined by measurement against a simultaneously-introduced reference O₂-Ar mixture (*BOC Australia*, 4.7% Ar in O₂) on an Isotope Ratio Mass Spectrometer (*Thermo Finnigan MAT 252*, Dual-Inlet Mode). Bellows were adjusted manually upon introduction of the sample and reference, in order to achieve a minimum difference in sample size between the reference and sample side. The used idle and integration times were 5 and 16 s

respectively, the signal height of m/z 32 was 2.5 V. Each sample was analysed during three runs of 30 cycles of sample-reference analysis, which each yielded an average $\delta^{17}\text{O}$ and $\delta^{18}\text{O}$ value. The average standard deviation and standard error over 30 mass-spectrometric measurements were 0.047 and 0.020‰ (SD) and 0.009 and 0.004‰ (SE), for $\delta^{17}\text{O}$ and $\delta^{18}\text{O}$ respectively.

As explained in **Chapter 1** and **2**, the isotope-ratio difference of a sample relative to a reference is, in standard delta-notation:

$$\delta\left(\frac{\text{sample}}{\text{reference}}\right) = \frac{R_{\text{sam}}}{R_{\text{ref}}} - 1,$$

$$R\left(\frac{^*\text{O}}{^{16}\text{O}}\right) = \frac{n(^*\text{O})}{n(^{16}\text{O})} \approx \frac{n(^*\text{O}^{16}\text{O})}{n(^{16}\text{O}^{16}\text{O})},$$

where R is the isotope ratio, the ratio of the abundance of the minor isotope over the major isotope (in this case the ratio of the amount of either ^{17}O or ^{18}O over ^{16}O), and $^*\text{O}$ is either ^{17}O or ^{18}O .

$\delta^{17}\text{O}$ and $\delta^{18}\text{O}$ were calculated from the measured ion beam intensities of m/z 34 or 33 relative to 32 in the sample and reference according to:

$$\begin{aligned} \delta^{17}\text{O}/\text{‰} &= \left[\frac{\left(\frac{n(^{17}\text{O})}{n(^{16}\text{O})}\right)_{\text{sam}}}{\left(\frac{n(^{17}\text{O})}{n(^{16}\text{O})}\right)_{\text{ref}}} - 1 \right] \cdot 1000 \approx \left[\frac{\left(\frac{n(^{17}\text{O}^{16}\text{O})}{n(^{16}\text{O}^{16}\text{O})}\right)_{\text{sam}}}{\left(\frac{n(^{17}\text{O}^{16}\text{O})}{n(^{16}\text{O}^{16}\text{O})}\right)_{\text{ref}}} - 1 \right] \cdot 1000 \\ &= \left[\frac{\left(\frac{U_{33}}{U_{32}}\right)_{\text{sam}}}{\left(\frac{U_{33}}{U_{32}}\right)_{\text{ref}}} - 1 \right] \cdot 1000 \\ \delta^{18}\text{O}/\text{‰} &\approx \left[\frac{\left(\frac{U_{34}}{U_{32}}\right)_{\text{sam}}}{\left(\frac{U_{34}}{U_{32}}\right)_{\text{ref}}} - 1 \right] \cdot 1000 \end{aligned}$$

At the end of each three blocks of measurements, an interfering-masses measurement was performed, during which the ion currents of m/z 28 (N_2), 40 (Ar) and 32 ($^{16}\text{O}_2$) were measured for both sample and reference.

$d(\text{N}_2/\text{O}_2)$ and $\delta(\text{O}_2/\text{Ar})$ were calculated according to

$$d(\text{N}_2/\text{O}_2)/\text{‰} = ((U_{28}/U_{32})_{\text{sa}} - (U_{28}/U_{32})_{\text{ref}}) \cdot 1000, \text{ and}$$

$$\delta(\text{O}_2/\text{Ar})/\text{‰} = \left(\frac{(U_{32}/U_{40})_{\text{sa}}}{(U_{32}/U_{40})_{\text{ref}}} - 1 \right) \cdot 1000,$$

where U_{28} , U_{32} and U_{40} are the voltages of the ion beam intensities (ion current · resistance) of m/z 28 (N_2), 32 ($^{16}O_2$) and 40 (Ar) respectively, ‘sa’ stands for sample and ‘ref’ for working reference.

Resulting $\delta^{17}O$ and $\delta^{18}O$ values were corrected for the effects of nitrogen and argon interference, and imbalance (difference in output voltage of m/z 32 signal between standard and sample), according to the linear relationships derived from dilution tests, imbalance tests and zero enrichments. Details are given in **Chapter 2**.

Based on dilution series (see **Chapter 2**), for nitrogen interference, $\delta^{17}O$ and $\delta^{18}O$ were corrected as follows:

$$\delta^{18}O_{\text{corr, N2}} = \delta^{18}O_{\text{meas}} - 0.052 \cdot (N_2/O_2)$$

$$\delta^{17}O_{\text{corr, N2}} = \delta^{17}O_{\text{meas}} - 0.1335 \cdot (N_2/O_2)$$

Note: $d(N_2/O_2)$ here refers to the absolute value.

For imbalance, the following corrections were applied, based on zero enrichments performed over the whole period of the biological experiments:

$$\delta^{18}O_{\text{corr, imb}} = \delta^{18}O_{\text{meas}} - 1.86 \cdot (U_{32,\text{sam}} - U_{32,\text{ref}}), \text{ and}$$

$$\delta^{17}O_{\text{corr, imb}} = \delta^{17}O_{\text{meas}} - (-0.45) \cdot (U_{32,\text{sam}} - U_{32,\text{ref}}),$$

where $U_{32,\text{sam}}$ and $U_{32,\text{ref}}$ are the ion beam intensities (V) of m/z 32 measured at the beginning of the run, for the sample and standard side, respectively.

Details on these corrections and argon corrections are supplied in **Chapter 2**.

Argon correction

Because the O_2 -Ar working reference gas has an O_2 -Ar composition close to that of atmospheric air (4.7% Ar in O_2), during the measurement of air samples, the difference in relative Ar content between the sample and reference is small ($\delta(O_2/Ar)_{\text{sample/ref}} < \sim 136\%$), and the effect of differences in $\delta(Ar/O_2)$ on the results would be expected to be very small or negligible (Barkan and Luz, 2003, J. Kaiser, pers. com. 2013). However, for the culture experiments, due to the presence of biological O_2 , the Ar/O_2 was much lower in the samples than in the reference gas ($\delta(O_2/Ar)_{\text{sam/ref}}$ of ~ 1000 - $10,000\%$, corresponding $\delta(Ar/O_2)_{\text{sam/ref}}$ down to $\sim -900\%$). Studies of Barkan and Luz (2003) and Abe and Yoshida (2003) indicate differences in relative Ar content of this magnitude could significantly affect the results. However, the exact effect depends on the used instrument and conditions around the time of measurement. Dilution tests were performed, adding different amounts of pure Ar to a pure O_2 gas (0-5% Ar in the mixture, in steps of 1%),

collecting the mixtures on molecular sieves and measuring their composition on the MAT 252 against the pure O₂ gas (0%) and against a different, O₂-Ar, reference gas (4.7% Ar in O₂, BOC). In all cases, results indicated differences in the Ar content between the sample and the reference in this range (0-5% Ar in O₂), did not significantly affect the Δ¹⁷O. A linear relationship was found between δ(Ar/O₂) and δ¹⁷O and δ¹⁸O, which increased with increasing δ(Ar/O₂) as reported by Barkan and Luz (2003) and Abe and Yoshida (2003). However, within this δ(Ar/O₂) range, the effect and thus corresponding correction of the δ¹⁷O and δ¹⁸O results was small. For biological samples, the effect of the correction was up to ~0.003‰ for δ¹⁷O and ~0.005‰ for δ¹⁸O. The corresponding effect on Δ¹⁷O was 0-1 ppm).

The δ¹⁷O and δ¹⁸O results of the three runs were corrected separately, after which corrected values were standardised against atmospheric air (see below) and used in the calculation of Δ¹⁷O. The Δ¹⁷O was calculated according to the definition:

$$\Delta^{17}\text{O}/\text{ppm} = (\delta^{17}\text{O} - 0.5179 \cdot \delta^{18}\text{O}) \cdot 1000,$$

where δ¹⁷O and δ¹⁸O are the values in ‘*per mil*’ (‰). For each sample, three corrected and air-standardised δ¹⁷O, δ¹⁸O and Δ¹⁷O values were thus obtained, which were averaged.

A ‘zero enrichment’ (measurement of reference gas against itself) was performed at the beginning of each day, in order to check for fluctuations in the functioning of the MS, and minimally one aliquot of cryogenically dried atmospheric air (‘dry air’ or ‘DA’) was always prepared and measured together with the samples. Averaged and corrected results of these dry air measurements versus the reference were used to standardise the corrected sample results with respect to atmospheric air, according to:

$$\delta_{\text{sa/air}}^*/\text{‰} \approx \delta_{\text{sa/DA}}^*/\text{‰} = \left[\frac{\delta_{\text{sa/ref}}^* - \delta_{\text{DA/ref}}^*}{\delta_{\text{DA/ref}}^* + 1} \right] \cdot 1000,$$

where ‘*’ can be ¹⁷O, ¹⁸O or O₂/Ar, ‘sa’ stands for sample, ‘DA’ stands for dry air and ‘ref’ stands for the working reference O₂-Ar mixture (note: δ-values in this equation are absolute values).

For each sample, three corrected and air-standardised δ¹⁷O, δ¹⁸O and Δ¹⁷O values were obtained, which were averaged, and one *d*(N₂/O₂) and δ(O₂/Ar) value. For each data point (examined moment in time), three culture bottles were sampled. Results are displayed in **Section 5.3**.

Note: For each sample, the pressure in the sample bellow of the MS at 100% opening was recorded. This does not give information on the exact O₂ content, but it makes it

possible to compare the sizes of the samples relative to each other, and thus gives an indication of the amount of produced oxygen (the samples should mostly contain O₂, with negligible amounts of N₂ and Ar). Sample sizes in the form of pressure in the bellow were also averaged per three bottles for each data point.

5.2.5 Initial trials and sampling strategy

Initial trials

Because it was not known a priori how fast the cultures would grow and how much oxygen they would produce, several trial experiments were performed. Initially, for first experiments (March 2013), the species *Picochlorum* was grown and sampled according to the methods described above, but the headspace was 3 ml and during sampling the gas was expanded into 4 ml of the line instead of the later ~180 ml. Ten bottles were inoculated simultaneously, of which 5 were sampled from growth day two and resampled every 24 hours for two weeks, and three were sampled from day 7 and resampled every 24 hours for a week. In order to keep track of the growth, fluorescence measurements were performed from the additional two bottles (from day 2 and 7 respectively). Results are displayed in **Figure 36**.

Unfortunately, none of the samples contained sufficient O₂ for MS measurements (first samples from day 7 contained almost sufficient oxygen, samples from resampling after 24 hours contained far from sufficient O₂ in any case). For later experiments, several adaptations were therefore made to increase oxygen content in the samples.

For a second set of experiments in May, it was decided to perform experiments with different headspace volumes (because increasing the headspace volume would lead to a larger O₂ content in the samples, J. Kaiser pers. com. 2013), to start sampling from a later growth day, allowing for more O₂ accumulation, and to increase the time between sample moments. In addition, it was decided to sample by expanding straight into the main part of the line (~200 ml) instead of the initial ~4 ml, thereby increasing the percentage of headspace gas sampled. Finally, a second species was also grown and sampled, which could potentially produce more oxygen (*E. huxleyi*).

For experiments with *E. huxleyi* in May 2013, four bottles were inoculated (8 ml inoculum to 160 ml of K/4) with a 3 ml headspace (more bottles were inoculated with larger (13 and 23 ml) headspace), and samples were expanded straight into the main part of the line (~200 ml instead of ~4 ml). One bottle was used for fluorescence and three were sampled from day 5, and resampled every 5 days, over a total period of 20 days. Samples yielded sufficient oxygen for isotopic analysis, and results are therefore included in **Section 5.3**. For *Picochlorum*, resampling still did not yield sufficient oxygen. For the final set of experiments, it was therefore decided to prepare more

bottles, and, in addition to resampling at different intervals, sample three new bottles at each sample moment (every two days over a period of 1-2 weeks). These bottles would have higher oxygen contents, and results could be compared to those from resampled bottles to assess the effect of sampling.

Experiments with different headspace volumes indicated increasing the headspace from 3 to 4 ml increased the oxygen content in the samples, but did not change the isotopic composition of the gas, or lead to additional problems. Increasing the headspace to either 13 or 23 ml led to problems in transfer and nitrogen separation (due to the large sample volume and nitrogen content). It was therefore decided to perform final experiments with a 4 ml headspace.

Summary and final sample strategy

A method was developed to grow phytoplankton and sample the produced oxygen without introducing air or fractionating the sample gas. Phytoplankton was grown in 165 ml glass bottles, sealed off from the atmosphere with a thick butyl rubber stopper. A 4 ml headspace was created by replacement of medium with nitrogen gas. Sampling of the headspace gas took place through a needle under vacuum into a ~200 ml volume on an extraction line.

From day 5 (*E. huxleyi*) and 6 (*Picochlorum*) samples of the headspace gas were taken every 48 hours, using a needle connected to an extraction line with liquid nitrogen trap, and frozen onto ten molecular sieve pellets at liquid N₂ temperature. Three new bottles were sampled every two days over a period of eight days. Three bottles were resampled every two days from sample day one, and three bottles were resampled every three days from sample day two. Bottles of sample day three and four were resampled for extra information. For *E. huxleyi*, a comparable set of experiments was conducted one month earlier, in which three bottles were resampled every five days over a period of 20 days.

Sampled gas, trapped on molecular sieves, was transferred to a line for separation of O₂ and Ar from CO₂, H₂O and N₂, after which oxygen isotope and O₂/Ar ratios were measured on a Dual-Inlet IRMS (*Thermo Finnigan MAT 252*).

Results of first time and repeated sampling of *Emiliana huxleyi* are displayed in **Figure 28 to 35**. For *Picochlorum*, oxygen contents were lower and, unfortunately, resampling did not yield sufficient oxygen for MS measurements. Results of newly sampled bottles are displayed in **Figure 29**.

Two bottles of *Picochlorum* were used for the daily measurement of fluorescence. One bottle of *E. huxleyi* was used for daily fluorescence and *Coulter Counter* (cell number) measurements. Results of the fluorescence and cell count measurements of *E. huxleyi* and *Picochlorum* are displayed in **Figure 37 and 38** respectively.

5.3 Results

5.3.1 First time sampling (new bottles)

Emiliana huxleyi

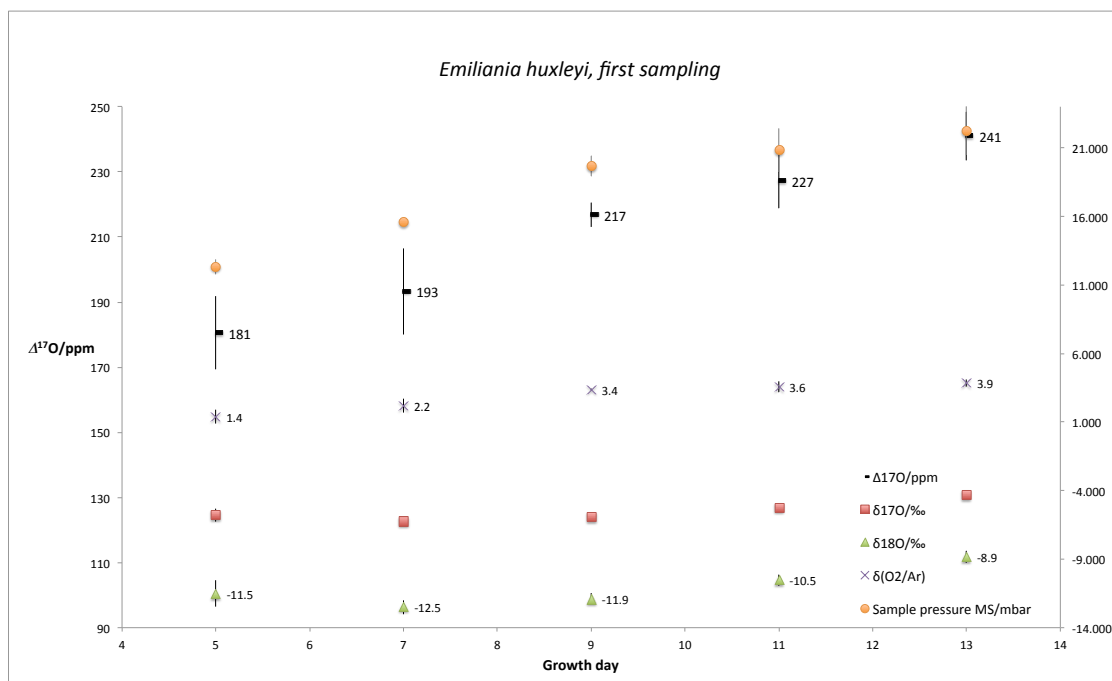


Figure 28: $\Delta^{17}\text{O}$, $\delta(\text{O}_2/\text{Ar})$, $\delta^{17}\text{O}$ and $\delta^{18}\text{O}$ results versus air- O_2 for *E. huxleyi*. On each sample day, three new bottles were sampled, and displayed values are averages of the three bottles. Results are imbalance and N_2 and Ar interference corrected and standardised with respect to air- O_2 . The number of days since inoculation (growth day) is displayed on the x-axis. $\Delta^{17}\text{O}$ results are plotted against the left y-axis, while other results are plotted on the right y-axis. $\Delta^{17}\text{O}$ results, calculated as $\Delta^{17}\text{O} = 1000(\delta^{17}\text{O} - 0.5179 \delta^{18}\text{O})$, are displayed in black. Purple crosses show the $\delta(\text{O}_2/\text{Ar})$ results, which are reported as absolute value, without conversion to ‰. $\delta^{17}\text{O}$ and $\delta^{18}\text{O}$ results are displayed in red squares and green triangles, respectively. Orange circles show the pressure in the sample bellow of the MS after loading of the sample, when the bellow was at its maximum opening. Error bars of $\Delta^{17}\text{O}$ results show ± 1 95% CI, while error bars of other results display ± 1 SD. Occasionally error bars are smaller than the displayed symbols.

E. huxleyi results show an increase in both $\delta(\text{O}_2/\text{Ar})$ (indicating net O_2 production) and $\Delta^{17}\text{O}$ over the sampling period (growth day 5-13), indicating steady-state was probably not yet reached. $\delta(\text{O}_2/\text{Ar})$ values increase from 1.4 to 3.9, but seem to stabilise near growth day 13. The same trend of increase over the period of sampling, and stabilisation near growth day 13, can be observed in the MS sample pressures. Both $\delta(\text{O}_2/\text{Ar})$ and sample pressure thus indicate net O_2 production up to growth day 13, but a tendency towards biological/concentration steady state near the final sample day(s). This is

confirmed by fluorescence and *Coulter Counter* results which indicate a stabilisation of growth (stationary phase) between growth day 10 and 14 (**Section 5.3.4., Figure 37**). It is also consistent with the observed stabilization in $\Delta^{17}\text{O}$ near day 13-14 in most *E. huxleyi* sample series (**Section 5.3.2, Figure 30-31**), which might indicate the observed value of 241 ppm is close to the maximum (or steady state) value.

$\delta^{17}\text{O}$ and $\delta^{18}\text{O}$ are in the range of -13 to -8‰ ($\delta^{18}\text{O}$) and -6.5 to -4 ‰ ($\delta^{17}\text{O}$), and thus in between the expected values for VSMOW or photosynthetic oxygen and those expected for air or steady state (see **Table 7**). A decrease is visible from sample day 1 to 2, but an enrichment in ^{17}O and ^{18}O is visible from sample day 2.

In comparison to for *Picochlorum* (**5.3.1, part two**), for *E. huxleyi* $\Delta^{17}\text{O}$, $\delta(\text{O}_2/\text{Ar})$ increase up to higher levels, indicating this species reaches biological steady state at higher $\Delta^{17}\text{O}$ and $\delta(\text{O}_2/\text{Ar})$, or O_2 concentration levels. In addition, the $\delta^{17}\text{O}$ and $\delta^{18}\text{O}$ are slightly more negative ($\delta^{18}\text{O}$ -13 to -8 vs. -6 to -2.5‰) than observed for *Picochlorum* over sample period, which might be related to the fact that the situation for *Picochlorum* was already closer to steady state (see page 120).

The standard deviation of $\Delta^{17}\text{O}$ between three bottles of the same sample day was on average ~13 ppm (comparable to the standard deviation between the results of reference gas mixtures ran through the separation line and then measured) corresponding to a 95% CI of ~10 ppm, and the increase in ^{17}O excess is visible over the whole range of sample points.

Purple crosses in **Figure 28** show the $\delta(\text{O}_2/\text{Ar})$ (vs. air) of the different sample days. Very high $\delta(\text{O}_2/\text{Ar})$ (vs. air) values were obtained in all samples (~1-4 (~1,000-4,000‰)), indicating a strong presence of biological oxygen in comparison to atmospheric air. Just as the ^{17}O excess, the $\delta(\text{O}_2/\text{Ar})$ was found to increase over the period of growth, from 1.4 for bottles sampled on growth day 5, to 3.9 for bottles sampled on growth day 13 (absolute values). This indicates an increase in the amount of biologically produced oxygen in the bottles, and thus net production. The fact that the $\delta(\text{O}_2/\text{Ar})$ in the bottles is still rising up to the final sample day indicates a biological steady state has not yet been reached. The $\delta(\text{O}_2/\text{Ar})$ value does however seem to start stabilising near the final sample days (growth day 10-13), indicating the system might be approaching steady state conditions, which is indicated by a tendency to stabilization in fluorescence, cell number and MS sample pressure for these sample days (**Figure 28**

and 37). The same trend can be observed in the average sample pressure after loading of the samples in the MS, which gives an indication of the oxygen content of the samples. Just as the $\delta(\text{O}_2/\text{Ar})$, the observed sample pressure increased over the period of sampling, indicating an increase in the oxygen content in the bottles over the period between growth day 5 and 13. Again, the increase became less strong near the final sample days, possibly indicating approach of steady state conditions.

$\delta^{17}\text{O}$ and $\delta^{18}\text{O}$ values versus air are negative (between ~ -4 and -6‰ for $\delta^{17}\text{O}$ and ~ -9 and -13‰ for $\delta^{18}\text{O}$), indicating the presence of biological oxygen. Values are more positive than those of VSMOW or pure photosynthetic oxygen (**Table 7**), which could be expected due to the involvement of respiration in the bottles. $\delta^{17}\text{O}$ and $\delta^{18}\text{O}$ values are more negative for bottles sampled on growth day 7 than for bottles sampled on growth day 5.

The decrease in delta values from sample day one to two could be a result of the fact that the $\delta^{17}\text{O}$ and $\delta^{18}\text{O}$ values are slightly more positive initially because not all atmospheric oxygen had been removed yet. Alternatively or additionally, it could indicate an increased contribution of photosynthesis relative to respiration between sample day one and two. From sample day 2 to 5 (growth day 7-13) $\delta^{17}\text{O}$ and $\delta^{18}\text{O}$ values become more positive, indicating the presence of respiration (which leads to an enrichment in ^{17}O and ^{18}O relative to ^{16}O).

Both $\Delta^{17}\text{O}$ and $\delta^{17}\text{O}$ and $\delta^{18}\text{O}$ values indicate an isotopic steady state has not yet been reached in the bottles on growth day 13, although $\delta(\text{O}_2/\text{Ar})$, fluorescence and cell number results indicate conditions are approaching biological steady state. This is confirmed by stabilising $\Delta^{17}\text{O}$ values observed in the repeated sampling *E. huxleyi* series (**Section 5.3.2, Figure 37**).

The standard deviation between three bottles of the same sample day is slightly larger than the uncertainty introduced by the method (~ 0.1 - 0.5‰ for $\delta^{18}\text{O}$ vs. 0.025 - 0.050‰ for DA (dry air) aliquots processed in a similar way as samples, see **Section 2.4**). The standard deviation of $\Delta^{17}\text{O}$ between results of three bottles of the same day is small (~ 13 ppm), and comparable to that of DA aliquots processed similarly to the samples, indicating variations in $\delta^{17}\text{O}$ and $\delta^{18}\text{O}$ values are largely related to mass-dependent processes. The standard deviation of $\delta^{17}\text{O}$ and $\delta^{18}\text{O}$ for sample day 1 is slightly larger than for the other sample days, which could be explained by the fact that any differences in inoculation density, growth or initial air content would be expected to be more pronounced initially.

The fact that the $\Delta^{17}\text{O}$ is increasing from sample day one until five (growth day 5-13), might indicate, that although it was initially expected that all oxygen would have been recycled after 5-7 days (E. Buitenhuis, pers. com. 2013), there was still atmospheric air present in the bottles during the first sample days (from the initially present dissolved oxygen). Alternatively, it could be a result of the fact that steady state had not been reached yet (the ratio of net to gross production, f was not zero). If f is not zero, the $\Delta^{17}\text{O}$ will be different from the biological or concentration steady state value (see Kaiser and Abe 2012, and **Appendix Figure 41-44**) However, in this case (for *E. huxleyi* and normal respiration) you would have expected $\Delta^{17}\text{O}$ to be higher if f is above zero, not lower (Kaiser and Abe 2012, **Appendix**, and **Section 5.4.1**).

Picochlorum

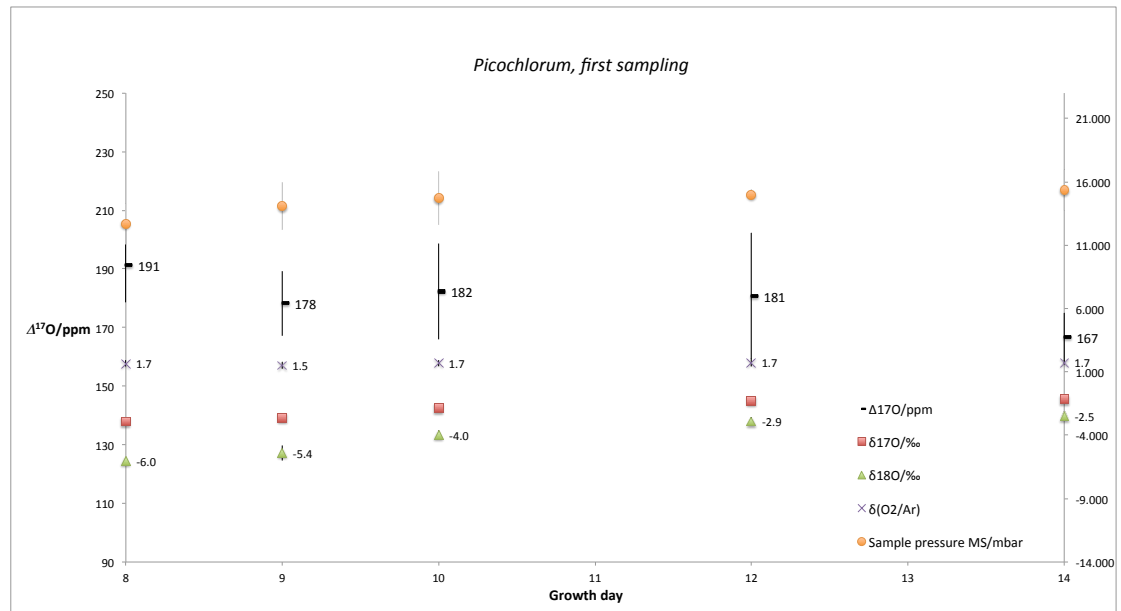


Figure 29: Average $\Delta^{17}\text{O}$ versus air- O_2 , for *Picochlorum* first time sampling (new bottles), calculated from corrected and air-standardised $\delta^{17}\text{O}$ and $\delta^{18}\text{O}$. Each value represents the average result of three bottles. Average 5 sample days: 180 ± 9 (± 1 SD) or ± 8 ($\pm 95\%$ CI).

$\Delta^{17}\text{O}$, $\delta(\text{O}_2/\text{Ar})$, $\delta^{17}\text{O}$ and $\delta^{18}\text{O}$ results for *Picochlorum* are displayed in **Figure 29**. On each sample day, three new bottles were sampled, and displayed values are averages of the three bottles. The number of days since inoculation (growth day) is displayed on the x-axis. $\Delta^{17}\text{O}$ results are plotted against the left y-axis, while other results are plotted on the right y-axis. $\Delta^{17}\text{O}$ results are displayed in black. Purple crosses show the $\delta(\text{O}_2/\text{Ar})$ results, which are reported without conversion to ‰. $\delta^{17}\text{O}$ and $\delta^{18}\text{O}$ results are displayed in red squares and green triangles, respectively. Orange circles show the pressure in the sample bellow of the MS after loading of the sample, when the bellow was at its maximum opening. Error bars of $\Delta^{17}\text{O}$ results show ± 1 95% CI, while error bars of other

results display ± 1 SD. Occasionally error bars are smaller than the displayed symbols. The unequal distribution of sample days is due to the fact that three bottles were sampled on growth day 6, 8, 9 (extra), 10, 12 and 14, but samples of day 6 were lost due to separation line problems.

For *Picochlorum*, $\Delta^{17}\text{O}$ is relatively constant over the sample period (180 ± 9 ppm) (growth day 8-14). This is accompanied by a constant $\delta(\text{O}_2/\text{Ar})$ (~ 1.7), and a relatively constant sample pressure from sample day 2 (day one sample pressure based on only two results of which one was comparable to those of other days), both indicating O_2 concentration has stabilised, indicating steady-state between production and respiration might have been reached. This is also indicated by the fluorescence data of *Picochlorum*, which indicate stationary growth phase is reached between day 8 and 10 (see **Section 5.3.4 Figure 38**). A relatively high value (191 ± 13 ppm (± 1 SD)) was obtained for sample day 1, while a relatively low value (167 ± 8 ppm) was obtained for sample day 5. These values are however not significantly different from those of other days, and in both cases one out of three bottles had a value strongly different from the other two, while the other two bottles produced identical results to bottles from other sample days (a value of 180 ± 2 ppm was obtained for sample day 2-4).

However, it cannot be excluded the relatively high value obtained for sample day one indicates steady state had not completely been reached (in which case slightly higher values could be expected, see **Table 7**, Kaiser and Abe 2012-Table 3, **Appendix**), and/or that the relatively low value for the final sample day indicates something changed in the bottles after a week of stationary phase. Since cultures were batch cultures with limited nutrients, maybe the cultures started dying or the involved respiration processes changed. The relatively low value of 167 ppm is mainly the result of one sample yielding a relatively low value (bottle 17: 157 ppm). As can be observed from **Figure 38**, the bottle in question also yielded a relatively low fluorescence compared to the other bottles, when this was measured a few days after the final sample day. This might indicate something affected growth, or maybe death phase started earlier, in this particular bottle.

Although $\Delta^{17}\text{O}$ is relatively constant from growth day 8 to 14, $\delta^{17}\text{O}$ and $\delta^{18}\text{O}$ are still increasing ($\delta^{18}\text{O} \sim -6$ to -2.5‰), which indicates an isotopic steady state has not been reached. The fact that the $\Delta^{17}\text{O}$ is rather stable indicates isotopes are fractionated along a slope of approximately 0.5179, probably as a result of (normal) dark respiration.

Observed $\delta^{17}\text{O}$ and $\delta^{18}\text{O}$ values were more positive for *Picochlorum* than for *E. huxleyi*, which could be a result of the fact that at the start of sampling *Picochlorum*, biological

steady state had already been reached and delta values had been increasing (due to respiration) longer. The increase in $\delta^{17}\text{O}$ and $\delta^{18}\text{O}$ values for *Picochlorum* over the last two sample days seems to become less strong, which could indicate approach of isotopic steady state.

$\delta(\text{O}_2/\text{Ar})$ values for *Picochlorum* stabilize at a lower value than for *E. huxleyi* (~1.7 vs. ~4), which indicates biological steady state is reached at lower oxygen concentrations. In addition, the $\Delta^{17}\text{O}$ seems to stabilize at a lower value for *Picochlorum* (~180 ppm) than for *E. huxleyi* (~250 ppm).

As mentioned above, although $\Delta^{17}\text{O}$ is very constant between sample day 2 and 4 ((180±2) ppm, ±1 SD), a slightly higher $\Delta^{17}\text{O}$ was obtained for sample day 1 ((191±13) ppm) and a slightly lower value was obtained for sample day 5 ((167±8) ppm). Values are not significantly different from those obtained for other sample days, and the difference could be a coincidence. In both cases one sample was present with a relatively higher (day 1, ~203 ppm) or low (day 5, ~157 ppm) value, while the other two samples produced values that were occasionally also observed for other sample days. (in the case of day 1, the other samples produced a value of 182 and 185 ppm). In the case of sample day 5, the sample with a relatively low ^{17}O excess came from a bottle which initially contained a relatively large air bubble. Since you would expect all initial oxygen to have been replaced after 14 days, this should however not have affected the sample. In addition, the fluorescence of this bottle, determined after the period of sampling, was remarkably low compared to that of other bottles (**Figure 38**).

Since all three samples of sample day 5 yielded relatively low ^{17}O excess values, this could also indicate that something changed in the bottles after ~7 days of stationary phase (at which stage you might expect nutrients to become limited and cultures to start declining). This could for instance be a small change from $f = 0$, or biological steady state, to $f < 0$ (net respiration) (see **Appendix, Figure 39-40**), or a change in the relative contribution of different O_2 uptake mechanisms, each with slightly different fractionation slopes and/or isotope effects. It could, for instance, indicate increased involvement of a respiration process with a fractionation slope (γ_{R}) below 0.5179 (such as photorespiration or the Mehler reaction, which are both known to become more important at lower CO_2 (and/or high O_2) concentrations (Angert et al. 2003, Helman et al. 2005) and fractionate along a lower triple isotope slope ($\gamma_{\text{R}} = 0.512$ for photorespiration and 0.497 for Mehler (Helman et al. 2005)). These O_2 consumption processes are in nature generally not expected to be important in marine phytoplankton (Luz and Barkan 2000, Kaplan et al. 1999, Kaiser 2011). However, in this case conditions were different from those in nature, and since conditions in the bottles would favour these reactions, their involvement cannot be excluded. Finally, changes in the

relative contribution of the dark respiration processes COX (ordinary dark respiration) and AOX (alternative oxidase pathway) might also have played a role.

A slightly higher $\Delta^{17}\text{O}$ for sample day one could in theory also be explained by a situation slightly before reaching biological steady state, with a $f > 0$, as shown by **Figure 39-40 (Appendix)** (as changes in f would lead to changes in the obtained $\Delta^{17}\text{O}$, depending on the definition used, $\delta^{17}\text{O}_\text{P}$ and $\delta^{18}\text{O}_\text{P}$ and $^{18}\epsilon_\text{R}$ and γ_R values (Kaiser 2011a, Kaiser and Abe 2012, Luz and Barkan 2005).

5.3.2 *E. huxleyi* different sample series

$\Delta^{17}\text{O}$ results

Results of both single and repeated sampling (first time sampling and different repeated sampling patterns) of *Emiliana huxleyi* are displayed in **Figure 30 and 31**.

For *Picochlorum*, unfortunately, none of the repetition samples contained sufficient oxygen for IRMS analysis.

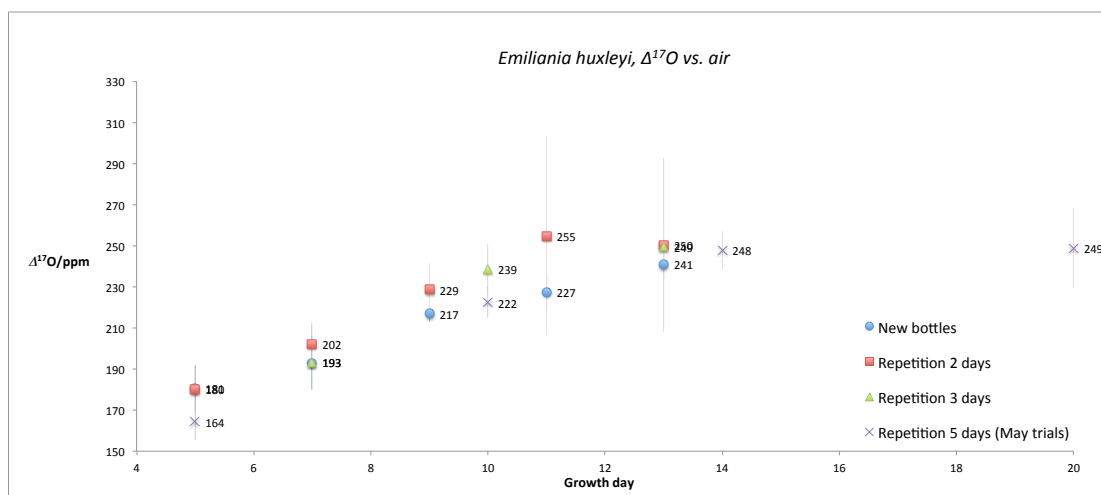


Figure 30: *Emiliana huxleyi*, $\Delta^{17}\text{O}$ results of different sample patterns. $\Delta^{17}\text{O}$ was calculated from corrected, air-referenced $\delta^{17}\text{O}$ and $\delta^{18}\text{O}$ using $\Delta^{17}\text{O} = 1000(\delta^{17}\text{O} - 0.5179\delta^{18}\text{O})$. Values are averages of results of three bottles, error bars show ± 1 95% confidence interval.

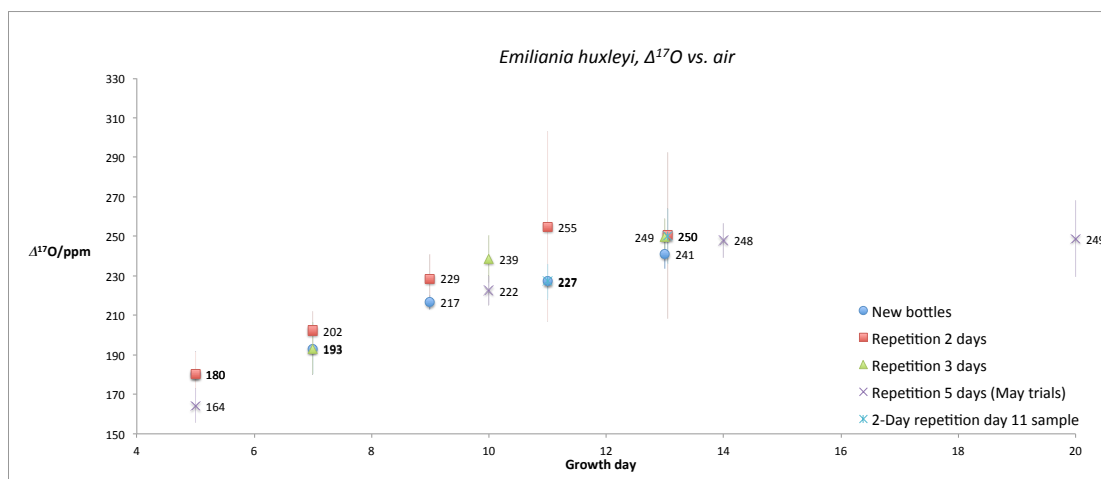


Figure 31: *Emiliana huxleyi*, $\Delta^{17}\text{O}$ results of different sample patterns. $\Delta^{17}\text{O}$ was calculated from corrected, air-referenced $\delta^{17}\text{O}$ and $\delta^{18}\text{O}$ using $\Delta^{17}\text{O} = 1000(\delta^{17}\text{O} - 0.5179\delta^{18}\text{O})$. Values are averages of results of three bottles, error bars show ± 1 95% confidence interval. Purple crosses refer to results of experiments with *E. huxleyi* from May 2013, in which bottles were resampled every 5 days. All other results are from June-July 2013 experiments. Values for day 13 were displayed with a slight offset to improve visibility. Bold values belong to two series.

As can be observed from **Figure 30 and 31**, the trend is the same for all patterns, with an increase from ~160-180 to ~250 ppm. Values of all repetition patterns approach (~249 \pm 1) ppm around day 13-14. The value for the newly sampled bottles is slightly lower, but the difference is small considering the uncertainties, and the newly sampled bottle results were increasing up to the final sample day (see **Section 5.3.1**). Values of 3 and 5-day repetition seem to stabilise around this value. Values are slightly higher, and seem to stabilise earlier, for bottles that were resampled every 2 or 3 days in comparison to either newly sampled bottles or resampled bottles from May (which were resampled every 5 days). Differences are however small considering the standard deviations. Overall, it seems values stabilise around ~250 ppm, which is also indicated by the fact that the $\Delta^{17}\text{O}$ does not change between growth day 14 and 20 of the 5-day repetition series.

In general, the standard deviation between results of one three bottles sampled at the same time was 5-15 ppm, comparable to the variation between results of zero enrichments or O₂-Ar or DA aliquots ran through the separation line, and the accompanying 95% CI was ~10 ppm (<13 ppm) in most cases. However, for the two final sample days of the 2-day repetition series and the final sample day of the 5-day repetition series, the variability between results was much larger (95% CI: 40-50 ppm for the final days of the 2-day repetition and 19 ppm for the final day of the 5-day repetition). The large error in the results of the final days of the 2-day repetition series,

results from the fact that these samples contained relatively little oxygen (m/z 32 signal intensity < 2 V, where 2.5 V was required), which, in combination with relatively high nitrogen contents (1-1.3 V) for these particular samples, led to a strongly increased imbalance and nitrogen effect and consequent increased variability in the MS results. However, resulting averages based on three samples were very close to those obtained for the other sample series (see **Figure 30-31**).

The slightly larger uncertainty observed for the final sample day of the 5-day repetition is due to the fact that for this day there were only two samples available instead of three.

A bottle from day 11 that was resampled after two days yielded a value of 250 ppm for growth day 13, very similar to values obtained for other series. This similarity in results between series with different sample frequencies, newly sampled bottles and resampled bottles, and experiments from May and June/July, can also be observed in the $\delta^{18}\text{O}$ (and $\delta^{17}\text{O}$) results (see **Figure 32-33**).

Interestingly, 2, 3 and 5-day repetition series yielded a practically identical value, of 248-250 ppm, for growth day 13-14, even though their sample frequency was different and the 5-day repetition results were obtained from an earlier set of experiments. In addition, one bottle that was first sampled on growth day 11 and resampled on growth day 13 also yielded a value of 250 ppm for this day (other bottles not resampled due to time limitations). For the newly sampled bottles, the obtained value on growth day 13 is slightly lower (241 ppm), than for the repeated sampled bottles. However, as mentioned above, $\Delta^{17}\text{O}$ in the newly sampled bottle results is increasing almost linearly up to the final sample day, which could indicate isotopic steady state was not yet reached for this series.

The fact that it seems steady state, or a stabilisation in $\Delta^{17}\text{O}$, is reached slightly earlier for frequently (every 2 or 3 days) resampled bottles than for newly sampled bottles and every 5-days resampled bottles (observable in **Figure 30-33**), could indicate steady state is reached earlier due to the resampling. This might be related to the movement of bottles during sampling, and/or the decreased oxygen content in the bottles. Finally, it could also be related to more rapid removal of initial atmospheric oxygen in these bottles. However, differences are very small and mainly observed in the 2-day repetition results, which have a relatively large uncertainty. They might therefore be based on coincidence.

For most sample patterns the increase over time in obtained $\Delta^{17}\text{O}$ seems to stabilise between growth day 10 and 14. Values of all repeated sample patterns seem to stabilise around 249 ppm at growth day 13-20.

For the June-July experiments, no samples were collected after growth day 13. However, samples from growth day 20 of the May trials (5-day repetition) show an almost identical value for growth day 14 and 20 (248 vs. 249 ppm). Since results of the May trials are very comparable to those of the June-July repetitions, this seems to indicate the $\Delta^{17}\text{O}$ indeed stabilizes around this value.

Results are very comparable between sample patterns (whether 2, 3 or 5-day repetition), values plotting approximately on the same line and following the same trend over the period of growth, so the sampling frequency does not seem to strongly affect the results. The average result of growth day 11 of the 2-day repetition series is slightly higher than the general trend (255 ppm), it should however be noted that the uncertainty of this data point is relatively large.

$\delta^{18}\text{O}$ results

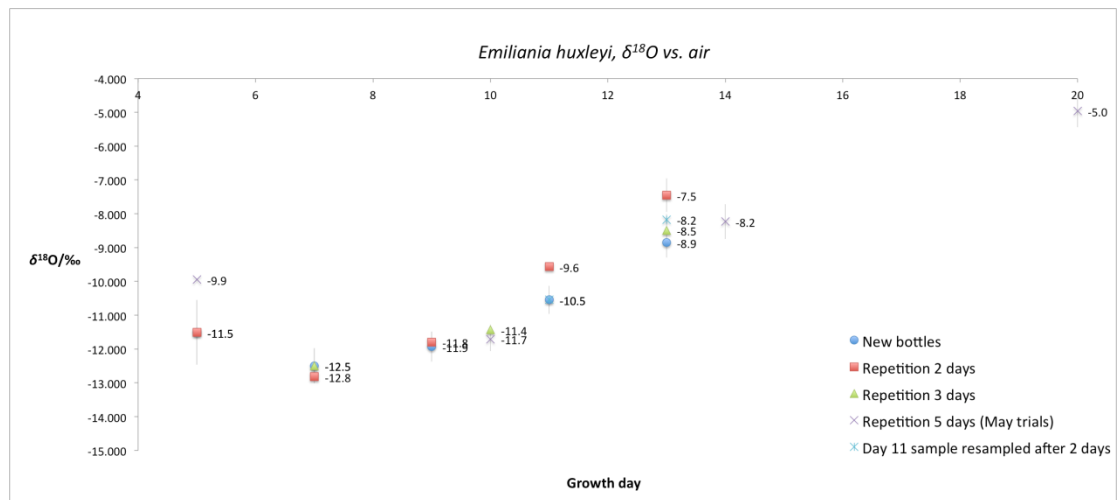


Figure 32: $\delta^{18}\text{O}$ results of *E. huxleyi* different sample patterns. $\delta^{18}\text{O}$ was corrected for imbalance and nitrogen and argon interference and standardised against air. Values are averages of 3 bottles, Error bars show ± 1 standard deviation.

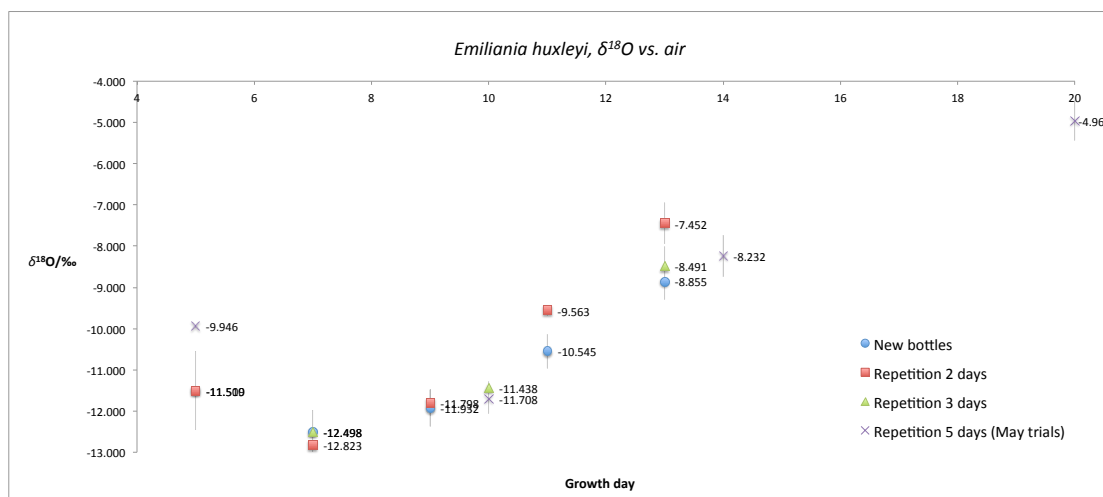


Figure 33: $\delta^{18}\text{O}$ results of *E. huxleyi* different sample patterns. $\delta^{18}\text{O}$ was corrected for imbalance and nitrogen and argon interference and standardised against air. Values are averages of 3 bottles, Error bars show ± 1 standard deviation.

Just as the $\Delta^{17}\text{O}$ results, $\delta^{18}\text{O}$ results are very comparable between different sample patterns, (newly sampled or resampled, May or June experiments), all showing an increase over the period of sampling ($\delta^{18}\text{O}$: ~ -12 to $\sim -8\text{‰}$ (-5‰ for May trials, which were continued until a later growth day), and a decrease between growth day 5 and 7)), and yielding very similar values for the same growth day. This seems to indicate sampling and repressurising, and the frequency hereof, did not significantly influence the triple isotopic composition of O_2 in the bottles. Results are relatively consistent between the 3 bottles of 1 sample moment, the standard deviation (SD) of $\delta^{18}\text{O}$ (~ 0.1 - 0.5‰ for most samples) being slightly higher than for DA and O_2 -Ar processed through the preparation line, but the SD of $\Delta^{17}\text{O}$ being comparable to that of zero enrichments and the above mentioned tests.

The results of different sample series show approximately the same trend, with a decrease between growth day 5 and 7 and a subsequent increase of $\delta^{18}\text{O}$ until the final sample day. The fact that the values are still increasing indicates isotopic steady state has not been reached. In case of the May experiments, sampling continued until growth day 20, and results obtained for this day indicate the $\delta^{18}\text{O}$ between day 14 and 20 continued to rise along approximately the same slope. The increase can be explained by respiration in the bottles. The slight decrease between sample day 1 and 2 might be a result of the initial presence of atmospheric air, or a change in the relative contribution of production and respiration.

As can be observed, for growth day 11 and 13, slightly more positive values were obtained for the 2-day repetition series than for the less frequently or not resampled series. This might indicate the resampling (possibly through movement of the bottles and/or decrease in oxygen content, or faster removal of initial atmospheric oxygen) led to a faster approach of steady state conditions. However, differences are small and the 2-day repetition series samples of these particular days had a relatively low oxygen content which decreased measurement precision (see above).

The differences in the values obtained for sample day 1, and the relatively large standard deviation for the 2-day repetition value, might be a result of differences in growth between bottles, which would be expected to be more pronounced initially, further away from steady state.

5.3.3 Additional results ($\delta(O_2/Ar)$, $d(N_2/O_2)$)

$\delta(O_2/Ar)$

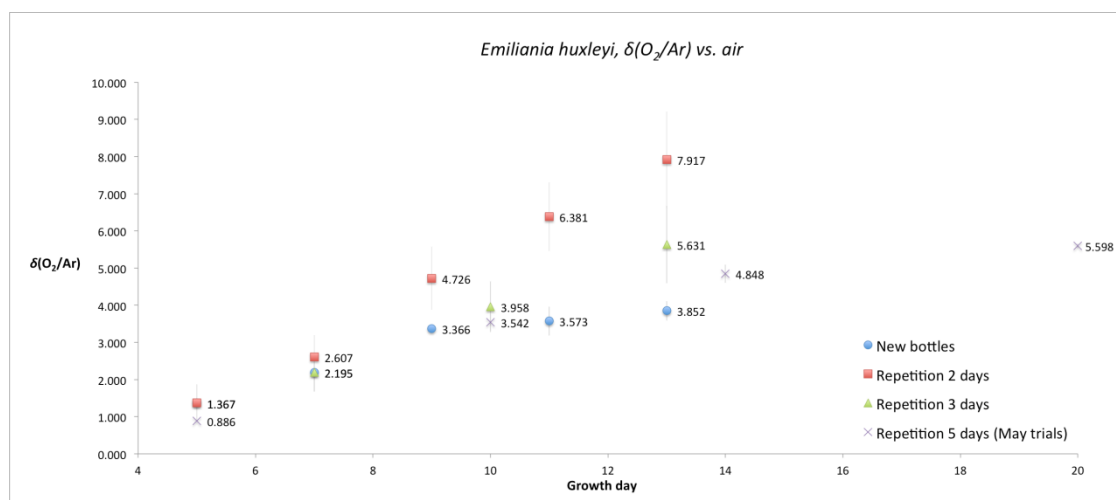


Figure 34: $\delta(O_2/Ar)$ results vs. air for all *E. huxleyi* series

As can be observed from the $\delta(O_2/Ar)$ results plotted in **Figure 34**, the $\delta(O_2/Ar)$ vs. air is far above zero in all cases (~1-8, or 1,000-8,000‰) indicating a large contribution of biologically produced oxygen in the bottles relative to initially present atmospheric air- O_2 . In addition, it gives no indication of air contamination during repressurising or handling of the samples. The $\delta(O_2/Ar)$ increases over the total period of sampling (growth day 5 to 13 or 20) for all *E. huxleyi* sample series. In case of the series with newly sampled bottles, this indicates the biological oxygen concentration in the bottles is still rising (net production), and a biological or concentration steady state had not yet been reached (see **Section 5.3.2**, The increase in $\delta(O_2/Ar)$ does however seem to slow down during the final days of sampling (growth day 10-13), indicating the system is

approaching steady state conditions, which was also indicated by a tendency to stabilisation in fluorescence, cell number and ^{17}O excess for these sample days (**Figure 30 and 37**)) In case of the series with repeated sampling from the same bottles, the results cannot be interpreted in the same way, since in these bottles the argon concentration was not constant, as argon was removed during sampling. As a result, for the same rise in biological oxygen concentration, you would expect a stronger increase in $\delta(\text{O}_2/\text{Ar})$ over time in resampled bottles, as can be observed in **Figure 34**.

Sample pressure

In case of repeated sampling, also no extra information could be obtained from the sample pressure on the MS (an additional indicator of O_2 -content), as oxygen was removed during sampling. For all repeated samples (except for 5-day repetition sample day 1-2) the sample pressure and thus oxygen content of the samples decreased over time, indicating more oxygen was removed during sampling than produced between sample days.

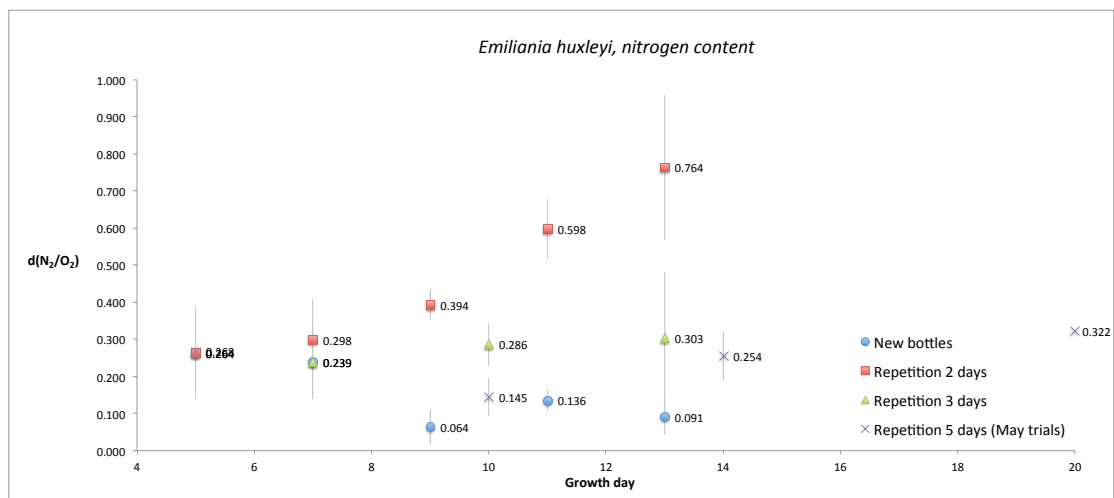


Figure 35: Nitrogen content of *E. huxleyi* samples

Nitrogen content

After separation, nitrogen content was around 0.5 V ($d(\text{N}_2/\text{O}_2)$: 50-300 ‰) in most samples, occasionally up to 1 V, indicating sufficient separation (and N_2 contents that could be corrected for using linear relationships described in **Chapter 2**). Relatively high $d(\text{N}_2/\text{O}_2)$ values were obtained for the final sample days of the 2-day repetition (~600-800 ‰). This is due to the fact that in these samples the oxygen content was relatively low (because more oxygen was removed during sampling than produced in two days, leading to a strong decrease in oxygen content over time for the 2-day

repetition series). Next to a relatively large variability in these samples, this would have led to a relatively large effect of the nitrogen correction for these days. It was however found that using different nitrogen correction slopes, based on tests with the used MS conducted over the past years, did not significantly change the value (more than (± 5 ppm for obtained steady state values and) ± 10 ppm (for final days of the 2-day repetition/most extreme cases) and results of 2-day repetition final days were always within ~ 10 ppm of those of the other sample patterns.)

Used definition of $\Delta^{17}\text{O}$

Reported results are based on the linear definition of $\Delta^{17}\text{O}$, with a slope of 0.5179. When values are recalculated using the logarithmic ('ln') definition with slope 0.5154 (See **Chapter 1**), results are (< 10 ppm) lower in all cases, but the trend is the same as for the linear definition with 0.5179 (the difference is similar for *E. huxleyi* day 1 and 5) (see Appendix).

When the 'ln' definition with slope 0.5179 is used instead, values obtained for *Picochlorum* (all days) and *E. huxleyi* final days stay approximately the same (up to 5 ppm higher). However, the values obtained for the first days of *E. huxleyi* become significantly higher, and $\Delta^{17}\text{O}$ increases from ~ 180 -200 ppm to ~ 255 ppm over the period of sampling, instead of from ~ 160 -180 to ~ 250 ppm (see Appendix, **Figure 39-40**).

Isotopic composition of source water

Cultures were grown in a medium based on seawater collected by UEA near the coast of East Anglia. The triple oxygen isotope composition of the source water was measured (H_2O fluorination method) at the LSCE (Laboratoire des Sciences du Climat et l'Environnement, Saclay) in France against the ORSMOW standard (in-house standard LSCE, calibrated against VSMOW). The ^{17}O excess of the source water was (3.4 ± 5) ppm vs. ORSMOW, and the $\delta^{18}\text{O}$ was (-0.5 ± 0.2) ‰ vs. ORSMOW. Tests were performed prior to the measurement in order to assess whether the presence of salt would influence the measurement, by adding salt to the ORSMOW standard and then determining the triple oxygen isotopic composition. The addition of salt had no influence on the results (^{17}O excess = 0 ppm).

Variability $\Delta^{17}\text{O}$ results

The average standard deviation (SD) between three bottles was 13 ± 5 ppm, which is comparable to the results for DA or O_2 -Ar aliquots processed on the separation line. The only exceptions to this general trend are the samples from *E. huxleyi* 2-day repetition

sample day 4 and 5, with an O₂ signal intensity below 2 V, which had a much larger variability in results than all other sets of 3 samples (SD 64-73 instead of ~13 ppm) In repeated samples, the SD between bottles stays approximately the same over time/with more frequent sampling (values comparable to those for newly sampled bottles), indicating the sampling or repressurising method did not increase the variability or differences between bottles.

5.3.4 Fluorescence and Coulter Counter results

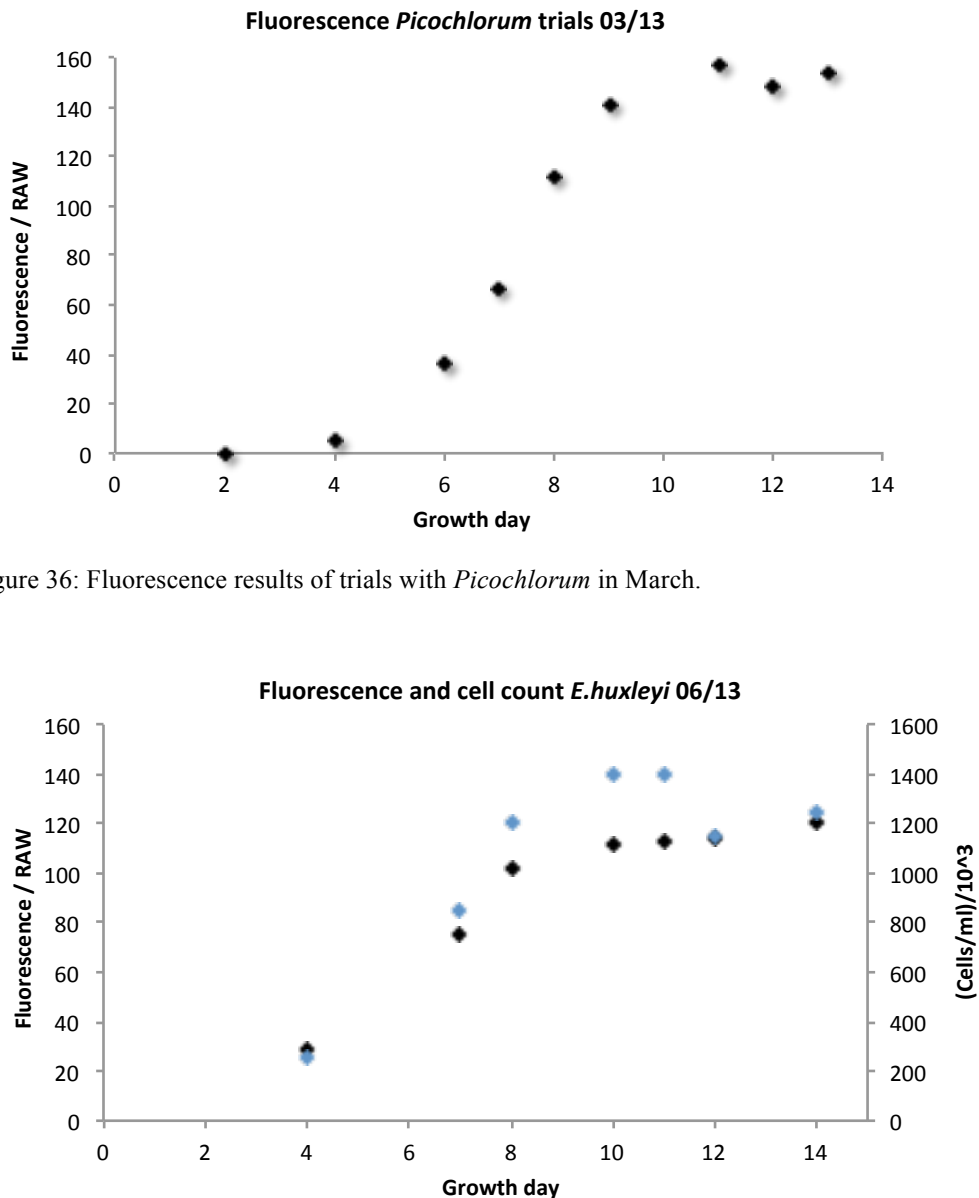


Figure 36: Fluorescence results of trials with *Picochlorum* in March.

Figure 37: Fluorescence and Coulter Counter results of *E. huxleyi* June experiments, Blue symbols show the results of *Coulter counter* measurements, while results of fluorescence measurements are displayed in black.

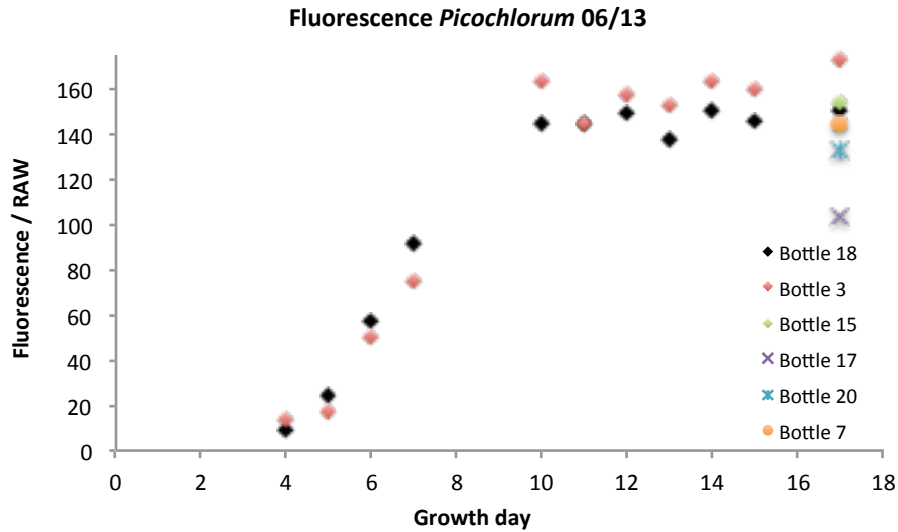


Figure 38: Fluorescence results for different simultaneously inoculated bottles of *Picochlorum* (June-July). Bottle 18 and 3 were used only for fluorescence measurements. The other bottles were tested for fluorescence after the end of the sampling period. At the time of measurement, bottle 15 and 20 had been sampled multiple times, 7 and 17 only once.

Results of the fluorescence and cell count measurements of *E. huxleyi* and *Picochlorum* are displayed in **Figure 37 and 38** respectively. For *E. huxleyi*, one bottle was used for both fluorescence and cell count measurements. Blue symbols show the results of *Coulter counter* measurements, while results of fluorescence measurements are displayed in black. Results indicate an increase in fluorescence and cell number up to day 8-9, and an indication of stabilisation (approaching stationary phase) for growth day 10-14. The slightly lower cell count numbers for the two final days of *E. huxleyi* could be related to problems with the instrument and/or dilution of the samples (the difference between results of three measurements was relatively large). Only the June '13 figure is shown, fluorescence and C.C. measurements of the May trials produced comparable results.

For *Picochlorum*, cells were too small for *Coulter counter* measurements, but two bottles were available for fluorescence measurements. Red and black symbols give the results of the different bottles, which show exactly the same trend, increasing exponentially from growth day 4, and reaching stationary phase around day 9. In addition, the growth curve is approximately identical to that obtained during trials with *Picochlorum* in March (**Figure 36**), which also shows stabilisation of the fluorescence around growth day 9-10. Three days after the final sample day, different sample bottles of *Picochlorum* were analysed for their fluorescence, in order to check whether fluorescence results gave a good indication of the growth in the real sample bottles. Results of most bottles, including bottles that were sampled once and bottles that were

sampled multiple times, are very close to those of the fluorescence bottles, indicating fluorescence results probably gave a good indication of growth in sample bottles and sampling and repressurising did not significantly affect growth (bottle 15 and 20 had been sampled multiple times, 7 and 17 only once). One *Picochlorum* bottle (17) had a relatively low fluorescence result, compared to all other bottles, including a bottle sampled on the same day (7). Interestingly, for this particular bottle, a relatively low $\Delta^{17}\text{O}$ was obtained (see **Section 5.3.1**), indicating something might have affected growth, or decline might have started earlier, in this particular bottle.

5.3.5 Variability in results

The standard deviation (SD) between results of one set of three bottles for $\delta^{17}\text{O}$ is between 0.05 and 0.25‰ in most cases, for $\delta^{18}\text{O}$, the SD of three samples varies between ~0.1 and ~0.5‰ for most sets of bottles.

The variation in $\delta(\text{O}_2/\text{Ar})$ (between 3 bottles of one set) is between ± 0.1 and 0.4 for most sets of 3 samples of both species (average SD ~0.25), but slightly higher for samples of 3- and 2-day repetition series (up to ~1 for final sample day 2-day repetition). For the 5-day repetition series this increase in variability is not visible.

Variation between samples collected in valved tubes (*E. huxleyi* and *Picochlorum* day 1, *E. huxleyi* May all samples) is not larger than between samples collected in cracker tubes. *Picochlorum* newly sampled bottles have a slightly lower SD for $\delta^{17}\text{O}$ and $\delta^{18}\text{O}$ than *E. huxleyi* newly sampled, which might be due to more equal inoculation between bottles. For *E. huxleyi* newly sampled bottles the first set of bottles has a relatively large variation between bottles in the small deltas (SD $\delta^{18}\text{O}$: 0.95‰), in combination with a relatively large variation (SD) in $\delta(\text{O}_2/\text{Ar})$ (0.5) suggesting a relatively large variation between bottles. This could be due to initial differences in inoculation density or growth rate between bottles. The first set of bottles of the *E. huxleyi* series from May in contrast shows a relatively small variability between bottles (SD $\delta^{18}\text{O}$: 0.03‰, SD $\delta(\text{O}_2/\text{Ar})$: 0.01).

Variations in $\delta^{17}\text{O}$ and $\delta^{18}\text{O}$ and $\Delta^{17}\text{O}$ are not significantly different between newly sampled and resampled bottles (the SD is slightly lower (~0.25‰ vs ~0.4‰) and more variable for resampled bottles from June-July and slightly higher for resampled bottles from May, suggesting the sampling and repressurising method does not lead to a significant increase in differences between bottles. The variation in $\delta(\text{O}_2/\text{Ar})$ does

increase for resampled bottles, (from 0.1-0.4 for most newly sampled bottles up to ~1 for four times resampled bottles).

The SD between $\Delta^{17}\text{O}$ results of three bottles of the same set is on average 13 ppm (95% CI: 9 ppm), which is comparable to the uncertainty of the experimental method (SD of $\text{O}_2\text{-Ar}$ and DA aliquots prepared in a similar way as samples). The SD is only significantly higher for the last two days of the 2-day repetition series, which is due to the low oxygen content in the samples of these days, which decreased the precision of the MS measurements.

The $d(\text{N}_2/\text{O}_2)$ is between 100 and 300‰ for most samples, exceptions are the last two days of the 2-day repetition ($d(\text{N}_2/\text{O}_2)$ up to ~600-800‰).

5.4 Discussion

5.4.1 Introduction: overview results.

Resulting $\Delta^{17}\text{O}_{\text{bio}}$ values for *E. huxleyi* and *Picochlorum*

For *Picochlorum*, biological steady state was assumed from sample day one and for *E. huxleyi* from day 13, based on stabilization of $\delta(\text{O}_2/\text{Ar})$, cell number and/or fluorescence and $\Delta^{17}\text{O}$.

For *E. huxleyi*, biological steady state was assumed from growth day 13, as all 3-sample averages from this day and later days were within ± 1 ppm of each other, and $\delta(\text{O}_2/\text{Ar})$, cell number and fluorescence were approximately constant. The May 5-day repetition series indicate the $\Delta^{17}\text{O}$ did not change between growth day 14 (248 ppm) and 20 (249 ppm). Since these values are very close to the values obtained for day 13 from the June/July experiments, it can be expected the $\Delta^{17}\text{O}$ indeed stabilises near this value. For calculation of the average and SD only the 3-day and 5-day repetition series were used, (and the sample from day 11 that was resampled on day 13 (see **Figure 31**), since results of the first time sampling series indicated steady-state might not yet have been reached (the obtained value was slightly lower, ~241 ppm, and the $\Delta^{17}\text{O}$ data showed a linear increase up to day 13), and results of the 2-day repetition series for the final days were less accurate (larger variability), due to the small sample size. The obtained average for day 13 of the 2-day repetition series was however within 1 ppm of the average (250 ppm) and including these results would not change the average of 249 ppm.

For *E. huxleyi*, the average at biological steady state (results from growth day 13-20) is

249±16(SD) (±6(SE)), based on individual MS measurements (2-day resampling results not included), 249±1(SD) (±1(SE)) based on averages per 3 samples (2-day resampling results included), and 249±11(SD) (±7(SE)) based on averages per sample (2-day resampling results not included).

For *Picochlorum*, the average biological steady state was taken over the whole period of sampling, as it was assumed the system was at biological steady state during all sample days. The average was 180±16(SD) (±5(SE)) based on individual MS measurements, 180±9(SD) (±8(SE)) based on averages per three samples and 180±13(SD) (±7(SE)) based on averages per samples (3 measurements per sample).

For completeness, when $\Delta^{17}\text{O}$ was calculated using the logarithmic definition ((‘ln’ definition: $\Delta^{17}\text{O}_{\text{ln}} = \ln(\delta^{18}\text{O}+1) - \lambda \ln(\delta^{17}\text{O}+1)$, see **Chapter 1**) with a λ coefficient of 0.5154, the resulting average for *Picochlorum* was 172 ppm (similar SD), and for the logarithmic definition with a slope 0.5179 183 ppm. For *E. huxleyi* the resulting $\Delta^{17}\text{O}$ for the ‘ln’ definition with slope 0.5154 was 239 ppm, while for the ‘ln’ definition with slope 0.5179, the result was 258 ppm.

5.4.2 Steady state

Was biological steady state reached?

Fluorescence, cell number, $\delta(\text{O}_2/\text{Ar})$ and sample pressure, independently indicated a biological or concentration steady state ($f = 0$) was reached from growth day ~9 for *Picochlorum* and ~13 for *E. huxleyi*. A similar stabilization was observable in the $\Delta^{17}\text{O}$ results, which were remarkably constant (considering the general uncertainty of the method) from these days (at ~180 ppm for *Picochlorum* (only ±2 ppm change from sample day 2 to 4) and ~249 ppm for *E. huxleyi* (only 1 ppm change between growth day 14 and 20 for the 5-day repetition series, and ±1 ppm difference between results of four different sample series, including two independent experiment series, for *E. huxleyi* growth day 13 and 14 (249±1 ppm). This all indicates, the obtained values are consistent and probably refer to biological steady state ($f = 0$) values.

It should however be noted isotopic steady state had not yet been reached, as the $\delta^{17}\text{O}$ and $\delta^{18}\text{O}$ values were still increasing up to the final sample day. This did however not change the $\Delta^{17}\text{O}$, which was approximately constant from the moment of reaching bio steady state, indicating that although respiration continued to enrich the oxygen in ^{17}O and ^{18}O , fractionation took place along a slope of approximately 0.518.

Resampled vs. newly sampled bottles: reaching steady state

The fact that it seems biological steady state is reached slightly earlier for the series in which the same bottle was sampled repeatedly (especially when the frequency was high, as for the 2-day repetition), compared to the samples from newly sampled bottles (indicated by slightly higher $\Delta^{17}\text{O}$ and $\delta^{18}\text{O}$ values for the same days in repetition samples), could possibly be explained by the fact that in the repeatedly sampled bottles, initial air- O_2 is removed more quickly than in the bottles that are allowed to accumulate until the moment of sampling (in which air- O_2 is only removed by biological uptake). In addition, the movement of bottles during the sampling procedure, and/or the decrease in gas content, might have contributed to a faster approach of steady state in the resampled bottles.

Increase in $\Delta^{17}\text{O}$ for *E. huxleyi*

The observation that the $\Delta^{17}\text{O}$ for *E. huxleyi* is increasing from sample day one to five, from a value of 160-180 ppm on growth day 5 to a (approximately steady state) value of ~250 ppm for growth day 13 to 20 is interesting. Since at the start of growth of the cultures, dissolved atmospheric oxygen was present in the bottles, you would expect the $\Delta^{17}\text{O}$ to be ~ 0 initially, and to increase towards a $\Delta^{17}\text{O}_{\text{max}^{\text{bio}}}$. This could explain the observed increase in $\Delta^{17}\text{O}$ over time. However, based on the volume of the bottles and headspace, and the expected growth rate of the phytoplankton, it was initially expected all oxygen would be replaced within approximately two days (E. Buitenhuis, pers. com. 2013, J. Kaiser pers. com. 2013). Of course, it is possible replacement of oxygen took place more slowly than expected. It should be noted bottles were not shaken during the period of growth, which might have led to slightly lower replacement rates, in addition, the start of logarithmic growth phase would depend on the growth phase of the inoculum and temperature and light conditions.

Another thing that should be taken into account is the fact that, due to its definition, the calculated $\Delta^{17}\text{O}$ is dependent on f (the ratio of net to gross production). When f is either lower or higher than zero (there is net production or consumption), the obtained value of $\Delta^{17}\text{O}$ generally differs from $\Delta^{17}\text{O}_{\text{S}_0}$ (the biological steady state value), the direction and size of the deviation depending on f , the chosen definition of $\Delta^{17}\text{O}$, and the respiratory fractionation ($^{18}\epsilon_{\text{R}}$ and γ_{R}) (thus involved oxygen consuming processes). (See **Appendix, Figure 41-44** (adapted from Kaiser 2011a,b) for calculations of the expected variation in $\Delta^{17}\text{O}$ with f , for different commonly used definitions, assuming average dark respiration, the VSMOW measurement of Barkan and Luz from 2005 and photosynthetic fractionation reported by Eisenstadt et al. (2010) for *E. huxleyi*).

However, as can be observed in Table 3 of Kaiser and Abe (2012) and **Appendix, Figure 41-44**, under average dark respiration conditions ($^{18}\epsilon_R = -20$ and $\gamma_R = 0.5179$), for *E. huxleyi* (assuming the photosynthetic fractionation reported for *E. huxleyi* by Eisenstadt et al. (2010)), $\Delta^{17}O_{P,(f=1)}$ is expected to be higher than $\Delta^{17}O_{S0,(f=0)}$, and since you would expect net production ($f > 0$) rather than net respiration ($f < 0$) during the first days of growth, you would expect the effect (of not reaching steady state yet) on $\Delta^{17}O$ to be the opposite of what was observed. As can be observed from **Appendix, Figure 39-40**, all three commonly-used definitions ($\Delta^{17}O_{\text{linear}, \lambda=0.5179}$, $\Delta^{17}O_{\text{ln}, \lambda=0.5179}$, $\Delta^{17}O_{\text{ln}, \lambda=0.5154}$ ($\Delta^{17}O_{\text{ln}} = \ln(\delta^{18}O+1) - \lambda \ln(\delta^{17}O+1)$, see **Chapter 1**) yielded lower values for the first sample days. Since the used $^{18}\epsilon_R$ is relatively uncertain (not known for *E. huxleyi* specifically), calculations of **Figure 41** were repeated with different $^{18}\epsilon_R$ values, but in all cases for $f > 0$, for $\Delta^{17}O_{\text{ln}, \lambda=0.5179}$ higher values were obtained than for $\Delta^{17}O_{\text{ln}, \lambda=0.5179(S0)}$.

Lower values for $f > 0$ than for $f = 0$ for all definitions were only obtained when the γ_R was increased to ~ 0.5225 , in which case resulting values for $f = 0$ became very high (~ 300 ppm). The observed values for $f > 0$ and $f = 0$ were only obtained when it was assumed the VSMOW measurement of Barkan and Luz 2005 or Kaiser and Abe 2012 was correct, there was no photosynthetic fractionation and γ_R was 0.5225. It is of course possible that before reaching steady state, f was lower than 0, instead of higher than 0. However, this seems unlikely. The fact that the $\Delta^{17}O_{\text{ln}, \lambda=0.5179}$ is higher than $\Delta^{17}O_{\text{linear}, \lambda=0.5179}$ (and $\Delta^{17}O_{\text{ln}, \lambda=0.5154}$) before steady state is reached, is consistent with expectations for $f > 0$ (see **Appendix, Figure 39-40**).

Therefore, the most likely explanation for the observed change in $\Delta^{17}O$ seems to be the presence of atmospheric air in the bottles. This could also explain the observed decrease in $\delta^{18}O$ and $\delta^{17}O$ from sample day one to two.

Possible deviations from biological steady state in *Picochlorum*

The effect of deviations from steady state (an f different from zero), can also not be excluded for *Picochlorum*. As described in the results, although $\Delta^{17}O$ values obtained for *Picochlorum* were very constant over the sampling period (day average 180 ± 9 ppm), a slightly lower $\Delta^{17}O$ was observed for final growth day (167 ppm), while a relatively high $\Delta^{17}O$ was observed for the first sample day (191 ppm). Although this could be a coincidence, due to the presence of one bottle with a slightly different behaviour (in both cases, one out of the three bottles yielded a $\Delta^{17}O$ relatively far from the average, see **Section 5.3.1**), it should be noted that in case of growth day one, fluorescence and $\delta(O_2/Ar)$ values are slightly below the value for the other sample days, which could indicate steady state was almost reached, but not completely for this day. Finally, for the

last sample day, although one bottle had a significantly lower $\Delta^{17}\text{O}$ in combination with a relatively low fluorescence (bottle 17, see **Section 5.3.4**), the other two bottles also had a $\Delta^{17}\text{O}$ slightly below the average. It can therefore not be ruled out that something changed in the bottles. Since it concerns a batch culture, with limited nutrients, you would expect cultures to start declining after a certain period. Fluorescence is however still constant for this day for the (not-sampled) fluorescence bottles. However, the low fluorescence value for bottle 17 might indicate decline in this bottle started earlier, or something affected growth in this bottle. If this was the case, it might have led to a change the balance of O_2 consuming reactions in the bottles (which could affect the $\Delta^{17}\text{O}$) or an increase in the relative contribution of respiration over photosynthesis. As shown in **Appendix, Figure 41-44** a change from $f = 0$ to $f < 0$ could (even under normal, dark respiration conditions) lead to lower $\Delta^{17}\text{O}_{\text{S}_0}$ for the same underlying $\delta^{17}\text{O}_{\text{P}}$ and $\delta^{18}\text{O}_{\text{P}}$ values. In addition, as can be observed, if steady state had not been completely reached at growth day 8, a $f > 0$ could also have led to a slightly higher $\Delta^{17}\text{O}$).

Interpretation of $\Delta^{17}\text{O}$ values

However, since the obtained $\Delta^{17}\text{O}$ for *Picochlorum* was relatively constant over the sample period, but especially from growth day 9-12 ($\sim 180 \pm 2$ ppm) (see **Figure 29**), while accompanying $\delta(\text{O}_2/\text{Ar})$ and fluorescence were also constant for these days (**Figure 29 and 38**, this strongly seems to indicate biological steady state was reached at least during this period).

In addition, for *E. huxleyi*, the $\Delta^{17}\text{O}$ of all independent sample series and experiments seems to stabilize around the same value (~ 249 ppm) from growth day 13, while also fluorescence, cell number and $\delta(\text{O}_2/\text{Ar})$ show a tendency to stabilisation indicating approach of concentration or biological steady state (see **Figure 28, 30-31 and 37**). Finally, the one series of *E. huxleyi* experiments for which sampling continued until growth day 20 (the May trials) shows almost exactly the same $\Delta^{17}\text{O}$ for day 20 as for day 14 (249 vs. 248 ppm), while up to day 14 its values are very close to those obtained for the other sample series (see **Figure 30-31**). This strongly indicates the $\Delta^{17}\text{O}$ indeed stabilised around this value.

Therefore, although $\delta^{17}\text{O}$ and $\delta^{18}\text{O}$ values are still increasing over the sample period, indicating an isotope steady state has not yet been reached, which complicates interpretation of the results and has to be realised, other data strongly indicate that a biological steady state was reached during the experiments. (In addition, $\Delta^{17}\text{O}$ was approximately constant from the moment of reaching bio steady state, indicating that although respiration continued to enrich the oxygen in ^{17}O and ^{18}O , fractionation

probably took place along a slope of approximately 0.518). In the remainder of this discussion the obtained average $\Delta^{17}\text{O}$ values will therefore be interpreted as (close to) biological steady state ($\Delta^{17}\text{O}_{\text{S0}}$) values and compared to $\Delta^{17}\text{O}_{\text{S0}}$ values from literature.

5.4.3 Comparison results to values from literature (Luz and Barkan 2000, Kaiser and Abe 2012)

Interpretation for different VSMOW estimates

As described in **Section 5.1**, Kaiser and Abe (2012) calculated expected $\Delta^{17}\text{O}_{\text{S0}}$ and $\Delta^{17}\text{O}_{\text{P}}$ values based on the different $\Delta^{17}\text{O}$ measurements of VSMOW, the species-specific photosynthetic fractionation observed by Eisenstadt et al. (2010), and the assumption that $^{18}\epsilon_{\text{R}} = -20$ and $^{17}\epsilon_{\text{R}}/^{18}\epsilon_{\text{R}} = 0.5179$ (average values for dark respiration in marine organisms (Barkan and Luz 2005, Kiddon et al. 1993)). Results are displayed in **Table 7**.

The here obtained ‘biological steady state’ $\Delta^{17}\text{O}$ values (~249 ppm for *E. huxleyi* and ~180 ppm for *Picochlorum*) are close to expectations based on $\Delta^{17}\text{O}_{\text{S0}}$ values reported in literature (Luz and Barkan 2000, Kaiser and Abe 2012). For *E. huxleyi*, the obtained $\Delta^{17}\text{O}_{\text{S0}}$ (249±11 ppm) is coincidentally identical to the average $\Delta^{17}\text{O}_{\text{S0}}$ obtained by Luz and Barkan in 2000 for two other marine species. In addition, the measured steady-state $\Delta^{17}\text{O}$ values of both species are very close to $\Delta^{17}\text{O}_{\text{S0}}$ values estimated by Kaiser and Abe (2012) based on different VSMOW measurements and the species-specific photosynthetic fractionation reported by Eisenstadt et al. (2010) (see **Table 7**). However, interestingly enough, the value for *Picochlorum* is very close to expectations (for comparable species) based on one VSMOW measurement, while the value obtained for *E. huxleyi* is very close to expectations based on the other measurement.

For *E. huxleyi*, as can be observed from **Table 7** (Kaiser and Abe 2012), the obtained $\Delta^{17}\text{O}_{\text{S0}}$ value (249±11 ppm) is very close to expectations based on the most recent measurements of VSMOW (Barkan and Luz 2011) and the photosynthetic fractionation reported by Eisenstadt et al. (2010) (255 ppm for *E. huxleyi*, see **Table 7**). However, compared to the VSMOW measurements by Barkan and Luz (2005) and Kaiser and Abe (2012), which yielded a ~50 ppm lower $\Delta^{17}\text{O}$, the value obtained for *E. huxleyi* is relatively high (compared to the expected value of 204 ppm). This could indicate that this VSMOW measurement is not correct, but it could of course also indicate the difference between $\Delta^{17}\text{O}_{\text{VSMOW}}$ and $\Delta^{17}\text{O}_{\text{S0}}$ is larger than expected based on the photosynthetic fractionation of Eisenstadt et al. (2010) and calculations of Kaiser and Abe (2012). This could for instance indicate stronger than expected photosynthetic

fractionation. However, a $^{18}\epsilon_R$ (respiratory isotope effect) less negative than -20‰, or γ_R ($=^{17}\epsilon_R/^{18}\epsilon_R$) above 0.5179 could also lead to higher $\Delta^{17}O_{S0}$ values for the same underlying $\Delta^{17}O_{VSMOW}$ (or $\Delta^{17}O_P$) values.

It should be noted that although higher γ_R values than 0.518 have so far not been reported for marine phytoplankton (Luz and Barkan 2005), $^{18}\epsilon_R$ is known to vary greatly depending on uptake processes and organisms involved. However, according to calculations as performed for **Figure 41-44** in the **Appendix**, for any value of $^{18}\epsilon_R$ (respiratory isotope effect) between -5 to -30‰, such a large difference cannot easily be explained without fractionation along a slope ($\gamma_R = ^{17}\epsilon_R/^{18}\epsilon_R$) above ~0.519. As so far no biological O_2 uptake processes have been reported with a fractionation slope higher than 0.519 (except for Mehler reaction in a higher plant (Helman et al. 2005)), this might indicate the difference is indeed caused by photosynthetic fractionation, if the lower $\Delta^{17}O_{VSMOW}$ measurement is correct, possibly even stronger than reported by Eisenstadt et al. (2010).

However, for *Picochlorum*, the opposite is the case. The obtained $\Delta^{17}O_{S0}$ value (180±9 ppm) is very close to expectations based on the lower (146 ppm) VSMOW measurement and the photosynthetic fractionation reported by Eisenstadt et al. (2010) for comparable species (expected $\Delta^{17}O_{S0}$ values being 183 ppm for *Nannochloropsis*, and 174 ppm for *C. reinhardtii*). However, if the higher (196 ppm) VSMOW measurement is assumed correct, the obtained steady-state value of 180 ppm for *Picochlorum* is much lower than expectations based on the photosynthetic fractionation for comparable species, and even lower than the expected $\Delta^{17}O_{S0}$ in the absence of photosynthetic fractionation (see **Table 7**). This could indicate weaker, absent or oppositely directed photosynthetic fractionation. In addition or alternatively, it could indicate involvement of a biological uptake mechanism with a triple isotope fractionation slope (γ_R) below 0.518, and/or an $^{18}\epsilon_R$ (respiratory isotope effect) larger than -20 as both would have a lowering effect on the $\Delta^{17}O_{S0}$ (see **Appendix, Figure 41-44**). Reported biological uptake mechanisms with a γ_R below 0.518 are photorespiration (0.512) and Mehler reaction (0.497) (Helman et al. 2005). Since the Mehler reaction has a relatively small $^{18}\epsilon_R$ (-10 to -15 ‰), photorespiration ($^{18}\epsilon_R$ -21.5) would seem more likely in this case (Guy et al. 1989, 1993, Helman et al 2005). Normally, these mechanisms are however not expected to play an important role in marine phytoplankton communities (Kaplan et al. 1999, Helman et al. 2005, Kaiser 2011). However, conditions in the bottles were not natural. CO_2 concentrations were probably low, in combination with high O_2 concentrations, which both favour these reactions. (Also, it is important to realize that light intensity in

Picochlorum experiments (150 μE) was slightly higher than in *E. huxleyi* experiments (50 μE). Their contribution can therefore not be excluded. Finally, since AOX (alternative oxidase) has approximately the same γ_{R} as ordinary dark respiration (COX) but a higher $^{18}\epsilon_{\text{R}}$ (~25 vs. 17 ‰) (Guy et al. 1989, 1993, Angert et al. 2003, Luz and Barkan 2005) a difference in the balance between COX and AOX might also have played a role.

Since the value obtained for one of the species is very close to expectations based on one VSMOW measurement, and the value for the other species is very close to expectations based on the other VSMOW measurement, results do not single out one measurement above the other, or give extra insight into the probability of each value. In addition, the uncertainty surrounding the value for VSMOW makes interpretation of the data complicated.

However, the large difference in steady state $\Delta^{17}\text{O}$ for *Picochlorum* (180 ppm) and *E. huxleyi* (~250 ppm), whether a result of differences in respiration/photosynthetic fractionation or both, strongly seems to indicate a difference in $\Delta^{17}\text{O}_{\text{bio}}$ between species. In addition, compared to either measurement of VSMOW vs. air, the value obtained for *E. huxleyi* is relatively high, which seems to indicate fractionation along a triple isotope slope higher than 0.518, which, as no common biological uptake processes with a slope above 0.518 have been reported, seems to lend additional credibility to the findings by Eisenstadt et al. (2010) that fractionation occurs during photosynthesis.

In addition, the observed difference in $\Delta^{17}\text{O}_{\text{bio}}$ between the studied species is in the direction expected based on results of Eisenstadt et al. (2010), who observed a stronger increase in $\Delta^{17}\text{O}$ due to photosynthetic fractionation for *E. huxleyi* than for the other studied species, including *Nannochloropsis*, a marine picoeukaryote the same size as *Picochlorum*. With the exception of *P. tricornutum*, it seemed that in the study by Eisenstadt et al. (2010), larger species displayed stronger fractionation (see **Table 6**). As in this case, stronger fractionation was observed for *E. huxleyi* than for *Picochlorum*, this might provide additional support to this idea. Especially since the difference between the species is large (70 ppm), if it has to be explained by differences in respiration processes only. However, the possible contribution of respiration processes other than ordinary dark respiration to the relatively low value for *Picochlorum*, should definitely not be overlooked.

Hopefully, the debate surrounding the $\Delta^{17}\text{O}$ of VSMOW vs. air will soon be resolved, so that the here obtained data can be more easily interpreted. However, independent of which VSMOW measurement is correct, the value obtained for *E. huxleyi* is

significantly higher than *either* measured VSMOW ^{17}O excess (and expected steady-state $\Delta^{17}\text{O}$ values in the absence of photosynthetic fractionation (see **Table 7**, Kaiser and Abe 2012), which might indeed indicate fractionation during photosynthesis. Respiratory processes with a γ_{R} above 0.518 or $^{18}\epsilon_{\text{R}}$ smaller than -20‰ could also lead to a higher ^{17}O excess, but no such high γ_{R} values have been reported for common biological uptake mechanisms, and a value as high as 250 is difficult to explain assuming either VSMOW measurement, an $^{18}\epsilon_{\text{R}}$ between \sim -5 and -30‰, and an γ_{R} below 0.519-0.520, without photosynthetic fractionation (see **Appendix**) Also, results indicate a higher $\Delta^{17}\text{O}_{\text{bio}}$ (and possibly photosynthetic fractionation) for *E. huxleyi*, than for the picoeukaryote and green algae *Picochlorum*, which is consistent with the results of Eisenstadt et al. (2010) for comparable species (which indicated stronger effects on $\Delta^{17}\text{O}$ due to photosynthetic fractionation for *E. huxleyi* than for any of the other examined species, including both a green alga (*C. Reinhardtii*), and a marine picoeukaryote the same size as *Picochlorum* (*Nannochloropsis*) (see **Table 6 and 7**). Finally, results are very consistent, in the sense that different sampling series led to the same results for the same days (see **Figure 30-32**, growth day 13), and independent experiments produced nearly identical results.

What is important to note, is that this study provides the first direct observations of a difference in $\Delta^{17}\text{O}_{\text{bio}}$ vs. air between marine species. A difference could be expected based on the results of Eisenstadt et al. (2010), but no measured differences in $\Delta^{17}\text{O}_{\text{bio}}$ vs. air have been reported before. Originally, the 2000 study by Luz and Barkan even concluded that $\Delta^{17}\text{O}_{\text{bio}}$ was independent of the species producing the oxygen. The results reported here clearly indicate a difference in $\Delta^{17}\text{O}_{\text{bio}}$ or $\Delta^{17}\text{O}_{\text{S0}}$ between species, which could have important implications for the derivation of gross oxygen production using triple isotopes. The difference between species in this study (\sim 70 ppm) is even larger than expected based on the results of Eisenstadt et al. (2010) for comparable species. The reason for this large difference (whether differences in photosynthetic or respiration fractionation) is difficult to assess, because of the current uncertainty surrounding the correct $\Delta^{17}\text{O}$ value of VSMOW vs. air. It might be a combination of differences in photosynthetic fractionation and respiratory fractionation. (As explained above, it might indicate a higher $\Delta^{17}\text{O}$ for *E. huxleyi* than expected based on the photosynthetic fractionation reported by Eisenstadt et al. (2010), which might indicate stronger photosynthetic fractionation. Alternatively, it could indicate weaker or absent photosynthetic fractionation in *Picochlorum*, and/or the involvement of a respiration process in *Picochlorum* cultures with a γ_{R} below 0.5179 (such as photorespiration) and/or $^{18}\epsilon_{\text{R}}$ larger than -20‰ (such as AOX).)

However, as mentioned above independent of which VSMOW measurement is correct, the high values obtained for *E. huxleyi* indicate the presence of photosynthetic fractionation, while results strongly indicate a difference between species, which independent of whether it was caused by differences in photosynthetic or respiratory fractionation, would have important implications for the calculation of gross oxygen production using triple oxygen isotopes, as it would make $GOP(^{17}\text{O})$ dependent on the species producing oxygen within a certain area. Since the here applied method yielded reproducible and consistent results, it would be interesting and useful to conduct similar experiments with different marine species, especially including important global primary producers such as cyanobacteria and diatoms, in order to increase our knowledge on $\Delta^{17}\text{O}_{\text{bio}}$.

5.4.4 Additional considerations

Unnatural growth conditions

Of course, growth conditions during these experiments were not natural. Cultures were grown in bottles with a small water volume (~165 ml) and headspace (4 ml) closed off from the atmosphere, with a limited supply of nutrients (batch cultures). In addition, cultures were uni-algal, and light was artificial. As a result, conditions were different from natural, and it cannot be excluded the organisms would behave or fractionate differently in nature (for instance, due to differences in the relative involvement of O_2 uptake mechanisms).

Effect respiration ($^{18}\epsilon_{\text{R}}$ and γ_{R})

As explained in the introduction, the $\delta^{17}\text{O}/\delta^{18}\text{O}$ (or $\ln(\delta^{17}\text{O}+1)/\ln(\delta^{18}\text{O}+1)$) fractionation slopes of various oxygen consuming processes vary slightly from 0.5179 (~0.497 for Mehler, ~0.512 for photorespiration to ~0.526 for Mehler in pea thylakoids (higher plant) Helman et al. 2005). It is unknown what the relative rates of different oxygen consuming processes were in these experiments. Since conditions and lighting were different from natural conditions, the dominant processes of respiration might also be different. Changes in the relative contribution of different O_2 consuming processes might have led to changes in the observed $\Delta^{17}\text{O}$, especially if the involved processes discriminated against ^{17}O and ^{18}O along a slope significantly different from 0.5179 (so if for instance photorespiration or Mehler reaction played a significant role).

Uncertainties and complications

As a result, the observed $\Delta^{17}\text{O}_{\text{S}_0}$ values are a result of the combination of the triple isotopic composition of VSMOW vs. air, currently debated as either ~146 or 196 ppm

(Kaiser and Abe 2012), a potential addition due to species-specific photosynthetic fractionation (Eisenstadt et al. 2010) and changes due to respiration, which could affect the $\Delta^{17}\text{O}_p$ in different directions and to different extents, depending on the $^{18}\epsilon_R$ and γ_R of the O_2 uptake processes involved. Finally, if the system is not exactly at steady state (f (ratio of net to gross production ratio) is not 0), the $\Delta^{17}\text{O}$ will deviate from $\Delta^{17}\text{O}_{S0}$, the amount and direction of deviation depending on f ($^{18}\epsilon_R$, γ_R) and the used definition (and lambda) as well as the underlying $\delta^{17}\text{O}_p$ and $\delta^{18}\text{O}_p$ values (in case of the linear definition) (Kaiser 2011a,b).

This all makes the observed $\Delta^{17}\text{O}$ results for a system with photosynthesis and respiration relatively difficult to interpret (even if we assume $f=0$, which is indicated by constant fluorescence/cell number, and $\delta(\text{O}_2/\text{Ar})$ and sample pressure values) since, at the moment, all input parameters ($\delta^{17}\text{O}_{\text{VSMOW}}$, photosynthetic fractionation, $^{18}\epsilon_R$ and exact γ_R of respiration processes involved) are relatively uncertain. In addition, it should be realized that $\delta^{17}\text{O}$ and $\delta^{18}\text{O}$ values are still increasing until the final sample day, and a complete isotopic steady state has thus not been reached, even though a biological steady state, and a constant $\Delta^{17}\text{O}$ value has been reached.

Air contamination

The fact that the $\delta(\text{O}_2/\text{Ar})$ vs. air was very high ($> 1,000\text{‰}$) in all samples, indicates the contamination with or presence of outside air was negligible. Also, the resampled bottle results give no indication of increased contamination due to the sampling or repressuring process (in form of lower $\delta(\text{O}_2/\text{Ar})$ or $\Delta^{17}\text{O}$ or more positive $\delta^{17}\text{O}$ and $\delta^{18}\text{O}$ values compared to newly sampled bottle samples).

$\Delta^{17}\text{O}$ definition

Because different definitions of $\Delta^{17}\text{O}$ have been used in the past, and the used definition affects the results (Kaiser 2011a,b, Kaiser and Abe 2011), for completeness, the $\Delta^{17}\text{O}$ was also calculated using the logarithmic definition ('ln' definition: $\Delta^{17}\text{O}_{\text{ln}} = \ln(\delta^{18}\text{O}+1) - \lambda \ln(\delta^{17}\text{O}+1)$, see **Chapter 1**) with slope 0.5179 (γ_R) and 0.5154 (θ_R). Results are displayed in **Appendix, Figure 39-40**. It can be observed, using another definition would not substantially change the results, either in terms of trend or obtained $\Delta^{17}\text{O}_{S0}$ values (which did not differ by more than 10 ppm), which could be expected for conditions near steady state ($\delta^{17}\text{O}$ and $\delta^{18}\text{O}$ values close to 0).

When $\Delta^{17}\text{O}$ was calculated using the logarithmic definition with a coefficient of 0.5154, the resulting average for *Picochlorum* was 172 ppm (similar SD), and for the logarithmic definition with a slope 0.5179 183 ppm. For *E. huxleyi* the resulting $\Delta^{17}\text{O}$ for

the 'ln' definition with slope 0.5154 was 239 ppm, while for the 'ln' definition with slope 0.5179, the result was 258 ppm.

Reliability results

For *E. huxleyi*, results for the same growth day are identical for once and multiple times sampled bottles, indicating the sampling and/or repressuring method did not significantly alter the composition of gas in the bottles. This was also indicated by fluorescence measurements for different bottles of *Picochlorum* conducted after the period of sampling, which produced comparable results for once and multiple times resampled bottles.

$\delta(\text{O}_2/\text{Ar})$ results show no indication of air contamination due to sampling and/or repressuring. Results of *Picochlorum* are very consistent between sample days, and for *E. huxleyi* (both in $\Delta^{17}\text{O}$ and $\delta^{17}\text{O}$ and $\delta^{18}\text{O}$) very consistent between independent experiments and different sampling approaches (either sampling from new bottles or resampling from the same bottles, at different frequencies).

Although the standard deviation (SD) of $\delta^{17}\text{O}$ and $\delta^{18}\text{O}$ was slightly higher than obtained during processing of O_2 -Ar reference gas aliquots, which could be expected due to small differences in growth and/or initial conditions between individual bottles, the SD of $\Delta^{17}\text{O}$ between three simultaneously sampled bottles was, with small exceptions, comparable to that of DA (dry air) or O_2 -Ar reference mixtures processed in the same way as samples, indicating the uncertainty was close to that introduced by the method itself.

Encountered problems

Due to separation line problems, *Picochlorum* day 6 samples were lost, but fortunately there were sufficient data left. O_2 content of repetition samples of *Picochlorum* was unfortunately too low for isotopic analysis. In addition, O_2 content during the final sample days of 2-day repetition series *E. huxleyi* was too low for accurate measurements, leading to a large variability in the results.

Collection tubes

All samples from May were collected in valved tubes, while samples from June-July were collected in flame-seal tubes from sample day 3 (*Picochlorum*) and 2 (*E. huxleyi*). Results between experiments with *E. huxleyi* from May and June-July were very similar, thus not indicating a substantial influence of the collection tube (it could however be expected to make a difference when samples are stored for longer periods of time, as flame-seal tubes are more leak-proof).

Future recommendations

E. huxleyi newly sampled bottles results indicate sampling stopped before a biological steady state was reached. Although repetition series (especially the 5-day repetition series which shows a similar $\Delta^{17}\text{O}$ between day 14 and 20) indicate $\Delta^{17}\text{O}$ was probably close to its steady state value, it would have been interesting to continue sampling over a longer period of time. For *Picochlorum* this would have been interesting as well, in order to see whether the lower value on sample day 5 was a coincidence or the $\Delta^{17}\text{O}$ started decreasing. For both species, $\delta^{17}\text{O}$ and $\delta^{18}\text{O}$ values were still increasing towards zero at the final day of sampling, so sampling over a longer period of time might be interesting because it might lead to the inclusion of a situation with isotopic steady state in the results. For repetition series, sampling longer would, with the currently used bottles, headspace and sampling method, not be possible due to the decrease in sample O_2 content over time, unless the oxygen content of the samples would be increased, for instance by increasing the bottle size (significantly increasing the headspace was not possible because N_2 contents became too high for effective removal on the separation line). For single sampling series, sampling longer would be possible, but require a larger quantity of bottles.

Since experiments seem to have yielded reliable results, consistent between species, between three bottles of the same sample day (small variability), newly sampled and repeatedly sampled bottles (at different time-intervals), and independent culture experiments in May and June, they yielded results that are within the expected range for biological oxygen at steady state produced by these types of marine phytoplankton, and they show no strong/unexplainable differences from the main trend, nor indication of air contamination, it would be very interesting to conduct similar experiments with additional species, preferably species that were either also used in the experiments of Eisenstadt et al. (2010) (as *Nannochloropsis*, in order to be able to properly compare the Luz and Barkan (2000) and Eisenstadt et al. (2010) results), or that are important global primary producers, such as cyanobacteria (*Prochlorococcus*, *Synechococcus*) or diatoms.

5.5 Conclusions

Results indicate the ^{17}O excess measured for both species is in the range of biological steady-state $\Delta^{17}\text{O}$ values calculated by Kaiser and Abe (2012) based on different measurements of VSMOW vs. air and species-specific photosynthetic fractionation reported by Eisenstadt et al (2010). In all cases, the ^{17}O excess for biological oxygen produced and recycled by *Emiliana huxleyi* was found to be significantly higher (249 ± 11 ppm) than the ^{17}O excess obtained for *Picochlorum* (180 ± 13 ppm), which seems in line with expectations based on results of Eisenstadt et al. (2010) for comparable phytoplankton species, and in disagreement with the original assumption that the ^{17}O excess of biological oxygen would be species-independent (Luz and Barkan, 2000). The observed difference between species was even larger than expected based on the results of Eisenstadt et al. (2010). Although the observed difference could originate from both differences in photosynthetic fractionation and respiratory fractionation, and it cannot be excluded the relative contribution of oxygen consuming processes in the bottles was different from that in nature, in either case, the resulting ^{17}O excess is significantly different between the two species, and the high ^{17}O excess obtained for *E. huxleyi* indicates fractionation along a triple isotope slope of > 0.519 which is difficult to explain based on respiratory fractionation only (Angert et al. 2003, Helman et al. 2005, Luz and Barkan 2005, Eisenstadt et al. 2010). Results therefore provide an additional indication of photosynthetic oxygen isotope fractionation and, more importantly, a species-dependent ^{17}O excess for biological oxygen, which would have important implications for the calculation of marine gross productivity using oxygen triple isotopes. Since a species-specific $\Delta^{17}\text{O}_{\text{bio}}$ would imply the relative contribution of different phytoplankton species to oxygen production would have to be accounted for in the calculation of $G(^{17}\text{O})$, this stresses the need to acquire more information on the specific $\Delta^{17}\text{O}_{\text{bio}}$ and O_2 production rate of more marine primary producers. Since the here applied culturing and sampling methods were found to produce consistent and reproducible results, it would be interesting to conduct similar experiments with additional phytoplankton species, specifically including globally important primary producers as marine cyanobacteria (*Synechococcus*, *Prochlorococcus*) which are important primary producers but were found sensitive to the helium purging method applied by Eisenstadt et al. (2010). In addition, it would be interesting to repeat the experiment with *Nannochloropsis* and compare results to those of similar experiments by Luz and Barkan (2000) and the $\Delta^{17}\text{O}_{\text{bio}}$ calculations by Kaiser and Abe (2012). Finally, more certainty regarding the $\delta^{17}\text{O}$ of VSMOW vs. air would make it easier to interpret the obtained results in the future.

Bibliography

Abe, O. (2008). Isotope fractionation of molecular oxygen during adsorption/desorption by molecular sieve zeolite. *Rapid Communications in Mass Spectrometry* , 22 (16), 2510-2514.

Abe, O., & Yoshida, N. (2003). Partial pressure dependency of $^{17}\text{O}/^{16}\text{O}$ and $^{18}\text{O}/^{16}\text{O}$ of molecular oxygen in the mass spectrometer. *Rapid Communications in Mass Spectrometry* , 17 (5), 395-400.

Angeles-Boza, A. M., Ertem, M. Z., Sarma, R., Ibanez, C. H., Maji, S., Llobet, A., et al. (2014). Competitive oxygen-18 kinetic isotope effects expose O–O bond formation in water oxidation catalysis by monomeric and dimeric ruthenium complexes. *Chem. Sci.* , 5, 1141-1152.

Angert, A., Rachmilevitch, S., Barkan, E., & Luz, B. (2003). Effects of photorespiration, the cytochrome pathway, and the alternative pathway on the triple isotopic composition of atmospheric O_2 . *Global Biogeochemical Cycles* , 17 (1), 1030.

Annan, J. N. (2008). *Growth response of the green alga Picochlorum Oklahomensis to nutrient limitation and salinity stress*. Ph.D. dissertation, Oklahoma State University.

Assonov, S. S., & Brenninkmeijer, C. A. (2005). Reporting small $\Delta^{17}\text{O}$ values: existing definitions and concepts. *Rapid Communications in Mass Spectrometry* , 19 (5), 627-636.

Assonov, S., & De Groot, P. A. (2009). Chapter 6 – Oxygen. In P. A. De Groot (Ed.), *Handbook of Stable Isotope Analytical Techniques* (pp. 405-618). Amsterdam: Elsevier.

Barford, C. C., Montoya, J. P., Altabet, M. A., & Mitchell, R. (1999). Steady-state nitrogen isotope effects of N_2 and N_2O production in *Paracoccus denitrificans*. *Applied and environmental microbiology* , 65 (3), 989-994.

Barkan, E., & Luz, B. (2007). Diffusivity fractionations of $\text{H}_2^{16}\text{O}/\text{H}_2^{17}\text{O}$ and $\text{H}_2^{16}\text{O}/\text{H}_2^{18}\text{O}$ in air and their implications for isotope hydrology. *Rapid Communications in Mass Spectrometry* , 21 (18), 2999-3005.

Barkan, E., & Luz, B. (2005). High precision measurements of $^{17}\text{O}/^{16}\text{O}$ and $^{18}\text{O}/^{16}\text{O}$ ratios in H_2O . *Rapid Communications in Mass Spectrometry* , 19 (24), 3737-3742.

Barkan, E., & Luz, B. (2003). High-precision measurements of $^{17}\text{O}/^{16}\text{O}$ and $^{18}\text{O}/^{16}\text{O}$ of O_2 and O_2/Ar ratio in air. *Rapid Communications in Mass Spectrometry* , 17 (24), 2809-2814.

Barkan, E., & Luz, B. (2011). The relationships among the three stable isotopes of oxygen in air, seawater and marine photosynthesis. *Rapid Communications in Mass Spectrometry* , 25 (16), 2367-2369.

- Bender, M. L., & Grande, K. D. (1987). Production, respiration, and the isotope geochemistry of O₂ in the upper water column. *Global Biogeochemical Cycles*, 1 (1), 49-59.
- Bender, M., Sowers, T., & Labeyrie, L. (1994). The Dole Effect and its variations during the last 130,000 years as measured in the Vostok Ice Core. *Global Biogeochemical Cycles*, 8 (3), 363-376.
- Benson, B. B., & Krause Jr., D. (1984). The concentration and isotopic fractionation of oxygen dissolved in freshwater and seawater in equilibrium with the atmosphere. *Limnology and oceanography*, 29 (3), 620-632.
- Benson, B. B., Krause Jr., D., & Peterson, M. A. (1979). The solubility and isotopic fractionation of gases in dilute aqueous solution. I. Oxygen. *Journal of Solution Chemistry*, 8 (9), 655-690.
- Bigeleisen, J., & Mayer, M. G. (1947). Calculation of equilibrium constants for isotopic exchange reactions. *The Journal of Chemical Physics*, 15 (5), 261-267.
- Blunier, T., Barnett, B., Bender, M. L., & Hendricks, M. B. (2002). Biological oxygen productivity during the last 60,000 years from triple oxygen isotope measurements. *Global Biogeochemical Cycles*, 16 (3), 1029.
- Boering, K. A., Jackson, T., Hoag, K. J., Cole, A. S., Perri, M. J., Thiemens, M., et al. (2004). Observations of the anomalous oxygen isotopic composition of carbon dioxide in the lower stratosphere and the flux of the anomaly to the troposphere. *Geophysical Research Letters*, 31, L03109.
- Brand, W. A. (2004). Chapter 38 – Mass spectrometer hardware for analyzing stable isotope ratios. In P. A. De Groot (Ed.), *Handbook of Stable Isotope Analytical Techniques* (pp. 835-856). Amsterdam: Elsevier.
- Brand, W. A., Coplen, T. B., Aerts-Bijma, A. T., Böhlke, J. K., Gehre, M., Geilmann, H., et al. (2009). Comprehensive inter-laboratory calibration of reference materials for δ¹⁸O versus VSMOW using various on-line high-temperature conversion techniques. *Rapid Communications in Mass Spectrometry*, 23 (7), 999-1019.
- Breck, D. W. (1964). Crystalline molecular sieves. *Journal of Chemical Education*, 41 (12), 678-689.
- Brenninkmeijer, C. A., & Louwers, M. L. (1985). Vacuum-actuated high-vacuum glass valve. *Analytical Chemistry*, 57 (4), 960-960.
- Buitenhuis, E. T., Li, W. K., Vaultot, D., Lomas, M. W., Landry, M. R., Partensky, F., et al. (2012). Picophytoplankton biomass distribution in the global ocean. *Earth System Science Data*, 4 (1), 37-46.
- Buitenhuis, E. T., Pangerc, T., Franklin, D. J., Le Quéré, C., & Malin, G. (2008). Growth rates of six coccolithophorid strains as a function of temperature. *Limnology and oceanography*, 53 (3), 1181-1185.

- Casciotti, K. L., McIlvin, M., & Buchwald, C. (2010). Oxygen isotopic exchange and fractionation during bacterial ammonia oxidation. *Limnology and Oceanography* , 55 (2), 753-762.
- Castro-Morales, K. (2010). *Marine productivity estimates from dissolved gas measurements in the Southern Ocean*. Ph.D. dissertation, University of East Anglia, Norwich, UK.
- Castro-Morales, K., Cassar, N., Shoosmith, D. R., & Kaiser, J. (2013). Biological production in the Bellingshausen Sea from oxygen-to-argon ratios and oxygen triple isotopes. *Biogeosciences* , 10 (4), 2273-2291.
- Clausen, J., & Junge, W. (2005). Search for intermediates of photosynthetic water oxidation. *Photosynthesis Research* , 84 (1-3), 339-345.
- Clayton, R. N., & Mayeda, T. K. (1988). Formation of ureilites by nebular processes. *Geochimica et Cosmochimica Acta* , 52 (5), 1313-1318.
- Clayton, R. N., & Mayeda, T. K. (1996). Oxygen isotope studies of achondrites. *Geochimica et Cosmochimica Acta* , 60 (11), 1999-2017.
- Clayton, R. N., Onuma, N., & Mayeda, T. K. (1976). A classification of meteorites based on oxygen isotopes. *Earth and Planetary Science Letters* , 30 (1), 10-18.
- Coleman, M., & Gray, J. (1972). An adjustable gas inlet system for an isotope mass spectrometer. *Review of Scientific Instruments* , 43 (10), 1501-1503.
- Corcoran, A. A., & Voorhies, W. A. (2012). Simultaneous measurements of oxygen and carbon dioxide fluxes to assess productivity in phytoplankton cultures. *Journal of Microbiological Methods* , 91 (3), 377-379.
- Craig, H. (1957). Isotopic standards for carbon and oxygen and correction factors for mass-spectrometric analysis of carbon dioxide. *Geochimica et Cosmochimica Acta* , 12 (1-2), 133-149.
- De Groot, P. A. (2009). Chapter 16 – Atmospheric - tropospheric - stratospheric compounds. In P. A. De Groot (Ed.), *Handbook of Stable Isotope Analytical Techniques* (pp. 957-988). Amsterdam: Elsevier.
- Dimier, C., Corato, F., Saviello, G., & Brunet, C. (2007). Photophysiological properties of the marine picoeukaryote picochlorum RCC 237 (Trebouxiophyceae, Chlorophyta). *Journal of Phycology* , 43 (2), 275-283.
- Ducklow, H. W., & Doney, S. C. (2013). What is the metabolic state of the oligotrophic ocean? A debate. *Annual Review of Marine Science* , 5 (1), 525-533.
- Dudley, W. C., & Goodney, D. E. (1979). Oxygen isotope content of coccoliths grown in culture. *Deep Sea Research Part A. Oceanographic Research Papers* , 26 (5), 495-503.

- Eisenstadt, D., Barkan, E., Luz, B., & Kaplan, A. (2010). Enrichment of oxygen heavy isotopes during photosynthesis in phytoplankton. *Photosynthesis Research* , 103 (2), 97-103.
- Emerson, S., Quay, P. D., Stump, C., Wilbur, D., & Schudlich, R. (1995). Chemical tracers of productivity and respiration in the subtropical Pacific Ocean. *Journal of Geophysical Research: Oceans* , 100 (C8), 15873-15887.
- Emerson, S., Stump, C., Wilbur, D., & Quay, P. (1999). Accurate measurement of O₂, N₂, and Ar gases in water and the solubility of N₂. *Marine Chemistry* , 64 (4), 337-347.
- Falkowski, P., Scholes, R. J., Boyle, E., Canadell, J., Canfield, D., Elser, J., et al. (2000). The global carbon cycle: A test of our knowledge of Earth as a system. *Science* , 290 (5490), 291-296.
- Field, C. B., Behrenfeld, M. J., Randerson, J. T., & Falkowski, P. (1998). Primary production of the biosphere: Integrating terrestrial and oceanic components. *Science* , 281 (5374), 237-240.
- Fontanier, C., Mackensen, A., Jorissen, F., Anschutz, P., Licari, L., & Griveaud, C. (2006). Stable oxygen and carbon isotopes of live benthic foraminifera from the Bay of Biscay: Microhabitat impact and seasonal variability. *Marine Micropaleontology* , 58 (3), 159-183.
- Fuller, N. J., Campbell, C., Allen, D. J., Pitt, F. D., Zwirgmaier, K., Le Gall, F., et al. (2006). Analysis of photosynthetic picoeukaryote diversity at open ocean sites in the Arabian Sea using a PCR biased towards marine algal plastids. *Aquatic Microbial Ecology* , 43 (1), 79-93.
- Garcia, H. E., & Gordon, L. I. (1992). Oxygen solubility in seawater: Better fitting equations. *Limnology and Oceanography* , 37 (6), 1307-1312.
- Ghosh, P., & Brand, W. A. (2003). Stable isotope ratio mass spectrometry in global climate change research. *International Journal of Mass Spectrometry* , 228 (1), 1-33.
- Gloël, J. (2012). *Triple oxygen isotopes and oxygen/argon ratio measurements to enhance coastal and open ocean production/respiration comparisons*. Ph.D. dissertation, Norwich, UK, University of East Anglia, School of environmental sciences.
- González-Posada, A. M. (2012). *Biological oxygen production from oxygen-to-argon ratios and oxygen isotopologues in the Atlantic Ocean*. Ph.D. dissertation, Norwich, UK, University of East Anglia, School of environmental sciences.
- Granger, J., Sigman, D. M., Needoba, J. A., & Harrison, P. J. (2004). Coupled nitrogen and oxygen isotope fractionation of nitrate during assimilation by cultures of marine phytoplankton. *Limnology and Oceanography* , 49, 1763-1773.
- Guy, R. D., Berry, J. A., Fogel, M. L., & Hoering, T. C. (1989). Differential fractionation of oxygen isotopes by cyanide-resistant and cyanide-sensitive respiration in plants. *Planta* , 177 (4), 483-491.

- Guy, R. D., Fogel, M. L., & Berry, J. A. (1993). Photosynthetic fractionation of the stable isotopes of oxygen and carbon. *Plant Physiology*, *101* (1), 37-47.
- Hamme, R. C., & Emerson, S. R. (2004). The solubility of neon, nitrogen and argon in distilled water and seawater. *Deep Sea Research Part I: Oceanographic Research Papers*, *51* (11), 1517-1528.
- Helman, Y., Barkan, E., Eisenstadt, D., Luz, B., & Kaplan, A. (2005). Fractionation of the three stable oxygen isotopes by oxygen-producing and oxygen-consuming reactions in photosynthetic organisms. *Plant physiology*, *138* (4), 2292-2298.
- Hendricks, M. B., Bender, M. L., & Barnett, B. A. (2004). Net and gross O₂ production in the Southern Ocean from measurements of biological O₂ saturation and its triple isotope composition. *Deep Sea Research Part I: Oceanographic Research Papers*, *51* (11), 1541-1561.
- Hendricks, M. B., Bender, M. L., Barnett, B. A., Strutton, P., & Chavez, F. P. (2005). Triple oxygen isotope composition of dissolved O₂ in the equatorial Pacific: A tracer of mixing, production, and respiration. *Journal of Geophysical Research: Oceans*, *110*, C12021.
- Juranek, L. W., & Quay, P. D. (2010). Basin-wide photosynthetic production rates in the subtropical and tropical Pacific Ocean determined from dissolved oxygen isotope ratio measurements. *Global Biogeochemical Cycles*, *24*, GB2006.
- Juranek, L. W., & Quay, P. D. (2005). In vitro and in situ gross primary and net community production in the North Pacific Subtropical Gyre using labeled and natural abundance isotopes of dissolved O₂. *Global Biogeochemical Cycles*, *19*, GB3009.
- Juranek, L. W., Quay, P. D., Feely, R. A., Lockwood, D., Karl, D. M., & Church, M. J. (2012). Biological production in the NE Pacific and its influence on air-sea CO₂ flux: Evidence from dissolved oxygen isotopes and O₂/Ar. *Journal of Geophysical Research: Oceans*, *117*, C05022.
- Juranek, L., & Quay, P. (2013). Using triple isotopes of dissolved oxygen to evaluate global marine productivity. *Annual Review of Marine Science*, *5* (1), 503-524.
- Kaiser, J. (2008). Reformulated ¹⁷O correction of mass spectrometric stable isotope measurements in carbon dioxide and a critical appraisal of historic 'absolute' carbon and oxygen isotope ratios. *Geochimica et Cosmochimica Acta*, *72* (5), 1312-1334.
- Kaiser, J. (2011). Technical note: Consistent calculation of aquatic gross production from oxygen triple isotope measurements. *Biogeosciences*, *8* (7), 1793-1811.
- Kaiser, J., & Abe, O. (2012). Reply to Nicholson's comment on "Consistent calculation of aquatic gross production from oxygen triple isotope measurements" by {Kaiser} (2011). *Biogeosciences*, *9* (8), 2921-2933.
- Kaiser, J., Röckmann, T., & Brenninkmeijer, C. A. (2004). Contribution of mass-dependent fractionation to the oxygen isotope anomaly of atmospheric nitrous oxide. *Journal of Geophysical Research: Atmospheres*, *109*, D03305.

- Kaiser, J., Reuer, M. K., Barnett, B., & Bender, M. L. (2005). Marine productivity estimates from continuous O₂/Ar ratio measurements by membrane inlet mass spectrometry. *Geophysical Research Letters*, *32*, L19605.
- Karlsson, H. R. (2004). Chapter 36 – The use of molecular sieves in stable isotope analysis. In P. A. De Groot (Ed.), *Handbook of Stable Isotope Analytical Techniques* (pp. 805-819). Amsterdam: Elsevier.
- Kiddon, J., Bender, M. L., Orchardo, J., Caron, D. A., Goldman, J. C., & Dennett, M. (1993). Isotopic fractionation of oxygen by respiring marine organisms. *Global Biogeochemical Cycles*, *7* (3), 679-694.
- Kowalczyk, K. (2006). *The isotopic composition of valves and organic tissue of diatoms grown in steady state cultures under varying conditions of temperature, light and nutrients – Implications for the interpretation of oxygen isotopes from sedimentary biogenic opal as proxies of environmental variations*. Ph.D. dissertation, Mathematisch-Naturwissenschaftlichen Fakultät, Universität zu Köln.
- Krause Jr., D., & Benson, B. B. (1989). The solubility and isotopic fractionation of gases in dilute aqueous solution. IIa. solubilities of the noble gases. *Journal of Solution Chemistry*, *18* (9), 823-873.
- Kroopnick, P. M. (1975). Respiration, photosynthesis, and oxygen isotope fractionation in oceanic surface water. *Limnology and Oceanography*, *20* (6), 988-992.
- Kroopnick, P., & Craig, H. (1972). Atmospheric oxygen: Isotopic composition and solubility fractionation. *Science*, *175* (4017), 54-55.
- Lämmerzahl, P., Röckmann, T., Brenninkmeijer, C. A., Krankowsky, D., & Mauersberger, K. (2002). Oxygen isotope composition of stratospheric carbon dioxide. *Geophysical Research Letters*, *29* (12), 1582.
- Lane, D., Beaumont, A., & Hunter, J. (1994). Primary production of prochlorophytes, cyanobacteria, and eucaryotic ultraphytoplankton: measurements from flow cytometric sorting. *Mar. Biol*, *114*, 85-95.
- Le Gall, F., Rigaut-Jalabert, F., Marie, D., Garczarek, L., Viprey, M., Gobet, A., et al. (2008). Picoplankton diversity in the South-East Pacific Ocean from cultures. *Biogeosciences*, *5* (1), 203-214.
- Luz, B., & Barkan, E. (2000). Assessment of oceanic productivity with the triple-isotope composition of dissolved oxygen. *Science*, *288* (5473), 2028-2031.
- Luz, B., & Barkan, E. (2009). Net and gross oxygen production from O₂/Ar, ¹⁷O/¹⁶O and ¹⁸O/¹⁶O ratios. *Aquat. Microb. Ecol*, *56* (2-3), 133-145.
- Luz, B., & Barkan, E. (2011). Oxygen isotope fractionation in the ocean surface and ¹⁸O/¹⁶O of atmospheric O₂. *Global Biogeochemical Cycles*, *25*, GB4006.
- Luz, B., & Barkan, E. (2011). Proper estimation of marine gross O₂ production with ¹⁷O/¹⁶O and ¹⁸O/¹⁶O ratios of dissolved O₂. *Geophysical Research Letters*, *38*, L19606.

- Luz, B., & Barkan, E. (2011). The isotopic composition of atmospheric oxygen. *Global Biogeochemical Cycles* , 25 (3), GB3001.
- Luz, B., & Barkan, E. (2005). The isotopic ratios $^{17}\text{O}/^{16}\text{O}$ and $^{18}\text{O}/^{16}\text{O}$ in molecular oxygen and their significance in biogeochemistry. *Geochimica et Cosmochimica Acta* , 69 (5), 1099-1110.
- Luz, B., Barkan, E., Bender, M. L., Thiemens, M. H., & Boering, K. A. (1999). Triple-isotope composition of atmospheric oxygen as a tracer of biosphere productivity. *Nature* , 400 (6744), 547-550.
- Luz, B., Barkan, E., Sagi, Y., & Yacobi, Y. Z. (2002). Evaluation of community respiratory mechanisms with oxygen isotopes: A case study in Lake Kinneret. *Limnology and Oceanography* , 47 (1), 33-42.
- Luz, B., Barkan, E., Yam, R., & Shemesh, A. (2009). Fractionation of oxygen and hydrogen isotopes in evaporating water. *Geochimica et Cosmochimica Acta* , 73 (22), 6697-6703.
- Man-Aharonovich, D., Philosof, A., Kirkup, B. C., Le Gall, F., Yogeve, T., Berman-Frank, I., et al. (2010). Diversity of active marine picoeukaryotes in the Eastern Mediterranean Sea unveiled using photosystem-II psbA transcripts. *The ISME journal* , 4 (8), 1044-1052.
- Marra, J. (2012). Comment on "Measuring primary production rates in the ocean: Enigmatic results between incubation and non-incubation methods at Station ALOHA" by P. D. Quay et al. *Global Biogeochemical Cycles* , 26, GB2031.
- Matsuhisa, Y., Goldsmith, J. R., & Clayton, R. N. (1979). Oxygen isotopic fractionation in the system quartz-albite-anorthite-water. *Geochimica et Cosmochimica Acta* , 43 (7), 1131-1140.
- McLaughlin, K., Silva, S., Kendall, C., Stuart-Williams, H., & Paytan, A. (2004). A precise method for the analysis of $\delta^{18}\text{O}$ of dissolved inorganic phosphate in seawater. *Limnol. Oceanogr.: Methods* , 2, 202-212.
- Miller, M. F. (2002). Isotopic fractionation and the quantification of ^{17}O anomalies in the oxygen three-isotope system: an appraisal and geochemical significance. *Geochimica et Cosmochimica Acta* , 66 (11), 1881-1889.
- Miller, M., Franchi, I., Sexton, A., & Pillinger, C. (1999). High-precision $\delta^{17}\text{O}$ isotope measurements of oxygen from silicates and other oxides: Method and applications. *Rapid Communications in Mass Spectrometry* , 13 (13), 1211-1217.
- Miyajima, T., Miyajima, Y., Hanba, Y. T., Yoshii, K., Koitabashi, T., & Wada, E. (1995). Determining the stable isotope ratio of total dissolved inorganic carbon in lake water by GC/C/IIRMS. *Limnology and Oceanography* , 40 (5), 994-1000.
- Moon-van der Staay, S. Y., De Wachter, R., & Vaultot, D. (2001). Oceanic 18S rDNA sequences from picoplankton reveal unsuspected eukaryotic diversity. *Nature* , 409 (6820), 607-610.

- Munro, D. R., Quay, P. D., Juranek, L. W., & Goericke, R. (2013). Biological production rates off the Southern California coast estimated from triple O₂ isotopes and O₂:Ar gas ratios. *Limnology and Oceanography* , 58 (4), 1312-1328.
- Nelson, S. T. (2000). Sample vial influences on the accuracy and precision of carbon and oxygen isotope ratio analysis in continuous flow mass spectrometric applications. *Rapid Communications in Mass Spectrometry* , 14 (4), 293-297.
- Nicholson, D. P. (2011). Comment on: "Technical note: Consistent calculation of aquatic gross production from oxygen triple isotope measurements" by Kaiser (2011). *Biogeosciences* , 8 (10), 2993-2997.
- Nicholson, D. P., Stanley, R. H., Barkan, E., Karl, D. M., Luz, B., Quay, P. D., et al. (2012). Evaluating triple oxygen isotope estimates of gross primary production at the Hawaii Ocean Time-series and Bermuda Atlantic Time-series study sites. *Journal of Geophysical Research: Oceans* , 117, C05012.
- Nicholson, D., Stanley, R. H., & Doney, S. C. (2014). The triple oxygen isotope tracer of primary productivity in a dynamic ocean model. *Global Biogeochemical Cycles* , 28 (5), 538-552.
- Oesselmann, J., Hilkert, A., & Douthitt, C. (2000). Trends in stable isotopic analyses and applications. *Nuclear techniques in integrated plant nutrient, water and soil management* , 16, 355-364.
- Ostrom, N. E., Carrick, H. J., Twiss, M. R., & Piwinski, L. (2005). Evaluation of primary production in Lake Erie by multiple proxies. *Oecologia* , 144 (1), 115-124.
- Ostrom, N. E., Russ, M. E., Field, A., Piwinski, L., Twiss, M. R., & Carrick, H. J. (2005). Ratios of community respiration to photosynthesis and rates of primary production in Lake Erie via oxygen isotope techniques. *Journal of Great Lakes Research* , 31, Supplement 2 (0), 138-153.
- Peterson, B. J., & Fry, B. (1987). Stable isotopes in ecosystem studies. *Annual Review of Ecology and Systematics* , 18 (1), 293-320.
- Prokopenko, M. G., Pauluis, O. M., Granger, J., & Yeung, L. Y. (2011). Exact evaluation of gross photosynthetic production from the oxygen triple-isotope composition of O₂: Implications for the net-to-gross primary production ratios. *Geophysical Research Letters* , 38, L14603.
- Quay, P. D. (2012). Reply to comment by J. Marra on "Measuring primary production rates in the ocean: Enigmatic results between incubation and non-incubation methods at Station ALOHA". *Global Biogeochemical Cycles* , 26, GB2032.
- Quay, P. D., Emerson, S., Wilbur, D. O., Stump, C., & Knox, M. (1993). The δ¹⁸O of dissolved O₂ in the surface waters of the subarctic Pacific: A tracer of biological productivity. *Journal of Geophysical Research: Oceans* , 98 (C5), 8447-8458.

- Quay, P. D., Peacock, C., Björkman, K., & Karl, D. M. (2010). Measuring primary production rates in the ocean: Enigmatic results between incubation and non-incubation methods at Station ALOHA. *Global Biogeochemical Cycles* , 24, GB3014.
- Quay, P., Stutsman, J., & Steinhoff, T. (2012). Primary production and carbon export rates across the subpolar N. Atlantic Ocean basin based on triple oxygen isotope and dissolved O₂ and Ar gas measurements. *Global Biogeochemical Cycles* , 26, GB2003.
- Quinones-Rivera, Z. J., Wissel, B., Justic, D., & Fry, B. (2007). Partitioning oxygen sources and sinks in a stratified, eutrophic coastal ecosystem using stable oxygen isotopes. *Marine Ecology Progress Series* , 342, 69-83.
- Reuer, M. K., Barnett, B. A., Bender, M. L., Falkowski, P. G., & Hendricks, M. B. (2007). New estimates of Southern Ocean biological production rates from O₂/Ar ratios and the triple isotope composition of O₂. *Deep Sea Research Part I: Oceanographic Research Papers* , 54 (6), 951-974.
- Robinson, C., Serret, P., Tilstone, G., Teira, E., Zubkov, M. V., Rees, A. P., et al. (2002). Plankton respiration in the Eastern Atlantic Ocean. *Deep Sea Research Part I: Oceanographic Research Papers* , 49 (5), 787-813.
- Sarma, V. V., Abe, O., & Saino, T. (2003). Chromatographic separation of nitrogen, argon, and oxygen in dissolved air for determination of triple oxygen isotopes by dual-inlet mass spectrometry. *Analytical Chemistry* , 75 (18), 4913-4917.
- Sarma, V. V., Abe, O., & Saino, T. (2008). Spatial variations in time-integrated plankton metabolic rates in Sagami Bay using triple oxygen isotopes and O₂:Ar ratios. *Limnology and Oceanography* , 53 (5), 1776-1783.
- Sarma, V. V., Abe, O., Yoshida, N., & Saino, T. (2006). Continuous shipboard sampling system for determination of triple oxygen isotopes and O₂/Ar ratio by dual-inlet mass spectrometry. *Rapid Communications in Mass Spectrometry* , 20 (23), 3503-3508.
- Sarma, V., Abe, O., Hashimoto, S., Hinuma, A., & Saino, T. (2005). Seasonal variations in triple oxygen isotopes and gross oxygen production in the Sagami Bay, central Japan. *Limnology and Oceanography* , 50 (2), 544-552.
- Sarma, V., Abe, O., Hinuma, A., & Saino, T. (2006). Short-term variation of triple oxygen isotopes and gross oxygen production in the Sagami Bay, central Japan. *Limnology and Oceanography* , 51 (3), 1432-1442.
- Schmidt, M., Botz, R., Rickert, D., Bohrmann, G., Hall, S., & Mann, S. (2001). Oxygen isotopes of marine diatoms and relations to opal-A maturation. *Geochimica et Cosmochimica Acta* , 65 (2), 201-211.
- Schmidt, M., Botz, R., Stoffers, P., Anders, T., & Bohrmann, G. (1997). Oxygen isotopes in marine diatoms: A comparative study of analytical techniques and new results on the isotope composition of recent marine diatoms. *Geochimica et Cosmochimica Acta* , 61 (11), 2275-2280.

- Sowers, T., Bender, M., & Raynaud, D. (1989). Elemental and isotopic composition of occluded O₂ and N₂ in polar ice. *Journal of Geophysical Research: Atmospheres* , 94 (D4), 5137-5150.
- Stanley, R. H., & Howard, E. M. (2013). Quantifying photosynthetic rates of microphytobenthos using the triple isotope composition of dissolved oxygen. *Limnology and Oceanography: Methods* , 11 (7), 360-373.
- Stanley, R. H., Kirkpatrick, J. B., Cassar, N., Barnett, B. A., & Bender, M. L. (2010). Net community production and gross primary production rates in the western equatorial Pacific. *Global Biogeochemical Cycles* , 24, GB4001.
- Stanley, R. H., Sandwith, Z. O., & Williams, W. J. (in press). Rates of summertime biological productivity in the Beaufort Gyre: A comparison between the low and record-low ice conditions of August 2011 and 2012. *Journal of Marine Systems* .
- Sturm, P., Leuenberger, M., Sirignano, C., Neubert, R. E., Meijer, H. A., Langenfelds, R., et al. (2004). Permeation of atmospheric gases through polymer O-rings used in flasks for air sampling. *Journal of Geophysical Research: Atmospheres* , 109, D04309.
- Tcherkez, G., & Farquhar, G. D. (2007). On the ¹⁶O/¹⁸O isotope effect associated with photosynthetic O₂ production. *Functional Plant Biology* , 34 (11), 1049-1052.
- Thiemens, M. H. (2013). Introduction to chemistry and applications in nature of mass independent isotope effects special feature. *Proceedings of the National Academy of Sciences* , 110 (44), 17631-17637.
- Thiemens, M. H. (1999). Mass-Independent Isotope Effects in Planetary Atmospheres and the Early Solar System. *Science* , 283 (5400), 341-345.
- Thiemens, M. H., & Heidenreich, J. E. (1983). The mass-independent fractionation of oxygen: A novel isotope effect and its possible cosmochemical implications. *Science* , 219 (4588), 1073-1075.
- Thiemens, M. H., & Meagher, D. (1984). Cryogenic separation of nitrogen and oxygen in air for determination of isotopic ratios by mass spectrometry. *Analytical Chemistry* , 56 (2), 201-203.
- Thiemens, M. H., Jackson, T. L., & Brenninkmeijer, C. A. (1995). Observation of a mass independent oxygen isotopic composition in terrestrial stratospheric CO₂, the link to ozone chemistry, and the possible occurrence in the Martian atmosphere. *Geophysical Research Letters* , 22 (3), 255-257.
- Tortell, P. D. (2005). Dissolved gas measurements in oceanic waters made by membrane inlet mass spectrometry. *Limnology and Oceanography: Methods* , 3 (1), 24-37.
- Urey, H. C. (1947). The thermodynamic properties of isotopic substances. *J. Chem. Soc.* , 562-581.
- Veldhuis, M. J., Timmermans, K. R., Croot, P., & van der Wagt, B. (2005). Picophytoplankton; a comparative study of their biochemical composition and photosynthetic properties. *Journal of Sea Research* , 53 (1-2), 7-24.

- Venkiteswaran, J. J., Wassenaar, L. I., & Schiff, S. L. (2007). Dynamics of dissolved oxygen isotopic ratios: a transient model to quantify primary production, community respiration, and air-water exchange in aquatic ecosystems. *Oecologia*, *153* (2), 385-398.
- Wanninkhof, R. (1992). Relationship between wind speed and gas exchange over the ocean. *Journal of Geophysical Research: Oceans*, *97* (C5), 7373-7382.
- Wassenaar, L. I., & Koehler, G. (1999). An on-line technique for the determination of the $\delta^{18}\text{O}$ and $\delta^{17}\text{O}$ of gaseous and dissolved oxygen. *Analytical Chemistry*, *71* (21), 4965-4968.
- Westberry, T. K., Williams, P. J., & Behrenfeld, M. J. (2012). Global net community production and the putative net heterotrophy of the oligotrophic oceans. *Global Biogeochemical Cycles*, *26*, GB4019.
- Wiegel, A. A., Cole, A. S., Hoag, K. J., Atlas, E. L., Schauffler, S. M., & Boering, K. A. (2013). Unexpected variations in the triple oxygen isotope composition of stratospheric carbon dioxide. *Proceedings of the National Academy of Sciences*, *110* (44), 17680-17685.
- Williams, P. J., Quay, P. D., Westberry, T. K., & Behrenfeld, M. J. (2013). The oligotrophic ocean is autotrophic. *Annual Review of Marine Science*, *5* (1), 535-549.
- Yeung, L. Y., Young, E. D., & Schauble, E. A. (2012). Measurements of $^{18}\text{O}^{18}\text{O}$ and $^{17}\text{O}^{18}\text{O}$ in the atmosphere and the role of isotope-exchange reactions. *Journal of Geophysical Research: Atmospheres*, *117*, D18306.
- Young, E. D., Yeung, L. Y., & Kohl, I. E. (2014). On the $\Delta^{17}\text{O}$ budget of atmospheric O_2 . *Geochimica et Cosmochimica Acta*, *135*, 102-125.
- Yung, Y. L., DeMore, W. B., & Pinto, J. P. (1991). Isotopic exchange between carbon dioxide and ozone via $\text{O}(^1\text{D})$ in the stratosphere. *Geophysical Research Letters*, *18* (1), 13-16.
- Yung, Y. L., Lee, A. Y., Irion, F. W., DeMore, W. B., & Wen, J. (1997). Carbon dioxide in the atmosphere: Isotopic exchange with ozone and its use as a tracer in the middle atmosphere. *Journal of Geophysical Research: Atmospheres*, *102* (D9), 10857-10866.
- Zonneveld, K. A., Mackensen, A., & Baumann, K.-H. (2007). Stable oxygen isotopes of *Thoracosphaera heimii* (Dinophyceae) in relationship to temperature; a culture experiment. *Marine Micropaleontology*, *64* (1-2), 80-90.

Appendix

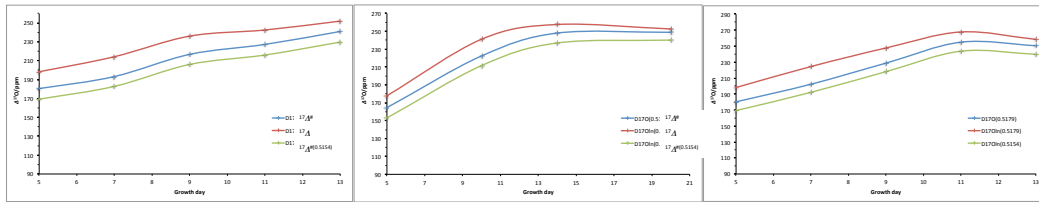


Figure 39: Figure showing the effect of using different definitions on the resulting $\Delta^{17}\text{O}$ for *E. huxleyi* first time sampling (left), 5-day (mid) and 2-day (right) repetition series.

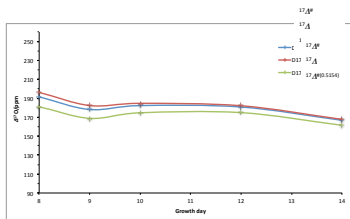


Figure 40: Shows the effect of the use of different definitions on the resulting $\Delta^{17}\text{O}$ for *Picochlorum* (differences are smaller than for *E. huxleyi*, as $f \sim 0$ and $\delta^{18}\text{O}$ values are closer to 0). $^{17}\Delta$ indicates $\Delta^{17}\text{O}$, ‘ln’ or ‘#’ refers to the logarithmic definition, λ is given between brackets. When no details are provided the definition is the linear definition with slope 0.5179.

As can be observed the used definition does not significantly change the observed trend or resulting $\Delta^{17}\text{O}$ value. (the ‘ln’ definition with slope 0.5179 consistently gives higher results than the linear definition with slope 0.5179, but the difference decreases when the situation becomes closer to steady state and $\delta^{18}\text{O}$ values approach zero. The ‘ln’ definition with slope 0.5154 consistently gives ~ 10 ppm more negative results but apart from that gives results with exactly the same trend as the linear definition results.)

Results show the used definition does not significantly change the observed trends or resulting $\Delta^{17}\text{O}_{s_0}$ values.

As expected, results of the different definitions are relatively far apart when conditions are away from biological steady state and/or $\delta^{18}\text{O}$ values are further away from zero, and become closer to each other when conditions approach $f = 0$ and/or $\delta^{18}\text{O}$ values become closer to 0. In all cases the result of the ‘ln’ definition with slope 0.5179 is slightly higher than that of the linear definition with slope 0.5179, although resulting values approach each other as $\delta^{18}\text{O}$ values and/or f approach zero. The ‘ln’ definition with slope 0.5154 yields more negative $\Delta^{17}\text{O}$ values in all cases, of approximately ~ 10 ppm with respect to the linear definition with slope 0.5179.

Variations in $\Delta^{17}\text{O}$ with f (ratio of net to gross production)

The result of the linear definition with 0.5179 is almost always slightly higher at $f = 0.5$ than at $f = 0$ or $f = 1$. It yields under general ($\gamma_R = 0.5179$, $^{18}\epsilon_R = -20\text{‰}$) respiration assuming the 2005-VSMOW and Eisenstadt et al. (2010) photosynthetic fractionation for *E. huxleyi*, a slightly higher $\Delta^{17}\text{O}_P$ than $\Delta^{17}\text{O}_{S0}$. In almost all cases the ‘ln’ definition with 0.5179 is higher at $f = 1$ than at $f = 0$. In all cases it is higher than linear(0.5179) at $f = 1$ (and approximately the same at $f = 0$). Under $\gamma_R = 0.5179$ and $^{18}\epsilon_R = -20\text{‰}$ respiration conditions, the ‘ln’ definition with 0.5154 gives approximately similar results for $f = 0$ and $f = 1$ (thus more constant results than the other two (with changing f)).

Increasing the γ_R or $^{18}\epsilon_R$ (more positive) leads to higher $\Delta^{17}\text{O}_{S0}$ values for the same $\Delta^{17}\text{O}_P$ values.

In order to get $\Delta^{17}\text{O}(\ln, 0.5179)$ values lower than $\Delta^{17}\text{O}_{S0}$ you need a γ_R of ~ 0.5225 . However, in this case (with the photosynthetic fractionation of Eisenstadt et al. (2010)), resulting values are too high.

If you would assume the VSMOW 2011 values, resulting steady state values are as predicted by the calculations of Kaiser and Abe (2012), but the lower values for the first days cannot be explained (unless by atmospheric air contribution).

If there would be no photosynthetic fractionation, definitions could give approx. the observed results ($\sim 150\text{-}200$ ppm for $\Delta^{17}\text{O}_P$, ~ 250 ppm $\Delta^{17}\text{O}_{S0}$ all definitions), if the γ_R is taken as 0.5225.

With values from Table 3 Kaiser and Abe (2012) ($\gamma_R = 0.5179 \pm 0.0006$, $^{18}\epsilon_R = (-20 \pm 4)\text{‰}$, ($\theta_R = 0.5154$) δ_P values from Luz and Barkan 2005-VSMOW and Eisenstadt et al. (2010) photosynthetic fractionation for *E. huxleyi*):

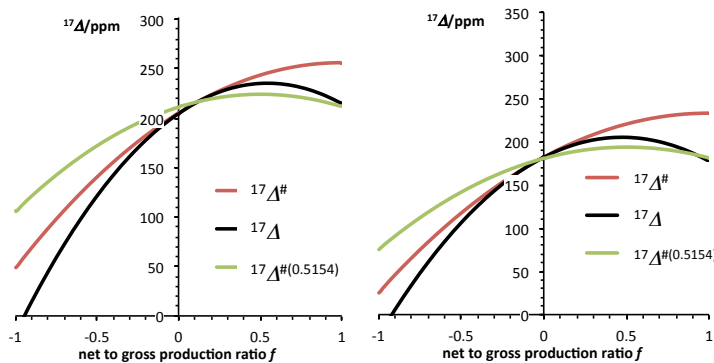


Figure 41 (left): Expected variation $\Delta^{17}\text{O}$ with f for different definitions, adapted Figure from Kaiser 2011a, calculations based on VSMOW 2005, ϵ_P Eisenstadt et al. (2010) for *E. huxleyi*, assuming $^{18}\epsilon_R = -20$ and $\gamma_R = 0.5179$ (as in Table 3 Kaiser and Abe (2012)) (if assuming VSMOW

values of Barkan and Luz 2011, results would be comparable but values ~ 50 ppm higher). As can be observed, for these input parameters, $\Delta^{17}\text{O}$ would be expected to be higher (for all tested definitions) for $f > 0$ than for $f = 0$.

Figure 42 (right): For *Nannochloropsis* you would expect, based on calculations/starting values (δ_P *Nannochloropsis* (Kaiser and Abe 2012 - Table 3 values, with -20.536, -10.458‰) (based on VSMOW Barkan and Luz 2005 + photosynthetic fractionation Eisenstadt et al. (2010)), $^{18}\epsilon_R$, γ_R) used by Kaiser in Table 3, with linear definition with 0.5179 a $\Delta^{17}\text{O}$ between 178 ($f = 1$) and 205 ($f = \sim 0.5$) between $f = 0$ and 1 (182 at $f = 0$). A lower $\Delta^{17}\text{O}$ could indicate $f < 0$.

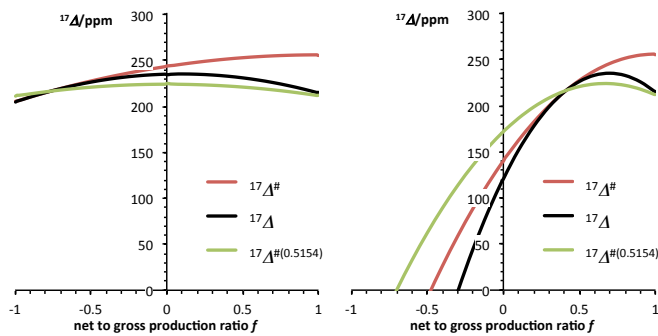


Figure 43: Same Figure (predictions for *E. huxleyi*) but with $^{18}\epsilon_R = -10$ (left) and -30 (right)

With changes in $^{18}\epsilon_R$, the $\Delta^{17}\text{O}_P$ stays the same but the $\Delta^{17}\text{O}_{S0}$ changes to ~ 121 - 140 (ln) ($^{18}\epsilon_R - 30$) or 235 - 244 (ln) ($^{18}\epsilon_R - 10$) (227 - 228 for $^{18}\epsilon_R = -15\%$).

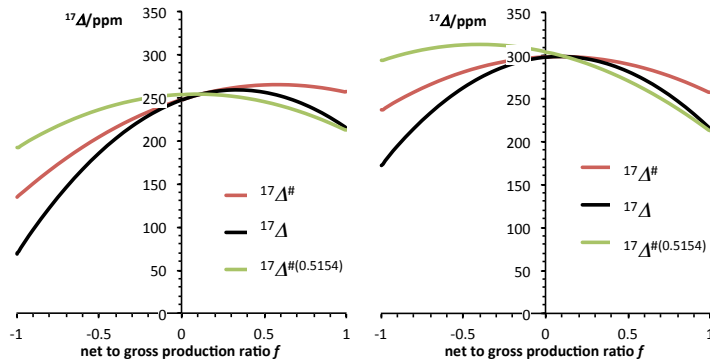
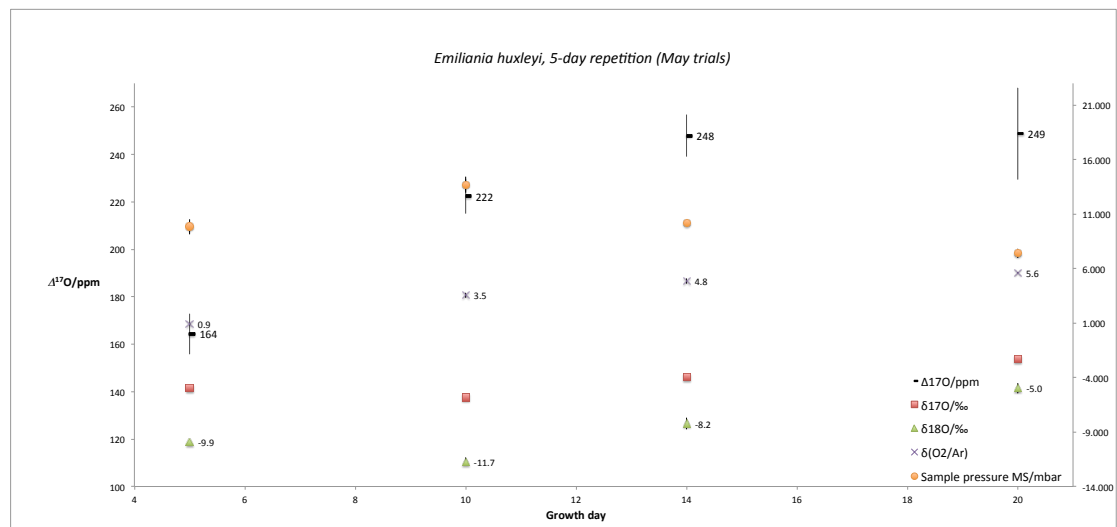


Figure 44: Figure for *E. huxleyi*, as above (VSMOW Barkan and Luz 2005, ϵ_P *E. huxleyi* Eisenstadt, $^{18}\epsilon_R = -20$) but with $\gamma_R = 0.52$ (left) and 0.5225 (right).

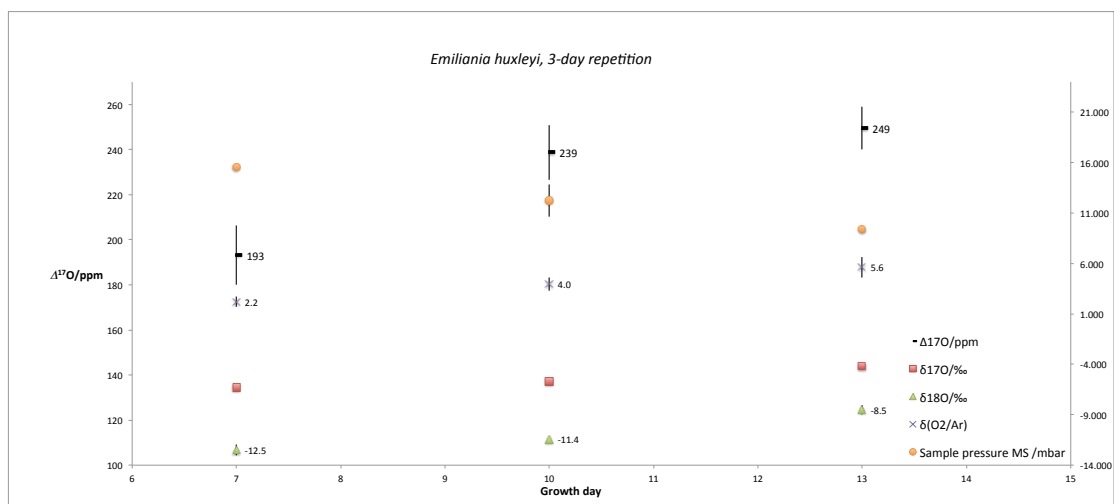
In all cases, calculations seem to indicate, if both $\Delta^{17}\text{O}$ (linear) and $\Delta^{17}\text{O}$ (ln) are lower than for $f = \sim 0$ (as in first days *E. huxleyi*), that $f < 0$.

Chapter 5: other sample patterns



The 5-day repetition series results from May experiments show exactly the same trend in the $\Delta^{17}\text{O}$ as the (*E. huxleyi*) repetition and single sampling series from June July, with an increase over the period of sampling towards a value of ~ 250 ppm. In this case the value obtained for growth day 5 is however slightly lower than for the other series (164 vs ~ 180 ppm), (in combination with slightly more positive $\delta^{17}\text{O}$ and $\delta^{18}\text{O}$ values for this day (compared to June-July *E. huxleyi* series) and a slightly lower $\delta(\text{O}_2/\text{Ar})$). This could however be related to small (initial) differences, in for instance inoculation density (or atmospheric air content) or differences in growth rates between individual bottles or bottles of May and June-July experiments). You could expect these (initial/individual differences (or differences in growth rate) to be more pronounced initially, when conditions are still further away from equilibrium (biological steady state). Apart from the slightly more positive values at sample day 1, $\delta^{17}\text{O}$ and $\delta^{18}\text{O}$ results are comparable to those of *E. huxleyi* single sampling and repeated sampling series of June-July, they are in the same range ($\delta^{18}\text{O} \sim -12$ to -8% up to day 14) and show the same trend with decreasing values from sample day 1 to 2 and increasing values (enrichment in ^{17}O and ^{18}O , indicating respiration) after day 2. The results of this set of experiments are thus very comparable to those of the June-July experiments, but in this case sampling was continued until day 20. It can be observed that the $\Delta^{17}\text{O}$ did not further increase after growth day 14, but instead is very comparable between growth day 14 and 20 (248 vs. 249 ppm). This might indicate (steady state is indeed reached around day 14 and) the $\Delta^{17}\text{O}$ indeed stabilises around this value. The small deltas however increase further (towards -5% for $\delta^{18}\text{O}$), probably as a result of normal (dark) respiration (with discrimination slope ~ 0.518), as the $\Delta^{17}\text{O}$ does not change anymore.

For these series, the variability between 3 bottles sampled at the same time is relatively small compared to for the June-July *E. huxleyi* series, which might be related to the fact that in these experiments, all bottles were inoculated with inoculum from the same tube, (while for the June-July experiments, inoculum was grown in 3 separate tubes (because of the larger volume needed) and bottles were inoculated from either one of these three. Bottles were however sampled (distributed over the sample days) so, that each set of three bottles contained one bottle of each inoculum tube). In this case the sample pressure slightly increases from sample day 1 to 2, indicating net production of oxygen between growth day 5 and 10 exceeded removal during sampling. After growth day ten, removal however exceeded net production over 5 days and the sample pressure (oxygen content) decreased with each time of sampling. $\delta(O_2/Ar)$ however increases, as for the other *E. huxleyi* repetition series, as a combination of net production of oxygen and removal of Ar.

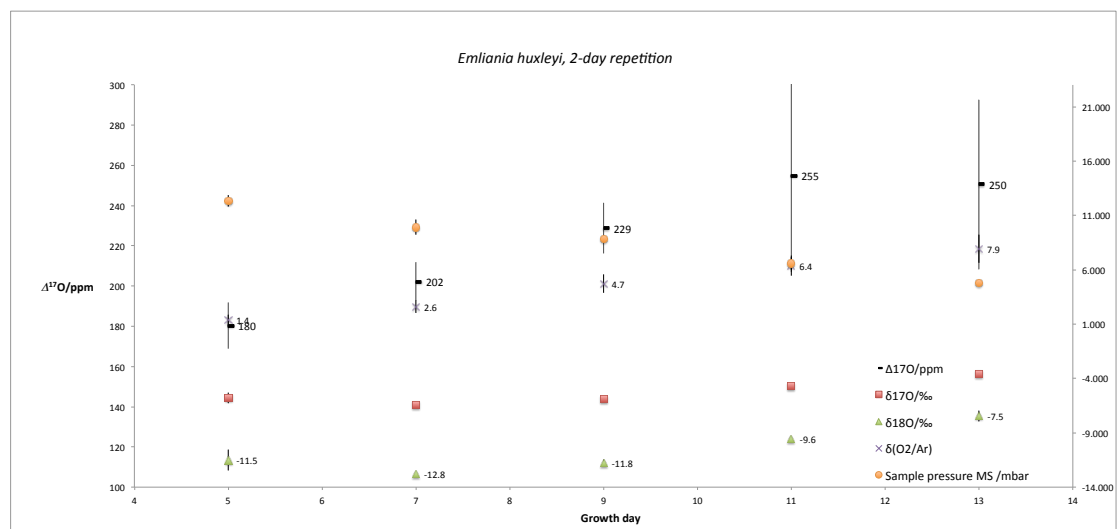


E. huxleyi 3-day repetition

$\Delta^{17}O$ and $\delta(O_2/Ar)$ trends are similar to those of 5-day and 2-day repetitions. $\delta^{17}O$ and $\delta^{18}O$ only increase due to later start sampling.

For the 3-day repetition series, the same trend in $\Delta^{17}O$ is observed as for the 2-day repetition series and 5-day repetition results from May, with values increasing towards ~250 (249) ppm around growth day 13. No difference in the moment of reaching this value can be observed between 2,3- and 5-day repetition series, indicating the sampling frequency does not affect the moment of reaching this value, the exact same trend being observed for the three sample patterns, which all seem to have a $\Delta^{17}O$ stabilising around growth day 13-14 and all reach exactly the same value for $\Delta^{17}O$ at growth day 13 or 14 (within 2 ppm). Compared to the single sampling series (with which this series shares

the data of growth day 7), results of resampled bottles are slightly higher, which might indicate resampling leads to a slightly higher $\Delta^{17}\text{O}_{\text{bio}}$ or $\Delta^{17}\text{O}_{\text{bio}}$ is reached faster for resampled bottles. However, as mentioned above, the frequency of resampling (whether once or multiple times) does not seem to have an effect on the results. In addition, the difference between the obtained values at growth day 13 for single and repeated sampling series is only ~ 8 ppm, so values are within each other's error (measurement uncertainty) and, even though results of resampled bottles are so close together in comparison to the result of single sampled bottles, this difference might be a coincidence. $\delta(\text{O}_2/\text{Ar})$, sample pressure and $\delta^{17}\text{O}$ and $\delta^{18}\text{O}$ results of the 3-day repetition series are comparable to those of the other repetition series.



$\Delta^{17}\text{O}$ results show the same trend as for the other sample patterns, increasing from 180 ppm to 250 ppm over the period of sampling. The last two values are relatively uncertain, but up to growth day 9, results are very comparable to those of other sample patterns, and the obtained averages are (although perhaps coincidentally) very close to averages of the other series. $\delta(\text{O}_2/\text{Ar})$ increases over the sampling period, but the increase is stronger than observed for newly sampled bottles, which is probably due to the removal of Ar during sampling in addition to the net oxygen production.

Sample pressure decreases, because there was (which only indicates) more removal of oxygen during sampling than net production over 2 days. (As a result sample pressure during the last two days became lower than preferable for accurate MS measurements, leading to the loss of precision for the MS results of these days.) $\delta^{17}\text{O}$ and $\delta^{18}\text{O}$ values are in the same range (~ -13 to -8 for $\delta^{18}\text{O}$, -6.5 to -4‰ for $\delta^{17}\text{O}$) as for the other sample series and show exactly the same trend as for the other patterns, with a decrease from sample day 1 to 2 and an increase from day 1 to 5.

